# Identifying Functional Links Between Kap121 and Chromosome Segregation in Yeast.

by

Lucas Vincent Cairo

A thesis submitted in partial fulfillment of the requirements for the degree of

Doctor of Philosophy

Department of Cell Biology
University of Alberta

**Abstract**

Nuclear pore complexes (NPCs) form aqueous portals in the nuclear envelope (NE) and are the sole sites for molecular exchange between nuclear and cytoplasmic compartments. While ions, small metabolites and molecules under ~40 kDa can freely passage through NPCs, most macromolecular transport across the NE is facilitated by a family of structurally related mobile transport receptors termed Karyopherins (Kaps). Kaps confer the ability to translocate through NPCs by establishing a series of low affinity interactions with Nups that contain phenylalanine-glycine repeat motifs (FG-Nups). While this general transport mechanism describes how the vast majority of macromolecular transport events are governed, far less is known about how nuclear transport is modulated in response to changes in cellular physiology. In budding yeast, which undergoes a closed mitosis, nuclear import mediated by Kap121 is inhibited in a regulated manner following arrest in metaphase with the microtubule-destabilizing drug nocodazole. The inhibition of Kap121-mediated import is facilitated by molecular rearrangements within the NPC, which prevent Kap121 and its cargos from moving through the NPC central channel. Here, we have investigated the underlying signaling mechanism required for triggering activation of the Kap121-transport inhibitory pathway (KTIP). We have discovered that the KTIP is activated in response to the loss of kinetochore-microtubule (KT-MT) attachments during mitosis. A key regulator of KTIP activation is the spindle assembly checkpoint (SAC) signaling protein, Mad1. Following KT detachment from spindle MTs, Mad1 participates in a signaling event and dynamically cycles between NPCs and KTs to initiate changes in the NPC driving the arrest of Kap121-mediated import. Activation of this signaling pathway requires the activity of the Aurora B-kinase Ipl1, and the resulting changes to transport prevent the

nuclear accumulation of the Kap121 cargo Glc7p, a phosphatase that functions as an antagonist of Ipl1-kinase activity. Thus, through reducing the nuclear accumulation of Glc7p, the KTIP fosters the establishment of a nuclear environment that promotes Ipl1-function and the eventual reorganization and proper assembly of the KT-MT interface. We have also uncovered a novel function for Kap121 in regulating KT bi-orientation and chromosome segregation during cell division distinct from its role in transporting proteins through the NPC. We present results showing that Kap121 physically interacts with Dam1 and Duo1, two key structural components of the Dam1 complex, which is an essential MT-bound assembly required for linking KTs to dynamic MT ends in yeast. We demonstrate that the interaction between Kap121 and the Dam1 complex is RanGTP-insensitive, suggesting this interaction occurs within the interior of the nucleus, potentially at the KT-MT interface. Kap121 binding to Dam1 and Duo1 promotes their stability, as a mutant version of Kap121 that can no longer bind these proteins leads to a significant decrease in their cellular levels. Our experimental results support a model where Kap121 confers a “chaperone-like” function within the nucleus where, through its physical association with Dam1/Duo1, contributes to the structural stability of the Dam1 complex by preventing Dam1 and Duo1 degradation.

**Dedication**

*To my remarkable parents,*

*for their love and support over the years….*

*And also to my newest little pal 'smelly Ellie' and her moderately smelly mother …*

**Acknowledgements**

It has been an absolute privilege to work in the Wozniak Lab. In particular, I am indebted to Dr. Rick Wozniak for sharing his unwavering passion for science. His work ethic, drive and determination are truly inspiring and for this, I am grateful to have worked alongside him over the years. I am also truly thankful for the help and support received from my committee members Drs. Richard Rachubinski and Gordon Chan. Their assistance over the years has been enormously helpful, and for this, I am extremely grateful.

I also consider myself blessed for working with a number of talented and interesting individuals over the years. This includes members of the Wozniak lab past and present as well as our great neighbors two meters to the north of us, the Rachubinski lab. And finally, I would also like to thank good coffee and good beer – without you I am nothing, with you I am everything.

## Table of Contents

Chapter I: *Introduction* ..... 1
1.1 Preface ..... 2
1.2 The nuclear envelope ..... 3
1.3 Nuclear pore complexes ..... 5
1.4 Nucleoporins ..... 9
1.4.1 Pore membrane proteins ..... 12
1.4.2 Core scaffold Nups ..... 14
1.4.3 FG-Nucleoporins ..... 16
1.4.4 NPC associated proteins ..... 19
1.5 The soluble transport machinery ..... 21
1.5.1 Karyopherins ..... 22
1.5.2 Nuclear signal sequences ..... 26
1.5.3 Ran ..... 28
1.6 Nuclear transport models ..... 32
1.6.1 The selective phase ..... 32
1.6.2 The virtual gate ..... 33
1.6.3 The affinity gradient ..... 34
1.7 Alternative Kap functions ..... 34
1.7.1 Cytoplasmic Kap functions ..... 35
1.7.2 Kaps, chromatin and mitosis ..... 38
1.8 Nuclear transport regulation ..... 42
1.8.1 Transport regulation through alterations to Kap-cargo interactions ..... 42
1.8.2 NPC-mediated transport regulation ..... 44
1.9 Mitotic NPC functions ..... 45
1.9.1 Nups and chromosome segregation ..... 46
1.9.2 KT proteins at NPCs ..... 48
1.10 KTs, chromosome segregation and the SAC ..... 51
1.10.1 KT morphology and structure ..... 52
1.10.2 The inner KT ..... 55
1.10.3 The outer KT ..... 56
1.10.4 The Dam1 complex ..... 58
1.10.5 KT bi-orientation in yeast ..... 60
1.10.6 Regulation of KT-MT interactions ..... 64
1.10.7 The Spindle Assembly Checkpoint ..... 66
1.11 Thesis focus ..... 73
Chapter II: *Experimental procedures* ..... 74
2.1 Yeast strains and media ..... 75
2.2 Plasmid ..... 87
2.3 Antibodies and buffers ..... 88
2.4 Immunopurification ..... 91
2.4.1 Immunopurification of protein A tagged proteins ..... 91
2.4.2 RanGTP release experiments ..... 92
2.4.3 IgG conjugation to epoxy-coated magnetic beads ..... 94
2.5 Western blotting ..... 95
2.5.1 Preparation of yeast whole cell lysates ..... 95

2.5.2 SDS-PAGE and western blotting analysis ..... 95
2.6 Benomyl sensitivity assay ..... 96
2.7 Chemically-induced cell cycle synchronization ..... 96
2.8 Galactose-induced overexpression ..... 97
2.9 Methionine-induced repression of *MET3* promoter controlled genes ..... 98
2.10 Inactivation of temperature-sensitive alleles ..... 98
2.11 FACS analysis ..... 98
2.12 Fluorescence and confocal microscopy ..... 99
2.13 Fluorescence recovery after photobleaching ..... 100
2.14 Image analysis and signal quantification ..... 101
2.15 Leptomycin-B inhibition of Xpo1 ..... 102
Chapter III: *Mitotic specific regulation of nuclear transport by the spindle assembly checkpoint protein Mad1* ..... 103
3.1 Overview ..... 104
3.2 Results ..... 105
3.2.1 Destabilization of MTs during metaphase alters nuclear transport ..... 105
3.2.2 Loss of KT-MT attachments activates the KTIP ..... 106
3.2.3 Mad1 activates the KTIP ..... 110
3.2.4 KTIP requires Mad1 association with NPCs and KTs ..... 113
3.2.5 Mad1 cycling between NPCs and KTs is required for KTIP activation ..... 120
3.2.6 Ipl1 function is necessary for activation of the KTIP ..... 121
3.2.7 The KTIP regulates the nuclear levels of Glc7p during SAC arrest ..... 124
3.3 Discussion ..... 129
Chapter IV: *A role for Kap121 in mitotic kinetochore bi-orientation* ..... 144
4.1 Overview ..... 145
4.2 Results ..... 146
4.2.1 Kap121 is required for KT bi-orientation ..... 146
4.2.2 Kap121 is required for accurate chromosome segregation ..... 151
4.2.3 Inhibition of Kap121-mediated import does not affect KT bi-orientation ..... 155
4.2.4 Kap121 binds the Dam1 complex and Ipl1 ..... 158
4.2.5 Carboxy-terminally tagging of Duo1 leads to the suppression of KT bi-orientation defects in *kap121-34* mutant cells. ..... 161
4.2.6. Loss of Kap121-Dam1 complex interactions leads to Dam1 complex destabilization ..... 165
4.3 Discussion ..... 169
Chapter V: *Perspectives* ..... 178
5.1 Synopsis ..... 179
5.2 Physiological output of the KTIP ..... 179
5.3 Mad1 and NPC molecular rearrangements ..... 182
5.4 KTIP in higher organisms ..... 183
5.5 Importins as intranuclear targeting factors ..... 186
5.6 Nups and chromosome segregation in yeast ..... 187
5.7 Kaps and KT assembly ..... 189
Chapter VI: *Appendix* ..... 230

## List of Tables

Table 1-1. Mammalian and yeast Nup homologs ..... 11

Table 1-2. Karyopherins of yeast and vertebrates ..... 24

Table 2-1. Yeast strains..... 77

Table 2-2. Antibodies..... 88

Table 2-3. Common buffers and solutions..... 89

## List of Figures

Figure 1-1. A composition and structural of nuclear pore complexes ..... 8

Figure 1-2. The nuclear transport cycle for import and export Kaps ..... 25

Figure 1-3. General organization of the budding yeast KT ..... 54

Figure 1-4. KT bi-orientation in budding yeast ..... 62

Figure 1-5. Ndc80 and Dam1 complexes in lateral to end-on attachments ..... 63

Figure 1-6. Spindle assembly checkpoint signaling at the KT ..... 71

Figure 3-1. MT destabilization during metaphase activates the KTIP ..... 108

Figure 3-2. MT depolymerization outside of metaphase has no effect on Kap121-mediated import ..... 109

Figure 3-3. KT detachment from spindle MTs is sufficient for KTIP activation. ..... 111

Figure 3-4. Mad1 is recruited to KTs in *ask1-2*, *ndc80-1*, and *mcd1-1* mutant cells grown at the non-permissive temperature ..... 112

Figure 3-5. KTIP activation requires Mad1, but not Mad2 ..... 114

Figure 3-6. Mad1 is recruited onto unattached KTs in the absence of Mad2 ..... 115

Figure 3-7. Dual association of Mad1 with both KTs and NPCs is necessary for KTIP activation ..... 118

Figure 3-8. mad1$^{318-749}$-GFP does not localize to Mlp bodies in *nup60*Δ cells ..... 119

Figure 3-9. KTIP activation requires the dynamic movement of Mad1 between NPCs and KTs ..... 123

Figure 3-10. Ipl1 is required for KTIP activation ..... 125

Figure 3-11. KTIP regulates nuclear import of Glc7p ..... 128

Figure 3-12. Model for Mad1 activation of the Kap121 transport inhibitory pathway ..... 132

Figure 3-13. *MPS1* overexpression induces the dissolution of Mlp bodies in *nup60Δ*

cells ..... 137
Figure 3-14. Nuclear import of Glc7p is inhibited by nocodazole-induced SAC arrest. ..... 140
Figure 4-1. Cells compromised for Kap121 function exhibit KT bi-orientation defects ..... 149
Figure 4-2. KT dynamics in *kap121-34* cells ..... 150
Figure 4-3. Loss of Kap121 function results in chromosomal segregation defects ..... 154
Figure 4-4. Arrest of Kap121-mediated import does not impact metaphase KT-alignment ..... 157
Figure 4-5. Kap121 interacts physically with the Dam1 complex and Ipl1 ..... 160
Figure 4-6. Carboxy-terminally tagging of Duo1 suppresses metaphase KT alignment defects in *kap121-34* cells ..... 163
Figure 4-7. GFP-tagged Duo1 suppresses metaphase KT bi-orientation defects in cells depleted of Kap121 ..... 164
Figure 4-8. kap121-34 fails to interact with the Dam1 complex or Ipl1. ..... 168
Figure 4-9. *duo1-2* and *kap121-34* mutant cells produce similar KT bi-orientation defects ..... 170
Figure 4-10. Kap121-GFP is not observed at KTs ..... 175
Figure 6-1. Nuclear accumulation of Kap121-GFP is inhibited in metaphase-arrested cells treated with nocodazole ..... 232

## List of Symbols, Abbreviations and Nomenclature

αF ..... alpha factor
APC ..... anaphase promoting complex
ATP ..... adenosine triphosphate
Ben ..... benomyl
BP ..... base pair
°C ..... degrees Celcius
CCD ..... charged coupled device
CPC ..... chromosomal passenger complex
ChIP ..... chromatin immunoprecipitation
cNLS ..... 'classical' NLS
d ..... days
Da ..... Dalton
DNA ..... deoxyribonucleic acid
ECL ..... enhanced chemoluminescence
EM ..... electron microscopy
ER ..... endoplasmic reticulum
Fig. ..... figure
FG ..... phenylalanine, glycine
FRAP ..... fluorescence recovery after photobleaching
FRET ..... fluorescence resonance energy transfer
g ..... gram
*g* ..... gravitational force
Gal ..... galactose
G1 ..... gap one phase
G2 ..... gap two phase
GAP ..... gtpase activating protein
GDP ..... guanosine diphosphate
GEF ..... guanosine exchange factor
GFP ..... green fluorescent protein
GFP+ ..... enhanced green fluorescent protein
Glc ..... glucose
GTP ..... guanosine triphosphate
GTPase ..... guanosine triphosphatase
H ..... hour
HA ..... hemagluttinin
HU ..... hydroxyurea
HRP ..... horseradishperoxidase
IgG ..... immunoglobulin G
INM ..... inner nuclear membrane
Kap ..... karyopherin
KBD ..... karyopherin binding domain
KT ..... kinetochore
LP ..... long pass
Min ..... minutes

μ ..... micro
μm ..... micron/micrometers
μg ..... microgram
μL ..... microlitres
m ..... milli
M ..... moles per litre/mitotic phase/mega ($1x10^6$)
mCh ..... mCherry
mRNA ..... messenger RNA
MT ..... microtubule
NE ..... nuclear envelope
NEBD ..... nuclear envelope breakdown
NES ..... nuclear export signal
NLS ..... nuclear localization signal
Noc ..... nocodazole
NPC ..... nuclear pore complex
Nup ..... nucleoporin
OD ..... optical density
ONM ..... outer nuclear membrane
ORF ..... open reading frame
pA ..... protein A
PAGE ..... polyacrylamide gel electropheresis
PCR ..... polymerase chain reaction
pH ..... -log[H]
pom ..... pore membrane protein
RFP ..... red fluorescent protein
RNA ..... ribonucleic acid
RNP ..... ribonucleoproteins
SAF ..... spindle assembly factor
sec ..... second
S ..... synthesis phase
SD ..... synthetic dropout media
SDS ..... sodium dodecyl sulphate
SM ..... synthetic media
SUMO ..... small ubiquitin-related modifier
TCA ..... trichloracetic acid
tRNA ..... transfer RNA
ts ..... temperature sensitive
U ..... unit
V ..... volt
WT ..... wild-type
YPD ..... yeast extract peptone and dextrose
YP-Gal ..... yeast extract peptone and galactose
YP-Raf ..... yeast extract peptone and raffinose

# **Chapter I:** *Introduction*

## 1.1. Preface

The eukaryotic cell is typified by the presence of a dynamic, complex and intricately organized internal membrane system that partitions the cell into discreet membrane-bound compartments termed organelles. The most predominant of these is the cell nucleus. As with all organelles, key to both the structural and functional integrity of the nuclear compartment is its membrane system referred to as the nuclear envelope (NE). This restrictive barrier encapsulates the nuclear genome and, with it, the diverse range of metabolic processes associated with maintaining nuclear physiology. Embedded within the NE are massive macromolecular assemblies called nuclear pore complexes (NPCs) that serve as selective gatekeepers for all macromolecular transport events across the NE. While ions and small metabolites can freely passage through NPCs, macromolecular trafficking across the NE requires the activity of soluble transport receptors, most of which belong to a family of structurally related proteins termed karyopherins (Kaps). These mobile transport receptors bind cargos containing nuclear localization signals (NLSs) or nuclear export signals (NESs) and function to dock them at the NPC for subsequent translocation through the NPC central channel. In addition to their roles in nucleocytoplasmic transport, it has become increasingly apparent that both NPCs and Kaps confer a variety of ancillary, transport-independent functions. The spatial juxtaposition of the nuclear transport apparatus relative to chromatin places this machinery at a locale ideal for influencing a variety of nuclear processes.

Individual NPC constituents and Kaps possess the ability to bind various elements of the mitotic apparatus, and through these interactions, are able to influence a variety of mitotic processes, including chromosomal transmission during cell division. These observations hold true across evolutionarily distant species, regardless of whether or not

the topological constraints of the NE are maintained over the course of mitosis. Thus, acquiring knowledge on the functional interrelationship between these disparate and unique cellular machineries is paramount to understanding the underlying mechanisms the cell has in place for maintaining genomic integrity.

**1.2 The nuclear envelope**

A defining hallmark of eukaryotic cells is the NE. Made up of two concentric lipid bilayers separated by a luminal space, the outer and inner nuclear membranes, referred to as the ONM and INM, encapsulate the nuclear genome (reviewed in Hetzer et al., 2005; Hetzer, 2010). Continuity between the ONM and INM is established at discreet topological regions within the NE dubbed the pore membrane (POM). Early electron microscopy (EM) studies investigating the basic morphology of the NE revealed that the ONM is continuous with the rough endoplasmic reticulum (RER) (Watson, 1955). Consistent with this, the ONM contains protein complexes also found at the RER, including membrane-attached ribosomes (Mattaj, 2004; Hetzer et al., 2005). Each membrane domain within the NE contains a unique protein complement, which contributes to the functional/structural specialization of each distinct stretch of membrane (Mattaj, 2004). The ONM, for instance, is host to a unique class of related integral membrane proteins that possess specialized sequence motifs referred to as KASH (Klarsicht, ANC-1, Syne Homology) domains (Hetzer, 2010). In metazoans, KASH domain-containing integral membrane proteins play a pivotal role in directly linking the NE to various elements of the actin cytoskeleton as several ONM constituents possess exposed actin binding domains (ABDs) (Wilhelmsen et al., 2005). In addition to binding

cytoskeletal components, KASH proteins also establish connections across the periplasmic space with Sad1/UNC-84 (SUN) domain-containing proteins of the INM, which physically interact with lamins and underlying chromatin (Starr and Han, 2003; Wilhelmsen et al., 2006). Such translumenal interactions are not only important for establishing physical linkages between the cell cytoskeleton and the nuclear interior but also for separating the ONM from the INM at equal distances through the NE (Voeltz and Prinz, 2007).

On the opposite side of the NE, the INM is defined by a unique array of proteins, which form extensive interactions with the underlying chromatin and a fibrous meshwork of intermediate filaments situated proximal to the NE termed the nuclear lamina (Hetzer, 2010). Accordingly, many INM proteins have been characterized on the basis of their interactions with chromatin or the lamins (i.e. lamin B receptor, lamin-associated peptide 1 and Man1) (Akhtar and Gasser, 2007; Dorner et al., 2007; Schirmer and Foisner, 2007). Notably, several human diseases have been linked to defects in the ability of INM proteins to target efficiently to the inner membrane (Worman and Bonne, 2007). This has fueled considerable interest in investigating the mechanisms by which these proteins target to the INM. A recent study has uncovered precisely how INM proteins are directed to the inner membrane revealing a bi-modal mechanism that involves both passive and active means of transport across the pore membrane (King et al., 2006). From this study, it was determined proteins with smaller nucleoplasmic domains (<25 kDa) destined for the INM are able to diffuse freely across the pore membrane and are eventually retained at this location through interactions with the nuclear lamins or chromatin (King et al., 2006; Lusk et al., 2007). Alternatively, proteins destined for the INM with larger exposed

soluble domains are actively transported across POM in a karyopherin-dependent manner. In either scenario, the pore membrane plays a key role in providing the pathway for the movement of INM proteins to their appropriate destination (Lusk et al., 2007).

Finally, the POM, or pore membrane, is largely defined as the site where the INM and ONM fuse and, consequently, serves as the entry point for INM proteins as discussed above. Topologically, the membrane at this location is highly curved and, resultantly, is energetically unstable (Mattaj, 2004; Alber et al., 2007; Hetzer, 2010). Therefore, one distinguishing feature of this stretch of NE is the presence of a specialized subset of integral membrane proteins that not only function to stabilize this energetically unfavorable membrane conformation but also serve as a scaffold to anchor NPCs to the NE (Alber et al., 2007). These proteins, referred to as the Poms, will be discussed in greater detail in section 1.4.1.

**1.3 Nuclear pore complexes**

Not long after the development of the electron microscope, this technology would become instrumental in the initial identification of NPCs. Described originally as ‘pores’, these electron-dense structures were observed at irregular frequency throughout the NE. In the years following, the term ‘pore complex’ was coined to better describe these cylindrical structures seen by EM (Watson, 1959). Since these initial pioneering studies, an enormous effort has gone into investigating the structural/functional features of these assemblies, and thanks to technological advances, a highly detailed picture has since emerged on the overall architecture of these assemblages. In particular, advances in microscopy have allowed for these structures to be visualized in greater detail. From

these studies, it was revealed that the NPC is built from repetitive, modular units, arranged with radial symmetry around the central transport channel, yielding a structure with apparent octagonal symmetry (Gall, 1967; Faberge, 1973; Kessel et al., 1973; Franke et al., 1981; Akey, 1989; Akey and Radermacher, 1993). Moreover, this structural organization appears to be conserved across evolutionarily divergent species (Stoffler et al., 1999; Fahrenkrog and Aebi, 2003). Despite the observed conservation in basic morphology, more empirical analyses revealed that there exist apparent dimensional and mass differences between distant eukaryotes. While vertebrate NPCs have a diameter of approximately 120-145 nm, the diameter of the yeast NPC is considerably smaller at ~96 nm (Akey and Radermacher, 1993; Yang et al., 1998). Consistent with this variation in size, proteomic analyses have yielded molecular mass estimates for yeast and vertebrate NPCs at ~40 MDa and ~60 MDa, respectively (Yang et al., 1998; Rout et al., 2000; Cronshaw et al., 2002). Despite these empirical differences, these complex assemblages, on a morphological, compositional and functional level, have remained remarkably well conserved throughout evolution (Yang et al., 1998; Vasu and Forbes, 2001; Cronshaw et al., 2002; Alber et al., 2007).

A recent study has yielded a high-resolution map of the entire NPC (See Figure 1-1) (Alber et al., 2007). This was achieved by utilizing a multi-disciplinary approach where proteomic, biophysical and imaging data were systematically acquired and then integrated using an advanced computational analysis. From this undertaking, a model of the NPC was made where the predominant structural/sub-structural features of the NPC were defined and the spatial positioning of each constituent nucleoporin within the NPC was predicted, thus yielding a detailed map of these structures (Figure 1-1) (Alber et al.,

2007). From this study, it was determined that the fundamental unit of symmetry of the NPC core is a 'spoke' subunit (Hinshaw et al., 1992; Beck et al., 2003; Stoffler et al., 2003; Kielsleva et al., 2004; Alber et al., 2007). The arrangement of the constituent proteins within each spoke yields a structural unit with nearly identical nucleoplasmic and cytoplasmic halves that are conjoined at the NPC's equator. In total, eight individual spokes are organized in an interconnected fashion to form the NPC structural core, which is comprised of a co-axial, triple-ring network including inner, outer, and membrane rings (Alber et al., 2007). These rings, stacked upon each other, form a cylindrical structure that encircles the NPC central channel. The outer rings, which are situated at the nucleoplasmic and cytoplasmic periphery of the NPC core, come together with the inner rings to form the NPC core scaffold. The membrane ring, positioned within the luminal space of the NE, is immediately proximal to the pore membrane and is sandwiched in between inner/outer rings. Included in this stacked coaxial ring structure are linker nucleoporins, which are effectively connected to the surface of the core scaffold where they face the interior of the central channel. Positioned here, linker Nups bridge the NPC core to the more functionally important unit of the NPC known as FG-nucleoporins, which are necessary for transport. Projecting from the walls of the central channel, FG-nucleoporins, being largely filamentous and unstructured, come together to crowd and occlude the central channel forming a physical zone of selectivity within the central conduit. The space occupied by FG-nucleoporins creates an opening of approximately 10 nm, which, intuitively, is similar to the maximal size of molecules that can freely diffuse through these structures (Alber et al., 2007). FG-nucleoporins and their roles in establishing the permeability barrier and facilitating karyopherin-dependent transport

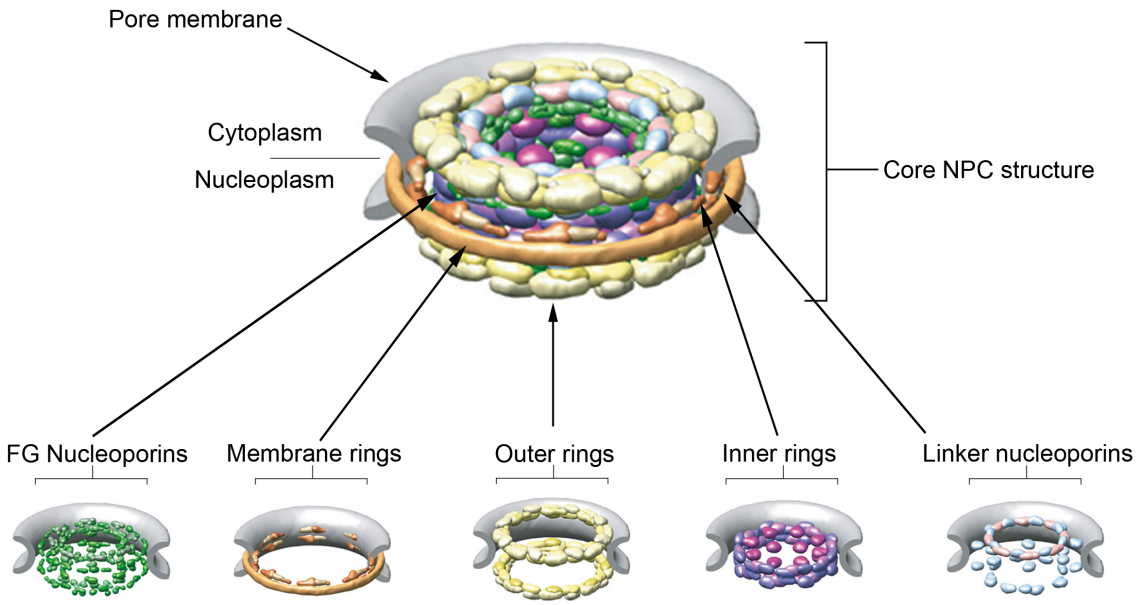


**Figure 1-1. A composition and structural model of yeast nuclear pore complexes.** Displayed is a schematic representation of the NPC embedded within the NE (grey). Individual nucleoporins have been color-coded on the basis of their localization volumes within the five substructures that comprise the NPC. The NPC core structure is comprised of a series of co-axial rings stacked on top of each other and include the inner rings (purple), outer rings (yellow) and linker nucleoporins (blue/pink). The core structural unit of the NPC is physically anchored to the pore membrane by the most outer ring termed the luminal ring and is depicted in orange. Lining the NPC central conduit through attachments to linker Nups are FG-nucleoporins (green). Finally, emanating from opposing faces of the NPC are the nuclear basket nucleoporins and the cytoplasmic filaments (not shown here). Adapted from Alber et al., 2007.

will be discussed in greater detail in section 1.4.3.

Finally, emanating off both nucleoplasmic and cytoplasmic faces of the NPC are filamentous structures that reach into both the interior of the nucleus and cytoplasm. On the cytoplasmic side, these unique structures, termed cytoplasmic filaments, are thought to play a key role in both initiation and termination of nuclear import and export (Rout et al., 2000; Beck et al., 2004; Wente and Rout, 2010; Aitchison and Rout, 2012). On the opposite side, extending into the nuclear interior, are nuclear filaments that come together to form a structural unit termed the nuclear basket (Wente and Rout, 2010; Aitchison and Rout, 2012). The position of the nuclear basket makes this structure amendable to partaking in a variety of nuclear functions outside of transport, and, as such, this structural unit not only interacts with the nuclear lamina in higher eukaryotes, but also with underlying chromatin across species (reviewed in Strambio-De-Castillia et al., 2010). In addition to interacting with various nuclear structures, the NPC acts as a molecular docking site for a plethora of proteins involved in a range of functions including sumoylation homeostasis, RNA biogenesis, chromatin metabolism and chromosome segregation (Strambio-De-Castillia et al., 2010).

## 1.4 Nucleoporins

The individual proteins that comprise the NPC are referred to as nucleoporins, or Nups. Thanks to a combination of genetic, biochemical and proteomic approaches, the constituent proteins that comprise the NPC have largely been inventoried across phylogenetically divergent eukaryotes. Remarkably, despite being among the largest macromolecular assemblies in the cell (~40-60 MDa), the NPC is comprised of a

relatively small number of individual constituent proteins (see Table 1-1) (Cronshaw et al., 2002; Rout et al., 2000). For example, by comparison, the eukaryotic ribosome, which has a predicted mass of approximately 4 MDa, contains in excess of 80 individual proteins (Wool et al., 1995; Fatica and Tollervey, 2002). This is in striking contrast to the NPC, which is comprised of only ~30 different proteins (Rout et al., 2000; Cronshaw et al., 2002; Alber et al., 2007). How such a massive and extraordinarily complex assemblage is made up of so few constituent proteins is reconciled by the observation that the architecture of the NPC is based on repetitive modules and, as a result of structural repetition, each Nup is present in multiple copies per NPC resulting in a total of 456 proteins per structure (Rout et al., 2000; Alber et al., 2007).

Computational fold prediction analyses and biochemical domain mapping reveal that the vast majority of Nups is comprised of surprisingly few repetitive protein fold types (Devos et al., 2004; Devos et al., 2006). On the basis of this analysis, the majority of Nups can effectively be segregated into three unique groups and includes the following: (1) Nups which possess transmembrane domains within their sequence and are housed within the pore membrane known as 'Poms' (pore membrane proteins), (2) Nups which possess β-propeller- and/or α-solenoid- fold-types commonly referred to as core scaffold Nups, and (3) Nups characterized by the presence of repetitive phenylalanine-glycine (FG) dipeptide repeats known as FG-Nups, which form the functional unit of the NPC involved in establishing the permeability barrier and facilitating nucleocytoplasmic transport. The next sections focus on the structural and functional elements of these distinct groups of Nups.

**Table 1-1 Mammalian and yeast Nup homologs**

| Mammalian Nucleoporin | *S. cerevisiae* Nucleoporin | Nucleoporin type |
|---|---|---|
| Nup358 | - | FG |
| Nup214 | Nup159 | FG |
| Nup153 | Nup1/Nup2/Nup60 | FG |
| Nup98 | Nup145/Nup110/Nup116 | FG |
| Nup62 | Nsp1 | FG |
| Nup58/Nup45 | Nup49 | FG |
| Nup54 | Nup57 | FG |
| Nup53 (Nup35) | Nup53/Nup59 | FG |
| Nup50 | Nup2 | FG |
| NLP1 (hCG1) | Nup42 | FG |
| Nup205 | Nup192 | Non-FG |
| Nup188 | Nup188 | Non-FG |
| Nup160 | Nup120 | Non-FG |
| Nup155 | Nup157/Nup170 | Non-FG |
| Nup133 | Nup133 | Non-FG |
| Nup107 | Nup84 | Non-FG |
| Nup96 | Nup145 | Non-FG |
| Nup93 | Nic96 | Non-FG |
| Nup88 | Nup82 | Non-FG |
| Nup85 (Nup75) | Nup85 | Non-FG |
| Nup43 | - | Non-FG |
| Nup37 | - | Non-FG |
| ALADIN | - | Non-FG |
| Gle1 | Gle1 | Non-FG |
| RAE1 (Gle2) | Gle2 | Non-FG |
| Sec13 | Sec13 | Non-FG |
| Seh1 | Seh1 | Non-FG |
| Tpr | Mlp1/Mlp2 | Non-FG |
| Pom121 | - | Pom |
| Gp210 | - | Pom |
| NDC1 | Ndc1 | Pom |
| - | Pom34 | Pom |
| - | Pom152 | Pom |

* Adapted from: D'Angelo and Hetzer, 2008.

### 1.4.1 Pore membrane proteins (Poms)

Positioned within the pore membrane is a family of integral membrane proteins termed 'Poms'. Together, through extensive physical interactions, these proteins form a distinct NPC subcomplex that encircles the pore (Alber et al., 2007; Onischenko et al. 2009). In yeast, there are three Poms including Pom34, Pom152, and Ndc1 (Wozniak et al. 1994; Chial et al., 1996; Tcheperegine et al. 1999; Miao et al., 2006). All three proteins are predicted to possess transmembrane α-helices within their sequence. This shared structural motif has considerable functional importance as it is required for anchoring the NPC to the NE, bridging intra-complex interactions with NPC core constituents, and, potentially, contributing to the stabilization of the energetically unstable pore membrane (Chial et al., 1998; Miao et al., 2006; Aitchison and Rout, 2012). The first of the yeast pore-membrane proteins to be described was Pom152 (Wozniak et al., 1994). Based on secondary structure predictions, Pom152 is perhaps structurally unique in that, contained within its luminal domain is a series of tandem repetitive motifs that are thought to come together to form cadherin folds (Devos et al., 2006). The presence of cadherin fold domains within Pom152 is predicted to form homophilic binding interfaces required for complex oligomerization (Aitchison and Rout, 2012). Although it is apparent that Pom152 contributes to NPC structure, cells are able to survive in the absence of this protein. Cell viability in the absence of Pom152 is likely attributed to functional redundancy with the other members of this subcomplex. This notion is supported by the observation that both *POM152* and *POM34* share a significant number of overlapping genetic interactions with scaffold Nups (Marelli et al., 1998; Tcheperegine et al., 1999; Miao et al., 2006; Onischenko et al., 2009). Unlike Pom152,

significantly less is known about the function of Pom34. Other than the reported structural features of this protein in that it contains two transmembrane domains and two domains that face the NPC core scaffold, little functional information has been described for this pore membrane constituents.

In contrast to the other Poms, Ndc1 is required not only for NPC assembly but also for insertion of spindle pole bodies (SPBs) into the NE (Winey et al., 1993; Chial et al., 1998; Araki et al., 2006; Casey et al., 2012). This dual role in both NPC and SPB assembly is presumably why *NDC1* is essential. Structurally, this protein possesses six transmembrane helices and a carboxy-terminal domain that forms an interaction interface with the NPC core Nups (Alber et al., 2007; Onischenko et al., 2009). Of the three Poms, loss of Ndc1 results in the most severe defects in NPC assembly. Depletion of this protein results in the mislocalization of both cytoplasmic and nucleoplasmic Nups and nuclear transport defects (Madrid et al., 2006).

Similar to yeast, vertebrate Poms also play a pivotal role in NPC assembly. Not only are they involved in the insertion of *de novo* NPCs into the NE while the envelope is still intact (interphase), they are also required for post-mitotic NPC re-assembly following NE breakdown. Using *Xenopus laevis* oocytes for reconstituting post-mitotic NPC reassembly, it was determined that both Pom121 and Ndc1 are required for the formation of NPC structural intermediates needed for the recruitment of core scaffold Nups to assembling NPCs (Antonin et al., 2005; Mansfeld et al., 2006). Consistent with this, *in vitro* data demonstrated that Pom121 interacts directly with both Nup160 and Nup155, which are both core scaffold Nups previously implicated in NPC re-assembly (Antonin et al., 2005; Mansfeld et al., 2006; Mitchell et al., 2010). Therefore, across

species, it is clear that the function of the Poms is highly conserved in that they are involved in NPC assembly and anchoring the core scaffold to the NE.

### 1.4.2 Core scaffold Nups

In yeast, the core scaffold is a substructure within the NPC comprised of twelve evolutionarily related structural proteins that are arranged together to form the inner and outer rings of the NPC (Alber et al., 2007). Based on fold composition analyses, core scaffold Nups consist predominantly of two varying protein fold types (Devos et al., 2004; Devos et al., 2006). These include β-propeller and α-solenoid-like folding domains. Depending on the Nup, these folding domains are generally found in three different arrangements whereby a given scaffold Nup consists almost entirely of either a β-propeller or α-solenoid-like folding domain or where both domains are found together in the same protein. Intriguingly, these exact fold types are highly characteristic of clathrin, COPI, and COPII membrane vesicular coating complexes. The observation that both scaffold Nups and these specialized membrane-bending complexes share fold types led to the proposal of the 'protocoatomer hypothesis', which posits that the fold types shared between these functionally divergent groups of proteins are the result of shared ancestry of a single membrane bending module (Field and Dacks, 2009). Shared ancestral origins between these functionally divergent complexes are further supported by the observation that Sec13, a member of the Sec13/31 COPII vesicle coating complex, is also found in the core-scaffold-containing Nup84 subcomplex (Devos et al., 2004). In addition, the topology of the core-scaffold appears to resemble that of a vesicle coat as it forms a discreet structure that encases the pore membrane (Devos et al., 2004; Alber et al., 2007).

Ultimately, at this position, the core scaffold defines the geometry of the pore in that both the height of the NPC and the width of the central channel are dictated by this structure (Alber et al., 2007). Moreover, given its centralized location, this structure interfaces with all other Nups and Poms, either on its inner or outer structural surface.

In its totality, the core scaffold in yeast is comprised of three major subcomplexes. These include the highly studied, seven member Nup84 complex, which comes together to form the outer ring of the core scaffold, the four member Nup170 complex that forms the inner ring, and the Nic96 complex that is thought to be the physical basis for establishing connections between the core scaffold and the FG-Nups (Alber et al., 2007). The structure of the Nup84 complex has been extensively studied revealing that it adopts a y-shaped conformation (Siniossoglou et al., 2000; Lutzmann et al., 2002; Hsia et al., 2007; Debler et al., 2008; Kampmann and Blobel, 2009). This y-shaped structural conformation is analogous to the structure formed by the COPII vesicle coating complex, thereby further supporting the 'protocoatomer' hypothesis discussed above. Functionally, this complex has been implicated in mRNA export and also in maintaining NPC distribution throughout the NE (Doye et al., 1994; Aitchison et al., 1995). Similarly, the mammalian counterpart to the Nup84 complex, the Nup107-160 complex, has also been implicated in mRNA export and NPC assembly (Vasu et al., 2001; Walther et al., 2003a).

Aligning with the NPC equator and in close spatial proximity to the three Poms, the inner rings formed by the Nup170 subcomplex are positioned to form extensive physical interactions with the pore membrane and resident proteins. The interactions formed between these NPC sub-complexes contributes significantly to the overall

structure of the NPC, and such interactions are paramount for tethering the NPC core to the pore membrane (Alber et al., 2007; Onischenko et al., 2009). This notion is supported by genetic data demonstrating extensive genetic interactions between members of the Nup170 complex and the Poms (Miao et al., 2006; Onischenko et al., 2009). Moreover, this subcomplex is important for NPC assembly, as the simultaneous loss of both Nup170, and its binding partner Nup157 results in a decrease in NPC number and the formation of NPC assembly intermediates (Makio et al., 2009).

### 1.4.3 FG-Nucleoporins

In the initial cataloguing of all NPC constituents, it was determined that nearly one-third of Nups inventoried contain highly repetitive phenylalanine-glycine dipeptide repeats (FG-repeats) (reviewed in Wente and Rout, 2010; Aitchison and Rout, 2012). Dubbed FG-Nups, regions of these proteins are characteristically unstructured as the FG-repeat domains of these proteins adopt a natively unfolded conformation forming intrinsically unstructured flexible filaments that fill the interior of the NPC central channel (Denning et al., 2003; Lim et al., 2006; Denning and Rexach, 2007; Lim et al., 2007; Patel et al., 2007; Lim et al., 2008; Yamada et al. 2010). Positioned here, FG-Nups directly interface with the soluble phase of the nuclear transport machinery, and in concert with nuclear transport factors (NTFs), they facilitate all macromolecular movement through NPCs. Ultimately, the movement of NTF/cargo complexes across NPCs relies upon direct physical interactions between NTFs and FG-repeats (Aitchison et al., 1996; Morianu and Blobel, 1997; Solsbacher et al., 2000; Allen et al., 2001; Ben-Efraim and Gerace, 2001; Gilchrist et al., 2003; Phytia and Rexach, 2003; Wente and

Rout, 2010; Aitchison and Rout, 2012). In particular, the importance of these interactions for nucleocytoplasmic transport was elegantly highlighted in separate studies in which the three-dimensional structure of the NTF Importin-β was solved in complex with FG-containing peptides (Bayliss et al., 2000; Bayliss et al., 2002). From this structural analysis, it was revealed that Importin-β makes direct contacts with phenylalanine residues contained within the sequence of the FG peptides. Moreover, mutating critical amino acid residues within Importin-β that form direct contact sites with FG-repeats not only resulted in reduced binding affinities between Kap and FG-peptide but also negatively affected nuclear import efficiencies *in vivo*, as judged by the localization of an import reporter (Bayliss et al., 2000). These experimental data thus underscore the essential contribution that FG-Nups play in facilitating nuclear transport.

It is predicted that the interactions between NTFs and FG-Nups are cooperative in nature as two to four FG-repeats are thought to bind to a single NTF (Bayliss et al., 2002; Grant et al., 2003; Isgro and Schulten, 2005; Liu and Stewart, 2005). As a single NPC is thought to contain more than 200 FG-Nups per NPC, and each FG-Nup contains anywhere between five and fifty FG repeats, these numbers suggest that there are literally thousands of potential binding sites for a single NTF upon entry into the NPC central channel (Rout et al., 2000; Strawn et al., 2004). Consistent with this, the over abundance of FG-binding sites is reflected in the observation that nearly 50% of the total mass of FG repeats can be deleted without having an impact on cellular viability (Strawn et al., 2004). Moreover, the sporadic dynamics and trajectories of a single molecule moving through the NPC central channel supports the notion that there exist thousands of binding sites for a single transport receptor within the pore (Yang et al., 2004; Kubitscheck et al.,

2005; Yang and Musser, 2006; Tu and Musser, 2011). Ultimately, this densely packed and crowded meshwork of FG-Nups that lines the central channel is necessary for the establishment of an entropic barrier that prohibits macromolecules from freely entering while allowing small molecules such as ions and nucleotides to freely enter.

In addition to their positioning in the NPC central channel, FG-Nups are also situated asymmetrically on cytoplasmic and nucleoplasmic faces of the NPC (Rout et al., 2000; Strawn et al., 2004; Wente and Rout, 2010; Aitchison and Rout, 2012). Arranged with 8-fold symmetry, the so-called cytoplasmic fibrils stretch into the cytoplasm and are thought to play important roles in both the initiation of nuclear import and termination of nuclear export. In yeast, Nup159, Nup82, and Nup49 contribute to the cytoplasmic basket (Kraemer et al., 1995; Hurwitz et al., 1998; Strahm et al., 1999; Rout et al., 2000; Alber et al., 2007). On the nucleoplasmic face reside the FG-Nups, Nup60, Nup2 and Nup1 in budding yeast and Nup153 and Nup50 in mammals (Sukegawa and Blobel, 1993; Guan et al., 2000; Rout et al., 2000; Dilworth et al., 2001). Extending off this face of the NPC are the myosin-like proteins, Mlp1 and Mlp2, that contribute to the nucleoplasmic basket (Kolling et al., 1993; Strambio-De-Castillia et al., 1999). Similar to the interior of the NPC where the FG-meshwork resides, both the nuclear basket and the cytoplasmic filaments are highly flexible and are structurally disordered. Therefore, there is an unvaried theme throughout the NPC in that those regions interfacing with the surrounding environment are relatively disordered and, on a mechanistic level, this disorder throughout the pore is a key physical and mechanical feature necessary for nuclear transport.

### 1.4.4 NPC-associated proteins

An emerging theme in NPC biology is that NPCs act as molecular docking sites for a plethora of functionally diverse proteins that are not considered *bona fide* Nups. In particular, the constituents of the NPC that interact most extensively with the surrounding nuclear and cytoplasmic milieu, namely the nuclear basket and cytoplasmic filaments, serve as physical tethering sites for a panoply of functionally diverse proteins. This interaction network formed at NPCs enables these structures to exert control over a number of cellular activities, while the converse is also true in that the structural and functional properties of the NPC can be directly influenced through their association with non-NPC proteins. In yeast, a clearly documented example of this comes from the cytoplasmic filament component Nup159, which serves as a sequestration site for both dynein light chain, Dyn2, and the DEAD-box RNA helicase, Dbp5 (Weirich et al., 2004; Stelter et al., 2007). In an unusual mechanism, the physical association of Dyn2 with Nup159 is thought to influence the structural properties of the cytoplasmic filaments causing them to become structurally rigid and, thus, inducing their projection outwards from the cytoplasmic face of the NPC (Stelter et al., 2007). Although the functional significance of this observation remains ill defined, this example illustrates how NPC structure, and potentially function, is subject to influence by non-NPC binding partners. In another example, Nup159 aids in the directionality of mRNA export by physically associating with Dbp5, which positions the DEAD-box RNA helicase at a location that enables it to interact with exiting mRNP particles in order to terminate mRNA export (Schmitt et al., 1999; Weirich et al., 2004; Montpetit et al., 2011). In vertebrates, cytoplasmic filaments provide docking sites for the SUMO-ligase UBC9 (Lee et al.,

1997; Saitoh et al., 1997). UBC9 and the cytoplasmic filament constituent Nup358 bind to RanGAP1 and perform several essential functions including mediating the dissociation of exiting NTF/cargo complexes and triggering the release of ribonucleoproteins from exported mRNP particles through UBC9-dependent sumoylation (Bernad et al., 2004; Vassileva et al., 2004).

On the opposite face of the NPC, the nuclear basket functions as a molecular hub for a number of proteins involved in a range of nuclear functions. An apparent unifying theme amongst proteins docked at the nuclear basket is their involvement in regulating some aspect of genomic integrity. For instance, proteins bound to the basket include regulators of mRNA surveillance, chromatin structure, as well as several players that influence chromosome segregation (Reviewed in Strambio-De-Castillia et al., 2010). In yeast, components essential for the nuclear basket are the coiled-coil myosin-like proteins Mlp1 and Mlp2, which are homologous with one another and their mammalian counterpart TPR (Kolling et al., 1993; Strambio-De-Castillia et al., 1999). Tethered to the nucleoplasmic face of the NPC, these proteins form lengthy, unstructured filaments that adopt a tentacle-like conformation. This structural consideration, in addition to their spatial positioning relative to chromatin, is a palatable explanation as to why the nuclear basket is functionally and physically linked to a variety of nuclear processes. For example, in yeast, Mlp2 physically interacts with SPBs, and, positioned there, is directly involved in mediating SPB assembly (Niepel et al., 2005). In an entirely unrelated example, both Mlp1 and Mlp2 are reported to be involved in sub-telomeric gene silencing through an association with yKu70, indicating that the nuclear basket has a direct role in anchoring telomeres to the nuclear periphery (Galy et al., 2000). This observation, plus

others, links the nuclear basket in yeast to telomere organization. Although this specific observation is somewhat controversial, other experimental data point to a role for the nuclear basket in influencing chromatin structure (Hediger et al., 2002a; Hediger et al., 2002b; Texari et al., 2014). Specifically, Mlp1/Mlp2 play a direct role in mediating transcriptional derepression of the *GAL1* gene loci through associating with the SUMO protease Ulp1 (Texari et al., 2014). In an intriguing mechanism, Mlp1/Mlp2 tethers Ulp1 to NPCs where it partakes in desumoylating the transcriptional derepressors Ssn6 and Tup1, leading to their inactivation and subsequent upregulation of *GAL1* transcriptional activity (Texari et al., 2014). In another study, the nuclear basket has been implicated in regulating transcriptional memory by associating with topologically distinct regions of DNA referred to as memory gene loops (MGLs) (Tan-Wong et al., 2009).

The nuclear basket has also been linked to cell-cycle control and chromosome segregation by physically associating with components of the spindle assembly checkpoint (SAC) signaling machinery. Multiple members of the SAC machinery, including Mps1, Mad1 and Mad2, are physically sequestered at NPCs until they are needed at kinetochores (KTs) upon SAC arrest (Campbell et al., 2001; Iuok et al., 2002; Ikui et al., 2002; Liu et al., 2003; Scott et al., 2005; Chi et al., 2008; Katsani et al., 2008; Lince-Faria et al., 2009). The interaction between NPCs and the SAC constituents will be discussed in greater detail in section 1.9.2.

### 1.5 The soluble transport machinery

Nucleocytoplasmic transport is regulated by the NPC through two basic mechanisms: (1) on a physical and structural level, NPCs provide conduits through which

molecules less than 9 nm in diameter can freely diffuse through and (2), through their distinct binding properties, they facilitate the translocation of macromolecules across the NE by directly interfacing with the soluble phase of the nuclear transport machinery. Macromolecules entering or exiting the nucleus rely upon specific amino acid sequences termed nuclear localization signals (NLSs) or nuclear export signals (NESs) that specify either nuclear or cytoplasmic compartmental localization. Recognition of NLS- or NES-bearing cargos and their subsequent translocation through NPCs is mediated by NTFs. The following section discusses the functional elements of the soluble phase of the nuclear transport apparatus.

### 1.5.1 Karyopherins

Stemming from a steadfast effort over the past three decades, the constituent proteins that comprise the soluble phase of the nuclear transport apparatus have largely been characterized. Overall, this effort has resulted in the identification of a conserved family of structurally related mobile transport receptors collectively termed karyopherins (Kaps). In total, 15 Kaps have been identified in yeast and 22 Kaps in vertebrates that specialize in nuclear import (Import Kaps; Importins) or export (Export Kaps; Exportins) (Table 1-2) (Wozniak et al., 1998; Gorlich and Kutay, 1999; Strom and Weis, 2001; Fried and Kutay, 2003; Pemberton and Paschal, 2005; Wente and Rout, 2010). Categorically, the karyopherin family is partitioned into two separate, but functionally related groups on the basis of structural similarity; these include β-Kaps and α-Kaps. Of these groups, the β-Kap family is the largest in the cell as 14 β-Kaps have been identified in yeast and in excess of 20 have been found in higher eukaryotes. There are significantly fewer α-Kaps,

of which one has been identified in yeast (Goldfarb et al., 2004). For the most part, β-Kaps facilitate macromolecular transport by directly binding cargos containing NLSs or NESs and subsequently interacting with the NPC (see Figure 1-2) (Aitchison and Rout, 2010; Wente and Rout, 2012). In a similar fashion, α-Kaps (Kap60 in yeast) directly bind classical NLS (cNLS)-containing cargos and they rely on an interaction with Kap-β (Importin-β1; Kap95 in yeast), which, in turn, binds FG-repeats required for their translocation through the NPC. Thus, Kap-α functions as an adaptor molecule bridging interactions between cNLS-containing cargos and Kap-β (Enenkel et al., 1995; Gorlich et al., 1995; Pemberton et al., 1998; Radu and Blobel, 1995; Goldfarb et al., 2004).

Biochemically, molecules that belong to the β-Kap family are typically acidic in nature and generally fall within a relative molecular mass range of between 95-130 kDa (Strom and Weis, 2001). On the basis of sequence, β-Kaps share minimal homology with each other (< 20% sequence identity) with the exception of the highly conserved amino-terminal Ran binding domain (Gorlich et al., 1997; Wozniak et al., 1998; Strom and Weis, 2001; Fried and Kutay, 2003). However, as alluded to earlier, despite the overall lack of sequence identity, β-Kaps bear significant tertiary structural similarity (Fukuhara et al., 2004; Stewart, 2007). Consistent amongst all β-Kaps whose three-dimensional structures have been elucidated (i.e. Importin-β1, Importin-β2, Crm1 and Cse1), it is apparent that they are built from a series of tandem helical HEAT repeats (Chook and Blobel, 1999; Cingolani et al., 1999; Vetter et al., 1999; Matsuura and Stewart, 2004; Stewart, 2007; Kobayashi and Matsuura, 2013). As a structural entity, the HEAT repeat is a 40 residue long motif that folds into two α-helices containing a short linker sequence (Andrade and Bork, 1995; Strom and Weis, 2001; Stewart, 2007).

**Table 1-2 Karyopherins of yeast and vertebrates**

| *S.cerevisiae* Karyopherin | Vertebrate Karyopherin | Cargo examples: (v)-vertebrate, (sc)-*S. cerevisiae* |
|---|---|---|
| Kap95 | Importin- β1 | Imports via sc-Kap60/v-importin-a adaptor proteins with cNLS; Imports via v-Snurportin the UsnRNPs; with no adaptor, imports v-cargo SREBP-2, HIV Rev, HIV TAT, cyclin B |
| Kap104 | Transportin or Transportin 2 | Imports sc-cargo – Nab2, Hrp1; v-cargo – PY-NLS proteins, mRNA-binding proteins, histones, ribosomal proteins |
| Kap108/Sxm1 | Importin 8 | Imports sc-cargo – Lhp1, ribosomal proteins; v-cargo – SRP19, Smad |
| Kap109/Cse1 | CAS | Imports sc-cargo – Kap60/Srp1; v-cargo – importin as |
| Kap111/Mtr1 | Transportin SR1 or SR2 | Sc-cargos – Npl3, tRNAs<br>v-cargo – SR proteins, HuR |
| Kap114 | Importin 9 | Sc-cargos – TBP, histones, Nap1, Sua7<br>v-cargos – histones, ribosomal proteins |
| Kap119/Nmd5 | Importin 7 | Sc-cargos – Hog1, Crz1, Dst1, ribosomal proteins, Histones |
| Kap120 | HsRanBP11 | Sc-cargos – Rpf1 |
| Kap121/Pse1 | Importin 5/Importin β3/RanBP5 | Sc-cargos – Yra1, Spo12, Ste12, Yap1, Pho4, histones, ribosomal proteins<br>v-cargos – histones, ribosomal proteins |
| Kap122/Pdr6 | - | Sc-cargos – Toa1 and Toa2 TFIIA |
| Kap123 | Importin 4 | Sc-cargos – SRP proteins, histones, ribosomal proteins<br>v-cargos –Transition Protein 2, histones, ribosomal |
| Kap127/Los1 | Exportin-t | Exports tRNAs |
| Kap142/Msn5 | Exportin 5 | Sc-cargos – Imports replication protein A; exports Pho4, Crz1, Cdh1; |
| - | Importin 13 | v-cargos - imports UBC9, Y14; exports eIF1A |
| Crm1/Xpo1 | CRM1/Exportin 1 | Exports proteins with leucine-rich NES, 60S ribosomal subunits (through NMD3 adaptor), 40S ribosomal |
| - | Exportin 4 | imports SOX2, SRY; exports Smad3, eIF5A |
| - | Exportin 6 | Exports profilin, actin |
| - | Exportin 7/ RanBP16 | Exports p50-RhoGAP |

*Adapted from Wente and Rout, 2010.

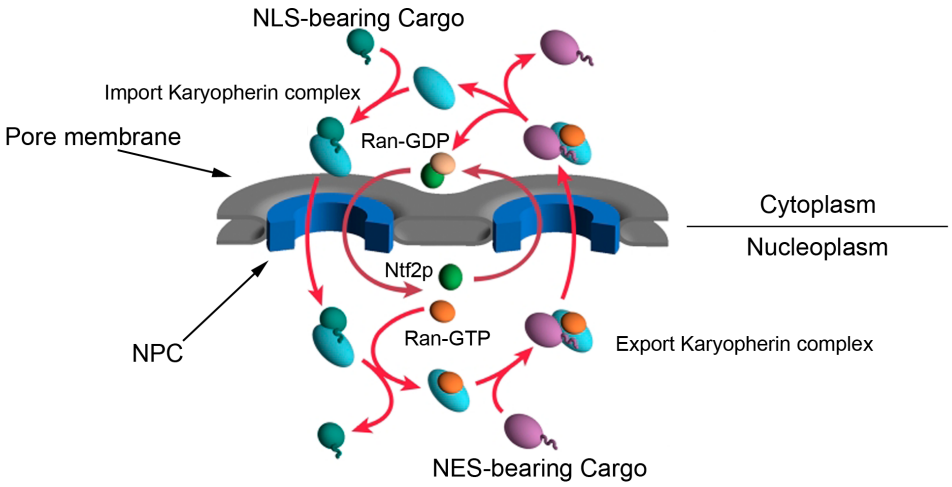


**Figure 1-2. The nuclear transport cycle for import and export Kaps.** Nuclear import is initiated in the cytoplasm through importin-mediated recognition of cargos bearing NLSs. Following the assembly of the Kap/cargo complex in the cytoplasm, translocation of this complex through the NPC is facilitated by low-affinity interactions between import Kaps and FG-Nups that line the NPC central channel. Upon entry into the nuclear interior, the incoming Kap/cargo complex encounters RanGTP, and subsequent binding leads to the dissociation of the import complex appropriately in the nucleoplasm. In the opposing direction, nuclear export is initiated through exportin-mediated recognition of cargos with exposed NESs. Conversely, RanGTP binding to the export Kap/cargo complex in the nucleoplasm enhances the affinity between Kap and NES-containing cargo and the resulting trimeric complex is exported out of the nucleus. As the trimeric complex enters the cytoplasm, RanGAP (Ran GTPase activating protein) is encountered, and subsequent binding stimulates GTP hydrolysis by Ran leading to the dissociation of the export Kap/cargo complex. Adapted from Aitchison and Rout, 2012.

In β-Kap structure, successive HEAT repeats are joined together and stack upon each other creating a polypeptide with a right-handed, superhelical twist. Intriguingly, this structural feature bears resemblance to the helix-turn-helix motifs possessed by core scaffold Nups and raises the possibility that Kaps may have diverged from a common structural entity involved in both the stationary and soluble phase of the transport apparatus (Wente and Rout, 2010).

A key biophysical feature of HEAT repeats is that they allow for significant structural flexibility (Stewart, 2007). Molecular elasticity is key for β-Kap function as it endows these molecules the ability to interact with a plethora of structurally varied molecules including diverse cargo sets, Nups, and Ran (Stewart, 2007). Consistent with this, structural analysis of Importin-β reveals this molecule contains nineteen successively arranged HEAT repeats forming an elongated helicoidal molecule that resembles a tightly wound spring (Cingolani et al., 1999; Lee et al., 2003; Lee et al., 2005; Liu and Stewart, 2005; Stewart, 2007). From this, slight changes in individual HEAT repeat positioning can cumulatively result in substantial changes to the helical pitch of the entire molecule enabling significant structural malleability. As such, changes in helical pitch in Importin-β are observed depending on its functional state, i.e. whether it is in complex with cargos, Nups, or RanGTP (Chook and Blobel, 1999; Bayliss et al., 2000; Lee et al., 2003; Lee et al., 2005; Liu and Stewart, 2005; Stewart, 2007).

### 1.5.2 Nuclear signal sequences

The most basic requirement for a macromolecule to translocate through the NPC is the presence of a specialized signal sequence that facilitates their association with the

soluble phase of the nuclear transport apparatus. These signal sequences, termed NLSs or NESs are topogenic sequence determinants that ultimately influence the compartment in which proteins bearing these signal motifs will reside. Proteins harboring NESs are destined for nuclear export, while the presence of an NLS facilitates macromolecular movement into the nucleus (Figure 1-2).

In general, there are varied flavors of NLSs. The cNLS, for instance, is a characteristically short amino acid residue sequence (KKKRK) recognized by the Kap α/β heterodimer (Fried and Kutay, 2003; Goldfarb et al., 2004; Wente and Rout, 2010). Many proteins also contain more complex bi-partite NLSs consisting of two separate clusters of basic residues spaced by approximately ten amino acid residues (Dingwall et al., 1988; Wente and Rout, 2010). However, despite these classifications, certain signal sequences exhibit degeneracy that enables a single cargo to, in some cases, interact with multiple Kaps. A prime example of this comes from the analysis of nuclear import of the histone proteins H2A and H2B in yeast where multiple Kaps, including Kap121, Kap95 and Kap114, bind to the same NLS and cooperatively mediate the import of these molecules into the nucleus (Mosammaparast et al., 2001). Another example arises from the ability of both Kap121 and Kap104 to recognize an arginine- and glycine- rich NLS (RG-NLS) found in the nucleolar protein Nop1 (Leslie et al., 2004). In this case, both Kap104 and Kap121 can functionally substitute for each other and both Kaps can import Nop1 into the nucleus. This observed redundancy in cargo recognition is a likely explanation for why loss-of-function of some Kaps results in lethality while others do not (Wozniak et al., 1998; Jans et al., 2000).

### 1.5.3 Ran

As a key regulator of β-Kap/cargo interactions, the small GTPase Ran is an integral component of the soluble nuclear transport machinery (Gorlich and Kutay, 1999; Macara, 2001; Weis, 2003; Fried and Kutay, 2003). While NPCs and Kaps provide the physical basis for nucleocytoplasmic transport, Ran provides the spatial cues that drive the formation/dissociation of import and export complexes in the appropriate compartments. Ran establishes a precipitous potential energy gradient across the NE, and in doing so, provides an energy source for the nuclear transport cycle. The establishment of this steep energy gradient across NPCs is achieved through the orchestrated activities of a variety of proteins. Among these is the small nuclear transport factor Ntf2 whose primary cellular duty is to mediate the trafficking of Ran through NPCs and into the nucleoplasm (see Figure 1-2) (Ribbeck et al., 1998; Smith et al., 1998). Although Ntf2 function is limited to importing a single cargo into the nucleus, it is estimated that millions of Ran molecules are imported into the nuclear compartment every minute in actively dividing cells as a result of Ntf2 activity (Gorlich and Kutay, 1999; Mattaj and Englmeier, 1998). Constitutive Ntf2-mediated transport contributes to the generation of a nuclear environment that is Ran-rich relative to the surrounding cytoplasm and estimates suggest that there is approximately a 500 fold difference between nuclear and cytoplasmic compartments (Kalab et al., 2002; Gorlich et al., 2003; Weis, 2003). Therefore, through this seemingly one-dimensional activity, Ntf2 plays an incredibly important role in establishing the Ran gradient within cells.

Other factors paramount for the establishment of the Ran gradient include the conserved nucleotide exchange factor RanGEF (Prp20 in yeast and RCC1 in vertebrates)

and the RanGTPase activating protein RanGAP (Rna1 in yeast and RanGAP1 in vertebrates) (Ohtsubo et al., 1989; Bischoff and Ponstingl, 1991; Bischoff and Ponstingl, 1995). RanGEF, which is housed within the nuclear interior and tethered to chromatin through an interaction with histone proteins H2A and H2B, functions to convert Ran into its GTP bound form thus contributing to the formation of a nuclear environment rich in RanGTP (Bischoff and Ponstingl, 1991; Nemergut et al., 2001). In order to accommodate for the huge flux of Ran into the nucleus, RanGEF is highly abundant and estimates suggest that this protein is present in up to one copy per nucleosome (Dasso et al., 1992). On the opposite side of the NE, the cytoplasmic pool of Ran is maintained in its GDP bound form through the activity of RanGAP, which, while tethered to Nup358/RanBP2, functions to stimulate the intrinsic GTPase activity of Ran resulting in GTP to GDP conversion (Matunis et al., 1996; Mahajan et al., 1997; Saitoh et al., 1997). Therefore, in concert with the transport activity of Ntf2, the spatial partitioning of these regulatory factors is what allows Ran to be maintained predominantly in its GDP bound form in the cytoplasm and GTP bound form in the nucleoplasm. The resulting biochemical variation between compartments provides the necessary biochemical gradient required for spatial directionality of nucleocytoplasmic transport.

The RanGTP gradient ultimately modulates nuclear transport by regulating the formation and disassembly of nuclear transport complexes in the appropriate compartments (Gorlich and Kutay, 1999; Macara, 2001; Weis, 2003; Fried and Kutay, 2003). Import Kap/cargo complexes are stable in the presence of RanGDP, and can, therefore efficiently assemble in the cytoplasm. However, as import complexes traverse NPCs and enter the nuclear interior, they encounter RanGTP. RanGTP binding leads to a

conformational change in the Kap that results in cargo release within the nuclear compartment (Figure 1-2). In contrast, nuclear export complexes form within the nuclear interior together with RanGTP (Fornerod et al., 1997). The resulting trimeric complex (Kap/Cargo/Ran) transits through the pore and is subsequently disassembled upon entry into the cytoplasm through RanGAP activity leading to cargo release in the cytoplasm.

#### 1.5.3.1 Mitotic Ran functions

In addition to regulating transport directionality, Ran also influences a multitude of mitotic processes including mitotic spindle assembly and post-mitotic NPC re-assembly (Dasso, 2002; Clarke and Zhang, 2009). Early clues of Ran's involvement in spindle formation/dynamics came from a basic set of experiments where the levels of RanGTP were artificially altered in *Xenopus* egg extracts. Decreased RanGTP levels resulted in low spindle density, as where the overproduction of RanGTP resulted in unregulated microtubule (MT) proliferation (Zhang et al., 1999; Wilde et al., 2001; Carazo-Salas et al., 2001). Later work revealed that these observed effects were largely attributed to a spatially confined biochemical gradient of RanGTP in the immediate vicinity of chromatin, a consequence of chromatin-localized Ran-GEF activity (discussed above). In fact, experiments using fluorescence resonance energy transfer (FRET) reporters of RanGTP demonstrated that this molecule effectively forms a dense "biochemical cloud" that directly surrounds chromatin in the absence of an intact NE (Caudron et al., 2005). Although RanGTP does not participate directly in spindle assembly or post-mitotic NPC re-assembly, this region of concentrated RanGTP surrounding chromatin functions as a spatial release mechanism that allows for the

dissociation of inhibitory Importin-β complexes in the immediate vicinity of mitotic chromosomes (Gruss et al., 2001; Nachury et al., 2001; Wiese et al., 2001; Clarke and Zhang, 2009). For example, Importin-β binds to multiple spindle assembly factors (SAFs) in the cytoplasm and functions to negatively regulate their activity by inhibiting their association with microtubules (MTs) (Kalab and Heald, 2008; Clarke and Zhang, 2009). These inhibitory interactions are relived once Importin-β/SAF complexes encroach upon regions surrounding mitotic chromosomes where RanGTP concentrations are highest. RanGTP-mediated dissociation of these complexes thus enables SAFs to participate in spindle assembly in a spatially regulated manner (discussed in greater detail below; section 1.7.2).

The spatially confined RanGTP gradient surrounding chromosomes also plays a pivotal role in directing post-mitotic NE and NPC reassembly through a mechanism similar to that described above. Following NPC disassembly at the onset of mitosis, Importin-β binds to specific Nup subcomplexes and functions as an inhibitor of Nup-Nup interactions required for the formation of higher order Nup assemblies (Zhang et al., 2002; Walther et al., 2003a; D'Angelo et al., 2006; Guttinger et al., 2009; Clarke and Zhang, 2009). One Nup subcomplex that is regulated in this manner is the Nup107-160 complex. During late mitosis, Nup107-160 complexes assemble on decondensing chromatin where they form 'pre-pore' structures from which NPCs are formed. Importin-β binding to Nup107-160 functions to prevent these Nup assemblages from seeding NPC re-assembly until such an association is relieved through RanGTP binding near chromatin at the end of mitosis (Walther et al., 2003a; Walther et al., 2003b; D'Angelo et al., 2006). In addition, RanGTP is also required for post-mitotic NE re-assembly, as NE vesicle

fusion on the surface of chromatin is severely compromised following immunodepletion of Ran (Hetzer et al., 2000).

### 1.6 Nuclear transport models

Despite the accumulated and vast knowledge acquired on both functional and structural aspects of the nuclear transport apparatus, molecular details regarding the mechanism of translocation through the NPC central channel largely remain elusive. Resultantly, various hypotheses have been proposed to help explain, on a mechanistic level, how the biophysical properties of the NPC contribute to the establishment of a highly selective barrier that allows the passage of some molecules while excluding others. To help shed light on the minutiae of this process, several investigators in the field have put forth models to help explain the intricacies of this process, and these models are briefly described in the following sections.

#### 1.6.1 The Selective Phase

The selective phase model, proposed by Ribbeck and Gorlich, posits that the interior of the central channel is a meshwork of interconnected FG-Nups creating a hydrophobic barrier or, “selective phase”, that functions to repel large hydrophilic molecules while selectively “solvating” molecules that have an affinity for the hydrophobic meshwork. Therefore, the biophysical nature of the matrix established by FG-repeats allows molecules with affinity for the meshwork, like Kaps, to locally disrupt regions and penetrate into the channel. The primary tenet of this model is largely supported by observations suggesting molecular trafficking through the NPC central

channel appears to be largely non-directional and energy independent (Nakielny and Dreyfuss, 1998; Ribbeck et al., 1998; Schwoebel et al., 1998; Englmeier et al., 1999; Nachury and Weis, 1999; Wente and Rout, 2010). Moreover, the NPC permeability barrier can effectively be disrupted with aliphatic alcohols thereby suggesting that the central channel may be comprised entirely of hydrophobic interactions (Ribbeck and Gorlich, 2002). Although the selective phase model puts forth a satisfactory mechanism for import, it fails to explain how transport directionality is established once Kap/cargo complexes infiltrate the hydrophobic FG matrix (Bickel and Bruinsma, 2002).

### 1.6.2 The Virtual Gate

The virtual gate model, as proposed by Rout and colleagues, puts forth the proposition that the vast majority of molecules encountered by NPCs are rejected from entering the central channel due to an entropic barrier (Rout et al., 2000; Rout et al., 2003). This model predicts that the flexible disordered regions of FG-Nups that pack the central channel and emanate from either face of the NPC effectively function as a physical repellent by brushing away molecules that fail to establish an interaction with them. Due to both the biophysical nature and spatial organization of the FG-Nups, they function to increase the entropic barrier imposed by the NPC. However, at the same time, the FG-regions that extend into either compartment act as a sink to concentrate Kap/cargo complexes at either entry point to the NPC. After an interaction is established between FG-Nup and Kap, the entropic barrier is overcome and the Kap/cargo complex can passage through the central channel. This model is supported by the observation that the physical nature of FG-Nups are altered upon Kap binding in that the flexible and

extended polymeric state of these Nups become less rigid and eventually collapse upon forming contacts with Kaps (Denning et al., 2003; Lim et al., 2006; Lim et al., 2007). Once partitioned into the NPC central channel, the model proposes that vectorial translocation of Kap/cargo complexes is accomplished through Brownian motion (Rout et al., 2000; Rout et al., 2003).

### 1.6.3 The Affinity Gradient

Transport rates across the NE have been estimated at approximately 100 MDa/sec and 1,000 translocation events/sec per individual NPC (Ribbeck and Gorlich, 2001). In order to accommodate for this gargantuan flux of molecules, both the selective phase and virtual gate models rely on the idea that interactions between Kaps and FG-Nups are weak in nature (Bayliss et al., 1999; Ribbeck and Gorlich, 2001; Bayliss et al., 2002). However, these models are somewhat flawed in that there exists experimental evidence to suggest that there are quantifiable differences in the affinities of various Kap/Nup interactions. Moreover, there is an observable increase in binding affinities from the cytoplasmic filaments to the nuclear basket (Ben-Efraim and Gerace, 2001; Phytia and Rexach, 2003). Therefore, the affinity gradient model incorporates these differences in Kap-Nup binding affinities and suggests that Kaps are guided through the NPC central channel by a gradient of increasingly strong interactions along their path.

## 1.7 Alternative Kap functions

As an increasingly thorough understanding of Kap structure/function has emerged, so to has a body of evidence implicating a number of Kaps as key regulators of

processes outside of nuclear transport. A variety of studies, spanning a range of disciplines, has revealed that several Kaps confer the ability to function as either positive or negative regulators of a diverse array of cellular activities ranging from ciliary transport at the apical membrane of epithelial cells to influencing mitotic spindle and NPC assembly following NE breakdown during mitosis. The following section focuses on the transport-independent duties performed by Kaps across evolutionarily divergent species.

### 1.7.1 Cytoplasmic Kap functions

In vertebrates, Importin-β1 and Importin-β2 have been shown to participate in a diverse range of cytoplasmic tasks (Twyffels et al., 2014). Perhaps the best-characterized example among these is the role of Importin-β2 possesses in actively targeting various factors to discrete cytoplasmic structures termed cilia. Primary cilia are MT-based, membrane-sheathed projections that emanate from most eukaryotic cells where they perform a variety of chemosensory functions depending on cell type (Yuan and Sun, 2013). As these structures form distinct compartments separable from the rest of the cytoplasm and have a distinct proteomic composition, a specialized transport system is required to deliver various cargos to these localized assemblies. In a mechanism that parallels nucleocytoplasmic transport, the directed targeting of the Kinesin-2 motor protein KIF17 to these cytoplasmic locales requires the activity of Importin-β2 (Dishinger et al., 2010; Gruss, 2010). Binding of Importin-β2 to KIF-17 is contingent upon a highly basic ‘NLS-like’ sequence termed a ciliary localization signal (CLS), and the dissociation of this complex occurs in a RanGTP-dependent manner. Consistent with

this, RanGTP is concentrated within the ciliary compartment and is necessary for the accumulation of KIF-17 within these cytoplasmic structures. In addition to targeting KIF-17, Importin-β2 is also involved in delivering the retinitis pigmentosa 2 (RP2) protein to cilia, which is a finding that has disease relevance as certain human ciliopathies have been linked to the inability of RP2 to target to this cellular compartment (Hurd et al., 2011).

In addition to functioning as cytoplasmic targeting factors, β-Kaps also possess the ability to act as chaperones within the cytoplasmic compartment. The ability of Kaps to function in a chaperone-like manner is largely attributed to their inherent affinity for basic amino acid sequence. As highly basic proteins such as histones and ribosomal proteins are translated, they are susceptible to aggregation due to non-specific inter- and intra- molecular interactions (Young et al., 2004). Chaperones function to suppress aggregate formation by binding hydrophobic or basic sequences shielding these regions from the surrounding environment and, thus, inappropriate interactions. In an intriguing example in mammalian cells, Importin-β binds the basic histone protein, Histone-H1, during its translation to effectively preclude its aggregation in the cytoplasm (Jakel et al., 2002). Importin-β was also shown to bind the ribosomal proteins rpS7 and rpL18a to keep these proteins soluble in the cytoplasm prior to their interaction with nucleic acids. These examples therefore represent a general mechanism for Importin-β in the cytoplasm in its ability to confer a chaperone-like function.

As well as preventing aggregate formation, Kaps can also function to inhibit non-specific interactions between proteins and lipid membranes. For example, in yeast, the import Kap, Kap123, binds the monotopic membrane protein, Nbp1, during its translation

and functions to specifically inhibit its inappropriate incorporation into cytoplasmic membranes (Kupke et al., 2011). Nbp1 is an essential SPB constituent that possesses an amphipathic α-helix required for its membrane binding and insertion (Winey et al., 1991, Winey et al., 1993; Schramm et al., 2000; Araki et al., 2006; Kupke et al., 2011). This membrane-binding domain facilitates the efficient incorporation of the entire SPB into the NE. As Nbp1 is translated in the cytoplasm, Kap123 binds the NLS sequence directly adjacent to the amphipathic α-helix and masks the association of this motif with non-specific cytoplasmic membranes. It is not until the Kap123/Nbp1 complex is dissociated in the nucleus that Nbp1 is allowed to interact with membranes, thereby incorporating into the NE and eventually into SPBs.

There also exists evidence to suggest members of the β-Kap family may act as MT adaptor proteins in the cytoplasm. Over the years, several independent observations have revealed that a variety of cargos utilize MTs as a means of transport into the nucleus. In one example, the small hormonal protein PTH-HrP binds tubulin in the cytoplasm and requires intact MTs for its efficient import into the nucleus (Lam et al., 2002). The efficient association of PTH-HrP with MTs depends upon Importin-β and disrupting MTs with nocodazole effectively blocks the import of this molecule into the nucleus. In a similar example, in neuronal cells, Importin-β has also been implicated in facilitating retrograde transport of NLS-containing axoplasmic proteins in response to cell injury (Hanz et al., 2003). As part of the injury response, Importin-β binds NLS-bearing axonal signals and facilitates their transport to the cell body along MTs in a dynein-dependent mechanism.

In addition to these MT-related functions in the cytoplasm, several Kaps target to RNA stress granules (SGs) and, here, are thought to influence both the assembly and metabolism of these dynamic structures (Chang and Tarn, 2009; Fujimura et al., 2010; Mahboubi et al., 2013). In HeLa cells, Importin-α is recruited to SGs following arsenite treatment, and loss of Importin-α function under these conditions impacts the dynamic assembly of these structures, thereby influencing the survivability of these cells following this induced stress scenario. This led the authors to conclude that Importin-α plays an active role in SG assembly and formation (Mahboubi et al., 2013). In another example, Importin-β2 was found to localize to both processing bodies (P-bodies) and SGs where it was proposed this Kap functions to deliver various cargos to these cytoplasmic structures, including various RNA binding proteins like TTP, thus contributing to SG and P-body metabolism (Chang and Tarn, 2009).

### 1.7.2 Kaps, chromatin and mitosis

Over the last decade or so, an increasing number of observations has revealed the intricate and nuanced interplay between Kaps and the mitotic apparatus. The proper execution of a number of fundamental mitotic processes, ranging from NPC re-assembly to the targeting of mitotic factors to various structures that comprise the spindle apparatus, depends upon the functionality of several Kaps. Perhaps the best defined example of this is the role conferred by Importin-β in directing spindle assembly. Upon the onset of mitosis, Importin-β adopts a general inhibitory role and specifically interferes with the activities of a number of proteins that promote spindle assembly, known as spindle assembly factors (SAFs) (Gruss et al., 2001; Nachury et al., 2001; Wiese et al.,

2001; Kelab and Heald, 2007; Clarke and Zhang, 2009). Importin-β binding, through NLS-dependent recognition, prevents these proteins from inappropriately associating with MTs, thereby suppressing MT polymerization and thus spindle formation. This inhibitory interaction is eventually overcome by RanGTP binding, an event that is spatially restricted to regions immediately surrounding chromatin. The spatially and temporally coordinated release of SAFs from Importin-β in the vicinity of chromatin provides the molecular explanation as to why mitotic MT nucleation is restricted to the regions directly surrounding mitotic chromosomes (Clarke and Zhang, 2009).

A specific example of a SAF whose activity is negatively regulated by Kap binding is TPX2, which, when released from Importin-α/β, promotes MT polymerization and Aurora-A activation at the early stages of mitosis (Gruss et al., 2001). In another example, Importin-β has been shown to inhibit the MT-nucleating proteins HURP and NuSAP, which, when released by RanGTP, participate in cross-linking spindle MTs and thus contribute to the establishment of proper kinetochore (KT)-MT interactions (Koffa et al., 2006; Sillje´ et al., 2006; Ribbeck et al., 2007). Notably, the NE protein lamin-B, which makes structural contributions to the spindle matrix, is another protein whose function is negatively regulated by Importin-α/β (Tsai et al., 2006; Adam et al., 2008). Following nuclear envelope breakdown (NEBD), lamin-B assembles into the fibrous spindle matrix required for tethering SAFs and SAC proteins during mitosis. It is thought that Importin-α binds lamin-B and prevents it from polymerizing into the spindle matrix during interphase. Following NEBD, Ran binding relieves this inhibitory interaction allowing for the formation of the spindle matrix. The multitude of regulatory functions exerted by Importin-β is a likely explanation as to why ectopic overproduction of

Importin-β yields a plethora of spindle defects ranging from the formation of multi-polar spindles to errors in mitotic chromosomal alignment (Ciciarello et al., 2004; Roscioli et al., 2012).

In addition to exerting an inhibitory role required for spatio-temporal control of spindle assembly, Kaps also possess the ability to target specific mitotic factors to chromatin. In vertebrates, a key regulatory factor involved in delivering a number of mitotic effectors to KTs is the nuclear export factor Crm1/Xpo1 (Arnaoutov et al., 2005; Zuccolo et al., 2007; Roscioli et al., 2012). Normally involved in exporting proteins bearing leucine rich NESs during interphase, Crm1 adopts an essential mitotic function through its Ran-dependent KT targeting activities (Fornerod et al., 1997; Fukuda et al., 1997; Ossareh-Nazari et al., 1997; Stade et al., 1997; Arnaoutov et al., 2005; Zuccolo et al., 2007; Torosantucci et al., 2008). Among the proteins recruited to KTs in a Crm1-dependent manner are RanBP2 and RanGAP1 (Arnaoutov et al., 2005). At KTs, these proteins contribute to K-fiber integrity and, thus, the establishment of stable KT-MT interactions during mitosis. Consistent with this, Crm1 is also involved in delivering three chromosomal passenger complex (CPC) members to KTs including Aurora B, Borealin, and INCENP, where they directly associate with centromeric complexes (Knauer et al., 2006). A fraction of Crm1 has also been found in association with centrosomes where it is involved in the duplication of these structures as well as recruiting factors required for spindle assembly including pericentrin, γ-tubulin and B23 (Liu et al., 2009; Rousselet, 2009).

In yeast, the Crm1 homolog, Xpo1 confers mitotic activities similar to those of its mammalian counterpart. In actively cycling cells, Xpo1 is found localized at SPBs

throughout the cell cycle (Neuber et al., 2008; Scott et al., 2009). However, following nocodazole-induced metaphase-arrest, Xpo1 redistributes from SPBs to unattached KTs. In transiting between nuclear structures, it was uncovered that Xpo1 functions to target the SAC signaling protein Mad1 to detached KTs during SAC arrest (Scott et al., 2009). Xpo1-mediated KT targeting of Mad1 occurs in a manner analogous to the formation of nuclear export complexes in that Xpo1 recognizes and binds an NES contained within Mad1's sequence. This results in the formation of a heterotrimeric complex containing RanGTP, Xpo1, and Mad1. Consistent with this, disrupting Mad1's NES, blocking Ran activity, or inhibiting Xpo1 with leptomycin B attenuates the ability of Mad1 to target to unattached KTs and to dynamically cycle between binding sites at NPCs and KTs (Scott et al., 2009).

In yeast, the ability of Kaps to participate in subnuclear targeting events is not exclusively limited to export Kaps, as there are examples where nuclear import factors partake in targeting various factors to locations within the nucleus. A noteworthy example of this is the non-essential import Kap, Kap114, which is involved in delivering and depositing the transcription initiation factor Tbp1 (TATA-binding protein) to TATA-containing promoter sequences (Pemberton et al., 1999). Import of Tbp1 requires the activity of Kap114; however, upon entry into the nucleus, Tbp1 remains associated with Kap114, as this interaction is biochemically resistant to RanGTP-mediated dissociation. Intriguingly, the dissociation of this complex and subsequent deposition of Tbp1 onto chromatin require the concerted binding of both RanGTP and dsDNA containing TATA sequence. In an analogous example, a similar mechanism has also been proposed for another yeast import receptor, Kap104, as its ability to release the RNA binding protein

Nab2 within the nuclear interior requires the presence of RNA as well as RanGTP (Lee and Aitchison, 1999).

### 1.8 Nuclear transport regulation

Housed within the nucleus is a complex and dynamic biochemical environment that is subject to alterations in response to a variety of physiological stimuli. Fine-tuning the biochemical composition of the nuclear milieu can be achieved with rapid kinetics by controlling the flux of molecules both into, and out of, the nucleus through regulated changes to nuclear transport. Orchestrated alterations to nucleocytoplasmic transport can be executed through two separate mechanisms, including (1) regulating access of a given Kap to its cognate cargos and (2) regulating transport at the NPC by modulations to Kap-Nup interactions. In the next section, these two distinct transport regulatory mechanisms will be discussed briefly, with emphasis on these mechanisms functioning during mitosis.

#### 1.8.1 Transport regulation through alterations to Kap-cargo interactions

The most basic transport regulatory mode involves post-translational modifications to an NLS or NES contained within a cargo molecule. Like most protein-protein interactions, Kap-cargo binding affinities can be manipulated through post-translational modifications. Modifications such as phosphorylation, sumoylation, and, in some cases, methylation can result in enhanced or inhibited interactions between Kap and cognate cargos (Kaffman and O'Shea, 1999; Madison et al., 2002; Pichler and Melchior, 2002). There are many documented examples of this mode of transport regulation and they often occur in response to a variety of physiological changes. For example, the

subcellular distribution of the cell cycle regulator, Cdh1, is controlled through its interaction with two separate Kaps, the importin, Kap121, and the exportin, Msn5 (Jaquenoud et al., 2002). The latter of the two interactions is governed by Cdk1-dependent phosphorylation. During the G1-phase of the cell cycle, Cdh1 accumulates in the nucleus where it regulates mitotic-cyclin levels. As cells enter S-phase, Cdk1 phosphorylates Cdh1, stimulating Msn5 binding and export from the nucleus. Cdh1 remains excluded from the nuclear compartment until the end of mitosis at which point it is dephosphorylated and again accumulates in the nucleus (Jaquenoud et al., 2002). In vertebrates, a similar transport regulatory mechanism is observed for cyclin-B1, which is excluded from the nucleus throughout interphase until re-accumulating in the nuclear compartment just prior to the start of mitosis. Nuclear exclusion during interphase is mediated through Crm1-dependent export, and cell-cycle-dependent phosphorylation of cyclin-B1 prevents its association with Crm1, thus enabling its import into the nucleus at the start of mitosis (Yang et al., 1998).

In addition to post-translational modifications, Kap-cargo interactions can be fostered or inhibited by changes in protein-protein interactions between members of a complex that lead to either the exposure or burial of a transport signal. For example, in mammalian cells, the transcription factor p53 contains an NES within its sequence that overlaps with a domain required for its tetramerization (Stommel et al., 1999). In response to certain cellular stimuli, p53 forms a tetramer that enables it to bind DNA and activate a variety of transcriptional programs. The resulting tetramerization masks the NES contained within p53, and the complex is thus blocked from interacting with the

nuclear export factor Crm1. This enables p53 to remain nuclear and bound to chromatin to promote transcriptional activation.

### 1.8.2 NPC-mediated transport regulation

The physical dimensions of the NPC central channel are not fixed but rather are subject to size-dependent alterations in response to physiological stimuli (Feldherr and Akin, 1993). In analyzing the physical properties of NPCs in quiescent versus actively growing mammalian cells, it was shown that the apparent size of the NPC central channel was quantifiably larger in actively growing cells as compared to quiescent cell populations (Feldherr and Akin, 1993). Consistent with this, these cells also exhibited significant differences in NPC permeability throughout the cell cycle, suggesting that the physical properties of NPCs can be modulated, presumably to elicit specific physiological responses (Feldherr and Akin, 1993; Feldherr and Akin, 1994). These observations ultimately led to the hypothesis that regulated changes to the structure of NPCs could regulate nuclear transport events. However, in these studies, the underlying molecular mechanisms governing these regulated changes were not clearly defined.

It was not until a study in budding yeast that precise mechanistic insights were gained and specific molecular details emerged on how physical changes within NPCs can function to modulate nuclear transport pathways in organisms that undergo closed mitoses (Makhnevych et al., 2003). From this work, it was determined that the transport properties of NPCs could be altered in order to specifically inhibit the flux of Kap121 into the nucleus following metaphase arrest. Specifically, the inhibition of Kap121-mediated transport was driven by localized molecular rearrangements within the Nup53-

containing subcomplex of the NPC. This mechanism is contingent upon the unique biochemical properties of Nup53 which, within its sequence, contains a high affinity-binding site specific for Kap121 (Lusk et al., 2002; Makhnevych et al., 2003). This domain, termed the Kap121-binding domain (KBD), resembles a Kap121-specific NLS, which is masked in cycling cells through an interaction with its neighboring binding partner Nup170 (Lusk et al., 2002; Makhnevych et al., 2003). Under these conditions, the KBD is inaccessible to Kap121. However, under conditions of nocodazole-induced metaphase-arrest, molecular rearrangements occur within the NPC that lead to the exposure of the KBD thereby allowing binding to Kap121 and inhibiting the entrance of this Kap, and its cargo, into the nuclear interior. Transport arrest is specific to Kap121 as transport mediated by other Kaps was largely unaffected. This study, for the first time, revealed, on a mechanistic level, how the NPC can alter its structural properties to control transport events in response to a particular stimulus.

### 1.9 Mitotic NPC functions

As components of the nuclear transport apparatus have become increasingly well defined on both structural and functional fronts, mounting evidence has accumulated linking numerous components of the nuclear transport machinery to processes outside of nuclear transport. In fact, a burgeoning field of study has emerged investigating the intertwined functional relationship between NPCs and various components of the mitotic apparatus. The mitotic functions revealed for Nups are diverse in nature ranging from influencing aspects of KT function, including K-fiber formation during spindle assembly,

to contributing to the robustness of SAC signaling at the early stages of metaphase. In the following section, the details of this emerging field of study are discussed.

### 1.9.1 Nups and chromosome segregation

One of the earliest observations linking nucleoporin function to chromosome segregation came from a chromosome transmission fidelity screen (*ctf*-) performed in yeast to identify genes encoding proteins that contribute to KT function. From this genetic analysis, a core structural component of the NPC, Nup170, was identified as a determinant of both KT integrity and, thus, chromosome segregation (Kerscher et al., 2001). Although Nup170 could not be detected in physical association with centromeric DNA, cells lacking Nup170 yielded significant chromosome loss phenotypes as well as transcriptional read-through defects at the centromere, suggesting that the integrity of the centromeric chromatin, and potentially KT structure, is compromised.

In higher eukaryotes, the functional interrelationship between Nups and chromosome segregation is more clearly defined. This may, in part, be attributed to significant morphological differences between yeast and vertebrate mitoses. As vertebrate cells enter the early stages of mitosis, nuclear envelope breakdown (NEBD) is initiated and NE membranes are disassembled. In synchronicity with NEBD, NPCs are reversibly disassembled and individual Nups and Poms, or subcomplexes of these, redistribute to the cytoplasm and ER (Terasaki et al., 2001; Burke and Ellenberg, 2002; Hetzer et al., 2005; Terry et al., 2007; Dultz et al., 2008; Guttinger et al., 2009; Imamoto and Funakoshi, 2012). In addition to this general redistribution pattern, certain Nup subcomplexes also bind various mitotic structures. For instance, the evolutionarily

conserved Nup107-160 complex (yeast Nup84 complex), a subcomplex required for NPC assembly (D'Angelo et al., 2006), has been found in association with multiple mitotic structures including centrosomes, the minus ends of spindle MTs, and KTs (Belgareh et al., 2001; Boehmer et al., 2003; Loiodice et al., 2004; Orjalo et al., 2006; Zuccolo et al., 2007). Positioned at these mitotic assemblies, the Nup107-160 complex is involved in regulating multiple tasks.

In particular, the Nup107-160 complex confers an important functional role in regulating KT-MT interactions during mitosis. Following NEBD, a fraction of the Nup107-160 subcomplex targets to unattached KTs in a manner dependent upon the KT proteins Ndc80 and CENP-F (Zuccolo et al., 2007). Loss of Nup107-160 KT binding affects chromosome alignment on the metaphase plate and results in defects in mitotic progression (Zuccolo et al., 2007). Consistent with this observation, this Nup-subcomplex also interacts with the γ-tubulin ring complex (γ-TuRC) and is involved in recruiting this MT-nucleating complex to mitotic KTs (Mishra et al., 2010). Through this activity, the Nup107-160 complex plays an important functional role in regulating proper K-fiber formation, which is necessary for the establishment of proper KT-MT interactions during spindle assembly.

While at KTs, the Nup107-160 complex is also involved in mediating the targeting of other nuclear transport factors and Nups to KTs including Crm1, RanGAP1 and Nup358 (Arnaoutov et al., 2005; Zuccolo et al., 2007). Cellular depletion of the Nup107-160 complex significantly reduces the amounts Crm1, RanGAP1 and Nup358 at unattached KTs, suggesting that this Nup subcomplex acts as a scaffolding surface on KTs. The reliance of Nup107-160 for RanGAP1 and Nup358 KT targeting has significant

functional implications, as RanGAP1/Nup358 are involved in recruiting other KT components to these assemblies, including CENP-E, CENP-F, and the SAC effectors Mad1 and Mad2 (Joseph et al., 2004).

### 1.9.2 KT proteins at NPCs

Nups bind KTs. The reciprocal is also true as KT proteins associate with NPCs. For instance, the KT component CENP-F binds NPCs just prior to the onset of mitosis (Fletcher et al., 2003). During interphase, CENP-F localizes predominantly to the nucleoplasm. However, immediately prior to NEBD, this protein redistributes partially to the nuclear periphery where it is sequestered at NPCs just preceding their disassembly. Although the functional significance of this observation is not understood, there is evidence to suggest that CENP-F may contribute to the targeting of the Nup107-160 complex to KTs (Zuccolo et al., 2007).

The SAC proteins Mad1 and Mad2 also bind NPCs and, to date, are the best characterized examples of KT proteins associating with these structures. From yeast to vertebrates, Mad1 and Mad2 bind interphase NPCs, and the molecular basis for this interaction has been studied in significant detail (Campbell et al., 2001; Iouk et al., 2002; Ikui et al., 2002; Scott et al., 2005; Katsani et al., 2008; Lince-Faria et al., 2009; Wozniak et al., 2010). Through deletion analysis in budding yeast, it was determined that Mad1 is required for NPC association of Mad1-Mad2 as deletion of *MAD1* results in the release of Mad2 from the periphery while the converse (*mad2Δ*) has negligible impact on Mad1-NPC binding (Campbell et al., 2002). This Mad1-Mad2-NPC interaction is conserved, as

parallel analyses conducted in fission yeast and *Aspergillus* yielded identical results (Ikui et al., 2002; De Souza et al., 2009).

On the other hand, elucidating the exact Nup binding partners for Mad1-Mad2 at NPCs has proven to be slightly more challenging due to the compositional and structural complexity of NPCs. An initial clue into elucidating the Nup binding partners of the Mad1-Mad2 complex came from immunogold EM experiments in human cells showing that this complex localizes to the nucleoplasmic face of NPCs, in close spatial proximity to the nuclear basket (Campbell et al., 2002). It would later be confirmed that the nuclear basket proteins TPR and Nup153 are indeed the molecular determinants for the association of Mad1-Mad2 with NPCs in mammalian cells, as depletion of either Nup results in mislocalization of Mad1-Mad2 from the nuclear periphery (Lee et al., 2008; Yussi et al., 2010). The association of Mad1-Mad2 with the nuclear basket also holds true in yeast, flies and *Aspergillus* (Scott et al., 2005; Katsani et al., 2008; Lince-Faria et al., 2009; De Souza et al., 2009). However, Mad1-Mad2 binding to NPCs is somewhat convoluted in budding yeast, as not only does this complex rely on the nuclear basket proteins Mlp1 and Mlp2 for their peripheral association, they also directly bind two separate FG-Nups including Nup53 and Nup60 (Iouk et al., 2002; Scott et al., 2005; R. Scott personal communication). The functional significance of the interaction between Mad1 and Nup53 will be discussed in greater detail in Chapter III.

Upon activation of the SAC, both Mad1 and Mad2 target from binding sites at NPCs to unattached KTs (reviewed in Musacchio and Salmon, 2007; Foley and Kapoor, 2013; London and Biggins, 2014). In budding yeast, the entire NPC-associated pool of Mad2 redistributes off NPCs and onto KTs, while Mad1 partitions into NPC and KT

bound pools (Iouk et al., 2002; Scott et al., 2005). Under these conditions, fluorescence recovery after photobleaching (FRAP) reveals that the majority of Mad1 (>60%) dynamically exchanges between binding sites at NPCs and KTs (Scott et al., 2005). Dual Mad1 binding to nuclear basket proteins and KTs has also been detected in *Aspergillus* and *Drosophila* in which a fraction of Mad1 remains associated with the nuclear basket during SAC activation (Lee et al., 2008; De Souza et al., 2009; Lince-Faria et al., 2009; Yussi et al., 2010). Intriguingly, a recent study in human cells has revealed that the physical association of Mad1-Mad2 with the nucleoporin translocated promoter region (TPR) is critical to prevent proteasome-mediated degradation of either SAC protein, thus contributing to SAC signaling robustness by maintaining Mad1-Mad2 proteostasis (Schweizer et al., 2013). In contrast, the association of Mad1 with Nup153 does not appear to contribute to SAC function but, rather, Nup153 binding to Mad1 has an opposing function and is thought to contribute to silencing of the SAC by influencing Mad1 phosphorylation levels (Lussi et al., 2010).

The ability of the NPC to influence the signaling activities of Mad1-Mad2 was recently discovered to extend beyond mitosis. In fact, it was revealed that the physical tethering of Mad1-Mad2 to interphase NPCs allows for the Mad1-Mad2 dimer to contribute to the formation of the mitotic checkpoint complex (MCC) prior to mitosis and NEBD (Rodriguez-Bravo et al., 2014). In effect, at the stages of the cell cycle prior to the completion of KT assembly, the NPC functions in an analogous fashion to mitotic KTs, which serve as a structural hub for the Mad1-Mad2 complex and generation of the "wait-anaphase" signal (MCC production). The pre-mitotic NPC-derived inhibitory signal (APC/C inhibition) is a likely explanation for the exquisite sensitivity of the SAC in

response to a single unattached KT during mitosis (Rieder et al. 1994; Li and Nicklas 1995). Consistent with this, loss of tethering of the Mad1-Mad2 dimer at NPCs results in mitotic defects including accelerated anaphase onset and a reduction in the robustness of SAC signaling from KTs. In yeast, there is evidence of the formation of spindle checkpoint complexes prior to mitosis, but whether these complexes are derived from NPC-tethered Mad1-Mad2 remains to be determined (Brady and Hardwick, 2000).

**1.10 KTs, chromosome segregation and the SAC**

Similar to NPCs, KTs are massive macromolecular assemblies comprised of a multitude of individual constituent proteins that come together to form highly sophisticated molecular machines. Unlike NPCs, KTs are built upon specialized DNA sequences, termed centromeres, where they mediate the attachment of chromosomes to spindle MTs to facilitate accurate chromosome segregation upon cellular division. In addition to physically contributing to chromosome transmission, these assemblages also double as signaling beacons that relay the interaction status at the KT-MT interface to the SAC. Under conditions where interactions at the KT-MT interface are faulty or erroneous, the SAC functions to halt mitotic progression as a mechanism to prevent the missegregation of chromosomes. Therefore, through these essential activities, these molecular assemblages play a crucial role in maintaining genomic stability and, thus, cellular viability. In the next section, both the structural and functional elements of KTs and their functional interplay with the SAC signaling machinery will be discussed in significant detail.

### 1.10.1 KT morphology and structure

The general ultrastructural features of the vertebrate KT were initially determined from studies using thin-section transmission EM on vertebrate chromosomes within intact cells (Brinkley and Stubblefield, 1966; Jokelainen, 1967; Roos, 1973; Riedler, 1981). From this, it was revealed that the vertebrate KT adopts a distinctive trilaminar morphology as the structure is visibly divided into three sections: (1) the inner KT which interfaces directly with chromatin, (2) the outer KT which forms the interaction interface with spindle MTs and finally (3) the central KT, which forms the least electron dense region of the KT. When detached from spindle-MTs, a distinct, densely packed, fibrillar-like structure, appropriately termed the fibrous corona, extends from the outer face of the KT (Cassimeris et al., 1990; Cheeseman and Desai, 2008). Intriguingly, this outward extension disappears when KTs directly contact the spindle, which is consistent with the idea that KTs undergo a dynamic molecular change when bound to MTs (Dong et al., 2007; McEwen et al., 2007; Gonen et al., 2012).

A similar analysis to describe the morphological features of budding yeast KTs within intact cells has not been possible due to the inherently small size of these assemblages in yeast. However, a recent EM study was conducted utilizing isolated yeast KT particles (native KT assemblies isolated on mini-chromosomes) to determine the general morphological features of these structures (Gonen et al., 2012). Despite the fact these pseudo-KT assemblies contained the majority of the core KT subcomplexes, they did not conform to the distinctive three-tiered, tri-laminar structural organization observed previously in vertebrate cells. Instead, these 126-nm particles contained a dense central hub region with a series of distinctive globular domains situated on the surface

nearest to the MT attachment site. However, despite obvious morphological differences, there appear to be similarities in the mode with which yeast KT particles interface with the surface of the MT lattice in so much as these interactions are mediated through multiple contacts sites between several outwardly extended globular domains and the MT surface. However, given the observed morphological differences demonstrated between species, it is difficult to ascertain whether these observations truly reflect the actual structural conformation of yeast KTs in intact cells. Almost certainly, future studies will be geared towards analyzing these assemblies within intact yeast cells.

As the morphological characteristics of KTs have become better defined, so to has the molecular composition of these assemblies. Across species, KTs are comprised of multiple subcomplexes that are physically interconnected with each other from the surface of chromatin to the MT lattice (see Figure 1-3) (reviewed in McAnish et al., 2003; Westermann et al., 2007; Biggins, 2013). In budding yeast, the KT is comprised of seven distinct subcomplexes including Ndc80, Mtw1/Mis12, Spc105/KNL1, Ctf19/COMA, Dam1, Cse4 and CBF3 complexes (Biggins, 2013). Each subcomplex in the yeast KT is present in multiple copies and, from this, it has been estimated that the core KT assemblage contains up to 250 individual protein constituents in total, with a predicted mass in excess of 5 MDa, not including additional regulatory proteins such as SAC constituents or MT-associated proteins (MAPs) (De Wulf et al., 2003; Westermann et al., 2007; Gonen et al., 2012).

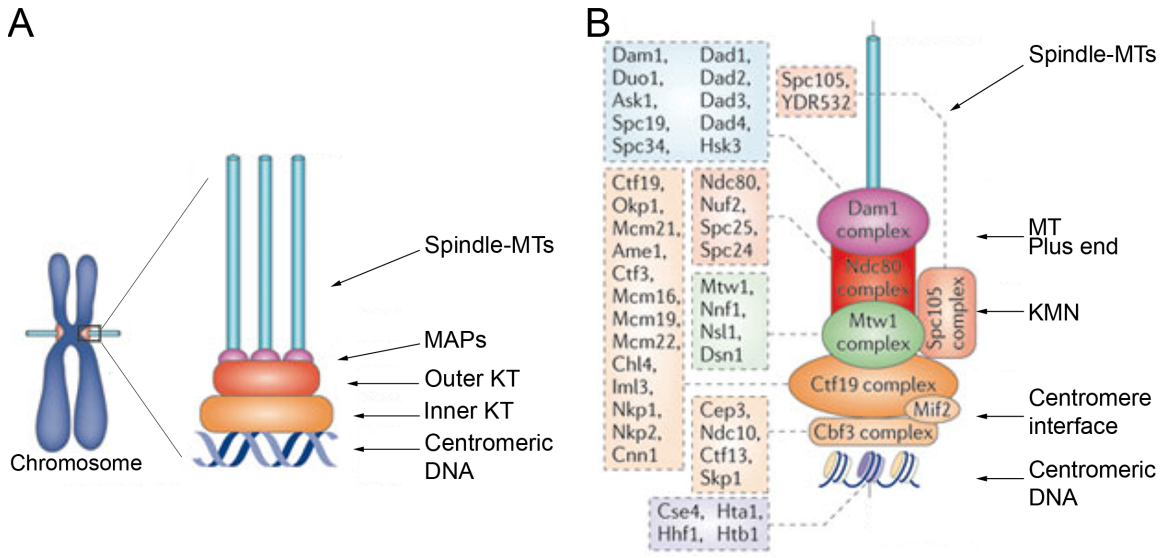


**Figure 1-3. General architecture of the budding yeast KT.** (a) Depicted is a schematic of the general organization of the core structure of the KT situated in between spindle-MTs and centromeric DNA. Generally, the core KT is largely comprised of two major multiprotein complexes referred to as the KT-MT network (KMN) and the constitutive centromeric-associated network (CCAN), which come together to form the inner and outer KT. The KMN is comprised of three constituent subcomplexes including the Spc105/Knl1, Ndc80, and Mtw1/Mis12 complexes. The CCAN contains three separate complexes that interact directly with DNA including Ctf19 (COMA), Mif2 and CBF3 complexes. In addition to these core constituent components, several regulatory proteins also associate with KTs, including the chromosomal passenger complex (CPC), MT-associated proteins (MAPs) and SAC regulators (not depicted). (b) The organization and relative distribution of individual KT constituents within the budding yeast KT. Localized to the distal, plus end tips of MTs is the heterodecameric Dam1 complex whose primary function involves forming the attachment site between dynamic MT ends and the outer KT. At the MT plus-end, the Dam1 complex interfaces directly with the KMN through interactions with the Ndc80 subcomplex. The KT subassembly largely responsible for anchoring the outer KT (KMN) to centromeric DNA is the Ctf19 subcomplex (CCAN in higher organisms) along with Mif2 (CENP-C homologue). The CBF3 complex directly associates with centromeric DNA and is thought to be involved in facilitating the deposition of the histone variant Cse4 onto centromeric DNA sequence. Adapted from Lampert and Westermann, 2011.

### 1.10.2 The inner KT

The inner KT is comprised of a highly conserved group of proteins, most of which are in direct physical contact with chromatin. Among the subcomplexes that reside at this location, the best characterized is the CBF3 subcomplex. This four-member complex was the first KT subassembly characterized in yeast and includes Ndc10, Cep3, Ctf13 and Skp1, all of which are necessary for viability. The CBF3 constituents come together to form a structural unit required to nucleate KT assembly (Doheny et al., 1993; Goh and Kilmartin, 1993; Jiang et al., 1993; Lechner, 1994; Strunnikov et al., 1995; Connelly and Hieter, 1996). The ability of this complex to directly interface with chromatin is dependent upon Ndc10 and Cep3, both of which possess classical DNA binding motifs. Cep3 contains a zinc cluster motif, a structural module found in most zinc finger transcription factors, and Ndc10 contains a sequence motif that bears structural similarity to tyrosine DNA recombinases (Dhawale and Lane, 1993; Strunnikov et al., 1995; Schjerling and Holmberg, 1996; Cho and Harrison, 2012; Perriches and Singleton, 2012). The presence of divergent DNA-binding domains allows both proteins to interface directly with specific A-T rich sequences found at centromeres and contributes to the stable association of this complex once bound to DNA.

In addition to CBF3, the yeast CENP-C homologue Mif2 and the COMA (Ctf19, Okp1, Mcm21, Ame1) subcomplex also comprise the inner KT. Although the exact functional contribution of these subcomplexes has remained somewhat ambiguous over the years, a recent report has implicated Mif2, and the COMA complex members Ame1 and Okp1, as key regulators of outer KT assembly in yeast by acting as scaffolding for Ndc80 recruitment to the KT (Hornung et al., 2014).

### 1.10.3 The outer KT

The outer KT is comprised of four essential subcomplexes including Mtw1/Mis12, Spc105/Knl1, Ndc80 and the Dam1 complex (reviewed in Biggins, 2013). The conserved Ndc80, Spc105/Knl1 and Mtw1/Mis12 complexes come together to form a specialized network that comprises the core MT binding module of the KT and has appropriately been dubbed the KT-MT network (KMN) (De Wulf et al., 2003; Desai et al., 2003; Nekrasov et al., 2003; Pinsky et al., 2003; Westermann et al., 2003; Cheeseman et al., 2004; Obuse et al., 2004; Liu et al., 2005; Cheeseman et al., 2006; Przewloka et al., 2007). Impairing the functional integrity of the KMN most often results in a KT null-phenotype whereby KTs cannot maintain load-bearing attachments and most often detach from spindle MTs (McCleland et al., 2003; Nekrasov et al., 2003; Cheeseman et al., 2004; Kerres et al., 2004; DeLuca et al., 2005; Emanuele et al., 2005; Cheeseman et al., 2006; DeLuca et al., 2006; Kline et al., 2006; Pinsky et al., 2006; Vorozhko et al., 2008; Pagliuca et al., 2009).

Among the constituent KMN subcomplexes, the Ndc80 complex confers the primary MT binding activity. Comprised of four essential proteins (Ndc80, Nuf2, Spc24, Spc25), three-dimensional structural analysis of this complex revealed that these proteins come together to a form a dumbbell shaped structure with two globular head domains connected by an extended α-helical coiled-coil shaft (Ciferri et al., 2005; Wei et al., 2007; Ciferri et al., 2008). In effect, this structural organization enables the Ndc80 complex to function as an extended head-to-tail linker whereby one globular head domain associates with MTs, and is comprised of Ndc80 and Nuf2, while the head on the opposite end binds to the core structure of the KT and is formed by Spc24 and Spc25 (Ciferri et al, 2005;

Wei et al, 2005). The intrinsic MT binding activity of the Ndc80 complex comes from the amino-terminal regions of both Ndc80 and Nuf2 (Cheeseman et al., 2006; Wei et al., 2007; Ciferri et al., 2008). Interactions between the Ndc80 complex and the MT surface are electrostatic in nature, as the globular head that interfaces with the negatively charged surface of tubulin contains two positively charged calponin homology (CH) domains (Wei et al., 2007; Ciferri et al., 2008). The presence of two CH domains within the Ndc80 and Nuf2 sequences is functionally significant, as this domain is a key characteristic of MT-associated proteins (MAPs) that mediates binding to the surface of the MT lattice (Hayashi and Ikura, 2003). Consistent with this, introducing mutations into the CH domains significantly lowers the binding affinity of the Ndc80 complex for MTs *in vitro* and results in chromosome-spindle attachment defects *in vivo* (Ciferri et al., 2007; Sundin et al., 2011; Tooley et al., 2011). Additional contributions to MT binding also come from a highly basic and structurally disordered region directly adjacent to the CH domains within the amino-terminus of Ndc80 (DeLuca et al., 2006; Guimaraes et al., 2008). Similar to CH domains, this intrinsically unstructured domain is highly positively charged and deletion of this region leads to errors in chromosome segregation. This region also serves as a point of regulation for KT-MT interactions, as it contains several Aurora B-kinase phosphorylation sites which, when modified, influence the electrostatic properties of this region and its MT-binding affinities (Guimaraes et al., 2008).

By contrast, the other complexes that make up the KMN (Spc105/Knl1 and Mtw1/Mis12) do not exhibit strong MT binding activity on their own *in vitro* (Cheeseman et al., 2006; Pagliuca et al., 2009; Hornung et al., 2011). However, it has been demonstrated that Spc105/Knl1 serves as a receptor for the SAC components Bub1

and Bub3 suggesting that the function of this complex is likely more pertinent for SAC signaling than mediating chromosome-spindle attachments (London et al., 2012). Despite the lack of MT binding activity possessed by the Mtw1 complex, the primary function of this four-member KT assembly (Mtw1, Dsn1, Nnf1, and Nsl1) is to form a structural linker bridging the gap between the MT binding interface and the inner centromere. The structure of this complex, as revealed by EM, shows a rod-like assembly with branched ends, which is consistent with the idea this complex serves as a molecular bridge between regions of the outer and inner KT (Westermann et al., 2003; Westermann et al., 2007). Therefore, each individual subcomplex that makes up the KMN is functionally distinct and together, in unison, they contribute to the overall structural integrity and functionality of the outer KT.

### 1.10.4 The Dam1 complex

Positioned on the opposite face of the KMN and directly bound to dynamic MT plus end tips is the Dam1 complex. Comprised of ten essential constituents (Dam1, Duo1, Dad1, Spc34, Ask1, Spc19, Dad2, Dad3, Dad4, Hsk3,) the individual members of this complex come together to form an intricate MT-coupling device whose primary function involves establishing and maintaining robust connections between MT distal ends and the outer KT (Hofmann et al., 1998; Cheeseman et al., 2001; Enquist-Newman et al., 2001; Janke et al., 2002; Li et al., 2002; De Wulf et al., 2003; Li et al., 2005; Miranda et al., 2005; Westermann et al., 2005). Significant gains in understanding the structural and biochemical activities of the Dam1 complex came from the development of an *in vitro* reconstitution assay whereby all ten members of this complex could be simultaneously

co-expressed in *E. coli* (Miranda et al., 2005; Westermann et al., 2005). Following their co-expression in the presence of MTs, it was uncovered that this complex oligomerizes on the surface of the tubulin lattice forming a ring-like structure encircling the circumference of the MT perpendicular to its axis (Westermann et al., 2005). Remarkably, the ability of the Dam1 complex to oligomerize is an intrinsic property as this complex can circularize in the absence of MTs (Westermann et al., 2005).

The interaction interface between the Dam1 complex and the MT surface is formed from a series of electrostatic interactions between the negatively charged E-Hook domains of αβ–tubulin and the highly basic carboxy-terminal regions of both Dam1 and Duo1 (Westermann et al., 2005). A closer inspection of this interface revealed that there is a lack of a fixed binding site on the MT surface and, in fact, there is a considerable gap between the inner ring of the Dam1 complex and the surface of the MT lattice. This observation proved to be significant for understanding the mechanistic nature of the Dam1 complex as these structural considerations implied that the complex possessed the ability to be mobile on the MT lattice. Further research revealed this to be precisely the case, as this complex confers the ability to translocate processively along the MT lattice while maintaining load-bearing attachments (Westermann et al., 2006). In addition to this activity, the Dam1 complex autonomously tracks the plus ends of MTs, allowing it to remain intimately coupled to dynamic MT plus ends (Westermann et al., 2006; Lampert et al., 2010). The plus-end tracking capability of the Dam1 complex is predicted to be a consequence of the affinity this assemblage has for GTP-bound tubulin, which is specifically enriched at the distal tips of MTs (Westermann et al., 2005). Thus, the highly processive nature of the Dam1 complex, in combination with its plus end tracking

capabilities, enable the Dam1 complex to couple chromosomes to highly dynamic MTs over the course of the cell cycle.

The physical link between the core KT assembly and the Dam1 complex is mediated through a bridging interaction between the KMN component Ndc80 and Dam1 (Lampert et al., 2010; Tien et al., 2010; Lampert et al., 2013; Tien et al., 2013). Although Ndc80 can bind the surface of MTs independently of the Dam1 complex, the Ndc80-Dam1 interaction is necessary for end-on, load-bearing KT-MT attachments required for KT bi-orientation. In the absence of Dam1 complex function, chromosomes fail to associate with MT plus ends and, as a result, sister chromatids fail to achieve bi-orientation on the mitotic spindle. This binding interface between Dam1 and Ndc80 also serves as a point of regulation of KT-MT interactions through Ipl1-activity (through Aurora B-kinase activity; discussed below).

### 1.10.5 KT bi-orientation in yeast

KT bi-orientation is an intricate, multi-step process that requires the coordinated activities of MT-associated motor proteins (i.e. Kar3 and Stu2), MT coupling devices like the Dam1 complex, and the activity of regulatory proteins like Ipl1, which, through its tension sensing activity, influences the attachment state between KTs and the spindle (see Figure 1-4) (reviewed in Tanaka et al., 2012). Effective KT bi-orientation is a requisite event for the faithful and error-free transmission of sister chromatids during cell division. The underlying molecular mechanisms that regulate this process have been the focus of a multitude of studies, with the most significant gains in understanding coming from studies performed in budding yeast. KTs exhibit two topologically distinct binding

modalities when interacting with spindle MTs; these include lateral (or side on) attachments where KTs interface with the lateral surface of the MT lattice and end-on attachments whereby KTs are bound to the distal tips (plus ends of the spindle) of MTs (Tanaka et al., 2010; Tanaka et al., 2012). Of the two binding modes, end-on attachments are the most stable and are an essential configuration for efficient KT bi-orientation during mitosis (Tanaka et al., 2005; Tanaka and Desai, 2008; Tanaka, 2010; Tanaka, 2012). However, during spindle assembly and initial KT capture, KTs typically associate with the lateral surface of MTs due simply to the large contact surface relative to the MT distal tips (Tanaka et al., 2005). The initial association of chromosomes with the lateral surface of MTs depends upon the MT binding activities of the Ndc80 complex (see Figure 1-5) (Ciferri et al., 2007; Lampert and Westermann, 2011; Tooley and Stukenberg, 2011; Deluca and Musacchio, 2012). Once associated with the lateral surface of MTs, these attachments must be converted to end-on attachments for the formation of stable KT-MT interactions. The precise mechanism by which this occurs has been determined in budding yeast and is, in part, reliant on the coordinated activities of the MT motor protein Kar3 and the outer KT components, Ndc80 and Dam1 (Tanaka et al., 2007). Following initial capture, chromosomes are transported pole-ward along MTs through the minus-end-directed MT motor protein Kar3 (Tanaka et al., 2007). However, as chromosomes move towards the minus end, MT depolymerization occurs at a more rapid rate than pole-ward chromosome migration; this allows for the plus ends of MTs to eventually catch up to the KT lateral attachment site (Tanaka et al., 2007; Tanaka, 2012). Once associated with MT distal tips, stable KT-MT interactions are facilitated by direct binding between Ndc80 and Dam1, which leads to the production of proper load-bearing

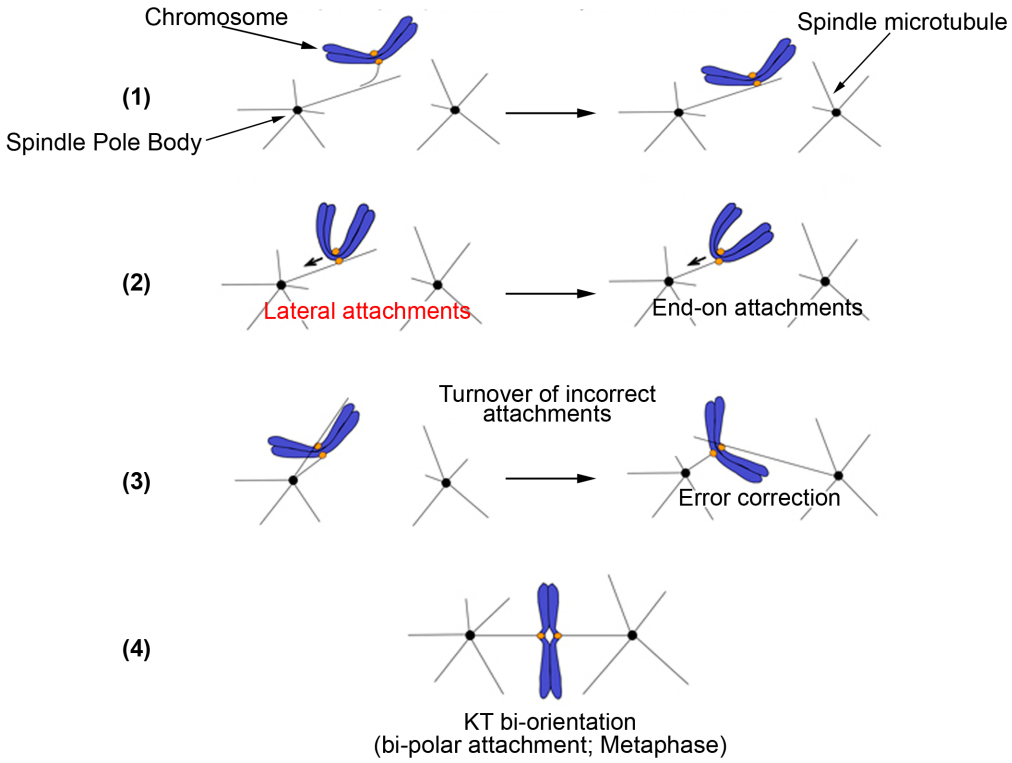


**Figure 1-4. KT bi-orientation in budding yeast.** Depicted is a schematic of the step-by-step process involved in KT bi-orientation in budding yeast. (1) Spindle MTs emanate from SPBs where KTs initially contact these structures by attaching to the lateral surface of these dynamic structures (lateral attachments). The lateral surface of MTs forms the initial contact sites for KTs due to the large surface area. (2) Once associated with the spindle, chromosomes are transported pole-ward (towards the minus end) through the activity of the MT motor protein Kar3. Due to rapid rates of MT depolymerization, the plus ends of MTs eventually associate with KTs to form more stable and robust end-on attachments. (3) In a scenario where both sister KTs engage MTs emanating from the same spindle pole (syntelic attachment), this erroneous KT-MT attachment must be corrected (through the activity of Ip1lp-kinase). (4) KT bi-orientation on the spindle is achieved when the opposing unbound KT (opposite sister chromatid) binds to a spindle-MT emanating from an opposing SPB. The pulling forces generated from opposing spindle MTs leads to the physical separation of sister KTs and tension is thus applied. Adapted from Tanaka, 2010.

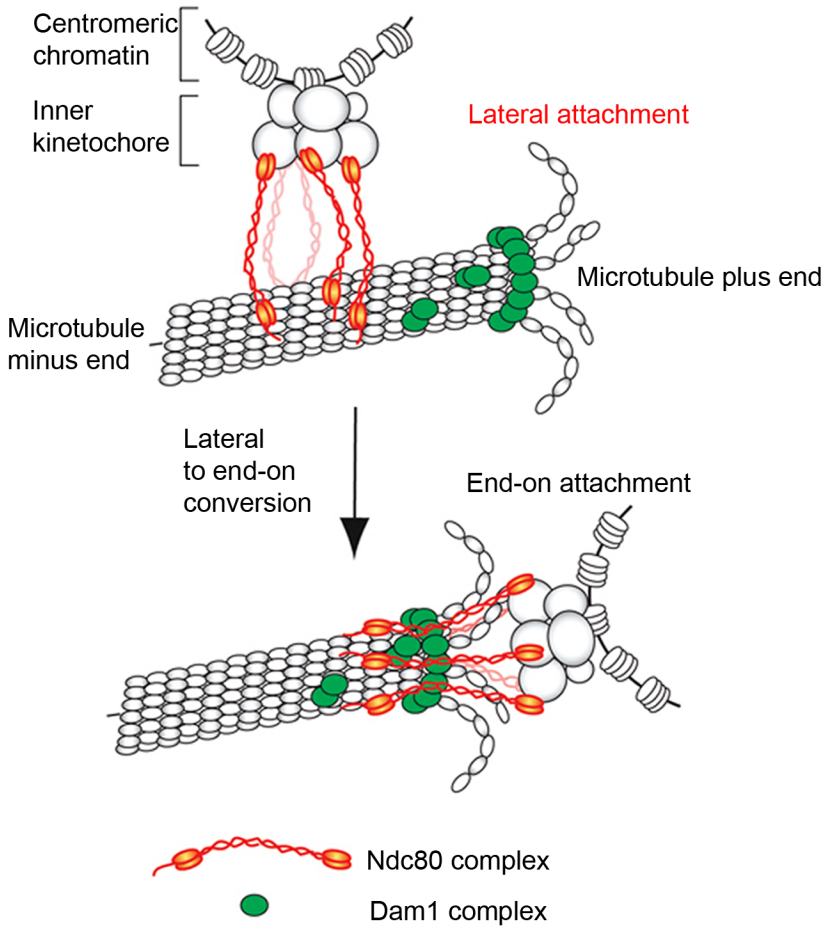


**Figure 1-5. Ndc80 and Dam1 complexes in lateral to end-on attachments.** The Ndc80 complex comprises the major MT-binding unit of the core KT and associates with the negatively charged lateral surface of MTs through a highly positively charged, globular calponin-homology domain (CH) within the amino-terminus of Ndc80. Lateral attachments do not support accurate chromosome segregation and must be eventually converted to end-on attachments. Key to the conversion of lateral to end-on binding modalities (an essential event necessary for KT bi-orientation) is the ability of the Ndc80 complex to eventually physically associate with the Dam1 complex situated at the MT plus-ends. Interactions between these interfaces are critical for the formation of stable attachments between KTs and MT plus-ends and, thus, are an absolute requirement for efficient KT bi-orientation. Adapted from Tanaka, 2010.

KT-MT attachments and, from this, sister chromatids achieve bi-orientation on the mitotic spindle (Tanaka et al., 2007; Lampert et al., 2010; Lampert et al., 2013). KT bi-orientation produces significant tension across sister KTs due to the pulling forces produced by opposing spindles MTs attached to sister chromatids linked by cohesin (Figure 1-4).

### 1.10.6 Regulation of KT-MT interactions

From yeast to mammals, the fundamental regulator of molecular interactions at the KT-MT interface is the highly conserved Aurora B-kinase (Ipl1 in yeast). Apart from the four member chromosomal passenger complex (also known as the CPC; Sli15, Bir1, Nbl1), Ipl1 binds KTs through an interaction with two separate inner KT complexes including COMA and CBF3 subcomplexes and, positioned here, functions to influence the attachment state of KTs to spindle MTs (Yoon and Carbon, 1999; Sandall et al., 2006; Knockleby and Vogel, 2009). Through this activity, Ipl1 plays an essential regulatory role in contributing to the efficient establishment of KT bi-orientation during mitosis. Cells that contain mutations that impair Ipl1 function fail to achieve KT bi-orientation on the spindle and possess tensionless, mono-oriented chromosome-spindle attachments whereby sister chromatids remain associated with MTs emanating from a single spindle pole (Biggins et al., 1999; Tanaka et al., 2002; Dewar et al., 2004; Tanaka et al., 2005). From this, it was proposed that Ipl1 is directly involved in a tension sensing, error correction mechanism whereby incorrect KT-MT attachments lacking tension are effectively disrupted and turned over through Ipl1-kinase activity (Biggins et al., 1999; Tanaka et al., 2002; Dewar et al., 2004; Tanaka et al., 2005).

Mechanistically, the weakening of interactions at the KT-MT interface is largely achieved through Ipl1-dependent phosphorylation of targets at this junction (Biggins et al., 1999; Cheeseman et al., 2002; Tanaka et al., 2002; Westermann et al., 2003; Dewar et al., 2004; Tanaka et al., 2005; Maskell et al., 2010). Over the past decade or so, numerous Ipl1 targets have been identified, including several members of both the Dam1 and Ndc80 complexes, which is important from a mechanistic standpoint as physical interactions between these complexes is key for the establishment of stable, end-on KT-MT interactions required for KT bi-orientation (Cheeseman et al., 2002; Akiyoshi et al., 2009a; Lampert et al., 2010; Lampert et al., 2013). Multiple Ipl1-phosphorylation targets have been identified in Dam1's sequence and depending on the phosphorylation site, the resulting effects on KT-MT interactions appear to vary considerably. For instance, phosphorylation of residues S20 of Dam1 reduces the binding affinity of the Dam1 complex for the surface of MTs resulting in more frequent dissociation of this entire assemblage from MTs *in vitro* (Gestault et al., 2008). Alternatively, Ipl1-mediated phosphorylation of other Dam1 sites can result in a range of effects including inhibition of Dam1 complex oligomerization (ring formation) on MTs to directly increasing the rates of MT catastrophe at the MT plus ends causing KT release (Wang et al., 2007; Akiyoshi et al., 2010; Sarangapani et al., 2013). On the other side of the KT-MT interface, several Ipl1-phosphorylation sites have also been identified in Ndc80, including in the positively charged unstructured amino-terminal domain, which directly interacts with tubulin (Akiyoshi et al., 2009a; Demeriel, 2012; Tien et al., 2014). Phosphorylation at these sites weakens MT binding *in vitro*. For example, phosphomimetic and non-phosphorylatable mutations destabilize and hyperstablize KT-MT interactions,

respectively (Umbreit et al., 2012; Sarangapani et al., 2013). In summary, across species, Ipl1 plays a critical role in regulating interactions at the KT-MT interface, and as a consequence of this activity, Ipl1 functions as a central regulator of KT bi-orientation.

### 1.10.7 The Spindle Assembly Checkpoint

The SAC monitors the attachment state of KTs to spindle MTs. In response to faulty interactions at the KT-MT interface, the SAC functions to arrest mitotic progression allowing the cell time to correct inappropriate interactions between chromosomes and the spindle (Musacchio and Salmon, 2007; Foley and Kapoor, 2013; London and Biggins, 2014). Genes encoding proteins involved in the SAC were originally identified in two separate screens conducted in yeast to identify mutants that fail to arrest in the presence of spindle damage. In total, each screen led to the identification of six genes including the mitotic arrest-deficient genes (*MAD1, MAD2* and *MAD3*) and the budding uninhibited by benzimidazole genes (*BUB1*, *BUB2* and *BUB3*) (Hoyt et al., 1991; Li and Murray, 1991). The SAC genes identified in these genetic screens are not essential for cell viability, as the SAC is dispensable during an unperturbed mitosis in yeast (Gillett et al., 2004). However, in animal cells, the SAC genes are necessary for viability as the checkpoint is activated every mitosis to prevent chromosome loss during spindle assembly (Basu et al., 1999; Kitagawa and Rose, 1999; Dobles et al., 2000; Kalitsis et al., 2000; Gillett et al., 2004). Five years following the initial identification of the *BUB* and *MAD* genes in yeast, the regulatory SAC kinase Mps1 was identified. Mps1 is essential due to its additional role in SPB duplication (Winey et al., 1991; Hardwick et al., 1996; Weiss and Winey, 1996; Jones et al., 2001).

The SAC mediates mitotic arrest by blocking Cdc20 activity, a co-activator of the anaphase-promoting complex/cyclosome (APC/C) (Li et al., 1997; Fang et al., 1998; Hwang et al., 1998; Kim et al., 1998). An E3 ubiquitin ligase, the multi-subunit APC/C promotes mitotic progression by specifically targeting two proteins for proteasomal degradation. These include securin, a protein involved in protecting sister-chromatid cohesion degradation during metaphase, and the Cdk1 co-activator cyclin B (see Figure 1.6) (Pds1 and Clb2 in yeast, respectively; King et al., 1995; Ciosk et al., 1998). Therefore, the SAC acts as a safety net to ensure that downstream mitotic events are prevented from being initiated in the presence of chromosome-spindle interaction defects. SAC signaling catalyzes the formation of a small protein complex termed the mitotic checkpoint complex (MCC). This complex is a heterotetramer that consists of the checkpoint proteins Mad2, Mad3 (BubR1), Bub3, and Cdc20 (Brady and Hardwick, 2000; Hardwick et al., 2000; Fraschini et al., 2001; Sudakin et al., 2001; Tang et al., 2001; Fang, 2002; Chao et al., 2012). This highly stable mitotic complex creates the "wait anaphase" signal as it forms an inhibitory complex with Cdc20. This prevents it from activating the APC/C, thus preventing mitotic progression.

Following the initial identification of the SAC genes in budding yeast, several laboratories began to speculate that the SAC exerts its effects on cell cycle progression specifically from KTs (Li and Murray, 1991; Hoyt et al., 1991; McIntosh, 1991; Gorbsky, 1995). Consistent with this hypothesis, early clues linking KT function and SAC signaling were derived from several observations showing that compromising the functionality of specific KT proteins through mutation resulted in SAC activation and metaphase arrest (Goh and Kilmartin, 1993; Wang and Burke, 1995; Pangilinan and

Spencer, 1996). In addition, laser ablation experiments in animal cells revealed that the photoablation of a single KT-MT attachment was sufficient to engage the SAC (Rieder et al., 1994; Rieder et al., 1995; Li and Nicklas, 1995). It would later be determined in significant molecular detail that KTs serve as the molecular hubs for the generation of the SAC signal as most SAC proteins are recruited to KTs upon spindle checkpoint activation (Musacchio and Salmon, 2007; Foley and Kapoor, 2013).

Across species, the SAC proteins Mps1, Mad1, Mad2, Bub1, Bub3 and BubR1, are recruited to unattached KTs in a hierarchical manner upon SAC activation, and they are subsequently removed from KTs following MT occupancy and SAC silencing (Musacchio and Salmon, 2007; Foley and Kapoor, 2013). This is mostly evident in budding yeast with the exception of Mad3, which is not detectable at unattached KTs during periods of SAC arrest (Gillett et al., 2004). While in most instances Mad1 and Mad2 target to KTs detached from the spindle, both Bub1 and Bub3 are found localized at these structures during an unperturbed mitosis (Iouk et al., 2002; Kerscher et al., 2003; Gillett et al., 2004). This observation was initially perceived as anomalous as, unlike the case in vertebrate cells, the SAC in yeast is not activated during an unperturbed cell cycle (Gillett et al., 2004). Subsequent experiments would reveal that, in addition to their roles in checkpoint signaling, Bub1-Bub3 are also involved in regulating KT-MT attachments and are required for efficient KT bi-orientation during mitosis (Fernius and Hardwick, 2007; Windecker et al., 2009; Kawashima et al., 2010; Storchova et al., 2011). This observation provided an explanation as to why *BUB1* and *BUB3* deletion mutants exhibit the highest rates of chromosome loss amongst the SAC genes in yeast (Indjeian et al., 2005; Fernius and Hardwick, 2007).

At the KT, elucidating the precise molecular binding sites for SAC proteins has proved to be challenging for the field due to the structural and compositional complexity of these macromolecular assemblies. However, from a series of recent studies, it was determined that the outermost KT assembly, the KMN (which includes Spc105/Knl1, Ndc80 and Mtw1/Mis12 complexes) constitutes the main docking hub for checkpoint proteins upon activation of the SAC (Cheeseman et al., 2006; Foley and Kapoor, 2013). As discussed in section 1.10.3, the KNM forms the major MT-binding module for the core KT, thus making it the ideal KT complex linking the topological state of KT-MT interactions to the SAC (Foley and Kapoor, 2013).

Of the KMN components, the Spc105/Knl1 complex plays a particularly important role in forming a 'landing pad' for SAC complexes, and mounting evidence suggests this outer KT component is crucial for the initiation of SAC signaling and the formation of higher order checkpoint signaling complexes (Figure 1-6) (Foley and Kapoor, 2013). In particular, it was revealed that Mps1-mediated phosphorylation of Spc105/Knl1 is a key initiating step in KT-based SAC signaling altogether (London et al., 2012; Shepperd et al., 2012; Yamagishi et al., 2012; Foley and Kapoor, 2013). Specifically, Mps1-modified Spc105/Knl1 is required for the recruitment of Bub1-Bub3 to KTs (Kiyomitsu et al., 2007; Kiyomitsu et al., 2011; London et al., 2012; Shepperd et al., 2012; Yamagishi, et al., 2012). This is a significant observation in regards to the hierarchy of checkpoint protein recruitment to KTs, as Bub1-Bub3 forms a scaffold for Mad1-Mad2 KT targeting. This step is key for catalyzing the formation of the MCC necessary for APC/C inhibition (London and Biggins, 2014). Thus, these results highlight

the importance of the KMN, in particular Spc105/Knl1, in acting as a scaffold for checkpoint complexes at the KT and in the initiation of SAC signaling from KTs.

Once SAC effectors are bound to KTs, how is the biochemical signal for APC/C inhibition generated? A few elegant structural and biochemical studies have determined that key to MCC formation and, thus, APC/C inhibition is a structural conversion event involving Mad2 at KTs. From these studies, it was determined that Mad2 has two functionally distinct structural conformations, including open Mad2 (O-Mad2) and closed Mad2 (C-Mad2). These findings led to the development of the "Mad2 template model" to explain KT-catalyzed inhibitory Mad2-Cdc20 complexes. In this model, the O-Mad2 conformer is soluble and unable to physically interact with the APC/C co-activator Cdc20. Thus, in this structural conformation, O-Mad2 cannot participate in SAC signaling and inhibit mitotic progression. The second conformer, C-Mad2, adopts a structural conformation that enables it to bind Cdc20 and, resultantly, can efficiently block mitotic progression by inhibiting APC/C activity (Luo et al., 2000; Luo et al., 2002; Luo et al., 2004; Sironi et al., 2002; De Antoni et al., 2005). Importantly, the conversion of O-Mad2 to C-Mad2 requires KT-bound Mad1 in stable association with C-Mad2 (De Antoni et al., 2005). At the KT, this complex actively recruits O-Mad2, resulting in the formation of a conformational dimer (O-Mad2/C-Mad2). This dimerization event leads to the rapid conversion of O-Mad2 to C-Mad2 that binds and inhibits Cdc20. Therefore, Mad1 in complex with C-Mad2 at KTs is non-exchanging and serves as a template for a rapidly exchanging pool of O-Mad2, which is proficient at inhibiting the APC/C and blocking mitotic progression (Figure 1-6) (DeAntoni et al., 2005; Mapelli et al., 2007).

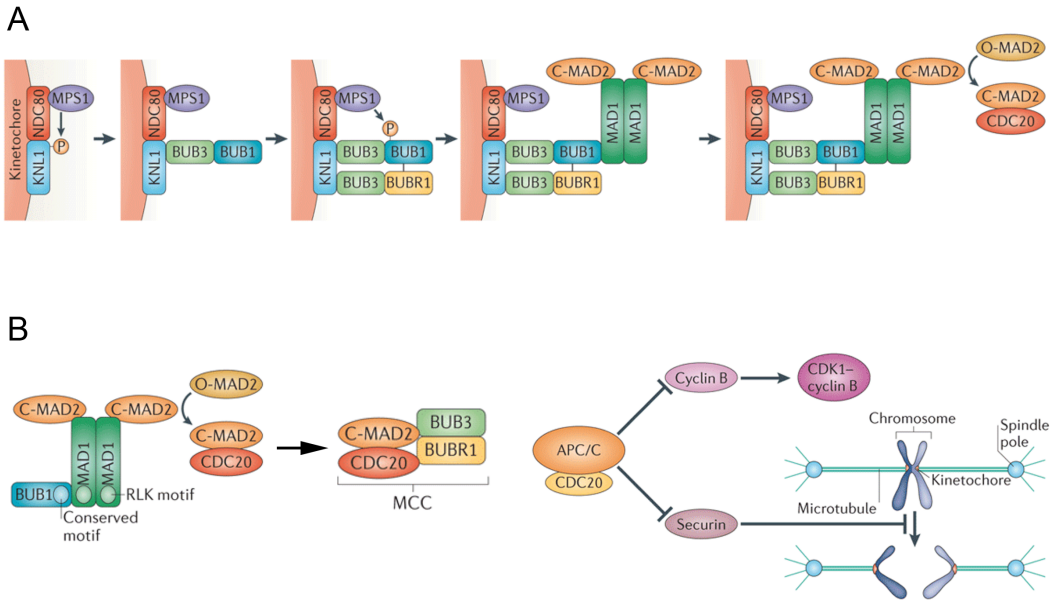


**Figure 1-6. Spindle assembly checkpoint signaling at the KT.** The outer KT components Spc105/Knl1 and Ndc80 come together to form the core KT scaffolding components required for the recruitment of SAC proteins upon checkpoint activation. Bound to Ndc80, Mps1-mediated phosphorylation of Spc105/Knl1 triggers the recruitment of Bub1-Bub3 to KTs. At KTs, Bub1-Bub3 seeds the assembly of higher-order checkpoint signaling complexes, as the recruitment of Mad1-Mad2 is dependent upon Bub1-Bub3 KT association. This recruitment event is initiated through Mps1-mediated phosphorylation of Bub1, which is required for Mad1 binding. The resulting Bub1-Mad1 complex acts to recruit the Mad1-Mad2 heterodimer to KTs. Positioned here, Mad1-Mad2 initiates SAC signaling through the conversion of 'open' (O)-Mad2 to 'closed' (C)-Mad2. (B) The closed version of Mad2 is competent to bind to the APC/C co-activator Cdc20 and, together with Bub3 and Mad3 (BubR1), these proteins form the mitotic checkpoint complex (MCC). The MCC blocks mitotic progression by preventing the APC/C from being activated. The resulting inhibition leads to the stabilization of cyclin-B and securin. This prevents chromosome segregation while the checkpoint is active and, thus, induces a mitotic delay. Adapted from London and Biggins, 2014.

### 1.10.7.1 SAC silencing

Extinguishing the checkpoint is arguably as important as its activation as SAC silencing is necessary for timely progression through mitosis and chromosome segregation. Recently, several laboratories have investigated the molecular mechanisms that contribute to silencing of the SAC. These laboratories have focused on two separate processes that accompany SAC silencing: the removal or stripping of Mad1/Mad2 from KTs and the reversal of SAC-activating phosphorylation events (Kops and Shah, 2012). The former process has been described in detail in mammalian cells and involves the MT motor protein dynein. Following MT occupancy at KTs, dynein is transported along MTs to KTs where it systematically strips multiple SAC components from the KT-MT interface, including Mad1-Mad2 and BubR1 (Howell et al., 2001; Gassmann et al., 2010). The systematic removal of these components from the KT attenuates Mad2 conversion and, thus, blocks continual MCC formation.

As SAC signaling requires the coordinated activity of a number of kinases and a multitude of phosphorylation events, the inhibition of this signaling event is assumed to depend upon the reversal of these modifications. Indeed, a universally conserved mechanism for SAC silencing involves the activity of the conserved phosphatase known as protein phosphatase-1 (PP1; Glc7 in budding yeast) (Pinsky et al., 2009; Vanoosthuyse and Hardwick, 2009; Rosenberg et al., 2011; Meadows et al., 2011; Wei et al., 2011). From yeast to vertebrates, PP1 exerts its ability to silence the SAC by de-phosphorylating a number of key substrates ranging from spindle checkpoint effectors to outer KT components, like Spc105/Knl1, which is a key recruitment site for the Bub1-Bub3 complex following SAC activation. Consistent with this, cells compromised for PP1

activity show delayed release from a SAC-mediated metaphase arrest, and disrupting the ability of this phosphatase from binding KTs results in constitutive checkpoint activation (Pinsky et al., 2009; Vanoosthuyse and Hardwick, 2009; Meadows et al., 2011; Rosenberg et al., 2011). Thus, the activity of this conserved phosphatase constitutes a major pathway by which cells are able to exit from a SAC-mediated mitotic arrest.

### 1.11 Thesis Focus

This thesis explores the functional interrelationship between the nuclear transport machinery and chromosome segregation in yeast. We have identified two interrelated functions of the nuclear transport factor Kap121 in regulating the fidelity of chromosome transmission during mitosis. First, we show that, through the signaling activity of Mad1, Kap121-mediated nuclear import is inhibited in response to the loss of KT-MT interactions during mitosis. A reduction in the nuclear flux of Kap121 and its cargos contributes to the establishment of a nuclear environment that promotes the activity of the checkpoint kinase Ipl1, thus promoting the reorganization and proper assembly of the KT-MT interface to facilitate accurate chromosome transmission. Second, we have identified a novel function for Kap121 in regulating mitotic KT bi-orientation. We have found that through its physical association with the Dam1 complex, Kap121 contributes to the formation of stable bi-polar KT-MT interactions by maintaining the stability of two essential structural components of the Dam1 complex, Dam1 and Duo1. Our data implicate Kap121 as a key regulator of chromosome transmission during cell division.

# **Chapter II:** *Experimental procedures*

**2.1 Yeast strains and media**

All yeast strains were grown in YPD (1% yeast extract, 2% bactopeptone, 2% glucose) at 23°C unless otherwise indicated. Cells harboring plasmids yielding prototropic markers were propagated in synthetic drop out medium (SM) containing 2% glucose (Sherman et al., 1983). In cases where strains utilized were deficient for adenine biosynthesis (w303 and YPH499), excess adenine was supplemented into the appropriate growth medium at a final concentration of 120 μg/mL. Yeast transformations involving autonomously replicating plasmids or PCR/plasmid-derived linear DNA fragments for targeted genomic integration were performed using the lithium acetate/polyethylene glycol (PEG)-based method (Schiestl and Gietz, 1989). Briefly, cell cultures (25 mL) were grown overnight to mid-logarithmic phase ($OD_{600}$ ~0.5-1.0), collected by centrifugation (Eppendorf 5810R, A-4-62 rotor at 4000 RPM for 5 min) washed twice with cold dd$H_20$ (25 mL), washed once with SORB transformation buffer (10 mM Tris-HCl, pH 8.0, 1 mM ethylenediaminetetraacetic acid {EDTA}/sodium hydroxide {NaOH}, pH 8.0, 100 mM lithium acetate {LiOAc}, 1 M sorbitol). Next, cells were resuspended in 250 μL of transformation buffer containing 5 μg/mL denatured salmon sperm DNA (ssDNA). The resulting slurry was aliquoted into 50 μL volumes and stored at -80°C.

For plasmid transformations, 1 μL of plasmid DNA was added to 50 μL of cell slurry. For transformations involving linear DNA fragments for targeted genomic integration, 10 μL of linear DNA (PCR or plasmid-based) were added to 50 μL of competent cells. Following DNA addition, cells were mixed thoroughly, and a 6-fold volume of PEG transformation buffer (100 mM LiOAc, 10 mM Tris–HCl, pH 8.0, 1 mM

EDTA/NaOH, pH 8.0, 40% polyethylene glycol {PEG} 3350) was added directly to the cell slurry. The resulting mixture was incubated at 23°C for 30 min while maintaining continual mixing at 5-min intervals. Dimethyl sulphoxide (DMSO) was added at a final concentration of 10%, and the cells were then placed in a 42°C water bath for ~15 min. Next, cells were sedimented (Beckman Coulter microfuge 18 centrifuge, 5000 rpm for 5 min), washed twice with dd$H_20$ (1 mL), and resuspended in the appropriate medium for overnight rescue at 23°C. The following day, the cells were sedimented and plated onto the appropriate medium. When prototropic selection markers were used, cells were plated ontoo SM medium lacking the corresponding amino acid. When cassettes containing dominant resistant markers were utilized, i.e. *KanMX6*, *NatMX6* or *HphMX6*, cells were plated onto YPD supplemented with the appropriate drug, i.e. kanamycin, nourseothricin, or hygromycin.

DNA cassettes for endogenous genomic integrations were produced using a one-step PCR-based method (Longtine et al., 1998), and the appropriate haploid yeast strains (w303a, DF5a, YPH499 and BY4741) were transformed. All DNA cassettes utilized for transformation were produced using either Expand High Fidelity or Expand Long Template PCR systems (Roche Applied Science, Indianapolis, IN). Template DNA utilized in the aforementioned PCR reactions were derived from either chromosomal or plasmid DNA. For endogenous integration of carboxy-terminal tags ($GFP_{S65T}$, *GFP+*, *mRFP*, *mCherry*, *pA*, $HA_3$, $MYC_{13}$), oligonucleotides, usually 80 base pairs (bp) in length, were designed with sequence homologous to regions immediately upstream and downstream (60 bp region in either direction) of the stop codon of the gene of interest, while the remaining 20 bp were homologous with the appropriate template DNA. For

endogenous integration of regulatable promoter sequences (*GAL1/10* and *MET3*), 80-bp oligonucleotides were designed with sequence homologous to regions immediately upstream and downstream (60 bp region in either direction) of the start codon of the gene of interest. All targeted genomic integrations were confirmed by either PCR or western blotting to ascertain the correct integration event.

**Table 2-1. Yeast strains**

| Name | Genotype | Source |
|---|---|---|
| W303-1a | *MATa ade2-1 ura3-1 his3-11 trp1-1 leu2-3,112 can1-100 (W303-1a)* | ATCC |
| YLC100 | *MATa ade2-1 his3-11 trp1-1 leu2-3,112 can1-100 ura3-1Δ::NLS$^{Pho4}$-GFP::URA3 (W303-1a)* | This study |
| YLC101 | *MATa ade2-1 ura3-1 his3-11 trp1-1 can1-100 leu2-3,112Δ::NLS$^{SV40}$-GFP::LEU2 (W303-1a)* | This study |
| YLC102 | *MATa ade2-1 his3-11 trp1-1 leu2-3,112 can1-100 ura3-1Δ::NLS$^{Pho4}$-GFP::URA3 cdc20Δ::KanR-P$_{MET3}$-HA3-CDC20 (W303-1a)* | This study |
| YLC103 | *MATa ade2-1 ura3-1 his3-11 trp1-1 can1-100 leu2-3,112Δ::NLS$^{SV40}$-GFP::LEU2 cdc20Δ::KanR-P$_{MET3}$-HA3-CDC20 (W303-1a)* | This study |
| YLC104 | *MATa ade2-1 his3-11 leu2-3,112 trp1-1 can1-100 ura3-1Δ::NLS$^{Pho4}$-GFP::URA3 cdc20Δ::KanR-P$_{MET3}$-HA3-CDC20 mad2Δ::HIS5 (W303-1a)* | This study |
| YLC105 | *MATa ade2-1 his3-11 trp1-1 leu2-3,112 can1-100 ura3-1Δ::NLS$^{Pho4}$-GFP::URA3 cdc20Δ::KanR-P$_{MET3}$-HA3-CDC20 mad1Δ::NatR (W303-1a)* | This study |
| Y1104 | *MATa ade2-1 ura3-1 his3-11 trp1-1 leu2-3,112 can1-100 ask1-2 (W303-1a)* | Li et al., 2002 |
| YLC106 | *MATa ade2-1 his3-11 trp1-1 leu2-3,112 can1-100 ura3-1Δ::NLS$^{Pho4}$-GFP::URA3 ask1-2 (W303-1a)* | This study |

| | | |
|---|---|---|
| SBY1117 | *MATa ade2-1 ura3-1 his3-11 trp1-1 leu2-3,112 can1-100 ndc80-1 (W303-1a)* | Sue Biggins |
| YLC107 | *MATa ade2-1 his3-11 trp1-1 leu2-3,112 can1-100 ura3-1Δ::NLS$^{Pho4}$-GFP::URA3 ndc80-1 (W303-1a)* | This study |
| SBY7211 | *MATa ade2-1 ura3-1 his3-11 trp1-1 leu2-3,112 can1-100 mcd1-1 (W303-1a)* | Sue Biggins |
| YLC108 | *MATa ade2-1 his3-11 trp1-1 leu2-3,112 can1-100 ura3-1Δ::NLS$^{Pho4}$-GFP::URA3 mcd1-1 (W303-1a)* | This study |
| SBY2189 | *MATa ade2-1 ura3-1 his3-11 trp1-1 leu2-3,112 can1-100 bar1-1 ip11-321 (W303-1a)* | Kotwaliwal e et al., 2007 |
| YLC109 | *MATa ade2-1 his3-11 trp1-1 leu2-3,112 can1-100 ura3-1Δ::NLS$^{Pho4}$-GFP::URA3 ipl1-321 (W303-1a)* | This study |
| YLC110 | *MATa ade2-1 ura3-1 his3-11 trp1-1 can1-100 leu2-3,112Δ::NLS$^{SV40}$-GFP::LEU2 ask1-2 (W303-1a)* | This study |
| YLC111 | *MATa ade2-1 ura3-1 his3-11 trp1-1 can1-100 leu2-3,112Δ::NLS$^{SV40}$-GFP::LEU2 ndc80-1 (W303-1a)* | This study |
| YLC112 | *MATa ade2-1 ura3-1 his3-11 trp1-1 can1-100 leu2-3,112Δ::NLS$^{SV40}$-GFP::LEU2 mcd1-1 (W303-1a)* | This study |
| YLC113 | *MATa ade2-1 his3-11 trp1-1 can1-100 leu2-3,112Δ::NLS$^{Pho4}$-GFP::LEU2 ura3-1Δ::P$_{GAL1}$-MPS1MYC::URA3 (W303-1a)* | This study |
| YLC114 | *MATa ade2-1 his3-11 trp1-1 can1-100 leu2-3,112Δ::NLS$^{SV40}$-GFP::LEU2 ura3-1Δ::P$_{GAL1}$-MPS1MYC::URA3 (W303-1a)* | This study |
| YLC115 | *MATa ade2-1 his3-11 trp1-1 leu2-3,112 can1-100 Mad1-GFP::HIS5 Mtw1-mRFP::NatR ura3-1Δ::P$_{GAL1}$-MPS1MYC::URA3 (W303-1a)* | This study |
| YLC116 | *MATa ade2-1 his3-11 trp1-1 leu2-3,112 can1-100 Mad1-GFP::HIS5 Mtw1-mRFP::NatR nup60Δ::HphR ura3-1Δ::P$_{GAL1}$-MPS1MYC::URA3 (W303-1a)* | This study |
| YLC117 | *MATa ade2-1 his3-11 trp1-1 leu2-3,112 can1-100 ura3-1Δ::NLS$^{Pho4}$-GFP::URA3 nup60Δ::KanR (W303-1a)* | This study |

| | | |
|---|---|---|
| YLC118 | *MATa ade2-1 his3-11 trp1-1 leu2-3,112 can1-100 ura3-1Δ::NLS$^{Pho4}$-GFP::URA3 mlp1Δ::KanR mlp2Δ::NatR (W303-1a)* | This study |
| KWY175 | *MATa ade2-1 ura3-1 his3-11 trp1-1 leu2-3,112 can1-100 (*p*xpo1T539C, HIS3) xpo1Δ::LEU2 (W303-1a)* | Stade et al., 1997 |
| YLC120 | *MATa ade2-1 ura3-1 his3-11 trp1-1 leu2-3,112 can1-100 Mad1-GFP::HIS5 Mtw1-mCherry::NatR (W303-1a)* | This study |
| YLC121 | *MATa ade2-1 ura3-1 his3-11 trp1-1 leu2-3,112 can1-100 Mad1-GFP::HIS5 Mtw1-mCherry::NatR ask1-2 (W303-1a)* | This study |
| YLC122 | *MATa ade2-1 ura3-1 his3-11 trp1-1 leu2-3,112 can1-100 Mad1-GFP::HIS5 Mtw1-mCherry::NatR ndc80-1 (W303-1a)* | This study |
| YLC123 | *MATa ade2-1 ura3-1 his3-11 trp1-1 leu2-3,112 can1-100 Mad1-GFP::HIS5 Mtw1-mCherry::NatR mcd1-1 (W303-1a)* | This study |
| YLC124 | *MATa ade2-1 ura3-1 his3-11 trp1-1 leu2-3,112 can1-100 Mad1-GFP::HIS5 Mtw1-mCherry::NatR ipl1-321 (W303-1a)* | This study |
| YLC125 | *MATa ade2-1 his3-11 trp1-1 leu2-3,112 can1-100 Mlp1-GFP::HIS5 Mad1-mCherry::NatR nup60Δ::HphR ura3-1Δ::P$_{GAL1}$-MPS1MYC::URA3 (W303-1a)* | This study |
| YLC126 | *MATa ade2-1 his3-11 trp1-1 leu2-3,112 can1-100 ura3-1Δ::NLS$^{Pho4}$-GFP::URA3 ipl1-321 cdc20Δ::KanR-P$_{MET3}$-HA3-CDC20 (W303-1a)* | This study |
| YLC127 | *MATa ade2-1 his3-11 trp1-1 leu2-3,112 can1-100 ura3-1Δ::NLS$^{Pho4}$-GFP::URA3 bar1Δ::KanR (W303-1a)* | This study |
| YLC128 | *MATa ade2-1 his3-11 trp1-1 leu2-3,112 can1-100 ura3-1Δ::mad1$^{318-749}$-GFP::URA3 nup60Δ::HphR Mlp1-RFP::NatR (W303-1a)* | This study |
| DF5a | *Mata ura3-52 his3Δ200 leu2-3,112 lys2-801 (DF5)* | Brachmann et al., 1998 |
| FSY160 | *Mata his3Δ200 leu2-3,112 lys2-801 tub1Δ::HIS3 tub3Δ::TRP1 (*p*tub1-729, LEU2) ura3-52Δ* | Abruzzi et al., 1998 |

| | | |
|---|---|---|
| KWY175 | *MATa ade2-1 ura3-1 his3-11 trp1-1 leu2-3,112 can1-100 (*p*xpo1T539C, HIS3) xpo1Δ::LEU2 (W303-1a)* | Stade et al., 1997 |
| YLC134 | *Mata his3Δ200 leu2-3,112 lys2-801 ura3-52Δ::NLS$^{Pho4}$-GFP::URA3 (DF5)* | This study |
| YPH499 | *MATa ura3-52 ade2-101 trp1-63 his3-200 leu2-1 trp1-63 lys2-801 (YPH499)* | Sikorski and Hieter, 1989 |
| YLC135 | *MATa ura3-52 ade2-101 trp1-63 his3-200 leu2-1Δ::NLS$^{Pho4}$-GFP::LEU2 trp2 lys2-801 Δ::P$_{GAL1}$-clb2$^{db}$::LYS2 (YPH499)* | This study |
| YLC136 | *MATa ade2-1 ura3-1 his3-11 leu2-3,112 trp1-1 can1-100 cdc20Δ::KanR-P$_{MET3}$-HA3-CDC20 Mad1-GFP::HIS5 Mtw1-mCherry::NatR (W303-1a)* | This study |
| YLC137 | *MATa ade2-1 ura3-1 his3-11 leu2-3,112 trp1-1 can1-100 cdc20Δ::KanR-P$_{MET3}$-HA3-CDC20 mad2Δ::HphR Mad1-GFP::HIS5 Mtw1-mCherry::NatR (W303-1a)* | This study |
| YLC202 | *Mata ura3-52 his3Δ200 leu2-3,112 lys2-801 (*p*kap121-34,TRP1) kap121Δ::LEU2 (DF5)* | Leslie et. al, 2002 |
| YLC215 | *Mata ura3-52 his3Δ200 leu2-3,112 lys2-801 Duo1-GFP::HIS5 (*p*kap121-34,TRP1) kap121Δ::LEU2 (DF5)* | This study |
| YLC242 | *MATa ade2-1 ura3-1 his3-11 trp1-1 leu2-3,112 can1-100 Glc7-GFP::HIS5 ndc80-1 (W303-1a)* | This study |
| YLC252 | *MATa ade2-1 his3-11 trp1-1 leu2-3,112 can1-100 ura3-1Δ::NLS$^{Pho4}$-GFP::URA3 (*p*xpo1T539C,HIS3) xpo1Δ::LEU2 (W303-1a)* | This study |
| YLC264 | *Mata ura3-52 his3Δ200 leu2-3,112 lys2-801 Glc7-GFP::HIS5 kap121::LEU2(* p*Kap121-34,TRP1) (DF5)* | This study |
| YLC288 | *MATa ade2-1 ura3-1 his3-11 trp1-1 leu2-3,112 can1-100 Glc7-GFP::HIS5 (W303-1a)* | This study |
| YLC298 | *Mata ura3-52 his3Δ200 leu2-3,112 lys2-801 Glc7-GFP::HIS5 (DF5)* | This study |
| YLC302 | *MATa ade2-1 ura3-1 his3-11 trp1-1 leu2-3,112 can1-100 nup53Δ::nup53ΔKBD-Nuf2 3'UTR-NatR (W303-1a)* | This study |

| | | |
|---|---|---|
| YLC306 | *MATa ade2-1 ura3-1 his3-11 trp1-1 leu2-3,112 can1-100 Glc7-GFP::HIS5 cdc20Δ::KanR-$P_{MET3}$-HA3-CDC20 ndc80-1 (W303-1a)* | This study |
| YLC324 | *MATa ade2-1 ura3-1 his3-11 trp1-1 leu2-3,112 can1-100 mad1Δ::NatR Glc7-GFP::HIS5 cdc20Δ::KanR-$P_{MET3}$-HA3-CDC20 ndc80-1 (W303-1a)* | This study |
| YLC326 | *MATa ade2-1 ura3-1 his3-11 trp1-1 leu2-3,112 can1-100 mad2Δ::NatR Glc7-GFP::HIS5 cdc20Δ::KanR-$P_{MET3}$-HA3-CDC20 ndc80-1 (W303-1a)* | This study |
| YLC343 | *Mata his3Δ200 leu2-3,112 lys2-801 tub1Δ::HIS3 tub3Δ::TRP1(*p*tub1-729, LEU2) ura3-52Δ::NLS$^{SV40}$-GFP::URA3 (DF5)* | This study |
| YLC344 | *Mata his3Δ200 leu2-3,112 lys2-801 ura3-52Δ::NLS$^{SV40}$-GFP::URA3 (DF5)* | This study |
| YLC351 | *MATa ade2-1 his3-11 trp1-1 leu2-3,112 can1-100 mad1Δ::NatR cdc20Δ::KanR-$P_{MET3}$-HA3-CDC20 ura3-52Δ::NLS$^{Pho4}$-GFP::URA3Δ::HIS5 (*p*MAD1, URA3) (W303-1a)* | This study |
| YLC352 | *MATa ade2-1 his3-11 trp1-1 leu2-3,112 can1-100 mad1Δ::NatR cdc20Δ::KanR-$P_{MET3}$-HA3-CDC20 ura3-52Δ::NLS$^{Pho4}$-GFP:: URA3Δ::HIS5 (*p*mad1$^{318-749}$, URA3) (W303-1a)* | This study |
| YLC353 | *MATa ade2-1 his3-11 trp1-1 leu2-3,112 can1-100 mad1Δ::NatR cdc20Δ::KanR-$P_{MET3}$-HA3-CDC20 ura3-52Δ::NLS$^{Pho4}$-GFP:: URA3Δ::HIS5 (*p*mad1$^{475-749}$, URA3) (W303-1a)* | This study |
| YLC354 | *MATa ade2-1 his3-11 trp1-1 leu2-3,112 can1-100 mad1Δ::NatR cdc20Δ::KanR-$P_{MET3}$-HA3-CDC20 ura3-52Δ::NLS$^{Pho4}$-GFP:: URA3Δ::HIS5 (*p*mad1$^{1-325}$, URA3) (W303-1a)* | This study |
| YLC356 | *MATa ade2-1 ura3-1 his3-11 trp1-1 leu2-3,112 can1-100 nup53Δ::nup53ΔKBD-Nuf2 3'UTR-NatR ipl1-321 (W303-1a)* | This study |
| SBY1306 | *MATa ade2-1 ura3-1 his3-11 trp1-1::glc7-10::TRP1 leu2-3,112 can1-100 glc7::LEU2 bar1-1 (W303-1a)* | Pinsky et al., 2006 |

| | | |
|---|---|---|
| YLC357 | *MATa ade2-1 ura3-1 his3-11 trp1-1::glc7-10::TRP1 leu2-3,112 can1-100 glc7::LEU2 bar1-1 nup53Δ::nup53ΔKBD-Nuf2 3'UTR-NatR (W303-1a)* | This study |
| YLC413 | *Mata ura3-52 his3Δ200 leu2-3,112 lys2-801 (*p*kap121-34,TRP1) kap121Δ::LEU2 Dam1-GFP::HIS5 (DF5)* | This study |
| YLC425 | *Mata ura3-52 his3Δ200 leu2-3,112 lys2-801 Mtw1-GFP::HIS5 (*p*kap121-34,TRP1) kap121Δ::LEU2 (DF5)* | This study |
| YLC427 | *Mata ura3-52 his3Δ200 leu2-3,112 lys2-801 nup53Δ::KanR-*$P_{GAL1}$*-HA3-NUP53 (DF5)* | This study |
| YLC431 | *Mata ura3-52 his3Δ200 leu2-3,112 lys2-801 (*p*kap121-34,TRP1) kap121Δ::LEU2 his3Δ200::*$P_{MET3}$*-GFPTUB1::HIS3 (DF5)* | This study |
| YLC435 | *Mata ura3-52 his3Δ200 leu2-3,112 lys2-801 his3Δ200::*$P_{MET3}$*-GFPTUB1::HIS3 (DF5)* | This study |
| YLC436 | *Mata ura3-52 his3Δ200 leu2-3,112 lys2-801 (*p*kap121-34,TRP1) kap121Δ::LEU2 his3Δ200::*$P_{MET3}$*-GFPTUB1::HIS3 Mtw1-mCherry::NatR (DF5)* | This study |
| YLC437 | *Mata ura3-52 his3Δ200 leu2-3,112 lys2-801 Mtw1-GFP::HIS5 (DF5)* | This study |
| YLC459 | *Mata ura3-52 his3Δ200 leu2-3,112 lys2-801 (*p*kap121-41,TRP1) kap121Δ::LEU2 (DF5)* | This study |
| YLC468 | *Mata ura3-52 his3Δ200 leu2-3,112 lys2-801 Duo1-GFP::HIS5 (DF5)* | This study |
| YLC485 | *Mata ura3-52 his3Δ200 leu2-3,112 lys2-801 Dam1-GFP::HIS5 (DF5)* | This study |
| YLC487 | *Mata ura3-52 his3Δ200 leu2-3,112 lys2-801 (*p*kap121-41,TRP1) kap121Δ::LEU2 Duo1-GFP::His5 (DF5)* | This study |
| YLC493 | *Mata ura3-52 his3Δ200 leu2-3,112 lys2-801 Dam1-GFP::HIS5 (DF5)* | This study |
| YLC500 | *MATa ade2-1 his3-11 trp1-1 leu2-3,112 can1-100 kap121Δ::KanR-*$P_{MET3}$*-HA3-KAP121 (W303-1a)* | This study |

| | | |
|---|---|---|
| YLC503 | *Mata ura3-52 his3Δ200 leu2-3,112 lys2-801 (*p*kap121-34,TRP1) kap121Δ::LEU2 mad1::KanR (DF5)* | This study |
| YLC516 | *Mata ura3-52 his3Δ200 leu2-3,112 lys2-801 mad2::HphR (DF5)* | This Study |
| YLC517 | *Mata ura3-52 his3Δ200 leu2-3,112 lys2-801 (*p*kap121-34,TRP1) kap121Δ::LEU2 mad2::HphR (DF5)* | This study |
| YLC540 | *Mata ura3-52 his3Δ200 leu2-3,112 lys2-801 (*p*kap121-34,TRP1) kap121Δ::LEU2 cdc20Δ::KanR-$P_{MET3}$-HA3-CDC20 Mtw1-GFP::HIS5(DF5)* | This study |
| YLC546 | *Mata ura3-52 his3Δ200 leu2-3,112 lys2-801 cdc20Δ::KanR-$P_{MET3}$-HA3-CDC20 Mtw1-GFP::HIS5(DF5)* | This study |
| YLC554 | *Mata ura3-52 his3Δ200 leu2-3,112 lys2-801 (*p*kap121-34,TRP1) kap121Δ::LEU2 Duo1-pA::HIS5 (DF5)* | This study |
| YLC559 | *Mata ura3-52 his3Δ200 leu2-3,112 lys2-801 Kap121-pA::HIS5 Duo1-13MYC::KanR (DF5)* | This study |
| YLC561 | *Mata ura3-52 his3Δ200 leu2-3,112 lys2-801 Kap121-pA::HIS5 Ipl1-13MYC::KanR (DF5)* | This study |
| YLC569 | *Mata ura3-52 his3Δ200 leu2-3,112 lys2-801 Kap121-pA::HIS5 Dam1-13MYC::KanR (DF5)* | This study |
| YLC577 | *Mata ura3-52 his3Δ200 leu2-3,112 lys2-801 Kap121-pA::HIS5 Mtw1-3HA::KanR (DF5)* | This study |
| YLC579 | *Mata ura3-52 his3Δ200 leu2-3,112 lys2-801 Kap121-13MYC::KanR Ipl1-pA::HIS5 (DF5)* | This study |
| YLC595 | *Mata ura3-52 his3Δ200 leu2-3,112 lys2-801 Mtw1-GFP::HIS5 kap123::KanR (DF5)* | This study |
| YLC597 | *Mata ura3-52 his3Δ200 leu2-3,112 lys2-801 (*p*kap121-34,TRP1) kap121Δ::LEU2 Duo1-pA::His5 (DF5)* | This study |
| YLC599 | *Mata ura3-52 his3Δ200 leu2-3,112 lys2-801 (*p*kap121-34,TRP1) kap121Δ::LEU2 Dam1-pA::His5 (DF5)* | This study |

| | | |
|---|---|---|
| YLC605 | *Mata ura3-52 his3Δ200 leu2-3,112 lys2-801 (*p*kap121-34,TRP1) kap121Δ::LEU2 Ipl1-pA::His5 (DF5)* | This study |
| YLC642 | *Mata ura3-52 his3Δ200 leu2-3,112 lys2-801 Mtw1-GFP::NatR Duo1-pA::His5 (*p*kap121-34,TRP1) kap121Δ::LEU2 (DF5)* | This study |
| YLC649 | *Mata ura3-52 his3Δ200 leu2-3,112 lys2-801 (*p*kap121-34,TRP1) kap121Δ::LEU2 Mtw1-GFP::His5 (pRS316KAP121) (DF5)* | This study |
| YLC652 | *Mata ura3-52 his3Δ200 leu2-3,112 lys2-801 (*p*kap121-34,TRP1) kap121Δ::LEU2 Mtw1-GFP::His5 (pRS316) (DF5)* | This study |
| YLC655 | *Mata ura3-52 his3Δ200 leu2-3,112 lys2-801 Mtw1-GFP::HIS5 Spc42-mCherry::NatR (DF5)* | This study |
| YLC657 | *MATa his3Δ1 leu2Δ0 ura3Δ0 met15Δ0 duo1-2::Kan Mtw1-GFP::NatR (BY4741)* | This study |
| YLC661 | *MATa his3Δ1 leu2Δ0 ura3Δ0 met15Δ0 kap121-34::KanR kap121-34-GFP::Nat Ndc1-mCherry::NatR (BY4741)* | This study |
| YLC665 | *Mata his3Δ200 leu2-3,112 lys2-801 (*p*kap121-34,TRP1) kap121Δ::LEU2 ura3-52::NLS$^{Pho4}$-GFP::URA3 Duo1-mCherry::NatR (DF5)* | This study |
| YLC666 | *Mata ura3-52 his3Δ200 leu2-3,112 lys2-801 (*p*kap121-41,TRP1) kap121Δ::LEU2 Mtw1-GFP::His5 Spc42-mCherry::NatR (DF5)* | This study |
| YLC675 | *MATa his3Δ1 leu2Δ0 ura3Δ0 met15Δ0 Mtw1-GFP::Nat Ndc1-mCherry::NatR (BY4741)* | This study |
| YLC676 | *MATa ade2-1 ura3-1 his3-11 trp1-1 leu2-3,112 can1-100 ndc80-1 Mtw1-GFP::NatR (W303-1a)* | This study |
| YLC694 | *Mata ura3-52 his3Δ200 leu2-3,112 lys2-801 Ame1-GFP::HIS5 (DF5)* | This study |
| YLC697 | *Mata his3Δ200 leu2-3,112 lys2-801 Kap121-pA::HIS5 Mtw1-mCherry::NatR ura3-52::NLS$^{Pho4}$-GFP::URA3 (DF5)* | This study |

| | | |
|---|---|---|
| YLC700 | *Mata ura3-52 his3Δ200 leu2-3,112 lys2-801 Duo1-GFP::HIS5 Spc42-mCherry::NatR (*p*kap121-34,TRP1) kap121Δ::LEU2 (DF5)* | This study |
| YLC712 | *Mata ura3-52 his3Δ200 leu2-3,112 lys2-801 Duo1-GFP::HIS5 Nup159-mCherry::NatR (DF5)* | This study |
| YLC713 | *Mata ura3-52 his3Δ200 leu2-3,112 lys2-801 Ipl11-GFP::HIS5 Nup159-mCherry::NatR (DF5)* | This study |
| YLC714 | *Mata his3Δ200 leu2-3,112 lys2-801 (*p*kap121-34,TRP1) kap121Δ::LEU2 ura3-52::NLS$^{Pho4}$-GFP::URA3 Mtw1-mCherry::NatR (DF5)* | This study |
| YLC718 | *Mata ura3-52 his3Δ200 leu2-3,112 lys2-801 (*p*kap121-34,TRP1) kap121Δ::LEU2 Ipl11-GFP::HIS5 Nup159-mCherry::NatR (DF5)* | This study |
| YLC719 | *Mata ura3-52 his3Δ200 leu2-3,112 lys2-801 (*p*kap121-34,TRP1) kap121Δ::LEU2 Duo1-GFP::HIS5 Nup159-mCherry::NatR (DF5)* | This study |
| YLC721 | *Mata ura3-52 his3Δ200 leu2-3,112 lys2-801 Dam1-GFP::HIS5 Nup159-mCherry::NatR (DF5)* | This study |
| YLC722 | *Mata ura3-52 his3Δ200 leu2-3,112 lys2-801 Spc105-GFP::HIS5 (DF5)* | This study |
| YLC723 | *Mata ura3-52 his3Δ200 leu2-3,112 lys2-801 Ame1-GFP::HIS5 (DF5)* | This study |
| YLC724 | *Mata ura3-52 his3Δ200 leu2-3,112 lys2-801 Duo1-3HA::KanR Mtw1-GFP::HIS5 (*p*kap121-34,TRP1) kap121Δ::LEU2 (DF5)* | This study |
| YLC735 | *MATa ade2-1 his3-11 trp1-1 leu2-3,112 can1-100 kap121Δ::KanR-P$_{MET3}$-HA3-KAP121 Mtw1-GFP::HIS5 Spc42-mCherry::NatR (W303-1a)* | This study |
| YLC743 | *MATa ade2-1 his3-11 trp1-1 leu2-3,112 can1-100 kap121Δ::KanR-P$_{MET3}$-HA3-KAP121 Duo1-GFP::HIS5 Spc42-mCherry::NatR (W303-1a)* | This study |
| YLC745 | *MATa ade2-1 his3-11 trp1-1 leu2-3,112 can1-100 kap121Δ::KanR-P$_{MET3}$-HA3-KAP121 Duo1-GFP::HIS5 Mtw1-mCherry::NatR (W303-1a)* | This study |
| YLC746 | *Mata ura3-52 his3Δ200 leu2-3,112 lys2-801 Kap121-13MYC::KanR Dam1-pA::HIS5 (DF5)* | This study |

| | | |
|---|---|---|
| YLC747 | *Mata ura3-52 his3Δ200 leu2-3,112 lys2-801 Kap121-13MYC::KanR Duo1-pA::HIS5 (DF5)* | This study |
| YLC752 | *Mata his3Δ200 leu2-3,112 lys2-801 (*p*kap121-34,TRP1) kap121Δ::LEU2 Duo1Δ::KanR-*$P_{MET3}$*-HA3-Duo1-GFP::HIS5 (DF5)* | This study |
| YLC754 | *MATa his3Δ1 leu2Δ0 met15Δ0 kap121-34::KanR ura3Δ0::NLS*$^{Pho4}$*-GFP::URA3 (*p*RS315KAP121) (BY4741)* | This study |
| YLC758 | *Mata his3Δ200 leu2-3,112 lys2-801 (*p*kap121-34,TRP1) kap121Δ::LEU2 Duo1Δ::KanR-*$P_{MET3}$*-HA3-Duo1 Mtw1-GFP::HIS5 (DF5)* | This study |
| YLC766 | *Mata ura3-52 his3Δ200 leu2-3,112 lys2-801 (*p*kap121-34,TRP1) kap121Δ::LEU2 Dam1-GFP::HIS5 Nup159-mCherry::NatR (DF5)* | This study |
| YLC768 | *Mata ura3-52 his3Δ200 leu2-3,112 lys2-801 Duo1-3HA::KanR (DF5)* | This study |
| YLC800 | *MATa his3Δ1 leu2Δ0 ura3Δ0 met15Δ0 kap121-34::Kan kap121-34-pA::HpHR Ipl1-13MYC::HIS5(BY4741)* | This study |
| YLC801 | *MATa his3Δ1 leu2Δ0 ura3Δ0 met15Δ0 kap121-34::Kan kap121-34-pA::HpHR Dam1-13MYC::HIS5(BY4741)* | This study |
| YLC804 | *MATa his3Δ1 leu2Δ0 ura3Δ0 met15Δ0 kap121-34::Kan kap121-34-pA::HpHR Duo1-13MYC::HIS5(BY4741)* | This study |
| YLC810 | *Mata ura3-52 his3Δ200 leu2-3,112 lys2-801 Nup53-pA::HIS5 Kap121-13MYC::KanR (DF5)* | This study |
| YLC816 | *Mata ura3-52 his3Δ200 leu2-3,112 lys2-801 Dam1-3HA::KanR (DF5)* | This study |
| YLC817 | *Mata ura3-52 his3Δ200 leu2-3,112 lys2-801 (*p*kap121-41,TRP1) kap121Δ::LEU2 Dam1-3HA::KanR (DF5)* | This study |

**2.2 Plasmids**

The plasmids listed in this section were acquired from a range of sources and used to complete this body of work. These include: pRS313*xpo1*$^{T539C}$*, CEN/HIS3* (a generous gift from Dr. Karsten Weis, University of California Berkeley, Berkeley, CA); pRS314*kap121-34*, *CEN/TRP1* (Leslie et al., 2002); pRS314*kap121-41*, *CEN/TRP1* (Leslie et al., 2002); pRS315, *CEN/LEU2* (Sikorski and Hieter, 1989); pRS315*KAP121, CEN/LEU2* (Leslie et al., 2002), pRS315*NLS*$^{Pho4}$*-GFP*$_3$*, CEN/LEU2* (a generous gift from Dr. Erin O'Shea, University of California San Francisco, San Francisco, CA) (Kaffman et al., 1998); pRS315*KAP121, CEN/LEU2* (Leslie et al., 2002); pRS316, *CEN/URA3* (Sikorski and Hieter, 1989); pRS316*NLS*$^{Pho4}$*-GFP*$_3$*, CEN/URA3* (Kaffman et al., 1998); pRS316*MAD1*, *CEN/URA3* (Scott et al., 2005); pRS316*MAD1*$^{318-749}$, *CEN/URA3* (Scott et al., 2005); pRS316*MAD1*$^{475-749}$, *CEN/URA3* (Scott et al., 2005); pRS316*MAD1*$^{1-325}$, *CEN/URA3* (Scott et al., 2005). The plasmid pFA6a-kanMX6-*P*$_{MET3}$*-HA* (pTM1046) provided the template for the construction of both the *P*$_{MET3}$*-HA-KAP121* and *P*$_{MET3}$*-HA-CDC20* cassettes (Makio et al., 2009). The plasmid pFA6a-kanMX6-*P*$_{GAL1}$*-HA* was utilized as template DNA for the production of the *P*$_{GAL1}$*-HA-NUP53* cassette (Longtine et al., 1998).

The following plasmids were utilized for the production of carboxy-terminal gene fusions and include the following: pGFP/HIS5 (*EGFP*$_{F64L,S65T}$*-HIS5*; Dilworth et al., 2001), pGFP/NAT (*EGFP*$_{F64L,S65T}$*-NatR*), pGFP+/NAT (GFP+-*NatR*), pmCherry/NAT (*mCherry-NatR*) and pRFP/NAT (*mRFP-NatR*) (generous gifts from Dr. Richard Rachubinski, University of Alberta, Edmonton, AB); pProtA/HU (*protein A-HIS3-URA3*; Aitchison et al., 1995a); pBXA (*protein A- HIS5*; Aitchision et al., 1995), pFA6a-13Myc-kanMX6 (*13xMYC-KanR*; Longtine et al., 1998); pFA6a-13Myc-His3MX6 (*13xMYC-HIS3*;

Longtine et al., 1998); pFA6a-3HA-kanMX6 (*3HA-KanR*; Longtine et al., 1998); pFA6a-3HA-HisMX6 (*3HA-HIS3*; Longtine et al., 1998).

The plasmids encoding for $P_{GAL1}$-*MYC-MPS1* (pAFS120; a generous gift from Dr. Mark Winey, University of Colorado, Boulder, CO) and $P_{GAL1}clb2^{db}$ (pSB102; a munificent gift from Dr. Sue Biggins, Fred Hutchinson Cancer Research Center, Seattle, WA) were subjected to single enzyme digestion (StuI and BstEII, respectively) and were subsequently utilized for targeted genomic integration at either the *URA3* or *LYS2* gene locus.

### 2.3 Antibodies and buffers

**Table 2-2. Antibodies**

| Antigen | Antibody ID | Raised in | Dilution (Immunoblotting) | Reference |
|---|---|---|---|---|
| Mad1 | 3I4, Final bleed | Rabbit | 1:2,000 in PBS-T | Scott, R.J. (PhD Thesis, 2008) |
| Gsp1 | 4G9, Final bleed | Rabbit | 1:10,000 in PBS-T | Scott, R.J. (PhD Thesis, 2008) |
| GFP | 3B4, Final bleed | Rabbit | 1:2,000 in PBS-T | Scott, R.J. (PhD Thesis, 2008) |
| Kap121 | 5T5, Final bleed | Rabbit | 1:10,000 in PBS-T | Leslie, D.M. (PhD Thesis, 2004) |
| Nup53 | H174, Final bleed | Rabbit | 1:5,000 in PBS-T | Marelli et al., 1998 |
| Nup60 | 4-5, Final bleed | Rabbit | 1:2,000 in PBS-T | Van De Vosse, D.W. (PhD Thesis, 2012) |
| Protein A (pA) | Anti-protein A IgG, from Rabbit (P3775) | Rabbit | 1:10,000 in PBS-T | Sigma Aldrich |
| Clb2 | Clb2 (y-180): sc-9071 | Rabbit | 1:1,000 in PBS-T | Santa Cruz Biotechnology |
| Mad2 | 1E2, Third bleed | Rabbit | 1:500 in PBS-T | Scott, R.J. (PhD Thesis, 2008) |

| | | | | |
|---|---|---|---|---|
| Phospho-Histone-H3 (Ser10) | 3H10 | Mouse | 1:2,000 in TBS-T | EMD Millipore |
| Histone-H3 | Ab1791 | Rabbit | 1:2,000 in TBS-T | Abcam |
| Myc | 9E10 | Mouse | 1:10,000 in PBS-T | Roche Applied Science |
| HA | F-7 (sc-7392) | Mouse | 1:5000 in PBS-T | Santa Cruz Biotechnology Inc. |
| Mouse IgG | Anti-mouse IgG, HRP-conjugated (NXA931) | Sheep | 1:10,000 in PBS-T | GE Healthcare |
| Rabbit IgG | Anti-mouse IgG, HRP-conjugated (NA934) | Donkey | 1:10,000 in PBS-T | GE Healthcare |

**Table 2-3. Common Buffers and solutions.**

| Buffer | Composition |
|---|---|
| Phosphate buffered saline (PBS-T) | 137 mM NaCl, 2.7 mM KCl, 4.3 mM $Na_2HPO_4$, 1.4 mM $KH_2O_4$, pH 7.5, 0.05% Tween-20 |
| Tris buffered saline (TBS-T) | 20 mM Tris-HCl, pH 7.5, 150 mM NaCl, 0.05% Tween-20 |
| 5 x SDS-PAGE running buffer | 0.25 M Tris-HCl, pH 8.8, 2 M glycine, 0.5% SDS |
| 1 x Blotting buffer | 20 mM Tris-HCl, 150 mM glycine, 20% methanol |
| SDS-PAGE sample buffer | 20% glycerol, 167 mM Tris-HCl, pH 6.8, 2% SDS, 0.05% bromophenol blue |
| DNA loading buffer | 0.30% bromophenol blue, 0.30% xylene cyanol, 45% glycerol |
| 10 x Tris Buffered EDTA | 0.89 M Tris-borate, 0.89 M boric acid, 0.02 M EDTA |
| IP wash buffer | 20 mM HEPES-KOH, pH 7.4, 110 mM potassium acetate (KOAc), 2 mM $MgCl_2$ |

| | |
|---|---|
| IP buffer | 20 mM HEPES-KOH, pH 7.4, 110 mM KOAc, 2 mM $MgCl_2$, 0.1% Tween-20, antifoam-B emulsion (1:5000 dilution), protease inhibitor pellets (complete EDTA-free) |
| Ran IP buffer A | 20 mM HEPES-KOH, pH 7.4, 110 mM KOAc, 2 mM $MgCl_2$, 0.1% Tween-20, antifoam-B emulsion (1:5000 dilution), protease inhibitor pellets (complete EDTA-free), 0.5% glycerol, 0.5 mM dithiothreitol (DTT) |
| Ran IP buffer B | 20 mM HEPES-KOH, pH 7.4, 110 mM KOAc, 2 mM $MgCl_2$, 0.1% Tween-20, antifoam-B emulsion (1:5000 dilution), protease inhibitor pellets (complete EDTA-free), 0.5mM ATP |
| Ran buffer | 20 mM Tris-HCL pH 8.0, 110 mM KOAc, 2.0 mM magnesium acetate {$Mg(OAc)_2$}, 1.0 mM EGTA, 10% glycerol, 5 mM β-mercaptoethanol |
| Yeast breaking buffer | 2% Triton X-100, 1% SDS, 100 mM NaCl, 10 mM Tris-HCl, pH 8.0, 1 mM EDTA, pH 8.0 |
| SORB transformation buffer | 10mM Tris-HCl, pH 8.0, 1 mM EDTA/NaOH, pH 8.0, 100 mM LiOAc, 1 M sorbital |
| PEG transformation buffer | 100 mM LiOAc, 10 mM Tris–HCl pH 8.0, 1 mM EDTA/NaOH, pH 8.0, 40% PEG 3350 |
| FACS buffer | 50 mM Tris-HCl, pH8.0 |
| Tris-EDTA (TE) | 10 mM Tris-HCl, 1 mM EDTA, pH 7.5 |
| PBS-T wash buffer | 0.1% Tween-20, 137 mM NaCl, 2.7 mM KCl, 4.3 mM $Na_2HPO_4$, 1.4 mM $KH_2O_4$, pH 7.4 |
| TBS-T wash buffer | 0.1% Tween-20, 20 mM Tris-HCl, pH 7.5, 150 mM NaCl, 0.05% |
| Milk blocking buffer | 5% skim milk powder, 0.1% Tween-20, 20 mM Tris-HCl, pH 7.5, 150 mM NaCl |
| BSA blocking buffer | 2.5 % bovine serum albumin, 0.1% Tween-20, 20 mM Tris-HCl, pH 7.5, 150 mM NaCl |
| Amido Black | 40% methanol, 10% acetic acid, 0.1% amido black |

## 2.4 Immunopurification

### 2.4.1 Immunopurification of protein A-tagged proteins

Kap121-pA, kap121-34-pA, Nup53-pA, Duo1-pA, Dam1A and Ipl1A fusion proteins were purified from yeast cell extracts as described previously (Alber et al., 2007). Yeast cells producing pA-tagged fusion proteins were grown overnight in large volume cultures (1 L of YPD) to an $OD_{600}$ of 1.0 at either 23°C (*kap121-34* cells) or 30°C, and cells were subsequently sedimented by centrifugation (Beckman Coulter; JLA 10.5, 5000 x g for 5 min at 23°C). Following sedimentation, cells were washed twice in $ddH_20$ (250 mL) and once with IP wash buffer (250 mL). Next, cell pellets were transferred to a 5-mL syringe and were extruded from the syringe tip into liquid nitogen to produce "cryo-yeast noodles" for storage at -80°C. The cryo-yeast noodles were then transferred into stainless steel jars (50 mL internal volume; Retsch, Haan, Germany) with three stainless steel balls (20 mm in diameter; Retch), which were cooled in liquid nitrogen. Cryogenic lysis was then performed by utilizing a planetary ball mill (PM100; Retch; 8 cycles at 400 rpm for 1.5 min with cooling in liquid nitrogen between grinding sessions) yielding ~1.0-2.0 g of yeast cell lysate in powder form. Lysates were then briefly warmed on ice (~2 min) and IP buffer containing complete protease inhibitor cocktail tablets (1 pellet per 50 mL of buffer; Roche Applied Science, Indianapolis, IN) was added at a 1:2 weight-to-volume ratio. The resulting slurry was kept on ice for ~30 min with vigorous mixing at 5-10 min intervals followed by centrifugation (Eppendorf 5810R, A-4-62 rotor at 1500 x g for 10 min at 4°C). Cleared lysates were then transferred to 2-mL tubes, and IgG-conjugated magnetic beads were added at a ratio of 3 mg of beads to 2 mL of lysate and incubated at 4°C with end-over-end rotation for a total of 1 h.

Following binding, beads were collected on the tube wall using a magnetic stand for ~2.5 min, and the remaining lysate was aspirated. Next, the beads were then resuspended in cold IP buffer. Following resuspension, the beads were gently mixed and placed on the magnetic stand for collection. This washing step was repeated a total of 10 times prior to elution. Elution of bead-bound protein complexes was performed at 4°C using a step gradient of $MgCl_2$ (50, 500, and 2000 mM; 500 µL volumes), as well as a final 0.5 M acetic acid elution for a total of 3 min per elution. Eluates were then precipitated overnight at 4°C using a 10 % trichloroacetic acid (TCA)/0.015 % sodium deoxycholate mixture. The following day, the protein precipitates were subject to centrifugation at 4°C (Eppendorf 5810R, F-45-30-11 rotor at 13,100 x g for 30 min) and supernatant was separated from pellet by aspiration. The remaining protein was resuspended in 1 mL of ice-cold acetone and incubated at -20 °C for 2 h. Next, the resulting resuspension was spun down (Eppendorf 5810R, F-45-30-11 rotor at 13,100 x g for 30 min at 4°C), the supernatant was carefully removed, and the remaining protein was lyophilized in a centrifugal speed vacuum apparatus for 30 min at 60°C (Labconco, Kansas City, MO). Finally, lyophilized protein was resuspended in sample buffer, heated for 10 min at 90°C, and then analyzed by SDS-PAGE and western blot.

### 2.4.2 RanGTP release experiments

Purified human recombinant Ran (hRan) (a generous gift from Dr. Yuh Min Chook, University of Texas Southwestern, Dallas, TX) was loaded with either GDP or GTP nucleotide as follows: first, aliquots of hRan (~10 mg/mL) resuspended in Ran buffer (see Table 2-3) was incubated in the presence of 25 mM EDTA, 0.5 mM GTP or

GDP nucleotide (Sigma-Aldrich, St. Louis, MO, USA) and 2 mM DTT for 90 min on ice. Ran was loaded with nucleotide at a concentration of 10 mg/mL. Next, the nucleotide loading reaction was quenched by adding $Mg(OAc)_2$ to a final concentration of 30 mM. The samples were incubated on ice for 30 min, at which point they were flash-frozen in liquid nitrogen and stored at -80°C.

To perform the release experiments, Nup53-pA and Duo1-pA fusion proteins were affinity-purified from cell lysates containing Kap121-13Myc as described above (section 2.4.1). Following binding of pA fusions to the beads, the bead-bound complexes were washed 5 times with cold IP buffer containing protease inhibitor cocktail tablets (1 pellet per 50 mL of buffer). Next, IP buffer containing 0.5 mM ATP (Ran IP buffer A; see Table 2-3) was used to wash the beads for 30 min at 23°C while maintaining continual mixing by orbital rotation. The beads were collected on a magnet (~2.5 min) then resuspended in IP buffer containing 1 % glycerol and 0.5 mM DTT (Ran IP buffer B; see table 2-3). Next, RanGDP (5 μg), RanGTP (5 μg), or 1 mM GTP alone (all resuspended in Ran IP buffer B) was added directly to the beads and incubated for a period of 30 min at 23°C with end-over-end rotation. Beads were collected on the tube wall using a magnetic stand, and the solution containing proteins released from the beads was transferred to new tubes (the released fraction after Ran treatment). The collected beads were resuspended with 0.5 M acetic acid and incubated for 3 min at 23°C, allowing for all the remaining proteins on the beads to be released. Beads were again collected on the tube wall using magnetic stand, and the solution were transferred into new tubes (the bound fraction after Ran treatment). The released and the bound fractions were then

concentrated by TCA precipitation as described above (section 2.4.1). The samples were then analyzed by SDS-PAGE and western blot analysis.

### 2.4.3 IgG conjugation to epoxy-coated magnetic beads

IgG conjugation to Epoxy M-270 Dynabeads (Invitrogen, Carlsbad, CA) was performed as described previously (Alber et al., 2007). Lyophilized IgG from rabbit serum (Sigma-Aldrich, St. Louis, MO) was resuspended in 1 mL of sodium-phosphate buffer (0.1 M $NaPO_4$, pH 7.4) and then cleared by centrifugation (Eppendorf 5810R, F-45-30-11 rotor at 13,100 x g for 10 min at 4°C). Sodium-phosphate buffer (2 mL) and 3 M ammonium sulfate, pH 7.5 (1.33 mL) were added to the cleared IgG solution. The resulting IgG solution was passed through a 0.22 μM polyvinylidene difluoride (PVDF; low protein binding) filter. In parallel, Epoxy M-270 Dynabeads were washed in 3.6 mL of sodium phosphate buffer for 10 min at 23°C followed by a final wash (1 mL) in the same buffer. Next, the filtered IgG solution was mixed with the beads, and the resulting mixture was allowed to incubate overnight at 30°C for 20 h while rotating. Following this conjugation reaction, the beads were subject to a series of washing steps carried out at 23°C and included the following: 1) 1 x 1 mL of 100 mM glycine, pH 2.5, for ~30 sec, 2) 1 x 1 mL 10 mM Tris-HCL, pH 8.8, for 5 min, 3) 1 x 1 mL 100 mM triethylamine, pH 6.0, for ~30 sec, 4) 4 x 1 mL PBS for 5 min, 5) 1 x 1 mL PBS + 0.5% Triton X-100 for 5 min, 6) 1 x 1 mL PBS + 0.5% Triton X-100 for 15 min, 6) 3 x 1 mL PBS for 5 min. Immediately following the final washing step, the beads were resuspended in 2 mL of PBS containing sodium azide at a final concentration of 0.02% and stored at 4°C.

## 2.5 Western blotting

### 2.5.1 Preparation of yeast whole cell lysates

To prepare whole cell lysates, cells were grown overnight to an $OD_{600}$ of 1.0 in the appropriate medium, 200 µl of cells were harvested by centrifugation, and then resuspended in SDS-PAGE sample buffer (50-100 µl; see Table 2-3 for composition). Samples were vigorously sonicated and then heated in boiling water for approximately 10 min. Following denaturation, samples were clarified by centrifugation and loaded onto SDS-PAGE gels for further analysis.

### 2.5.2 SDS-PAGE and western blotting analysis

Proteins analyzed by western blot were initially separated by SDS-PAGE using 8-10% acrylamide gels and BioRad Mini Protean III units (BioRad, Hercules, CA). Resolved protein was then transferred to nitrocellulose membranes using BioRad Mini Trans-Blot transfer cells. Post-transfer membranes were stained with 2% amido black, and excess stain was removed by washing membranes 4-5 times with water. In most cases, 5% skim milk powder resuspended in PBS-T (PBS containing 0.1% Tween-20) was used as the blocking reagent. In some instances, 2.5% BSA resuspended in TBS-T was used as an alternative blocking reagent. In both cases, membranes were blocked for a period of 1 h at 23°C. Blocked membranes were then probed with the desired antibody at the optimal concentration (listed in Table 2-2), and allowed to incubate overnight at 4°C. Next, membranes were washed three times in 50-100 mL of PBS-T for 10 min intervals. The appropriate horseradish peroxidase (HRP)-conjugated secondary antibody (either sheep anti-mouse IgG or donkey anti-rabbit IgG; see Table 2-2), suspended in PBS-

T/skim milk solution, was incubated with the membranes in PBS-T/skim milk solution for a period of ~1-2 h. Membranes were washed three times with PBS-T, and detection of bound secondary antibody was achieved using the enhanced chemiluminescence (ECL) detection system (GE Healthcare, Chalfont St. Giles, United Kingdom) and Fuji RX film (FUJIFILM Canada Inc., Mississauga, ON). Depending on the primary antibody used, exposure times varied significantly (between 2 sec to 1.5 h).

**2.6 Benomyl sensitivity assay**

To assess benomyl sensitivity, cells were grown overnight in YPD at 23°C to an $OD_{600}$ of 0.8-1.2, diluted to equivalent cell densities, then spotted onto YPD plates supplemented with either vehicle alone (1% DMSO) or benomyl (Sigma-Aldrich, St. Louis, MO) at varying concentrations (5, 10, 15, 20 or 25 μg/mL) dissolved in 1% DMSO. Plates were incubated at 30°C for 2 days.

**2.7 Chemically-induced cell cycle synchronization**

To achieve G1 synchronization, cells were grown overnight at 23°C to an $OD_{600}$ of 1.0-1.5 and subsequently diluted ten-fold. Cells were then shifted to 30°C until an $OD_{600}$ of 0.3-0.4 was reached and α-factor (Sigma-Aldrich, St. Louis, MO, USA) was added directly to the medium. Depending on the presence or absence of the *BAR1* gene, α-factor was added at a final concentration of 10 μg/mL or 50 ng/mL, respectively. For increased synchronization efficiency for *BAR1* cells, α-factor was added to low pH (pH = 5.0) YPD as a means to attenuate rapid degradation of the mating pheromone.

To arrest cells in S-phase, cells were grown overnight to early logarithmic phase ($OD_{600}$ 0.3-0.4), and hydroxyurea (HU; Sigma-Aldrich, St. Louis, MO) was added directly to the medium at a final concentration of 250 mM. Following HU addition, cells were allowed to grow for ~3-4 h at 23°C before analysis. To confirm synchronization, cells were inspected microscopically for the accumulation of medium- to large- budded cells.

To achieve a chemically induced metaphase arrest, the microtubule destabilizing drug nocodazole (Calbiochem, Darmstadt, Germany) was added to cells at an $OD_{600}$ of ~0.4-0.8 at a final concentration of 20 μg/mL. Following nocodazole addition, cells were propagated for a period of 2.5 h at 23°C, and arrest efficiencies were verified microscopically.

**2.8 Galactose-induced overexpression**

*MPS1, clb2$^{db}$,* and *NUP53* genes were placed under control of the *GAL1/10* promoter for the purpose of overexpression. Briefly, strains harboring galactose-inducible versions of these genes ($P_{GAL1}$-*MPS1*, $P_{GAL1}$-*clb$^{db}$*, $P_{GAL1}$-*NUP53*) were grown overnight to an $OD_{600}$ of ~0.4-0.5 in YP medium containing 2% raffinose. Galactose was then added directly to the medium at a final concentration of 3%. Depending on the gene subjected to overexpression, cells incubated in the presence of galactose for a period of 4 to 10 h at 23°C (4 h for *MPS1* and *clb2$^{db}$*; 10 h for *NUP53*). Overproduction of the gene of interest was monitored by western blot analysis.

**2.9 Methionine-induced repression of *MET3* promoter controlled genes**

For repression of either *KAP121* or *CDC20*, both genes were placed under control of the regulatable *MET3* promoter ($P_{MET3}$-*HA-CDC20* or $P_{MET3}$-*HA-KAP121*). Briefly, strains harboring either the endogenously integrated $P_{MET3}$-*HA-CDC20* or $P_{MET3}$-*HA-KAP121* alleles were grown to mid-logarithmic phase ($OD_{600}$ of ~0.5-0.6) in SD medium lacking methionine. Next, cells were collected by centrifugation (Eppendorf 5810R, A-4-62 rotor at 1500 x g for 2.5 min at 23°C), resuspended in YPD medium supplemented with excess methionine (200 μg/mL), and grown for either 2.5 h (Cdc20 depletion) or 4 h (Kap121 depletion) at 23°C. Cellular depletion of either protein was inspected by western blot analysis.

**2.10 Inactivation of temperature-sensitive alleles**

Strains harboring conditional alleles (*mcd1-1, ask1-2, ndc80-1, ipl1-321, kap121-34, kap121-41, duo1-2)* were grown overnight in YPD (25 mL) at 23°C to mid-logarithmic phase ($OD_{600}$ of 0.5-0.6). Cultures were then shifted to 37°C for a period of 3 h. Cells harboring the cold-sensitive *tub1-729* gene were grown overnight in YPD to an $OD_{600}$ of 1.0 at 23°C. Next, cells were diluted 10-fold and were shifted to 16°C for a period of 18 h to induce microtubule defects (Abruzzi et al., 2002).

**2.11 FACS analysis**

Cells interrogated by FACS analysis were harvested by centrifugation, washed twice in water (1 mL), and resuspended in 70% EtOH and incubated overnight at 4°C for fixation. Following fixation, cells were washed once in 50 mM Tris-HCl (FACS buffer)

and resuspended in FACS buffer containing 1 mg/mL of RNase A (Sigma-Aldrich, St. Louis, MO). For efficient digestion, cells were incubated at 37°C for 2 h. Next, cells were harvested by centrifugation and resuspended in a pepsin solution (pepsin 5 mg/mL in water, pH 2.0) for incubation at 37°C for 3 h. Following pepsin digestion, cells were washed once with FACS buffer and resuspended in 250 μL of propidium iodide solution (200 mM NaCl, 180 mM Tris-HCl, pH 7.5, 70 mM $MgCl_2$, propidium iodide 50 ng/mL) for a period of 1 h at 23°C. Cells were then diluted in FACS buffer (2.5 mL) and sonicated at the lowest setting with ~5 pulses prior to data collection by FACScan (BD Biosciences, San Jose, CA). Analysis of all acquired data was performed using CellQuest software (BD Biosciences, San Jose, CA).

**2.12 Fluorescence and confocal microscopy**

All live cell images of GFP- and RFP-tagged fusion proteins were acquired using either an epifluorescence or confocal microscope. Epifluorescence images were acquired using an Axio Observer.Z1 equipped with an UPlanS-Apochromat 100×/1.40 NA oil immersion objective lens (Carl Zeiss, Oberkochen, Germany) and an AxioCam MRm digital camera (Carl Zeiss, Oberkochen, Germany). Confocal images were obtained using an Axiovert 200M equipped with a confocal scanning system (LSM 510 META) and a Plan-Apochromat 63×/1.40 NA oil immersion objective lens (Carl Zeiss, Oberkochen, Germany). Acquired images were stored using Axiovision software (Carl Zeiss, Inc.) and they were analyzed using ImageJ software (National Institutes of Health, Bethesda, MD).

Image acquisition using the Zeiss LSM 510 confocal microscope was performed as follows: for GFP excitation, and Argon laser line emitting 488nm light was used.

Emission from excited GFP was collected using a long-pass filter (LP 505 nm). For colocalization of GFP and RFP (Mad1-GFP and Mtw1-RFP), GFP was excited with 488 nm light and, this time, emissions were collected using a band pass filter (BP 505-530 nm). For mRFP excitation, a Helium laser emitting at 543 nm was used, and the resulting emitted fluorescence was collected using a long-pass filter (LP 560 nm). The optical depth of all confocal images collected was 0.7 μm.

**2.13 Fluorescence recovery after photobleaching**

All fluorescence recovery after photobleaching (FRAP) experiments were performed using a confocal microscope (LSM 510 META). Both 488 nm (Mad1-GFP+) and 543 nm (Mtw1-mRFP) light scans were used to detect GFP and RFP signals. The initial scan employed both 488 and 543 nm light to identify KT-associated Mad1-GFP (overlapping with Mtw1-RFP) in cells arrested in metaphase with nocodazole or by Mps1-overexpression (see sections 2.7 and 2.8). KT-associated Mad1-GFP was defined as the region of interest (ROI). After the initial scan, subsequent scans only employed 488 nm light to follow the Mad1-GFP signal alone. KT bound Mad1-GFP was next bleached with 488 nm wavelength light at 100% intensity for 15 iterations. Following the bleaching step, images were acquired every 5 s for the duration of the experiment beginning at the pre-bleach scan (a total of 240 sec). Analysis of Mad1-GFP fluorescence recovery at KTs was performed as previously described (Scott et al., 2005; Ptak et al., 2007). Briefly, ImageJ was used to determine the integrated florescence values for the ROI and also to subtract the background fluorescence coming from within and outside the cell. To correct for ROI bleaching over the course of the experiment, ROI values were

multiplied by a factor equivalent to the pre-bleach whole cell fluorescence intensity value divided by the post-bleach whole cell fluorescence intensity value. At each time point, calculations of the final normalized fluorescence intensities for the ROI were derived by dividing the ROI fluorescence intensity by the pre-bleach ROI fluorescence intensity and this analysis was carried out for each replicate (+Gal -Noc, n = 5; +Gal +Noc, n = 6). Plotted time points were then fitted to a one-phase association curve. All data analysis was carried out using Prism 4 software (GraphPad Software, La Jolla, CA).

**2.14 Image analysis and signal quantification**

Image processing (image cropping and linear brightness/contrast adjustments) and quantification of NLS-GFP Nuclear/Cytoplasmic fluorescence intensity ratios were carried out using ImageJ software. To determine the Nuclear/Cytoplasmic fluorescence intensity ratio for an individual cell, the mean integrated fluorescence intensity was calculated for a 0.5 μm x 0.5 μm region centered within the nucleus and in a cytoplasmic region adjacent to the nucleus of a given live cell. Within each cell, the region of greater signal intensity of the import reporter demarcated the nucleus. The background signal was determined from a region outside of the cell. Background fluorescence intensity was subtracted from the nuclear and cytoplasmic values, and these adjusted values were used to calculate the Nuclear/Cytoplasmic ratio for each cell. For each experiment shown, the average nuclear/cytoplasmic ratio was calculated from measurements of fifty or more individual cells under each condition and at each time point indicated. The average ratios were plotted in a bar graph, and variability between individual cells was expressed as standard error of the mean.

**2.15 Leptomycin-B inhibition of Xpo1**

Yeast cells expressing the *xpo1-T539C* allele were grown overnight in YPD (5 mL) to an $OD_{600}$ of ~0.3-0.5. Next, a small volume of cells (1 mL) was harvested, and leptomycin B (LMB) was added directly to the media at a final concentration of 100 ng/mL (Neville and Rosbach, 1999). Following LMB addition, cells were grown for a period of 30 min prior to microscopic analysis. To test for LMB activity, the nuclear localization of the NLS-GFP-NES reporter (Stade et al., 1997) was analyzed in parallel cultures, both before and immediately after LMB addition.

**Chapter III:** *Mitotic-specific regulation of nuclear transport by the spindle assembly checkpoint protein Mad1**

* A version of this chapter has been published as Cairo et al., *Molecular Cell,* 2013, 49, pp 109-120

### 3.1 Overview

NPCs and KTs perform distinct tasks, yet their shared ability to bind several proteins suggests their functions are intertwined. Among these shared proteins is Mad1, a component of the yeast SAC. Here we describe a role for Mad1 in regulating nuclear import that employs its ability to sense a disruption of KT-MT interactions during mitosis. We show that KT-MT detachment arrests nuclear import mediated by the transport factor Kap121 through a mechanism that requires Mad1 cycling between unattached, metaphase KTs and binding sites at the NPC. This signaling pathway requires the Aurora-B kinase Ipl1, and the resulting transport changes inhibit the nuclear import of Glc7, a phosphatase that acts as an Ipl1 antagonist. We propose a distinct branch of the SAC exists in which Mad1 senses unattached KTs and, by altering NPC transport activity, regulates the nuclear environment of the spindle.

## 3.2 Results

### 3.2.1 Destabilization of MTs during metaphase alters nuclear transport

Treatment of yeast cultures with MT destabilizing drugs, e.g. nocodazole, disrupts the mitotic spindle and its attachments to KTs leading to activation of the SAC and metaphase arrest. In arrested cells, structural rearrangements occur within NPCs that inhibit translocation of Kap121 through the NPC and import of its cargos (Makhnevych et al., 2003). These events are readily monitored by a loss in the nuclear accumulation of a Kap121-specific import reporter, such as $NLS^{Pho4}$-GFP (Figure 3-1A). Using this assay, we investigated the mechanism underlying the nocodazole-induced activation of the Kap121-transport inhibitory pathway (KTIP). First, we tested whether metaphase arrest, independent of depolymerization of the mitotic spindle, was sufficient to activate the KTIP. For these experiments, Cdc20 was depleted to prevent activation of the APC/C, which in turn induces metaphase arrest in the presence of an intact spindle (Uhlmann et al., 2000). Under these conditions import of $NLS^{Pho4}$-GFP was robust, suggesting that metaphase arrest was not sufficient to activate the KTIP (Figure 3-1B). However, if the Cdc20-depleted cells were treated with nocodazole, nuclear accumulation of $NLS^{Pho4}$-GFP was lost, consistent with the inhibition of Kap121-mediated import. In contrast, import mediated by other NTFs (Kap60/Kap95) was not affected (Figure 3-1B, $NLS^{SV40}$-GFP). These results were consistent with the conclusion that MT depolymerization activates the KTIP. In support of this idea, we also observed that cells harboring a cold sensitive α-tubulin mutation (*tub1-729*), which exhibit MT defects at the non-permissive temperature (15°C) and arrest in metaphase (Schatz et al., 1988), also induce the KTIP (Figure 3-1C). Moreover, inhibition of Kap121 transport

appears restricted to periods of mitosis prior to chromosome segregation. Cells arrested in G1-phase, S-phase, or late anaphase and then treated with nocodazole exhibit no inhibition of $NLS^{Pho4}$-GFP import (Figure 3-2). Thus, the signal inducing the KTIP arises as a consequence of MT destabilization during metaphase.

### 3.2.2 Loss of KT-MT attachments activates the KTIP

Studies characterizing the *tub1-729* mutant reported that the mutant protein destabilized KT-MT interactions leading to KT detachment (Abruzzi et al., 2002). Therefore, we investigated whether KT detachment from MTs, rather than a global depolymerization of MTs, activates the KTIP. To test this idea, we examined the phenotype of two mutants, *ask1-2* and *ndc80-1*, that functionally compromise the outer KT complexes DAM/DASH and Ndc80. At the non-permissive temperature (37°C), these mutants exhibit KT detachment from spindle MTs, recruitment of Mad1 to KTs (Figure 3-4A), and SAC-dependent metaphase arrest (Pinsky et al., 2006a). Importantly, import of the Kap121, but not Kap60/Kap95, cargo was inhibited (Figures 3-3A and 3-3B).

The KTIP was also examined in a *mcd1-1* cohesin mutant at the non-permissive temperature (Figure 3-3C). This mutant was examined because it indirectly induces KT-MT detachment without disrupting KT structure. At the non-permissive temperature sister chromatid cohesion is lost, leading to a loss of tension at the KT-MT interface (Michaelis et al., 1997). In the absence of KT-MT tension, the Aurora B-like kinase Ipl1 induces KT detachment and SAC-mediated metaphase arrest occurs (Pinsky et al.,

**Figure 3-1. MT destabilization during metaphase activates the KTIP**

Localization of transport reporters imported by Kap121 ($NLS^{Pho4}$-GFP) or Kap60/Kap95 ($NLS^{SV40}$-GFP) was assessed by epifluorescence microscopy under the indicated conditions (left panels). Bar graphs represent a quantification of the reporter signals in cells visualized by microscopy and are given as Nuclear/Cytoplasmic fluorescence intensity ratios (right panels; $n \geq 50$ cells). Error bars express standard error. (A) WT cells expressing *$NLS^{Pho4}$-GFP* or *$NLS^{SV40}$-GFP* were grown to mid-log phase (-), treated with nocodazole, and analyzed at the indicated times (+Noc). (B) *$P_{MET3}$-CDC20 $NLS^{Pho4}$-GFP* and *$P_{MET3}$-CDC20 $NLS^{SV40}$-GFP* cells were grown in media lacking methionine (-Met). Methionine was added to the media alone (+Met) or with nocodazole (+Met +Noc) and the cultures incubated for 2.5 h. (C) WT (DF5) and *tub1-729* containing strains expressing *$NLS^{Pho4}$-GFP* or *$NLS^{SV40}$-GFP* were incubated at a permissive (30°C) or non-permissive (15°C) temperature for *tub1-729* growth.

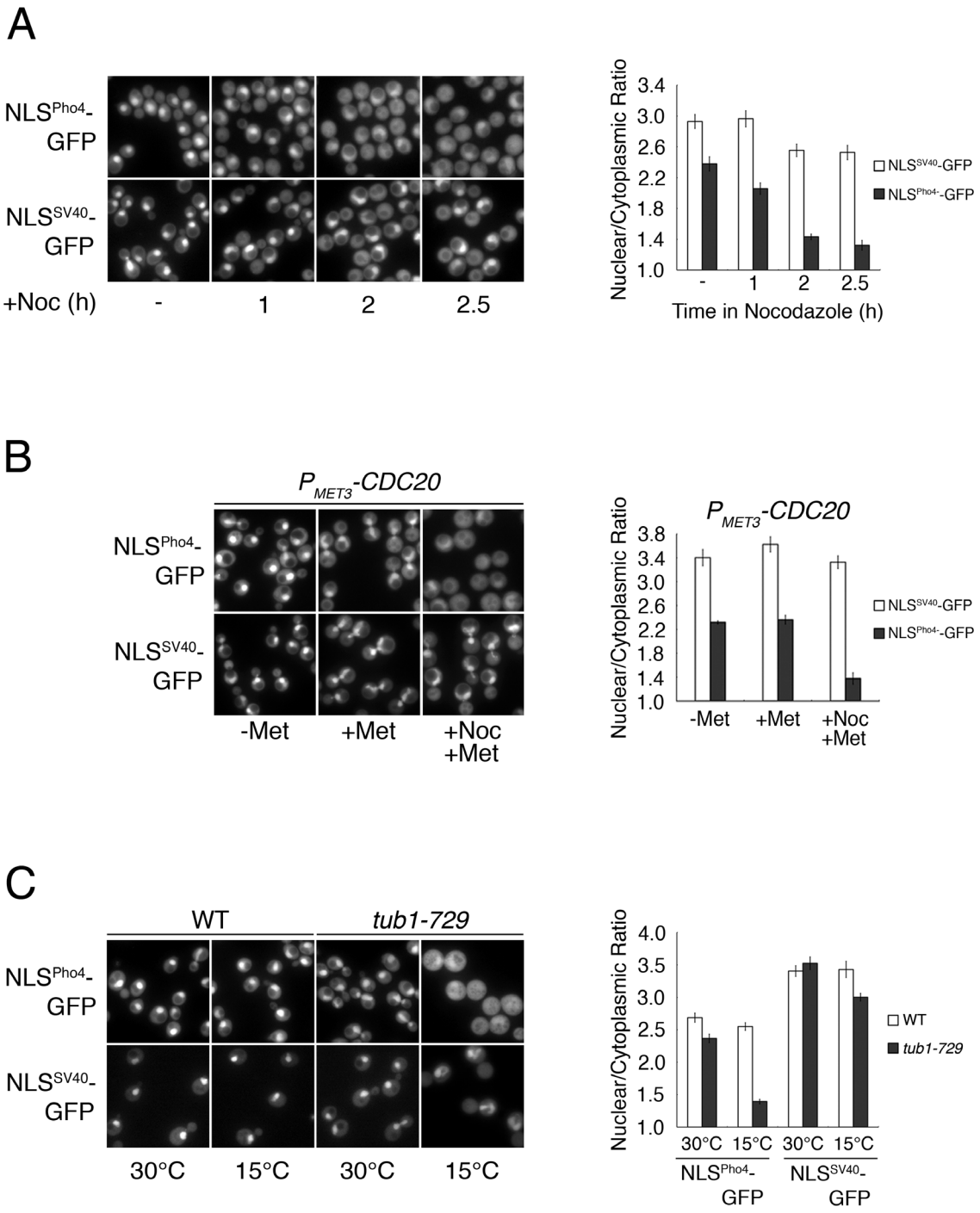


**Figure 3-1. MT destabilization during metaphase activates the KTIP.**

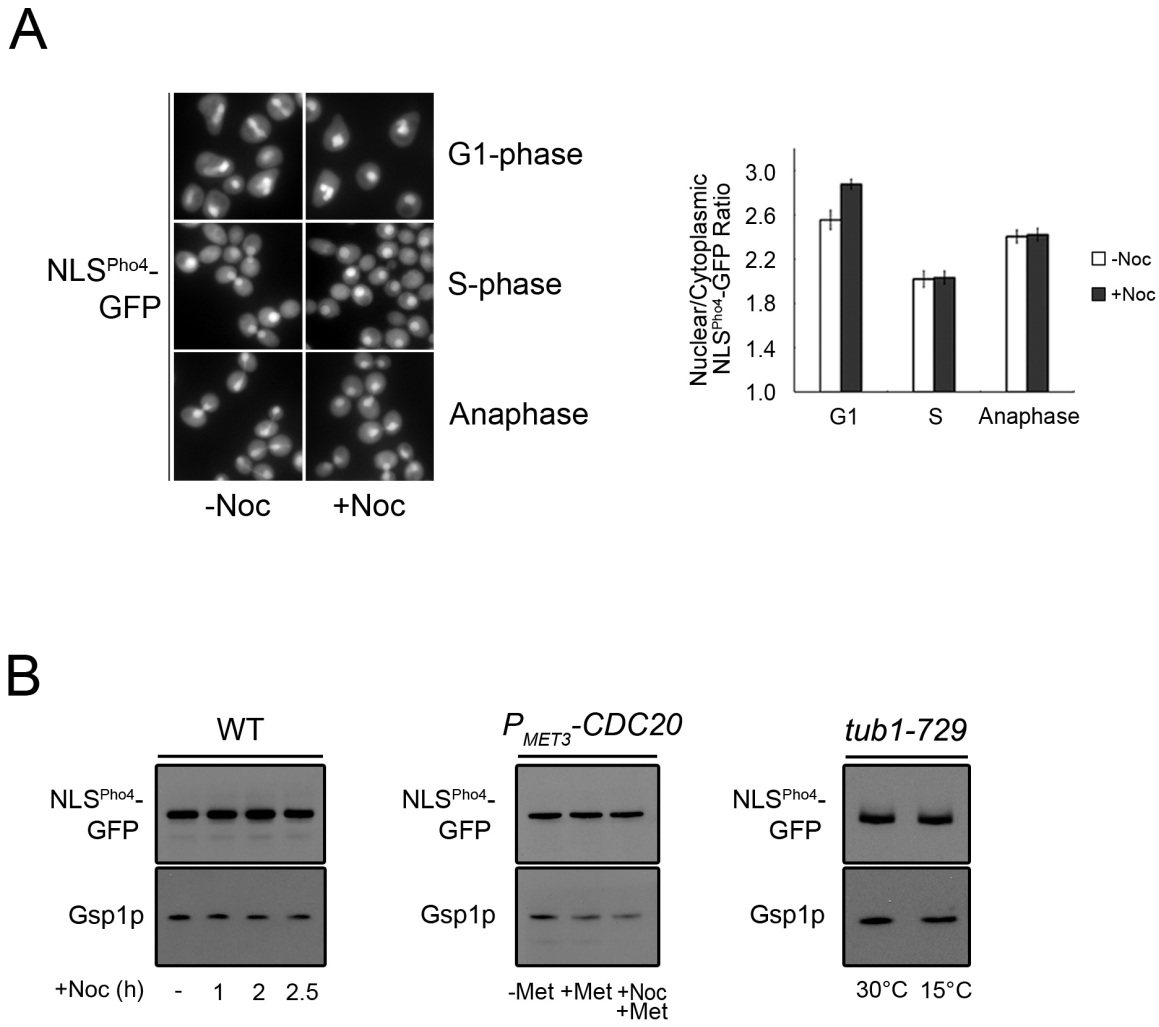


**Figure 3-2. MT depolymerization outside of metaphase has no effect on Kap121-mediated import.**

(A) WT cells expressing *NLS$^{Pho4}$-GFP* were synchronized in G1-phase (α-factor), S-phase (hydroxyurea), or late anaphase (*$P_{GAL1}$-clb2$^{db}$* strain, + galactose for 3h). Following cell cycle arrest, cultures were incubated in the absence (-Noc) or presence (+Noc) of nocodazole for 1 h at 30°C. NLS$^{Pho4}$-GFP localization was analyzed by epifluorescence microscopy (left panels) and its nuclear/cytoplasmic fluorescence intensity ratios were determined (right panels; n ≥ 50 cells). Error bars express standard error. (B) Western blots were performed using an anti-GFP antibody to assess NLS$^{Pho4}$-GFP levels within the indicated strains under each condition tested in Figure 1. Each blot was additionally probed with an anti-Gsp1 antibody as a loading control.

2006a). Accordingly, Mad1 is recruited to KTs in *mcd1-1* cells at 37 °C (Figure 3-4A). Under these conditions, we also observed activation of the KTIP and inhibition of $NLS^{Pho4}$-GFP reporter import (Figure 3-3C). Together, these data indicate that KT detachment from MTs is sufficient for KTIP activation.

### 3.2.3 Mad1 activates the KTIP

Conditions that disrupt KT-MT interactions induce the SAC and metaphase arrest. Two key players in the SAC, Mad1 and Mad2, are bound to NPCs in interphase (Campbell et al., 2001; Iouk et al., 2002). In yeast, when the SAC is activated, Mad1 partitions between NPCs and KTs, while Mad2 is only detected at KTs. These observations led us to examine the role played by the SAC and, more specifically, Mad1 and Mad2, in the KTIP. For these experiments, import of the $NLS^{Pho4}$-GFP reporter was monitored in metaphase-arrested cells lacking Mad1 or Mad2 following nocodazole-induced disruption of KT-MT interactions. The strain backgrounds used included a $P_{MET3}$-*CDC20* gene allowing metaphase arrest despite the absence of Mad1 or Mad2 and a functional SAC. Both the $P_{MET3}$-*CDC20 mad1Δ* and $P_{MET3}$-*CDC20 mad2Δ* mutants, arrested by depletion of Cdc20, exhibited robust import of the $NLS^{Pho4}$-GFP reporter similar to their WT counterpart ($P_{MET3}$-*CDC20*; Figure 3-5A). When MTs were disrupted (+nocodazole) in arrested $P_{MET3}$-*CDC20* cells, the KTIP was induced and nuclear levels of $NLS^{Pho4}$-GFP decreased. Similarly, MT disruption activated the KTIP and import was inhibited in a strain lacking Mad2 ($P_{MET3}$-*CDC20 mad2Δ*). Of note, Mad1 is localized to KTs in these cells (Figure 3-6). However, nocodazole treatment of $P_{MET3}$-*CDC20 mad1Δ* cells did not alter Kap121-mediated import as the $NLS^{Pho4}$-GFP

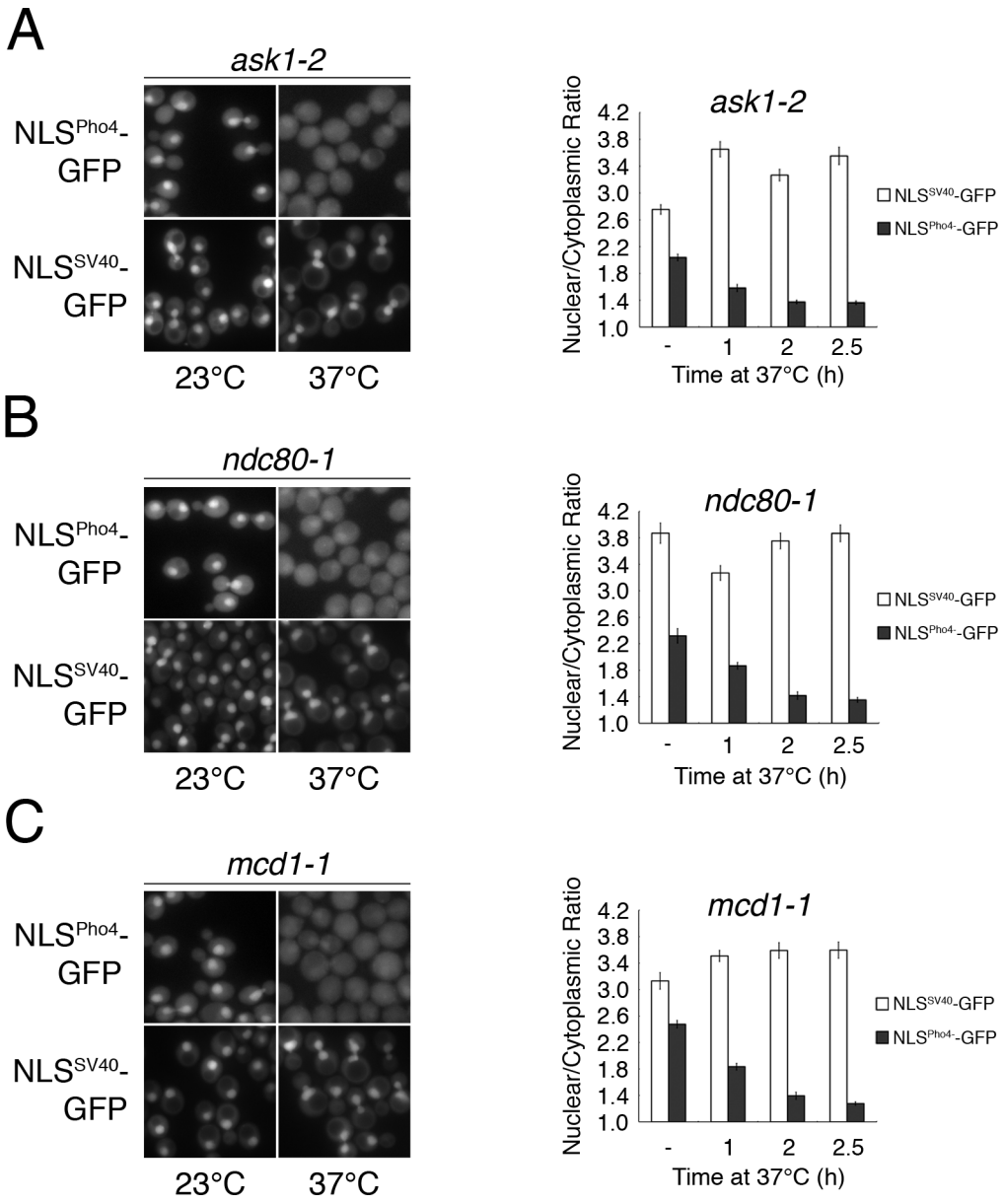


**Figure 3-3. KT detachment from spindle MTs is sufficient for KTIP activation.**

**(**A-C) Strains containing the mutation *ask1-2, ndc80-1,* or *mcd1-1*, and synthesizing $NLS^{Pho4}$-GFP or $NLS^{SV40}$-GFP, were grown at 23°C and then shifted to the non-permissive temperature (37°C) for 2.5 h. Localization of the transport reporters was determined by epifluorescence microscopy (left panels). Nuclear/Cytoplasmic fluorescence intensity ratios were determined for each reporter at the indicated times after a shift to 37°C (right panels; $n \geq 50$ cells). Error bars express standard error.

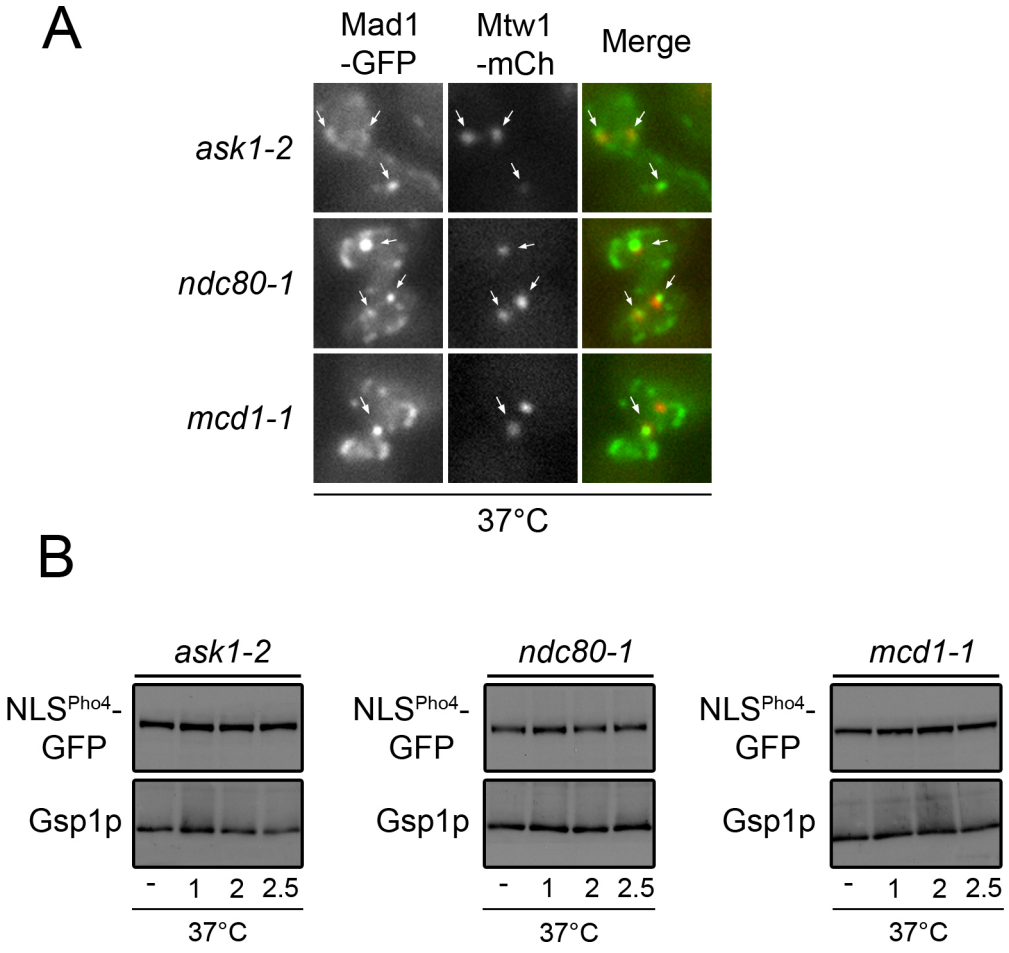


**Figure 3-4. Mad1 is recruited to KTs in *ask1-2*, *ndc80-1*, and *mcd1-1* mutant cells grown at the non-permissive temperature.**

(A) Localization of Mad1-GFP and the KT marker Mtw1-mCherry were assessed by epifluorescence microscopy in *ask1-2, ndc80-1, and mcd1-1* mutant cells following incubation at the non-permissive temperature (37°C) for 2 h. Arrows point to overlapping Mad1-GFP and Mtw1-mCherry foci. (B) Western blots were performed using an anti-GFP antibody to assess $NLS^{Pho4}$-GFP levels within the indicated strains under each condition tested in Figure 2. Anti-Gsp1 western blots were also carried out as loading controls.

reporter remained concentrated in the nucleoplasm (Figure 3-5A). Based on these results, we concluded that Mad1, but not Mad2, is required for the KTIP.

Our observations that the KTIP can function in the absence of Mad2, while requiring Mad1, suggests that Mad1 signals the presence of unattached KTs to NPCs through a mechanism that is independent of the Mad1/Mad2 complex and the Mad2-containing MCC. Thus, we investigated whether ectopic activation of the SAC, in the presence of intact KT-MT attachments, would trigger inhibition of Kap121-mediated import. This was accomplished by overproduction of the SAC kinase Mps1, which induces a SAC arrest independent of mitotic spindle depolymerization (Hardwick et al., 1996). Mps1 overproduction stimulates recruitment of Mad1 to bi-oriented, attached KTs (see Figure 3-9B) and Mad1/Mad2 dependent inhibition of the APC/C. Strikingly, cells arrested by overproduction of Mps1 showed no inhibition of $NLS^{Pho4}$-GFP import (Figure 3-5B). However, when these arrested cells were treated with nocodazole to induce KT-MT detachment, nuclear accumulation of $NLS^{Pho4}$-GFP was inhibited. These results support the conclusion that unattached KTs trigger a distinct function for Mad1 in the activation of the KTIP.

### 3.2.4 KTIP requires Mad1 association with NPCs and KTs

To determine how Mad1 communicates the existence of unattached KTs to NPCs, we investigated the relevance of its dual association with KTs and NPCs. We tested the effects of mutations that alter the association of Mad1 with either structure on the KTIP. An N-terminal region of Mad1 (residues 1-325) binds the NPC, while a C-

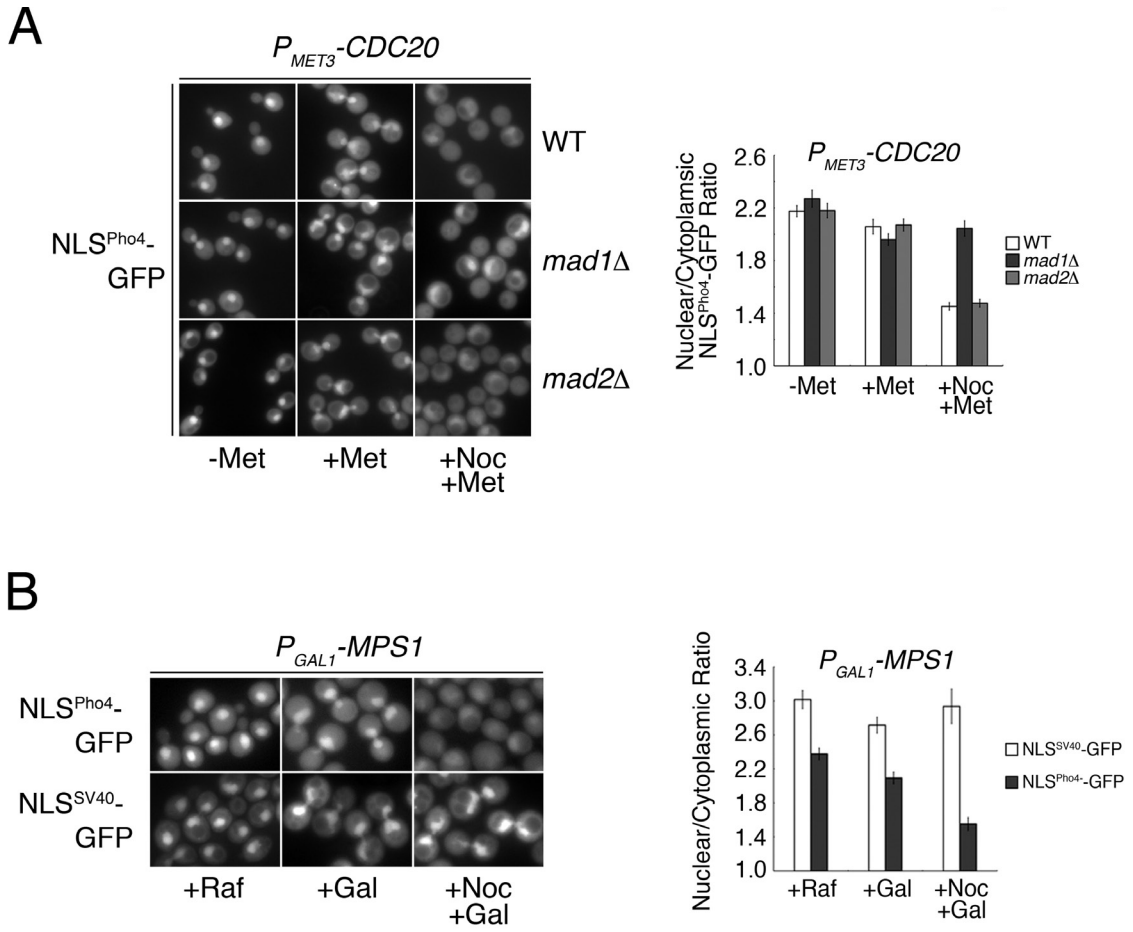


**Figure 3-5. KTIP activation requires Mad1, but not Mad2.**

(A) *$P_{MET3}$-CDC20* (WT), *$P_{MET3}$-CDC20 mad1Δ* (*mad1Δ*), and *$P_{MET3}$-CDC20 mad2Δ* (*mad2Δ*) strains, synthesizing the NLS$^{Pho4}$-GFP reporter, were grown in medium lacking methionine (-Met). Methionine was added to these cultures either alone (+Met) or with nocodazole (+Met +Noc) and incubated for 2.5 h prior to analysis. (B) Cultures of *$P_{GAL1}$-MPS1* cells were grown in raffinose medium (+Raf). Galactose was then added and the cells incubated for 3 h to induce Mps1-mediated metaphase arrest. Cultures were then maintained in galactose-containing medium for an additional 1 h in the absence (+Gal) or presence of nocodazole (+Gal +Noc). Localization of the indicated reporters was determined by epifluorescence microscopy (left panels) and the Nuclear/Cytoplasmic fluorescence intensity ratios calculated (right panels; n ≥ 50 cells). Error bars express standard error.

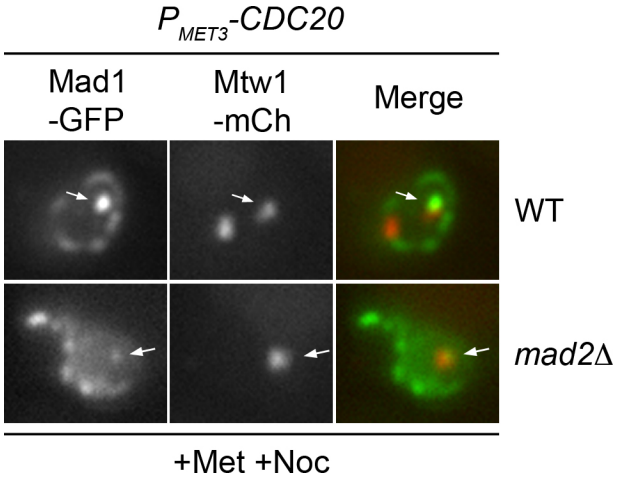


**Figure 3-6. Mad1 is recruited onto unattached KTs in the absence of Mad2.**

Mad1-GFP and the KT marker Mtw1-mCherry were examined by epifluorescence microscopy in $P_{MET3}$-*CDC20* and $P_{MET3}$-*CDC20 mad2Δ* cells after a 2.5 h incubation in medium containing methionine and nocodazole. Arrows point to overlapping Mad1-GFP and Mtw1-mCherry foci.

terminal region (residues 475-749) binds to KTs and is functional in the SAC (Figure 3-7A; Scott et al., 2005). This modular organization of Mad1 allowed us to test the function of each region in the KTIP. The function of individual fragments was tested in a $P_{MET3}$-*CDC20 mad1Δ* mutant background to allow uniform metaphase arrest. Unlike full-length Mad1, we observed that neither mad1$^{1-325}$ nor mad1$^{475-749}$ was capable of rescuing the KTIP defect of a *mad1*Δ mutant (Figure 3-7B). Although the C-terminus alone is insufficient, the likelihood that the KT-binding domain of Mad1 was required to produce a signal necessary to activate the KTIP seemed high, thus we examined the function of a shorter N-terminal deletion, mad1$^{318-749}$, that begins to encroach on the NPC binding regions of Mad1. mad1$^{318-749}$ binds directly to Nup53 (Scott et al., 2005), a key component of the KTIP, but it lacks a region within residues 1-325 that mediates the interaction of Mad1 with a second NPC-associated site formed by Mlp1 and Mlp2 (Figure 3-8; Scott et al., 2005; also see Lee et al., 2008; De Souza et al., 2009; Lince-Faria et al., 2009). As shown in Figure 3-7B, introduction of mad1$^{318-749}$ into the *mad1*Δ strain led to restoration of the KTIP. Thus, a Mad1 fragment capable of binding KTs and Nup53, but not the Mlp proteins, was both necessary and sufficient for the KTIP.

Although the role of Mad1 in the KTIP can be uncoupled from its interactions with the Mlp proteins, the interaction of Mlp proteins with Mad1, coupled with their positioning near Nups that function in the KTIP (Scott et al., 2005), prompted an examination of their role in the KTIP. We tested Kap121-mediated import in an *mlp1*Δ *mlp2*Δ mutant strain prior to and following nocodazole-induced SAC arrest. As shown in Figure 3-7C, the loss of Mlp proteins abolished the KTIP, as no inhibition of transport

**Figure 3-7. Dual association of Mad1 with both KTs and NPCs is necessary for KTIP activation.**

(A) Shown is a schematic representation of Mad1 and mad1 truncations used in this study. NPC and KT binding regions are indicated. (B) *$P_{MET3}$-CDC20 mad1Δ $NLS^{Pho4}$-GFP* strains containing a plasmid that expresses *MAD1* or a *mad1* truncation (*$mad1^{1-325}$*, *$mad1^{318-749}$*, or *$mad1^{475-749}$*) were used to evaluate the KTIP function of specific Mad1 domains. Cells were grown in medium lacking methionine (-Met) followed by the addition of methionine alone (+Met) or methionine plus nocodazole (20 μg/ml) (+Met +Noc) for 2.5 h prior to analysis. (C) WT, *nup60Δ*, and *mlp1Δ mlp2Δ* strains synthesizing $NLS^{Pho4}$-GFP were grown to mid-log phase (-Noc) then treated with nocodazole for 2.5 h (+Noc). Reporter localization was assessed by epifluorescence microscopy (left panels) and the Nuclear/Cytoplasmic fluorescence intensity ratios calculated (right panels; $n \geq 50$ cells). Error bars express standard error.

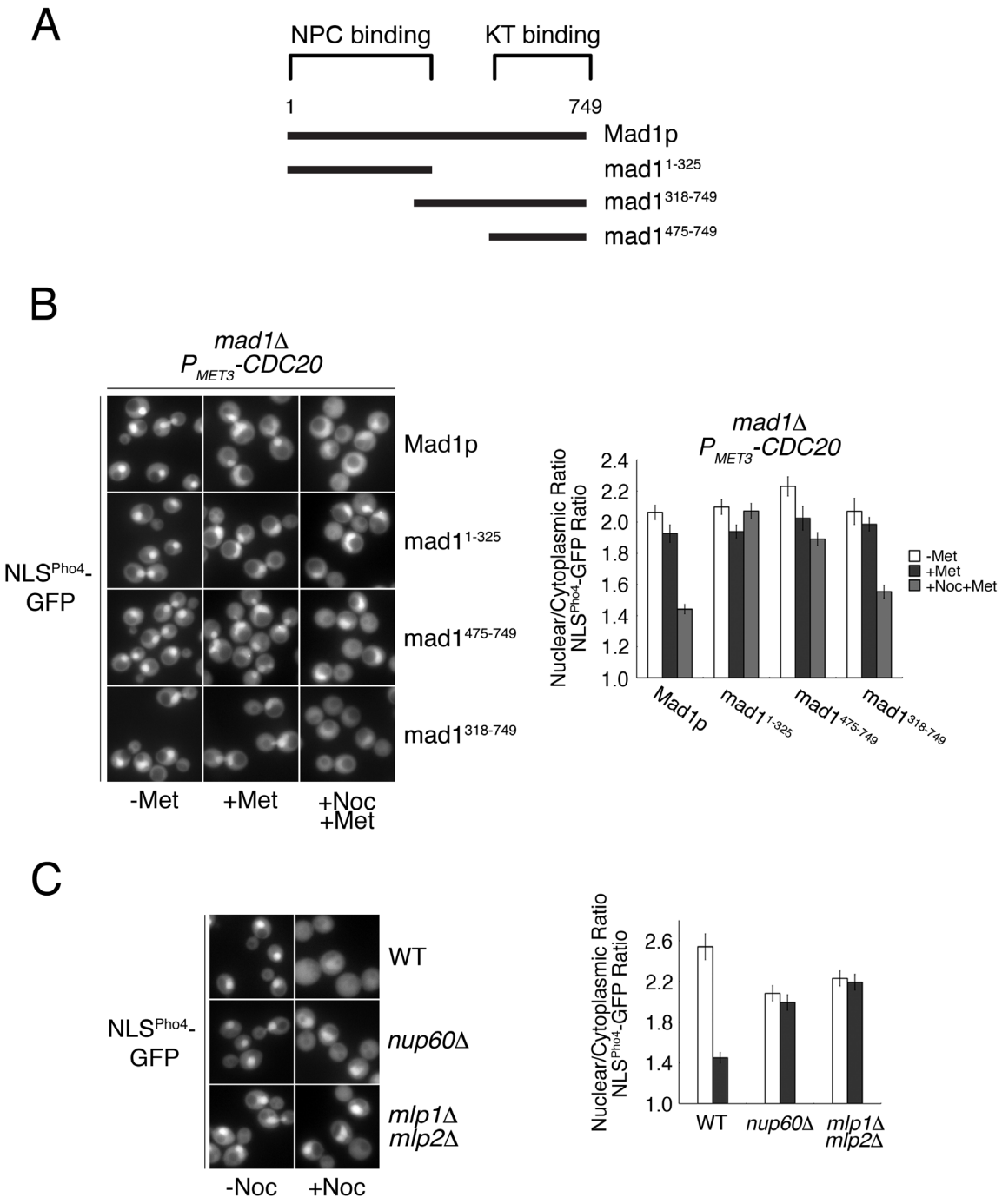


**Figure 3-7. Dual association of Mad1 with both KTs and NPCs is necessary for KTIP activation.**

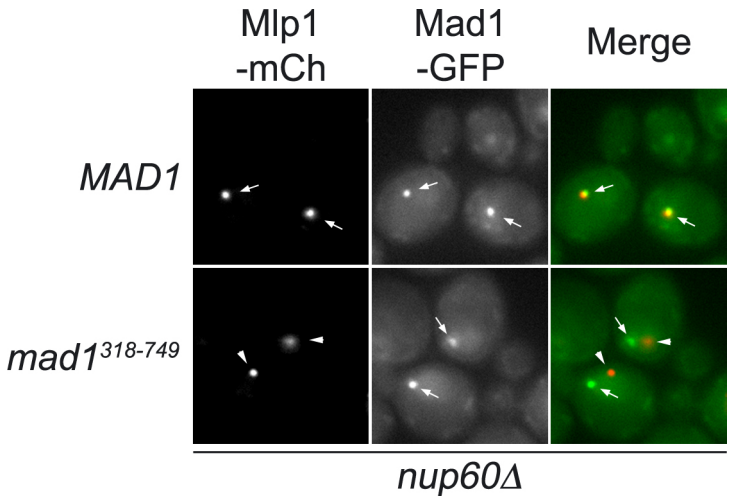


**Figure 3-8. mad1$^{318-749}$-GFP does not localize to Mlp bodies in *nup60*Δ cells**.

In *nup60Δ* cells, the Mlp1 and Mlp2 proteins relocalize from NPCs to a single focus in the nucleoplasm (termed an Mlp body), which binds Mad1 (Scott et al., 2005). However, an examination of *nup60Δ* cells synthesizing *mad1*$^{318-749}$-GFP (arrows) and Mlp1-mCherrry by epifluorescence microscopy revealed no association of *mad1*$^{318-749}$-GFP with Mlp bodies.

was detected in nocodazole-arrested *mlp1*Δ *mlp2*Δ mutant cells. Moreover, we observed that the mislocalization of the Mlp proteins from the NPC was also sufficient to block the KTIP. In the absence of Nup60, the Mlp proteins fail to associate with NPCs, and they concentrate at a single focus in the nucleoplasm (Feuerbach et al., 2002; Scott et al., 2005; Figure 3-8). Treatment of *nup60*Δ mutant cells with nocodazole induced a SAC-dependent arrest, but no inhibition of Kap121-mediated transport was observed (Figure 3-7C). Cumulatively, our data support a model in which the KTIP requires the association of Mad1 with both NPCs and unattached KTs, as well as the positioning of the Mlp proteins at the NPC.

### 3.2.5. Mad1 cycling between NPCs and KTs is required for KTIP activation

Previous work showed that Mad1 cycles between NPCs and unattached KTs in SAC-arrested cells (Scott et al., 2009). The movement of Mad1 between these platforms could serve to transduce a signal from unattached KTs that alters NPC function. To determine whether Mad1 cycling was required to activate the KTIP, we took advantage of the observation that Mad1 turnover requires the nuclear transport factor Xpo1. A point mutation in this transport factor, $xpo1^{T539C}$, renders it inactive in the presence of the anti-fungal leptomycin B (LMB). The addition of LMB to nocodazole-arrested $xpo1^{T539C}$ cells rapidly inhibits Mad1 cycling, but it does not disassociate Mad1 from NPCs or unattached KTs (Scott et al., 2009). Thus, we tested the effect of LMB on the localization of the $NLS^{Pho4}$-GFP reporter in nocodazole-arrested $xpo1^{T539C}$ cells where the KTIP is activated. Strikingly, LMB treatment induced the nuclear accumulation of the $NLS^{Pho4}$-GFP reporter (Figure 3-9A). These observations are consistent with the idea that Mad1 cycling between NPCs and detached KTs is necessary for the KTIP.

A link between Mad1 cycling and activation of the KTIP was also detected in cells overproducing Mps1. As described above, overexpression of *MPS1* induces a SAC-mediated mitotic arrest. In these arrested cells, we observed Mad1 at bi-oriented, MT-attached KT foci and at NPCs (Figure 3-9B, +Gal -Noc), but the KTIP is not activated (Figure 3-5B). When the turnover of KT-bound Mad1-GFP was assessed in these cells, fluorescence recovery after photobleaching (FRAP) revealed little or no recovery of the Mad1-GFP signal (Figure 3-9C and 3-9D). Thus, the lack of Mad1 turnover at KTs coincided with an inability to activate the KTIP. We further evaluated this relationship by treating the Mps1-arrested cells with nocodazole. These conditions disrupt KT-MT interactions leading to the collapse of the bi-oriented KTs into a single focus (Figure 3-9B and 3-9C) and activation of the KTIP (Figure 3-5B). Importantly, FRAP analysis showed a corresponding increase in Mad1-GFP turnover at KTs (Figure 3-9D). Mean fluorescence recovery occurred with a $t_{1/2}$ of ~ 30 s, similar to previously reported observations in nocodazole-arrested cells ($t_{1/2}$ = 33 s; Scott et al., 2009). These results further reveal a correlation between the movement of Mad1 between NPCs and KTs and the activation of the KTIP.

### 3.2.6 Ipl1 function is necessary for activation of the KTIP

KT-associated Ipl1 is thought to respond to the loss of intra-KT tension by phosphorylating outer KT components and destabilizing KT-MT interactions (reviewed in Maresca and Salmon, 2010). This function of Ipl1 contributes to the severing of

**Figure 3-9. KTIP activation requires the dynamic movement of Mad1 between NPCs and KTs.**

(A) *$NLS^{Pho4}$-GFP* and *$NLS^{Pho4}$-GFP $xpo1^{T539C}$* strains were grown to mid-log phase (-Noc) and then treated with nocodazole (+Noc) for 2.5 h. Leptomycin B was added and the cultures incubated an additional 0.5 h (+Noc +LMB). Under each growth condition, reporter localization was assessed by epifluorescence microscopy, and the Nuclear/Cytoplasmic fluorescence intensity ratios calculated (bottom panel; $n \geq 50$ cells). Error bars express standard error. (B) Cells containing the *$P_{GAL1}$-MPS1* cassette and producing Mad1-GFP and the KT marker Mtw1-RFP were grown in raffinose medium (+Raf) to mid-log phase. Galactose was added to the culture and cells incubated for 3 h. The culture was then split and incubated for an additional 1 h in the absence (-Noc) or presence (+Noc) of nocodazole. Arrows indicate positions of overlapping Mad1-GFP and Mtw1-RFP signals detected by confocal microscopy. (C) Shown are magnified images of representative cells, treated as in panel B, that were imaged by confocal microscopy and used in the FRAP analysis shown in panel D. (D) (Upper panel) The dynamic behavior of Mad1-GFP at KTs was assessed by FRAP analysis. *$P_{GAL1}$-MPS1* cells grown either in galactose media for 3 h (+Gal -Noc) or in galactose media for 3 h followed by a 1 h incubation in the presence of nocodazole (+Gal +Noc). Mad1-GFP associated with KTs (as defined by localization with Mtw1-RFP; arrows) ($0^-$ s) was bleached ($0^+$ s) and recovery of the Mad1-GFP fluorescence signal was monitored by confocal microscopy and image acquisition at 5 s intervals for 240 s. Top panels shown are images acquired every 10 s over a 140 s period. (Bottom panel) A graphic representation of Mad1-GFP recovery at bleached KTs is shown as a plot of mean relative fluorescence intensity vs. time (s) (+Gal –Noc open circles, n=5; +Gal +Noc closed circles, n=6). Data points have been fitted to give the curves shown (solid lines). No appreciable Mad1-GFP recovery could be detected within the +Gal -Noc treated cells. Mad1-GFP in +Gal +Noc treated cells recovered with a $t_{1/2}$ of 30.3 s and signal recovery of 36.2%. Error at each time point is given as standard deviation.

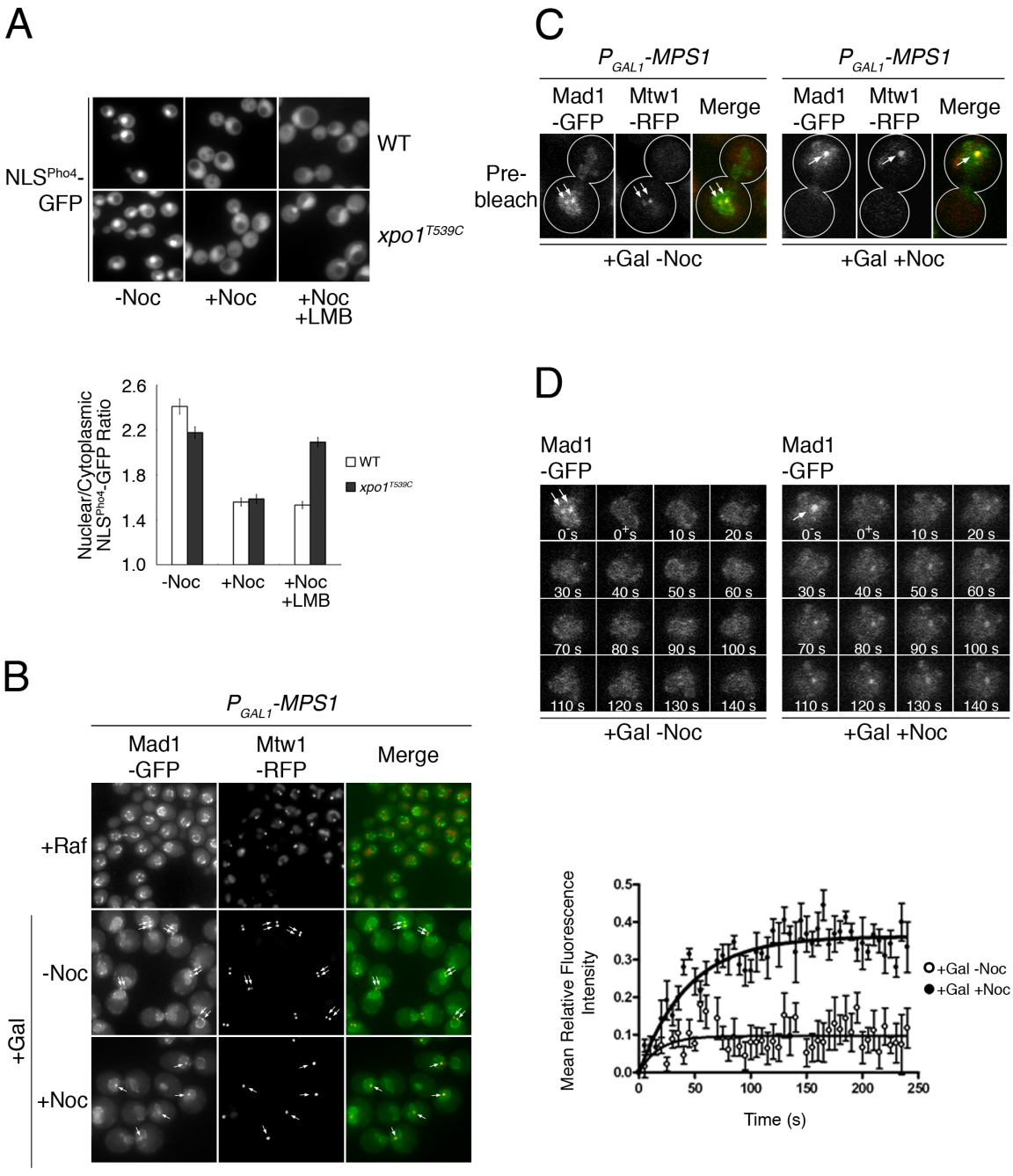


**Figure 3-9. KTIP activation requires the dynamic movement of Mad1 between NPCs and KTs.**

defective KT-MT attachments (Pinsky et al., 2006a; Shimogawa et al. 2009). The conditions we have used to activate the KTIP, including mutants such as *ask1-2* and *ndc80-1* (Figure 3-3A and 3-3B), are also thought to invoke Ipl1 activity to facilitate the disruption of KT-MT interactions leading to SAC arrest (Pinsky et al., 2006a). Therefore, we investigated whether Ipl1 was required for the KTIP using the temperature-sensitive *ipl1-321* mutant. Nocodazole treatment of the *ipl1-321* cells induced a metaphase arrest, similar to previous reports (Figure 3-10B; Biggins and Murray, 2001), that results in Mad1 targeting to detached KTs (Figure 3-10A). In these arrested cells, we also examined the localization of the $NLS^{Pho4}$-GFP reporter prior to and following a shift to 37ºC (Figure 3-10B), thus under conditions that induce KT-MT detachment and partially (23ºC) or fully (37ºC) inactivate the ipl1-321 protein. Unlike WT cells, the KTIP was inactive in cells containing the *ipl1-321* mutation and they continued to import the $NLS^{Pho4}$-GFP reporter, suggesting that the Ipl1 kinase is required for the KTIP.

### 3.2.7 The KTIP regulates the nuclear levels of Glc7 during SAC arrest

We hypothesize that the KTIP contributes to spindle function and chromosome segregation under conditions where these events are challenged and the SAC is activated. The influence of the KTIP on these events is presumed to occur through changes in the nuclear concentration of Kap121 and its cargos during SAC arrest. We have attempted to define candidate cargos as a step towards uncovering the contributions of the KTIP to mitotic progression. We targeted the protein phosphatase Glc7 based on several observations: 1) genetic analysis has uncovered a functional interaction between Glc7

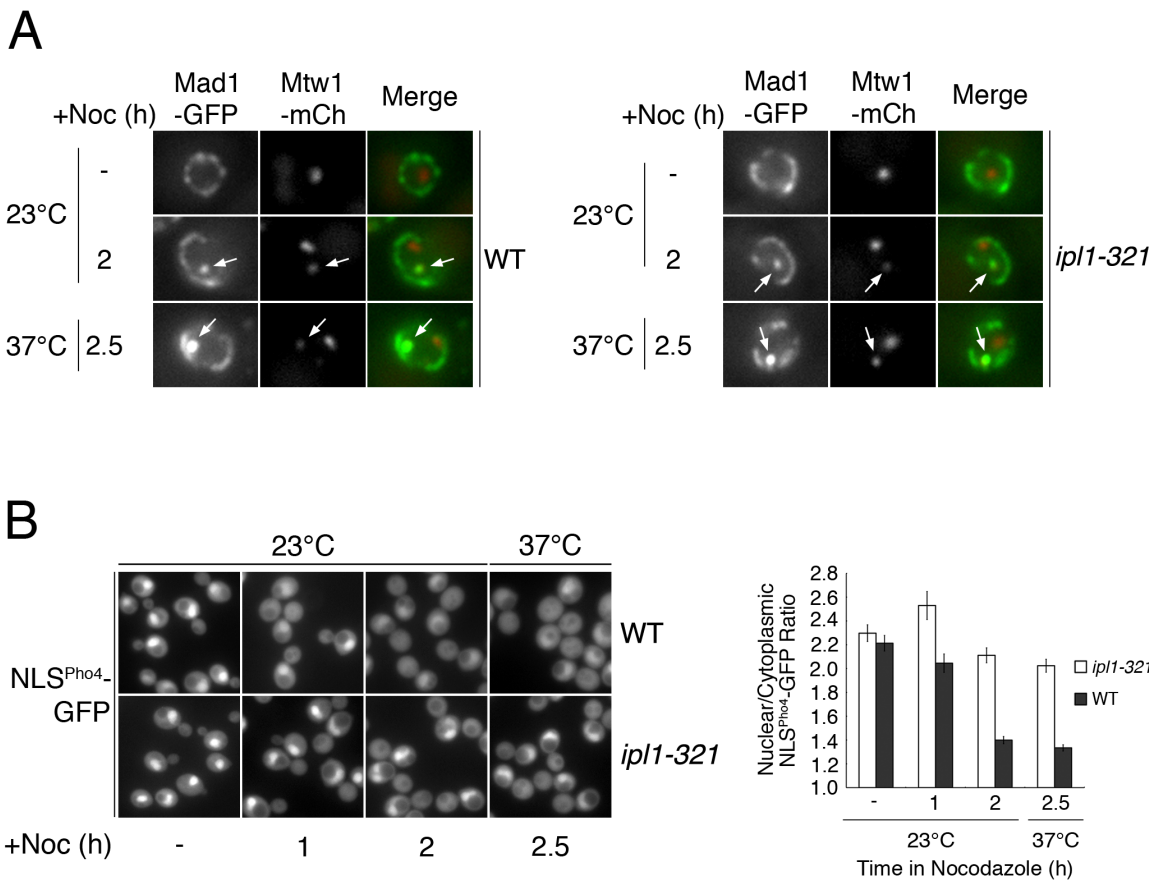


**Figure 3-10. Ipl1 is required for KTIP activation.**

The localization of Mad1-GFP and the KT marker Mtw1-mCherry was examined in WT and *ipl1-321* cells. Cells were examined by epifluorescence microscopy following growth at 23°C in the absence of nocodazole (-) or after treatment with nocodazole for 2 h. Cells arrested with nocodazole were also examined following incubation at 37°C for an additional 0.5 h (2.5 h). Arrows indicate the position of overlapping Mad1-GFP and Mtw1-mCherry foci. (B) Import of the $NLS^{Pho4}$-GFP reporter was also examined using epifluorescence microscopy in WT and *ipl1-321* cells. Cells were grown at 23°C in the absence (-) or presence of nocodazole for the indicated times. Cultures treated for 2 h with nocodazole were also shifted to 37°C for an additional 0.5 h to further inhibit ipl1-321 function (2.5 h). Nuclear/Cytoplasmic fluorescence intensity ratios for $NLS^{Pho4}$-GFP were determined under each condition ($n \geq 50$ cells). Error bars express standard error.

and Nup53 (Logan et al., 2008), a key component of the KTIP machinery, 2) Glc7 contains a putative Kap121 NLS and is concentrated in the nucleus of asynchronous cells, 3) Glc7 is an antagonist of Ipl1 function (reviewed in Lesage et al., 2011), and 4) mutations that reduce nuclear levels of Glc7 rescue growth of *ipl1*$^{ts}$ mutants (Pinsky et al., 2006b; Bharucha et al., 2008; Tatchell et al., 2011). Using Glc7-GFP and cells containing the *kap121-34* temperature-sensitive allele, we showed that nuclear accumulation of Glc7 was dependent on Kap121 (Figure 3-11A). Importantly, activation of the KTIP also leads to a decrease in nuclear levels of Glc7-GFP, and this inhibition of import is dependent on Mad1 (Figure 3-11B, 3-11C, 3-14A and 3-14B).

Dephosphorylation of KT proteins by Glc7 promotes KT-MT association, while phosphorylation of KT proteins by Ipl1 during SAC arrest induces a state of MT detachment that ultimately contributes to bipolar spindle attachment (Sassoon et al., 1999; Pinsky et al., 2006a; Pinsky et al., 2006b; Akiyoshi et al., 2009a). The reduced nuclear concentration of Glc7 arising from KTIP activation is predicted to attenuate its antagonistic effects on Ipl1 activity and thus promote KT-MT detachment. Thus, we hypothesized that the KTIP supports Ipl1 function, and mutations that compromise the KTIP (e.g. *nup53*Δ*KBD*; Makhnevych et al., 2003) would exhibit MT-related phenotypes similar to mutations in Ipl1 (e.g. *ipl1-321*). In this regard, we observed that the *ipl1-321* mutant cells grow more efficiently than WT cells on medium containing benomyl (a MT destabilizing drug) at semi-permissive temperatures for growth (Figure 3-11D), an observation consistent with an increased stability of KT-MT interactions in the absence of fully functional Ipl1. Examination of *nup53*Δ*KBD* cells revealed a similar benomyl-

**Figure 3-11. KTIP regulates nuclear import of Glc7.**

(A) Cultures of WT cells and a *kap121-34* temperature-sensitive strain producing Glc7-GFP were grown to mid-log phase at 23°C, and then shifted to 37°C for 3 h. Loss of kap121-34 function at 37°C inhibits nuclear accumulation of Glc7-GFP. The subcellular distribution of Glc7-GFP was examined in an *ndc80-1* strain (panel B) as well as *ndc80-1* $P_{MET3}$*-CDC20, ndc80-1* $P_{MET3}$*-CDC20 mad1Δ,* and *ndc80-1* $P_{MET3}$*-CDC20 mad2Δ* (panel C) strains using epifluorescence microscopy. (B) A mid-log phase culture was shifted from 23°C to 37°C and incubated at the non-permissive temperature for the indicated time. (C) Cultures of the indicated *ndc80-1* $P_{MET3}$*-CDC20* based strains (-Met) were arrested by addition of methionine (+Met). Each culture was then split in half and either maintained at 23°C or shifted to 37°C for an additional 2.5 h. Note, the bright fluorescent foci detected following KTIP-dependent nuclear exclusion of Glc7-GFP have also been seen in other studies where the inhibition of nuclear accumulation of Glc7 was documented (Bharucha et al., 2008; Tatchell et al., 2011). These foci remain undefined. Nuclear/Cytoplasmic fluorescence intensity ratios for Glc7-GFP were determined under each condition ($n \geq 50$ cells). Error bars express standard error. (C and D) Cultures of WT, *nup53ΔKBD*, *ipl1-321*, *ipl1-321 nup53ΔKBD*, *glc7-10,* and *glc7-10 nup53ΔKBD* cells were spotted as 10-fold serial dilutions onto YPD plates supplemented with vehicle alone (1% DMSO) or containing the indicated concentrations of benomyl (+Ben). Plates were then incubated at 25°C for 4 days or at 30°C for 2 days.

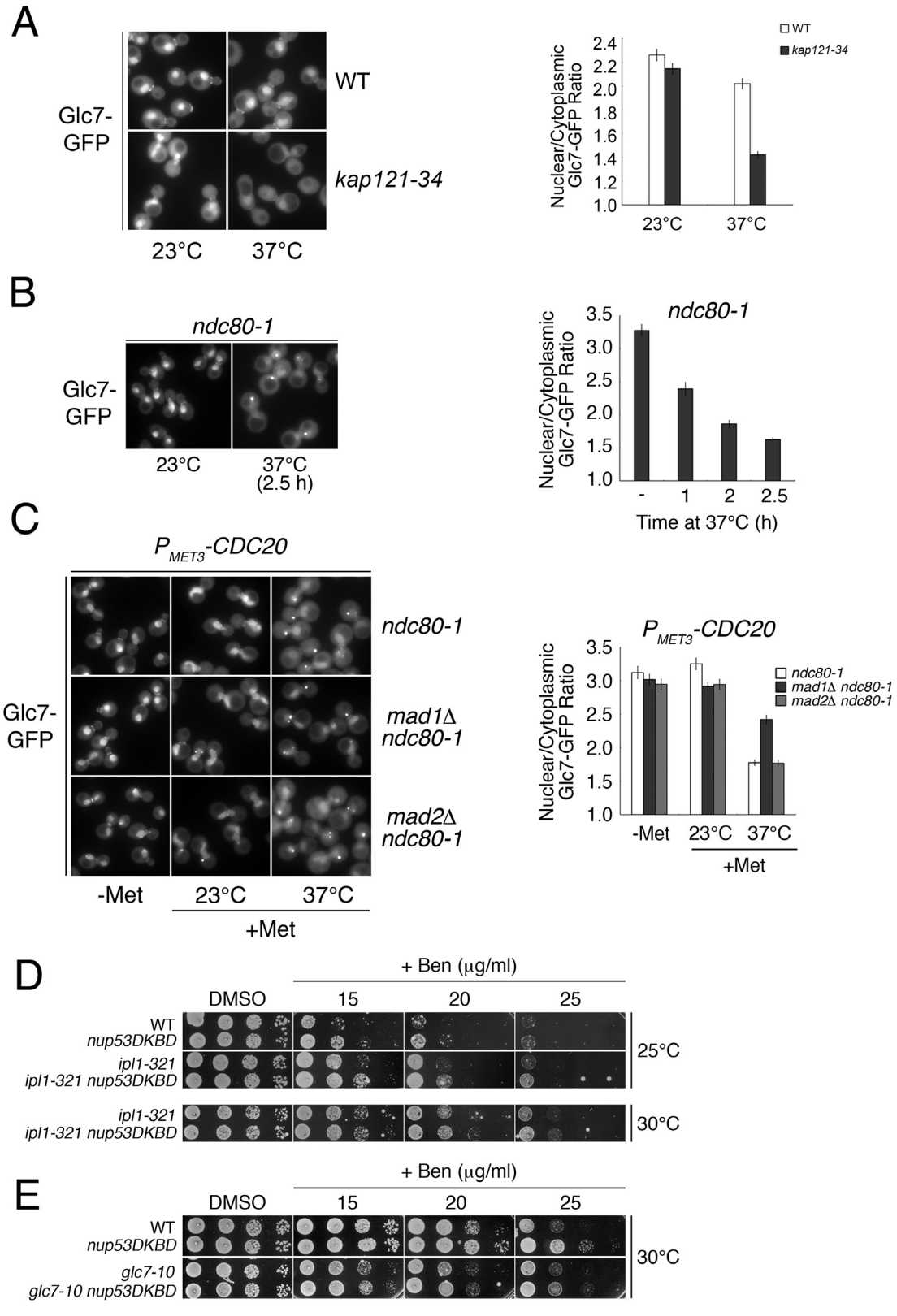


**Figure 3-11. KTIP regulates nuclear import of Glc7.**

resistant phenotype (Figure 3-11D). When we examined a *nup53ΔKBD ipl1-321* double mutant at 25ºC, we observed the mutations had an additive effect with the double mutant showing greater benomyl resistance than either of the single mutants (Figure 3-11D). However, at elevated temperatures (30ºC) that further compromised *ipl1-321* function, the benomyl resistance of the single *ipl1-321* mutant approaches that of the double mutant, i.e. the contribution of the *nup53ΔKBD* mutation to the benomyl resistance of the double mutant was no longer detected (Figure 3-11D). One explanation for these results is that the benomyl resistance conferred by the *nup53ΔKBD* mutation is linked to Ipl1 function. These results are consistent with the loss of KTIP function antagonizing Ipl1 function, potentially through an increased nuclear concentration of Glc7 (Figure 3-11C). This model predicts that mutations compromising Glc7 function would suppress the benomyl resistant phenotype of the *nup53ΔKBD* mutant. Indeed, we observed that a *glc7-10* mutation largely eliminated the benomyl-resistant phenotype associated with the *nup53ΔKBD* mutation (Figure 3-11E).

### 3.3 Discussion

NPCs bind several proteins with no previously defined role in nuclear transport; among these are Mad1 and Mad2. Here we report that, during mitosis, the transport properties of NPCs are regulated by the state of KT-MT interactions. Conditions that disturb KT-MT interactions and foster Ipl1-mediated phosphorylation of KT-associated proteins induce Xpo1-dependent cycling of Mad1 between KTs and NPCs. These events initiate changes in NPCs that inhibit Kap121-mediated import (see Model, Figure 3-12). Mad1 performs this function through a signaling mechanism independently of Mad2 and

the MCC but dependent on Ipl1. Furthermore, we show that the KTIP contributes to establishing a nuclear environment that supports Ipl1 function by reducing nuclear levels of the Glc7 phosphatase.

NPCs and KTs are generally viewed as separate macromolecular platforms that perform distinct biological functions. However, observations made over a number of years imply certain proteins, originally thought to function exclusively within one structure, play a role in the workings of both. For example, vertebrate NPCs are disassembled during mitosis and various Nups are recruited to KTs where they participate in KT-MT interactions (see Introduction). In addition, Mlp-like proteins positioned on the nuclear face of NPCs during interphase are associated with a mitotic spindle matrix, and possibly KTs, of various organisms that undergo an open, or partially open, mitosis, including human, *Drosophila*, and *Aspergillus nidulans* (Lee et al., 2008; De Souza et al, 2009; Lince-Faria et al., 2009). Here, as in interphase, the Mlp-like proteins are capable of binding Mad1 and Mad2. Thus, it has been proposed that they may establish a 'fence' or 'barrier' that assists in maintaining a higher concentration of Mad1 and Mad2 in the vicinity of KTs and, therefore, contribute to a robust SAC. Nups have also been detected in a spindle matrix fraction; however, their function at this locale has not been established (Ma et al., 2009; Zheng, 2010). In *S. cerevisiae*, Mlp proteins, Nups, and Mad1 associated with an intact NE during mitosis, i.e. closed mitosis, are likely to function analogously to the spindle matrix with the added topological constraints provided by the NE membrane. In this context, Mad1, through its interaction with NPCs, is positioned to regulate nuclear transport and the access of molecules to the spindle and chromosomes.

We have shown that Mad1 regulates Kap121-mediated nuclear import by

**Figure 3-12. Model for Mad1 activation of the Kap121 transport inhibitory pathway.**

(A) In cycling cells, bi-orientated chromosomes (grey ellipses) are established at metaphase through the attachment of spindle MTs (dashed line) to the SPB and KTs. This places KTs under tension (green KT), satisfying the SAC and allowing progression through M-phase. Under these conditions, Mad1 remains bound to the nucleoplasmic face of NPCs, and the import and nuclear accumulation of Kap121 cargos (NLS-containing cargos including Glc7) are unabated. (B) Disruption of KT-MT interactions (red X and red Kt) leads to detached KTs that induce the SAC arrest. As part of checkpoint signaling, Mad1 and Mad2 are released from NPCs and interact with detached KTs where they participate in the formation of the mitotic checkpoint complex (MCC) and suppression of the APC/C. Concomitant with this, a pool of KT-bound Mad1, potentially distinct from the Mad1/Map2 complex, cycles between KTs and NPCs. Mad1 cycling initiates changes in the NPC, possibly through Mad1 binding to alternative NPC sites, which inhibit passage of Kap121 and nuclear import of its cargos. This process is dependent on the Ipl1-kinase and serves to inhibit nuclear accumulation of the Glc7 phosphatase. NE, nuclear envelope.

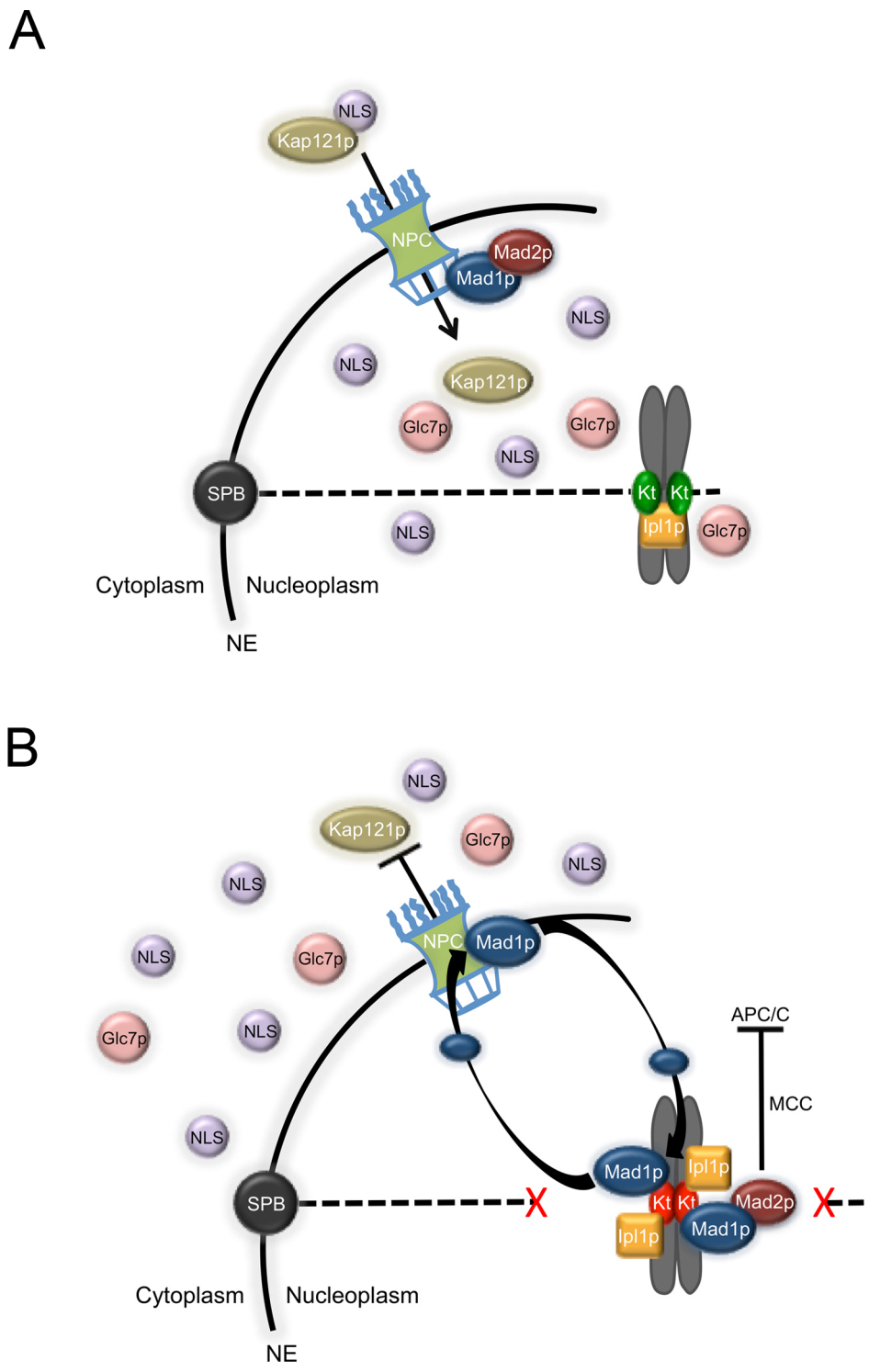


**Figure 3-12. Model for Mad1 activation of the Kap121 transport inhibitory pathway.**

activating the KTIP in response to disruption of KT-MT attachments (Figures 3-1 and 3-3). Under these conditions, Mad1 and Mad2 are bound to unattached KTs and the SAC is active (Gillett et al., 2004). Moreover, Mad1 is also detectable at NPCs, and FRAP experiments have shown that Mad1 is capable of exchanging between NPC- and KT-bound pools by a mechanism that uses the exportin Xpo1 (Scott et al., 2009). We have made several observations that lead us to conclude that this cycling phenomenon is required to inhibit Kap121-mediated transport. If Mad1 is mutated to disrupt its binding to NPCs or unattached KTs (Figure 3-7), or if its cycling is inhibited by blocking Xpo1 function, the KTIP is arrested (Figure 3-9). A correlation between Mad1 cycling and activation of the KTIP is also revealed in cells overexpressing *MPS1*. Mps1 overproduction induces a SAC-dependent metaphase arrest and Mad1 is visible at both NPCs and KTs, but we detect no turnover of Mad1 at KTs (Figure 3-9) and, importantly, no activation of the KTIP (Figure 3-5). Only after KT-MT interactions are disrupted in these cells are Mad1 turnover initiated and the KTIP activated (Figure 3-9). In the aggregate, these results lead us to propose that the cycling of Mad1 between unattached KTs and NPCs propagates the signal responsible for modifying the transport properties of the NPC, it is not, however, necessary for SAC-mediated cell cycle arrest, as the latter occurs in the absence of Mad1 cycling (Figure 3-9; Scott et al., 2009).

The role of Mad1 in sensing the state of KT-MT interactions and regulating the KTIP is also distinct from its well established function as a member of the Mad1/Mad2 complex. This conclusion is supported by data showing that a mutant lacking Mad2 possesses a functional KTIP (Figure 3-5). This is in sharp contrast to the essential role of Mad2 in the SAC, and the requirement for its interaction with Mad1 in the formation of

the MCC (consisting of Mad2, Cdc20, Mad3, and Bub3) that suppresses APC/C activity (see Musacchio and Salmon, 2007). This function for the Mad1/Mad2 complex is invoked during SAC arrest induced by *MPS1* overexpression, but it does not suffice to activate the KTIP (Figure 3-5). It is only after disruption of KT-MT interactions in these cells that the KTIP is activated (Figure 3-5) and the separate functional role of Mad1 revealed. Further support for this conclusion comes from the identification of truncations of Mad1 (mad1$^{475-749}$) capable of supporting SAC arrest but unable to activate the KTIP (Figure 3-7).

At the NPC, the KTIP is executed through structural changes in the NPC (Makhnevych et al., 2003). Key steps are the release of Nup53 from its neighbor Nup170, allowing Nup53 to bind Kap121, which, in turn, inhibits movement of Kap121 and its cargo into the nucleus. Our data lead us to conclude that a previously detected interaction between Mad1 and Nup53 (Scott et al., 2005) forms the mechanistic basis for activation of the KTIP. This idea is supported by our results showing that a C-terminal fragment of Mad1 (mad1$^{318-749}$), capable of binding Nup53 and KTs (Scott et al., 2005), can support the KTIP (Figure 3-7). By contrast, the mad1$^{318-749}$ truncation shows a decreased ability to bind the Mlp proteins, a known binding site for Mad1 at the NPC (Scott et al., 2005; Figure 3-7), suggesting Mad1 binding to the Mlp proteins is not a requirement for the KTIP. Irrespective of their interactions with Mad1, the Mlp proteins are, however, required for the KTIP (Figure 3-7). We speculate that their function in the KTIP occurs through an ability to modulate NPC structure independently of their interactions with Mad1. Consistent with this idea, Mlp1 and Mlp2 interact with Nup170 (Scott et al., 2005), a key Nup involved in the KTIP. Moreover, Mlp proteins appear to undergo

physical change during SAC arrest. For example, *MPS1* overexpression induces the dispersion of Mlp protein clusters present in the nucleoplasm of *nup60*Δ cells, implying that Mlp proteins are modified under conditions of SAC arrest (Figure 3-13). We would suggest that these modifications of the Mlp proteins contribute to changing their interactions with Nup binding partners. It is our working model that concerted changes in the interactions of Mad1 and the Mlp proteins with Nups drive changes in the transport properties of the NPC. Defining the nature of these molecular interactions and, more globally, changes in NPC structure in SAC- arrested cells will be of particular interest in future studies.

Activation of the KTIP occurs following disruption of KT-MT interactions, suggesting this pathway contributes to fostering a nuclear environment that facilitates the reorganization and proper assembly of the KT-MT interface. Consistent with this concept, activation of the KTIP is functionally linked to KT-bound Ipl1 (Figure 3-10). This kinase contributes to SAC arrest and senses the loss of intra-KT tension resulting from improper spindle attachment (Pinsky et al., 2006a). Ipl1 promotes correction of these errors by phosphorylating various KT proteins, inducing their detachment from spindle MTs (reviewed in Lampson and Cheeseman, 2011). Thus, conditions that promote Ipl1-mediated phosphorylation also elicit the KTIP. Importantly, in analyzing an *ipl1-321* mutant, we observed that, while this mutant is capable of sustaining SAC arrest (Biggins and Murray, 2001), including events such as Mad1 recruitment to KTs, these cells failed to support the KTIP (Figure 3-10). How Ipl1 contributes to the KTIP is unclear. We speculate that Ipl1 could phosphorylate Mad1, or a binding partner, in a manner that supports Mad1 cycling and interactions with the NPC necessary to alter

**Figure 3-13. *MPS1* overexpression induces the dissolution of Mlp bodies in *nup60Δ* cells**.

*$P_{GAL1}$-MPS1 nup60Δ* cells producing Mlp1-GFP and Mad1-RFP (panel A) or Mad1-GFP and Mtw1-RFP (panel B) were grown in raffinose medium (+Raf) to mid-log phase. Galactose was added to these cultures and incubation continued for 3 h. At 3 h, each culture was split and the two halves were incubated for an addition 1 h in the absence (+Gal) or presence of nocodazole (+Gal +Noc). Localization of Mlp1-GFP and Mad1-RFP (panel A) or Mad1-GFP and the KT marker Mtw1-RFP (panel B) was assessed by epifluorescence microscopy. Arrows highlight overlap between Mlp1-GFP and Mad1-RFP (A) or Mad1-GFP and Mtw1-RFP (B). Mps1 overproduction induces the recruitment of Mad1-GFP to KTs and the loss of visible Mlp bodies. (C) The loss of Mlp bodies was not due to the degradation of Mlp1-GFP. Mlp1-GFP levels, in *$P_{GAL1}$-MPS1 MAD1-RFP MLP1-GFP nup60Δ* cells (panel A) grown in either raffinose (Raf) or galactose (Gal)-containing medium for 4 h, were examined by western blot analysis of whole cell lysates using an anti-GFP antibody (Mlp1-GFP). Also shown for comparison are Mad1-GFP levels in a lysate derived from the *$P_{GAL1}$-MPS1 MTW1-RFP MAD1-GFP nup60Δ* cells detected using anti-GFP antibody (Mad1-GFP). An anti-Gsp1 antibody blot is shown as a loading control. Mass markers shown are in kilodaltons.

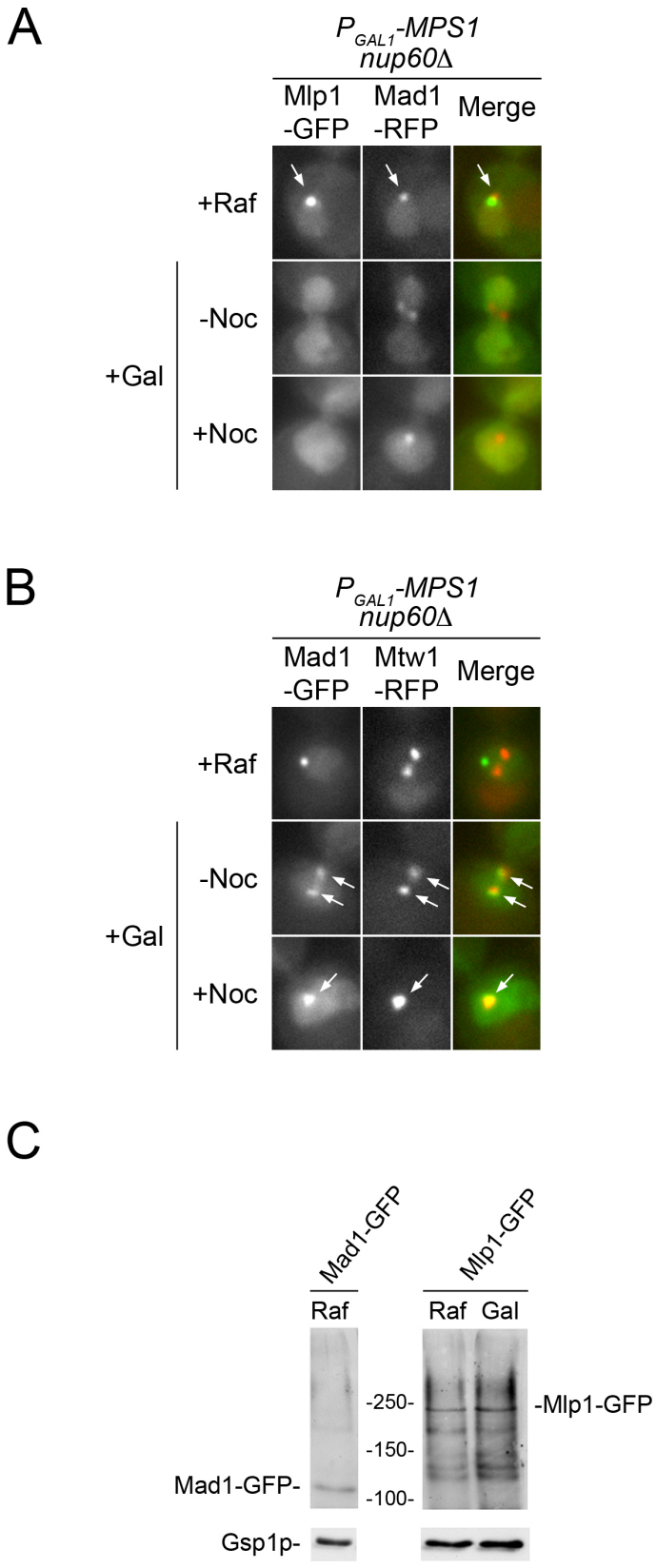


**Figure 3-13. *MPS1* overexpression induces the dissolution of Mlp bodies in *nup60Δ* cells**.

Kap121-mediated import. While Mad1 phosphorylation by Ipl1 has not as yet been described, this event seems plausible, as Mad1 binding to unattached KTs is likely to occur near Ndc80, a known target of Ipl1 (Martin-Lluesma et al., 2002; Akiyoshi et al., 2009b).

The correlation between KT-bound Ipl1 activity and the on state of the KTIP led us to conclude that the latter supports Ipl1 function. In support of this hypothesis, we have shown that, during SAC arrest, the KTIP prevents nuclear accumulation of the phosphatase Glc7, an antagonist of Ipl1 function (Figures 3-11 and 3-14). A link between SAC arrest and the loss of nuclear accumulation of Glc7 was also reported by Tatchell and colleagues (Bharucha et al., 2008). They showed that mutations in Ypi1, a protein suggested to regulate Glc7 function, elicits a SAC-dependent cell cycle arrest, decreases nuclear levels of Glc7, and suppresses an *ipl1*$^{ts}$ mutant. The role of the KTIP in these observations has not been explored, but its involvement in the observed phenotypes seems likely. We envisage that reduced nuclear levels of Glc7 established by the KTIP create an environment conducive to maintaining the phosphorylation state of Ipl1 targets. In support of this idea, the loss of KTIP function and the resulting increase in nuclear levels of Glc7 detected in a *mad1*Δ mutant (Figures 3-11 and 3-14) correspondingly lead to increased dephosphorylation of histone H3, a target of Glc7, when these cells are arrested in metaphase and treated with nocodazole (Figure 3-14).

The relationship between Ipl1, Glc7, and the KTIP is further supported by functional interactions between various mutants. Compromised Ipl1 function leads to the accumulation of hyperstable KT-MT attachments (Cimini et al., 2006; Pinsky et al.,

**Figure 3-14. Nuclear import of Glc7 is inhibited by nocodazole-induced SAC arrest.**

(A) Wild type cells synthesizing Glc7-GFP were grown to mid-log phase at 23°C (-), then treated with nocodazole (20 μg/ml) and analyzed at the indicated times (+Noc). As seen with other Kap121 cargos, nocodazole-induced M-phase arrest inhibits Glc7-GFP import. (B) $P_{MET3}$-*CDC20* (WT) and $P_{MET3}$-*CDC20 mad1Δ* (*mad1Δ*) cells producing Glc7-GFP were grown to mid-log phase in media lacking methionine (-Met). Methionine was subsequently added to the media, either alone (+Met) or with nocodazole (20 μg/ml; +Met +Noc), and cultures were then incubated for 2.5 h. We observed that nocodazole-induced M-phase inhibition of Glc7-GFP import is dependent on Mad1. In all panels, Glc7-GFP was visualized using epifluoresence microscopy. Nuclear/Cytoplasmic fluorescence intensity ratios for Glc7-GFP are shown (right panels; n ≥ 50 cells). Error bars express standard error. (C) $P_{MET3}$-*CDC20,* $P_{MET3}$-*CDC20 mad1Δ,* and $P_{MET3}$-*CDC20 mad2Δ* cells were grown to mid-log phase in media lacking methionine (-Met). Methionine was subsequently added to the media alone (+Met) or with nocodazole (20 μg/ml; +Met +Noc) and cultures were incubated for an additional 2.5 h. Whole cell extracts were analyzed by western blotting using a phospho-specific anti-histone H3 phosphoserine 10 antibody (H3{pSer10}) or anti-histone H3 antibody. In the WT and *mad2*Δ backgrounds, H3 serine 10 phosphorylation is observed in the nocodazole-treated cells. By contrast, $P_{MET3}$-*CDC20 mad1*Δ cells, lacking a functional KTIP, exhibited decreased levels of H3 serine 10 phosphorylation. (D) Western blots were performed using an anti-GFP antibody to assess Glc7-GFP levels within the indicated strains shown above and in Figure 7. anti-Gsp1 western blots were also carried out as loading controls.

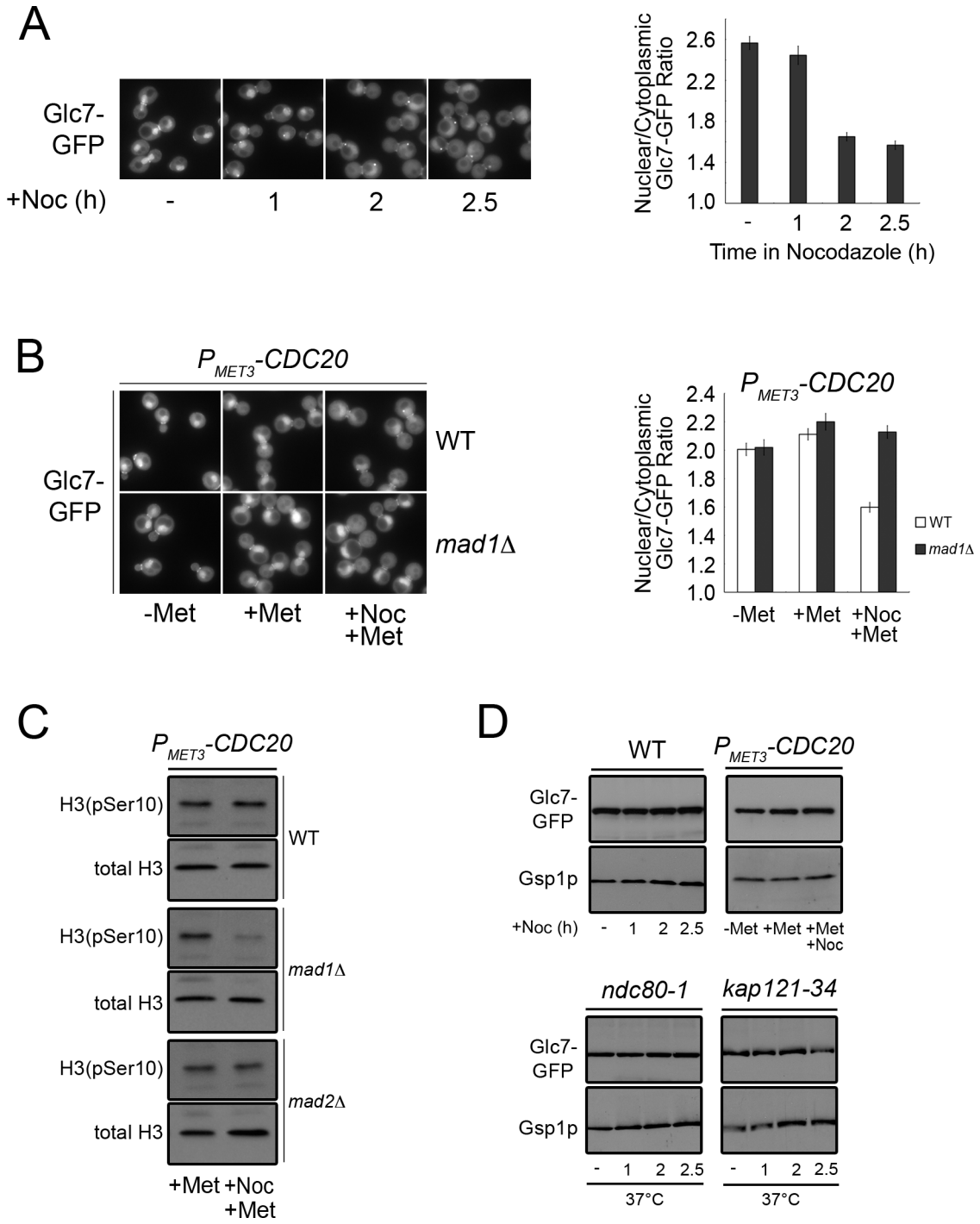


**Figure 3-14. Nuclear import of Glc7 is inhibited by nocodazole-induced SAC arrest.**

2006b) and, consistent with this, we observed that *ipl1-321* mutant cells appear more resistant to MT-destabilizing drugs and grow more robustly than WT cells in their presence (Figure 3-11). A similar phenotype is also detected in a *nup53ΔKBD* mutant, whose only known defect is the loss of the KTIP (Makhnevych et al., 2003). We postulated that increased nuclear Glc7 caused by the *nup53ΔKBD* mutant during SAC arrest would explain the phenocopy of the *ipl1-321* mutant. Consistent with this idea, we observed that the benomyl-resistant phenotype of the *nup53ΔKBD* mutant is dependent on Glc7 (Figure 3-11). These results further support a mechanistic link between the control of Kap121-mediated import and Ipl1 function.

It is also of note that a recent manuscript reported a physical interaction between Ipl1 and Kap121, providing evidence for a complex containing Ipl1, three previously identified Ipl1 interactors, and Kap121 (Breitkreutz et al., 2010). The functional significance of this observation remains to be clarified, as our data imply that Ipl1 is not an import cargo of Kap121 (Figure 4-7). As we have seen in this study and others, Kaps can function in roles outside of nuclear transport, e.g. Xpo1 acting as a signal transducer as shown here and R. Scott et al., 2009 (also see Harel and Forbes, 2004; Roscioli et al., 2012), and it will be of interest to determine whether Kap121 plays multiple roles in Ipl1 function.

In addition to its role in supporting Ipl1 activity, it seems plausible that the KTIP contributes to additional processes during SAC arrest. All Kap121 cargos are predicted to be affected by the KTIP. However, at present, the Kap121 cargo inventory is almost certainly incomplete (Leslie et al., 2004; Krogan et al., 2006; Breitkreutz et al., 2010), leaving unclear the list of potential functions that could be influenced by the

KTIP. Based on the observation that the KTIP is not required for SAC arrest, at least within the parameters we have used to examine its function, whatever role this pathway plays is likely to be, at least partially, redundant. This is not unusual for nuclear transport pathways as multiple factors, including both Importins and Exportins, often contribute to the localization of proteins. The processes that control the localization of Cdh1 underscore this idea. Cdh1, which regulates the activity of the APC/C, is imported into the nucleus by Kap121 during the G1/S-phase (Jaquenoud et al., 2002). However, phosphorylation-induced export mediated by the Kap, Msn5, drives Cdh1 into the cytoplasm during the G2/M-phase where it is sequestered away from the APC/C. Thus, in SAC-arrested cells, exclusion of Cdh1 from the nucleus is likely enhanced by Msn5-mediated export and the KTIP.

Through our characterization of the KTIP, we have uncovered an interwoven relationship between KTs, Mad1, and NPCs, and established a previously undefined functional relationship between Kaps that implicates Xpo1 in the regulation of Kap121-mediated import (Figure 3-9). We have shown that Mad1 can detect the assembly state of the KT-MT interface and, in response to and support of Ipl1 signaling, influence the structure and function of the NPC. We envisage that similar functional relationships are conserved throughout eukaryotes, including those undergoing open mitosis. Binding of Mad1 to both KTs and NPCs, including to mammalian Nup53( Hawryluk-Gara et al., 2005), as well as the interactions of Xpo1 (Crm1; Joseph et al., 2004) with KTs, is conserved in vertebrates. While open mitosis and disassembly of the NE in these organisms would preclude the need for transport regulation during metaphase, Mad1 is recruited to KTs in early prophase prior to NPC and NE disassembly that occurs in late

prophase (Campbell et al., 2001; Chi et al., 2008; reviewed in Güttinger et al., 2009). Thus, a role for Mad1 in the regulation of nuclear transport is plausible in early mitosis. It is also intriguing to consider that the functions we have uncovered for yeast Mad1 in modulating Nup-Nup and Nup-Kap interactions could be used to regulate other aspects of NPC biology, among these coordinating an arrest of NPC assembly until the SAC is satisfied.

# **Chapter IV:** *A role for Kap121 in mitotic kinetochore bi-orientation*[*]

[*] A similar work will be submitted for publication.

**4.1 Overview**

In addition to facilitating macromolecular transport through NPCs, emerging evidence has implicated a number of Kaps as key regulators of essential mitotic processes, including chromosome transmission. Here, we have uncovered a novel function for the essential importin, Kap121, in contributing to the formation of stable, bi-polar KT-MT attachments during mitosis in yeast. This function for Kap121 pertains to its ability to physically associate with Dam1 and Duo1, which are two essential structural constituents of the MT-bound Dam1 complex, an assembly required for linking dynamic MT ends to the outer KT. We show that the physical association of Kap121 with Dam1/Duo1 promotes the structural stability of these proteins *in vivo,* as the loss of Kap121 binding leads to their destabilization and degradation. Consequently, this gives rise to errors in KT bi-orientation resulting in inaccurate chromosome segregation. Moreover, we show that the physical association of Kap121 with Duo1 is resistant to RanGTP-mediated dissociation suggesting that this complex can form in the Ran-rich environment of the nucleus, including at the KT-MT interface. Taken together, we propose that Kap121 confers a "chaperone-like" function within the nucleus where, through its physical association with Dam1/Duo1, it contributes to the structural stability of the Dam1 complex by preventing Dam1 and Duo1 degradation.

## 4.2 Results

### 4.2.1 Kap121 is required for KT bi-orientation

Cells compromised for Kap121 function display defects in mitotic progression. In particular, cells harboring the *kap121-34* allele accumulate as large budded cells and are stalled at the metaphase-to-anaphase transition (Makhnevych et al., 2003). Stalled progression at this mitotic stage often arises due to defects in anaphase spindle elongation (He et al., 2001; Severin et al., 2001) or SAC-mediated arrest stemming from defective KT-MT interactions (reviewed in McAnish et al., 2003; Tanaka et al., 2005; Westermann, 2007; Biggins, 2013). To differentiate between these possibilities, we examined the distribution of KTs in cells by analyzing the localization of the KT protein Mtw1 tagged with GFP relative to SPBs containing Spc42-mCherry. If cells are stalled in metaphase as a result of faulty KT-MT interactions, sister KTs will fail to bi-orient on the mitotic spindle (Goshima and Yanagida, 2000; McAnish et al., 2003; DeWulf et al., 2003; Tanaka et al., 2005; Godek et al., 2014). By contrast, if anaphase spindle elongation is defective, metaphase KT alignment would appear normal, as defects in spindle mid-zone elongation do not impact metaphase KT bi-orientation (He et al., 2001; Severin et al., 2001; Gillet et al., 2004).

As WT cells enter the early stages of mitosis, KTs align synchronously on the mitotic spindle and adopt a "bi-lobed" configuration where two separate KT foci (~1 μM apart) are positioned along the spindle axis between separated sister SPBs (Goshima and Yanagida, 2000; He et al., 2000; Tanaka et al., 2000; McAnish et al., 2003; DeWulf et al., 2003; Tanaka et al., 2005). This distribution pattern indicates that sister KTs, i.e, those from opposite sister chromatids, have formed accurate and stable attachments to

MTs and are under tension (Figure 4-1A, WT) (McAnish et al., 2003; Tanaka et al., 2005; Kemmler et al., 2009). Strikingly, in analyzing the distribution of Mtw1-GFP in *kap121-34* cells, KT bi-orientation in metaphase cells appeared defective. The vast majority of *kap121-34* cells yielded multiple individual Mtw1-GFP foci distributed linearly along the length of the spindle axis between separated sister SPBs (Figure 4-1A, *kap121-34*). In addition, a subpopulation of cells contained KTs collapsed into a single focus. These observations were also supported by time-lapse imaging of *kap121-34* cells, which also revealed that KTs remain largely unclustered throughout the course of metaphase followed by either their collapse into a single focus or separation upon anaphase entry (Figure 4-2A). These phenotypes are characteristic of a failure to establish KT bi-orientation on the mitotic spindle, suggesting these cells are unable to maintain, or establish, load-bearing KT-MT attachments necessary for efficient chromosomal bi-orientation. By contrast, mutations in a structurally related Kap, Kap123 (*kap123*Δ), exhibited no mitotic KT alignment defects (Figure 4-2B).

The KT bi-orientation defect in cycling *kap121-34* cells was also detected when these cells were arrested in metaphase by depletion of the APC/C co-activator Cdc20 (Figure 4-1B; +Met). Moreover, to acquire a better understanding of the nature of the KT defects possessed by *kap121-34* cells, the distribution of KTs (Mtw1-mCh) was followed relative to the position of the mitotic spindle (GFP-Tub1). While two distinct KT foci are positioned along the spindle axis (GFP-Tub1) in WT cells, the *kap121-34* mutant presented with multiple KT foci, along the mitotic spindle. These data led us to conclude that despite the inability of KTs to achieve KT bi-orientation, they associate with the mitotic spindle (Figure 4-1C).

**Figure 4-1. Cells compromised for Kap121 function exhibit KT bi-orientation defects.**

The localization of KTs (Mtw1-GFP or Mtw1-mCherry) relative to SPBs (Spc42-mCherry) or spindle-MTs (GFP-Tub1) was assessed using epifluorescence microscopy under the indicated conditions for growth. Arrowheads indicate the positioning of KTs. (A, D) Wild-type (WT), *kap121-34* and *kap121-41* cells producing Mtw1-GFP and Spc42-mCherry were grown to mid-logarithmic phase at 23°C and were subsequently shifted to 37°C for 3 h. (B) $P_{MET3}$-*CDC20* and *kap121-34* $P_{MET3}$-*CDC20* cells synthesizing Mtw1-GFP were propagated overnight in medium lacking methionine (-Met) at 23°C. To cultures in mid-logarithmic phase, methionine was added (+Met) for 2.5 h to deplete Cdc20 to induce a metaphase arrest. (C) *kap121-34* $P_{MET3}$*GFP-TUB1* cells expressing Mtw1-mCherry were grown in YPD at 23°C and were shifted to medium lacking methionine for 45 min to induce GFP-Tub1 expression for imaging the spindle. (E) $P_{MET3}$-*KAP121* cells expressing Mtw1-GFP and Spc42-mCherry were propagated in medium lacking methionine (-Met) at 23°C. Methionine was added (+Met) to mid-logarithmic phase cultures for a total of 3.5 h to deplete Kap121. (F) Bar graphs display a quantification of the number of large budded cells containing duplicated SPBs situated in close proximity to the bud-neck, i.e. metaphase cells, with KTs in the bi-lobed configuration versus cells displaying either unclustered or collapsed KT foci. The data are expressed as percentages ($n \geq 100$ cells).

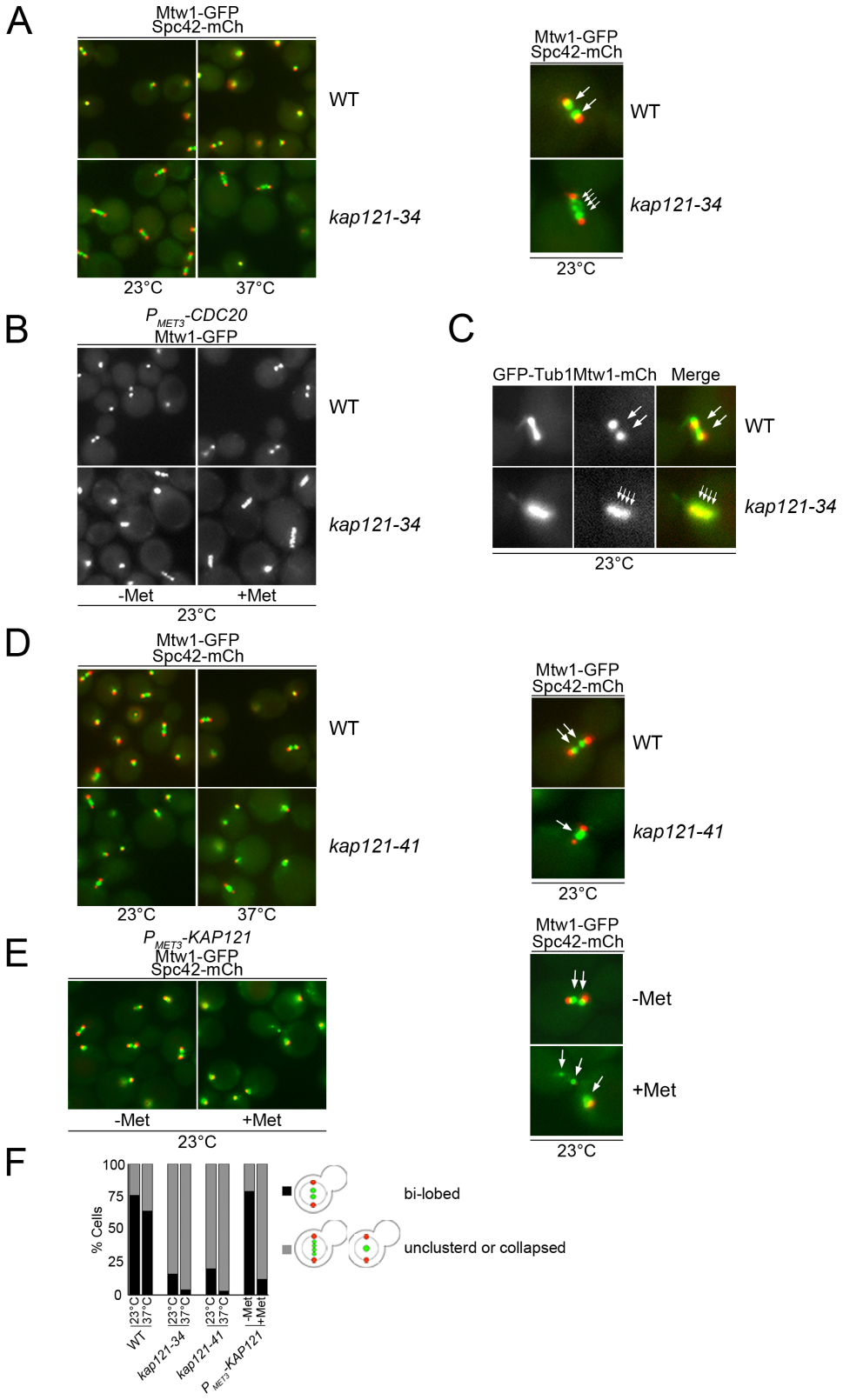


**Figur 4-1. Cells compromised for Kap121 function exhibit KT bi-orientation defects.**

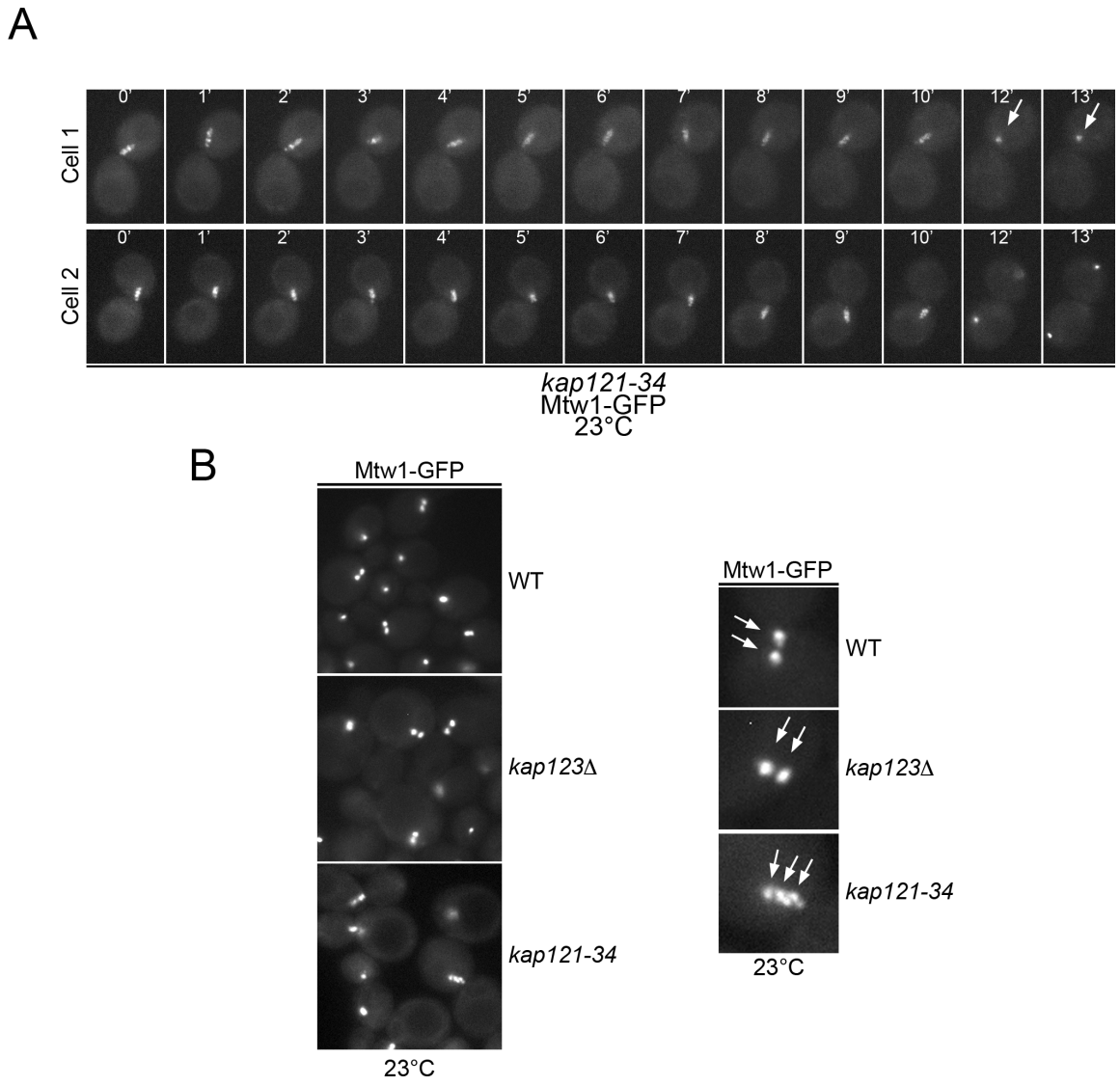


**Figure 4-2. KT dynamics in *kap121-34* cells.**

The distribution of KTs was analyzed in *kap121-34* and *kap123Δ* cells using an epifluorescence microscope. (A) Two separate metaphase *kap121-34* cells producing Mtw1-GFP (Cell 1 and Cell 2) were imaged at 1-min intervals for a total of 13 min at 23°C. Arrowheads point to collapsed KT foci. (B) Cultures of WT, *kap123Δ* and *kap121-34* cells synthesizing Mtw1-GFP were propagated at 23°C and then imaged. Arrowheads indicate the positioning of KTs.

We also investigated whether defects in mitotic KT bi-orientation were specific for the *kap121-34* allele or whether this phenotype is generally visible upon loss of Kap121 function. To test this, we examined KT bi-orientation in another Ts allele (*kap121-41*; Leslie et al., 2002) and cells depleted of WT Kap121 ($P_{MET3}$-*KAP121*, +Met). As with the *kap121-34* mutant, both the *kap121-41* mutant cells and cells depleted of Kap121 failed to properly bi-orient their sister KTs on the mitotic spindle (Figure 4-1D and 4-1E). Of note, cells depleted of Kap121 showed the most severe KT defects as Mtw1-GFP foci appeared off the spindle axis and randomly distributed throughout the nucleus suggesting that KTs are detached from spindle-MTs (Figure 4-1E). Quantification of the percentage of metaphase cells presenting KTs in the bi-lobed configuration revealed that all three alleles (*kap121-34, kap121-41* and $P_{MET3}$-*KAP121*) displayed a low percentage of cells with bi-oriented KTs subsequent to Kap121 inactivation (Figure 4-1F). Taken together, these results demonstrate that Kap121 function is required for KT bi-orientation during the early stages of mitosis.

### 4.2.2 Kap121 is required for accurate chromosome segregation

A failure to efficiently establish KT bi-orientation leads to defects in chromosome transmission (Goshima and Yanagida, 2000; He et al., 2000; Tanaka et al., 2000; DeWulf et al., 2003; McAnish et al., 2003; Tanaka et al., 2005; Westermann et al., 2007; Tanaka, 2010; Tanaka, 2012; Biggins, 2013; Cheeseman, 2014; Godek, 2014). Thus, we examined the fidelity of chromosome segregation in cells compromised for Kap121 function using FACS analysis. Cultures of WT cells exhibit characteristic 1N and 2N peaks, largely representative of G1 and M-phase cell populations. At the permissive

temperature for growth, the *kap121-34* cell population contains a higher percentage of large budded cells with a 2N DNA content as compared to WT cells, consistent with previous reports (Figure 4-3A; left and right panels) (Makhnevych et al., 2003). Following shift to the non-permissive temperature, a sub-population of *kap121-34* cells displayed a broadened 4N peak indicating abnormal chromosomal segregation (Figure 4-3A; left panel). Similarly, depletion of Kap121 ($P_{MET3}$-*KAP121,* +MET) also resulted in a robust mitotic delay (Figure 4-3B; 2.5 h +Met), with prolonged depletion (4 h) giving rise to severe chromosomal segregation defects (Figure 4-3B; 4h + MET).

If the mitotic delays observed upon loss of Kap121 function are linked to defects in KT-MT interactions, they are likely to arise as a consequence of SAC activation. To test this, FACS analysis was performed on *kap121-34* cells lacking an essential SAC component, Mad1 (*kap121-34 mad1Δ*). At 23°C, FACS analysis of *kap121-34 mad1Δ* cells revealed an increase in the 1N peak relative to the *kap121-34* single mutant indicating that SAC abrogation relieves the observed mitotic delay in *kap121-34* cells (Figure 4-3C). Furthermore, at the non-permissive temperature, the increased frequency of chromosome missegregation detected in *kap121-34* cell populations is further exacerbated in the absence of Mad1 (Figure 4-3C). The loss of SAC function in *kap121-34* cells also reduces the viability of this mutant (*kap121-34 mad2Δ*) at various temperatures (Figure 4-3D). Taken together, these data reveal that cells lacking Kap121 function present mitotic delays likely as a consequence of defects in KT-MT interactions and the recognition of these defects by the SAC.

**Figure 4-3. Loss of Kap121 function results in chromosomal segregation defects.**

Cell cultures of the indicated genotypes were propagated overnight to mid-logarithmic phase, and cellular DNA content was assessed using FACS analysis under the indicated conditions. The positions of 1N, 2N and 4N peaks are indicated with arrows (A, B, C). (A) DF5 (WT) and *kap121-34* cells were grown at 23°C and were subsequently shifted to 37°C for 4.5 h. Quantification of the percentage of large budded cells was also determined under the indicated conditions (Right panel; n ≥ 100 cells). (B) $P_{MET3}$-*KAP121* cells were grown overnight in medium lacking methionine (-Met). Methionine was added to the medium (+Met) to repress *KAP121* expression, and cells were analyzed at the indicated times. Percent large budded cells are also displayed (Right panel; n ≥ 100 cells). (C) Cultures of WT, *kap121-34*, and *kap121-34 mad1Δ* cells were grown overnight at 23°C and shifted to 37°C for 4.5 h. (D) Cultures of DF5 (WT), *mad2Δ, kap121-34,* and *kap121-34 mad2Δ* cells were serially diluted, spotted onto YPD plates, and incubated at the indicated temperatures for 2-3 days.

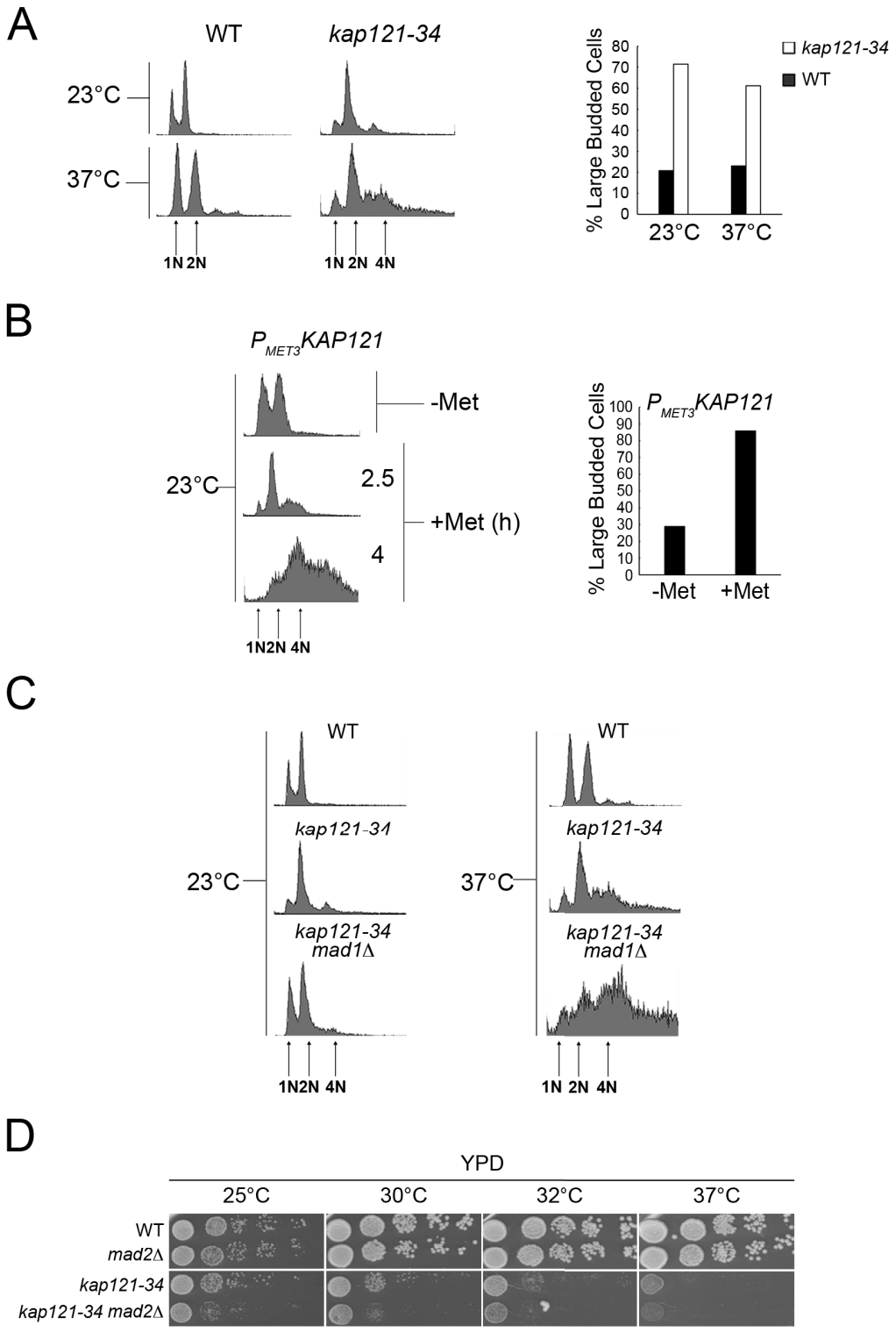


**Figure 4-3. Loss of Kap121 function results in chromosomal segregation defects.**

### 4.2.3 Inhibition of Kap121-mediated import does not affect KT bi-orientation.

As yeast cells undergo a closed mitosis, a potential explanation for the KT bi-orientation defects seen in the *kap121* mutants was the inhibition of nuclear import of proteins responsible for proper KT or spindle function. If correct, we would predict a direct correlation between conditions that inhibited Kap121-mediated import and defects in KT bi-orientation. To test this, we examined KT alignment in cells over producing the FG-nucleoporin Nup53 ($P_{GAL1}$*NUP53*). In these cells, Kap121-mediated import is specifically inhibited despite the presence of WT Kap121 (Marelli et al., 2001). Within the $P_{GAL1}$*NUP53* strain background, we simultaneously followed Kap121-mediated transport, using an $NLS^{Pho4}$-GFP reporter, and KT positioning, using Mtw1-mCherry, following induction of *NUP53* overexpression. Prior to induction ($P_{GAL1}$*NUP53*, +Raf), $NLS^{Pho4}$-GFP accumulates in the nucleus and KT distribution in mitotic cells appeared normal (Figure 4-4A). By contrast, following overproduction of Nup53 ($P_{GAL1}$*NUP53*, +Gal), nuclear levels of $NLS^{Pho4}$-GFP were greatly reduced (Figure 4-4A, +Gal; $NLS^{Pho4}$-GFP). Despite the inhibition of Kap121-mediated import under these conditions, mitotic chromosome alignment appeared normal, as indicated by the consistent presence of bi-lobed, bi-oriented KTs in cells transiting through metaphase (Figure 4-4A, +Gal; Mtw1-mCherry). Two additional observations also support a transport independent role for Kap121 in KT bi-orientation. First, we have detected that the addition of a protein A tag to the C-terminus of Kap121 (Kap121-pA) inhibited nuclear import of the $NLS^{Pho4}$-GFP reporter (Figure 4-4B), potentially by altering cargo binding sites near the C-terminus of Kap121 (Kobayashi and Matsuura, 2013).

**Figure 4-4. Arrest of Kap121-mediated import does not impact metaphase KT-alignment.**

Kap121-mediated transport ($NLS^{Pho4}$-GFP) and KT localization (Mtw1-mCherry) were monitored using epifluorescence microscopy under the indicated conditions (left panels; A, B, C). The Nuclear/Cytoplasmic fluorescence intensity ratios for $NLS^{Pho4}$-GFP were also calculated under the indicated conditions of growth (A and B; $n \geq 50$ cells). Error bars represent standard error (right and middle panels). (A) A culture of *$P_{GAL1}$-NUP53 $NLS^{Pho4}$-GFP MTW1-MCHERRY* cells was propagated in medium containing raffinose (+Raf) as the sole carbon source at 23°C. Once cultures reached early-logarithmic phase, galactose was added (+Gal) for 10 h to overproduce Nup53 to inhibit Kap121-mediated import. Western blot analysis using an anti-Nup53 antibody was performed in parallel to follow Nup53 cellular levels following galactose addition (Right panel). (B) WT, *KAP121-PA* and *kap121-34* cells synthesizing $NLS^{Pho4}$-GFP and Mtw1-mCherry were grown overnight to mid-logarithmic phase at 23°C. (C) *kap121-34 MTW1-GFP* and *kap121-34 $NLS^{Pho4}$-GFP* cells transformed with either p*EMPTY* or p*KAP121* were propagated overnight at 23°C to mid-logarithmic phase. The number of cells containing a nuclear $NLS^{Pho4}$-GFP signal, as well as the number of large budded cells presenting KTs in the bi-lobed configuration, was quantified in *kap121-34* p*EMPTY, kap121-34* p*KAP121* and WT cell populations. The data were plotted on the same graph for a compare-wise analysis (Right panel; $n \geq 100$ cells). (D) Cultures of *kap121-34* p*EMPTY* and *kap121-34 pKAP121 cells* were serially diluted, spotted onto CM-Leu plates, and incubated at the indicated temperatures for 3-4 days.

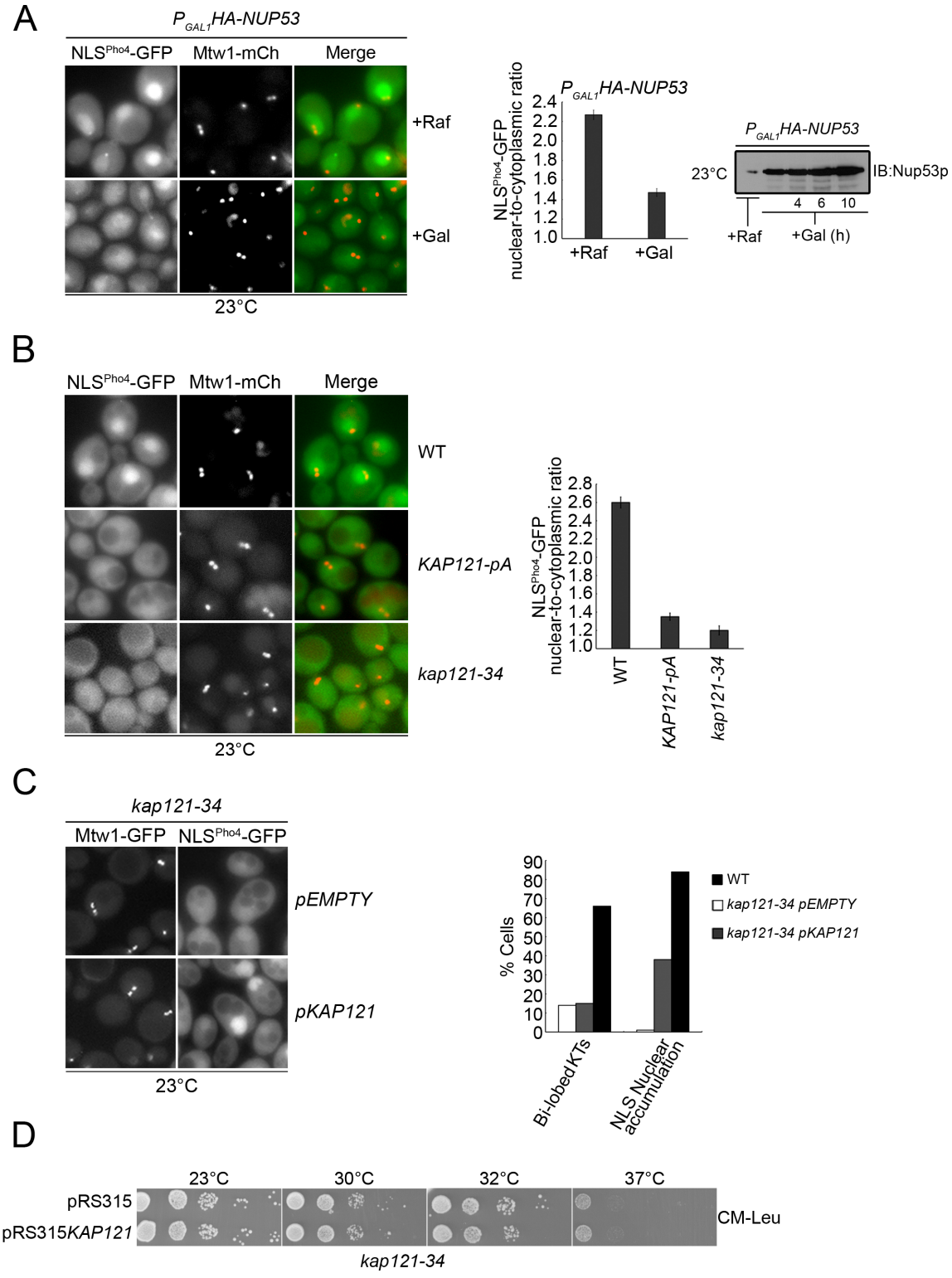


**Figure 4-4. Arrest of Kap121-mediated import does not impact metaphase KT-alignment.**

However, cells synthesizing the Kap121-pA fusion showed no defects in KT bi-orientation (Figure 4-4B). Second, ectopic expression of WT *KAP121* in *kap121-34* cells leads to the restoration of import (Leslie et al., 2002; Figure 4-4C). Despite this restored nuclear import, *kap121-34* cells expressing ectopic *KAP121* exhibit similar growth rates compared to *kap121-34* cells transformed with plasmid alone (Figure 4-4C and 4-4D). On the basis of these data, we conclude that the KT bi-orientation defects observed in the various *kap121* mutant alleles cannot be explained by the inhibition of cargo import.

### 4.2.4 Kap121 binds the Dam1 complex and Ipl1

Various proteins have been detected in association with Kap121, with many established or potential import cargos. Most of these have no obvious functional link to KTs, with the exception of Duo1, a protein identified in association with Kap121 in a high-throughput protein-protein interaction screen (Krogan et al., 2006). Furthermore, a genetic screen previously conducted in our laboratory identified a mutation synthetically lethal with the *kap121-34* allele, which could be suppressed by *DUO1* (Axel Dienemann, University of Alberta, personal communication). Duo1 is a structural component of the Dam1 complex, an essential MT-bound assembly required for physically linking dynamic MT tips with the outer KT (Hoffman et al., 1998; Cheeseman et al., 2001; Janke et al., 2002; Tanaka et al., 2005; Westermann et al., 2005; Miranda et al., 2005; Wang et al., 2007; Westermann et al., 2007; Lampert et al., 2010; Tien et al., 2010; Biggins 2013; Lampert et al., 2013; Tien et al., 2013; Umbreit et al., 2014). On the basis of these data, we examined the interactions of Kap121 with the Dam1 complex. Kap121-pA was purified from cells also producing Duo1-13Myc or Dam1-13Myc. Western analysis of

Kap121-pA bound proteins revealed both Duo1-13Myc and Dam1-13Myc co-purified with Kap121-pA (Figure 4-5A). Consistent with these data, reciprocal purifications of Dam1-pA or Duo1-pA contained bound Kap121-13Myc (Figure 4-5B). Also detected in association with Kap121 was the Aurora B-kinase Ipl1, a protein that interacts with the Dam1 complex and modulates its interactions with KTs (Kang et al., 2001; Cheeseman et al., 2002). We conclude from these results that Kap121 physically interacts with the Dam1 complex.

RanGTP binding to Kap121 induces the release of bound cargos (reviewed in Wente and Rout, 2010; Aitchison and Rout, 2012). However, intranuclear interacting partners of Kap121, such as Ulp1 (Panse et al., 2003), and other Importins have, in some cases, been shown to form RanGTP-resistant complexes that function in the RanGTP-rich environment of the nucleoplasm (Lee and Aitchison, 1999; Pemberton et al., 1999; Mosammaparast et al., 2002). Given that the nuclear localization of the Dam1 complex and its interactions with Kap121, we examined whether this complex was sensitive to RanGTP. We affinity-purified Duo1-pA or Nup53-pA from cell extracts containing Kap121-13Myc. Isolated complexes were then incubated with either RanGTP or RanGDP. The Kap121-Nup53 complex was previously shown to be disrupted by RanGTP (Marelli et al., 1998), and consistent with these reports, Kap121-13Myc was efficiently released from Nup53-pA upon treatment of the complex with RanGTP but not RanGDP (Figure 4-5C). By contrast, the Duo1-pA-Kap121-13Myc complex was unaffected by the addition of RanGTP (Figure 4-5C). On the basis of these data, we conclude that Duo1 is unlikely to be an import cargo of Kap121. Instead, this

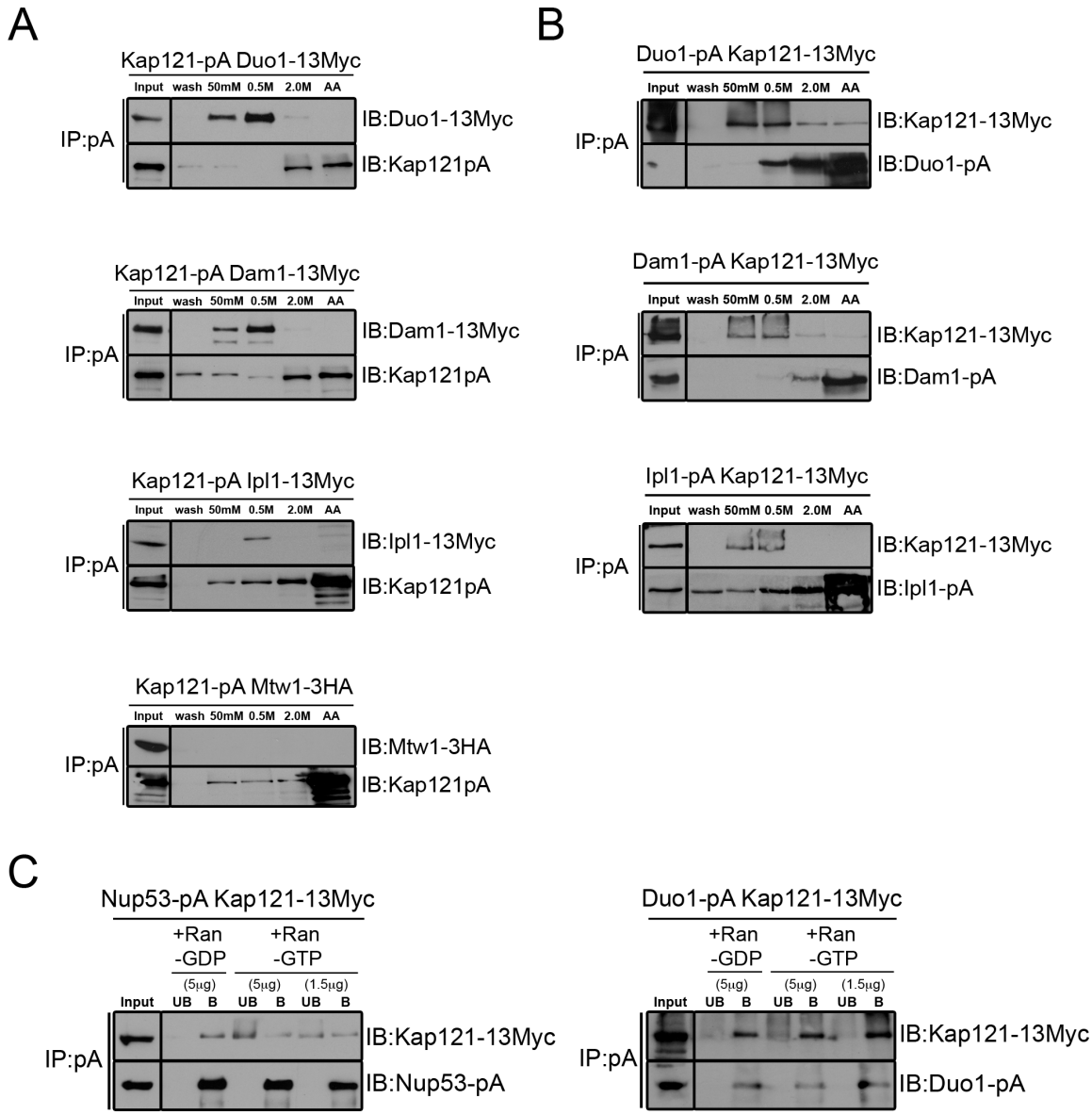


**Figure 4-5. Kap121 interacts physically with the Dam1 complex and Ipl1.**

(A) The Kap121-pA fusion protein was affinity purified from cells producing Dam1-13Myc, Duo1-13Myc, Ipl1-13Myc or Mtw1-3HA fusion proteins. Bound proteins were eluted using a stepwise gradient of magnesium chloride ($MgCl_2$) and a final 0.5 M acetic acid wash (AA). The eluted fractions were analyzed by western blot analysis to detect the indicated proteins. Samples of the protein input (input) and the final wash (wash) are included in each panel. (B) IP experiments reciprocal to those described in (A) were performed using strains that produced the indicated pA and Myc-tagged proteins. (C) The ability of RanGTP to release Kap121-13Myc from Duo1-pA and Nup53-pA complexes was analyzed. Equivalent amounts of either immunopurified complex were incubated with RanGTP or RanGDP. Bound (B) and released (UB) fractions were analyzed by western blot analysis using anti-Myc and anti-protein A antibodies.

interaction may occur within the nuclear interior, presumably at the KT-MT interface, where the Dam1 complex resides.

### 4.2.5 Carboxy-terminal tagging of Duo1 leads to the suppression of KT bi-orientation defects in *kap121-34* mutant cells

Our data led us to conclude that the KT bi-orientation defect in the *kap121-34* mutant is unlikely to be linked to Kap121-mediated import. Consistent with this idea, an examination of GFP-tagged Dam1, Duo1, or Ipl1 in the *kap121-34* mutant revealed that each GFP fusion protein targeted to the nucleus (Figure 4-6A). In WT cells, Duo1-GFP was visible at KTs, with metaphase cells exhibiting a linear, bi-lobed distribution of KT-associated Duo1-GFP. Surprisingly, the localization pattern of Duo1-GFP in *kap121-34* cells appeared largely indistinguishable from WT at both 23°C and 37°C (Figure 4-6A). A partial phenotypic suppression effect was also observed in *kap121-34* cells synthesizing Dam1-GFP (Figure 4-6A). Since the observed phenotypic suppression effect was more robust in cells producing Duo1-GFP, we more closely examined the effects this fusion protein had on KT bi-orientation in *kap121-34* cells. When analyzing Duo1-GFP relative to KTs (Mtw1-mCh), GFP and mCherry signals colocalized in the *kap121-34* mutant at 23°C and 37°C (Figure 4-6B), and Duo1-GFP was also positioned between separated SPBs, labeled with Spc42-mCherry (Figure 4-6C). These results implied that the production of the Duo1-GFP fusion protein was capable of suppressing the KT bi-orientation defect observed in the *kap121-34* mutant. Similarly, the expression of *DUO1-GFP* also suppressed the KT bi-orientation defect in Kap121-depleted cells (Figure 4-7, $P_{MET3}$-*KAP121*, + Met for 3.5 h). This rescue effect was not limited to the GFP fusion, as

**Figure 4-6. Carboxy-terminal tagging of Duo1 suppresses metaphase KT alignment defects in *kap121-34* cells.**

(A-E) The subcellular distribution of GFP and mCherry tagged proteins was examined using an epifluorescence microscope. In all instances, cells were grown overnight at 23°C to mid-logarithmic phase and were subsequently shifted to 37°C for 3 h. Arrows indicate the positioning of KTs. (A) Dam1-GFP, Duo1-GFP and Ipl1-GFP were analyzed in WT and *kap121-34* cells expressing Nup159-mCherry. (B, C) The localization of Duo1-GFP was followed relative to either SPBs (Spc42-mCherry) or KTs (Mtw1-mCherry) in *kap121-34* cells. Bar graphs represent a quantification of the number of large budded cells containing KTs in the bi-lobed configuration versus cells yielding either unclustered or collapsed KT foci and are expressed as percentages ($n \geq 100$ cells). (D) The distribution of KTs (Mtw1-GFP) was analyzed in *kap121-34* cells producing Duo1 (untagged), Duo1-pA or Duo1-3HA. (E) Kap121-mediated import was monitored ($NLS^{Pho4}$-GFP) in cells producing Duo1-mCherry grown at permissive (23°C) and non-permissive (37°C) temperatures for 3h.

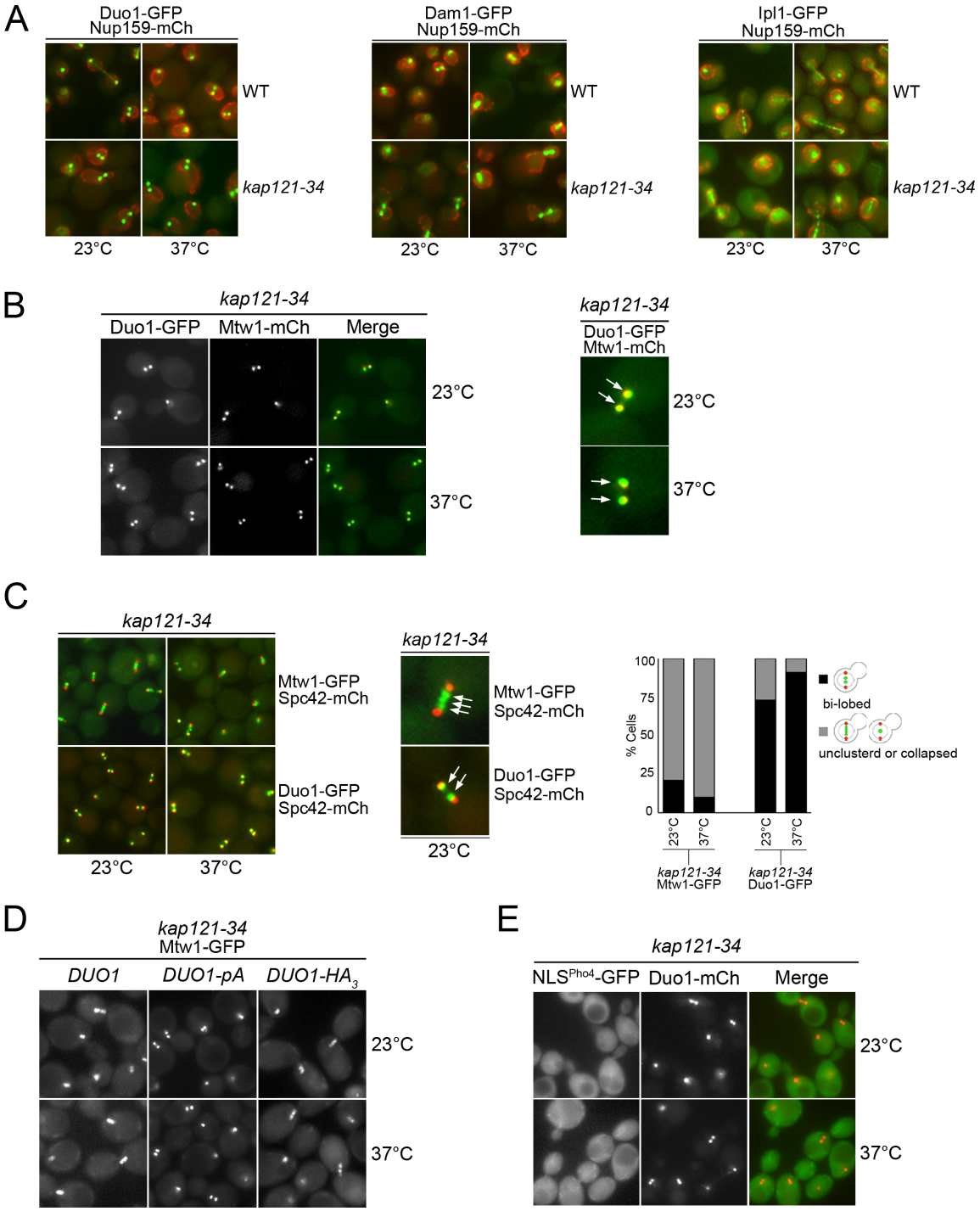


**Figure 4-6. Carboxy-terminal tagging of Duo1 suppresses metaphase KT alignment defects in *kap121-34* cells.**

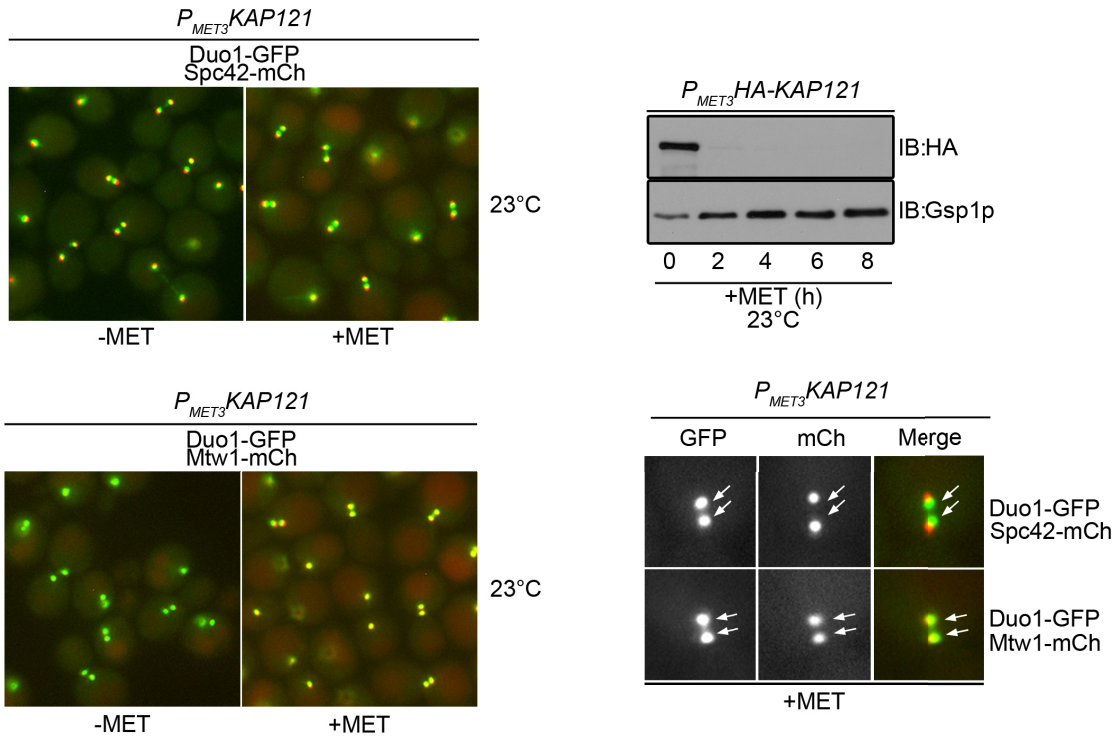


**Figure 4-7. GFP-tagged Duo1 suppresses metaphase KT bi-orientation defects in cells depleted of Kap121.**

(A) *$P_{MET3}$-KAP121* cells expressing either Duo1-GFP in combination with Mtw1-mCherry (KTs) or Spc42-mCherry (SPBs) were grown overnight at 23°C in the absence of methionine (-Met) to mid-logarithmic phase. Cultures were subsequently shifted into methionine-containing medium (+Met) for 3.5h to repress *KAP121* expression. The distribution of Duo1-GFP relative to SPBs (Spc42-mCherry) or KTs (Mtw1-mCherry) was documented using an epifluorescence microscope. Arrowheads indicate the location of KTs. In parallel, whole cell lysates were collected and Kap121 levels were analyzed by western blot using an anti-HA (HA-Kap121) and anti-Gsp1 (load control) antibodies to determine the efficiency of Kap121 depletion.

Duo1 constructs containing a carboxy-terminal protein-A epitope were also capable of suppressing the KT bi-orientation defect in the *kap121-34* mutant (Figure 4-6D). However, the addition of smaller peptide tags (3 x hemagglutinin or 3HA) to Duo1failed to restore KT-alignment, suggesting a bulky Carboxy-terminal tag contributes to the phenotypic suppression effect (Figure 4-6D). While the presence of the Duo1-GFP fusion rescued sister KT bi-orientation, it did not rescue the import defect of *kap121-34* mutant cells. In *kap121-34* cells expressing *DUO1-mCherry*, the $NLS^{Pho4}$-GFP reporter failed to accumulate in nuclei (Figure 4-6E).

### 4.2.6 Loss of Kap121-Dam1 complex interactions leads to Dam1 complex destabilization

The ability of the Duo1-GFP or -pA fusions to restore normal KT bi-orientation in the *kap121-34* mutant led us to hypothesize that mitotic defects associated with this mutant reflect changes in interactions of Kap121 with the Dam1 complex. To further evaluate this idea, we examined whether these interactions were altered in the *kap121-34* mutant. In contrast to the binding of WT Kap121 to the Dam1 complex components (see Figure 4-5), no Dam1-13Myc, Duo1-13Myc, or Ip1l-13Myc was detected in association with purified mutant kap121-34-pA (Figure 4-8A). Similarly, experiments performed using Duo1-pA, Dam1-pA or Ipl1-pA also failed to detect the kap121-34 mutant protein (Figure 4-8B).

Our results support an interaction of the Dam1 complex with Kap121 and a role for this Kap in the function of this complex. As both the assembly and overall integrity of the Dam1 complex are compromised upon the loss of individual complex members (Li et

al., 2002), we examined whether the decreased association of the kap121-34 mutant protein with this complex altered cellular levels of Duo1 and Dam1. Using western blotting analysis, we examined cellular levels of Duo1-3HA and Dam1-3HA in *kap121-34* cells at both permissive and non-permissive temperatures for growth. Strikingly, the levels of both HA-tagged proteins were lower in *kap121-34* cells as compared to WT cells grown at 23°C (Figure 4-8C). Moreover, following a shift to 37°C for 3 h, both proteins showed a further reduction to barely detectable levels (Figure 4-8C). These results imply that the physical association of Kap121 with the Dam1 complex contributes to maintaining normal cellular levels of the complex. The reduction in the Dam1 complex members in the *kap121-34* mutant offers a likely explanation for its observed KT bi-orientation defects. Suppression or partial suppression of these defects by expression of Duo1-GFP or Dam1-GFP led us to test whether the GFP fusions driven by their endogenous gene promoters were stable in the *kap121-34* mutant. We monitored the levels of GFP-tagged Duo1 and Dam1 in *kap121-34* cells, and as shown in Figure 4-8D, both fusion proteins were detectable at 23°C and 37°C, and their levels were comparable to those in WT cells (Figure 4-8D). These data imply that the addition of a bulky C-terminal tag stabilizes Duo1 and Dam1 in *kap121-34* cells.

To assess further the functional relationship between KT-MT defects in *kap121-34* cells and reduced levels of Duo1 detected in these cells, we analyzed whether over producing Duo1 would suppress the KT bi-orientation defects in *kap121-34* cells. For these experiments, the endogenous *DUO1* promoter was replaced with the inducible *MET3* promoter. We could visualize using a $P_{MET3}$-*DUO1-GFP* cassette that induction of

**Figure 4-8. kap121-34 fails to interact with the Dam1 complex or Ipl1.**

(A) kap121-34-pA was immunopurified from cells producing either Dam1-13Myc, Duo1-13Myc or Ipl1-13Myc. Bound complexes were released with increasing concentrations of magnesium chloride ($MgCl_2$) and a final 0.5 M acetic acid wash (AA). Eluted fractions were analyzed by SDS-PAGE and western blot to detect the indicated proteins using anti-MYC and anti-protein A antibodies. Samples of the protein input (input) and the final wash (wash) are included in each panel. (B) Experiments parallel to those described in part (A) were performed using strains producing Duo1-pA, Dam1-pA or Ipl1-pA. Co-purifying proteins were analyzed by SDS-PAGE and western blot using anti-Kap121 and anti-protein A antibodies. (C, D) *kap121-34* and WT cells expressing Duo1-3HA, Dam1-3HA, Duo1-GFP or Dam1-GFP were grown overnight at 23°C and then shifted to 37°C for 3 h. Aliquots of cells were collected for lysis and whole cell extracts were analyzed by both SDS-PAGE and western blot using anti-HA, anti-GFP and anti-Gsp1 (loading control) antibodies. (E) *Kap121-34 DUO1-GFP*, *kap121-34* $P_{MET3}$*-DUO1-GFP*, *kap121-34 MTW1-GFP* and *kap121-34* $P_{MET3}$*-DUO1 MTW1-GFP* strains were propagated in the indicated media at 23°C. The localization of Mtw1-GFP and Duo1-GFP was documented using an epifluorescence microscope.

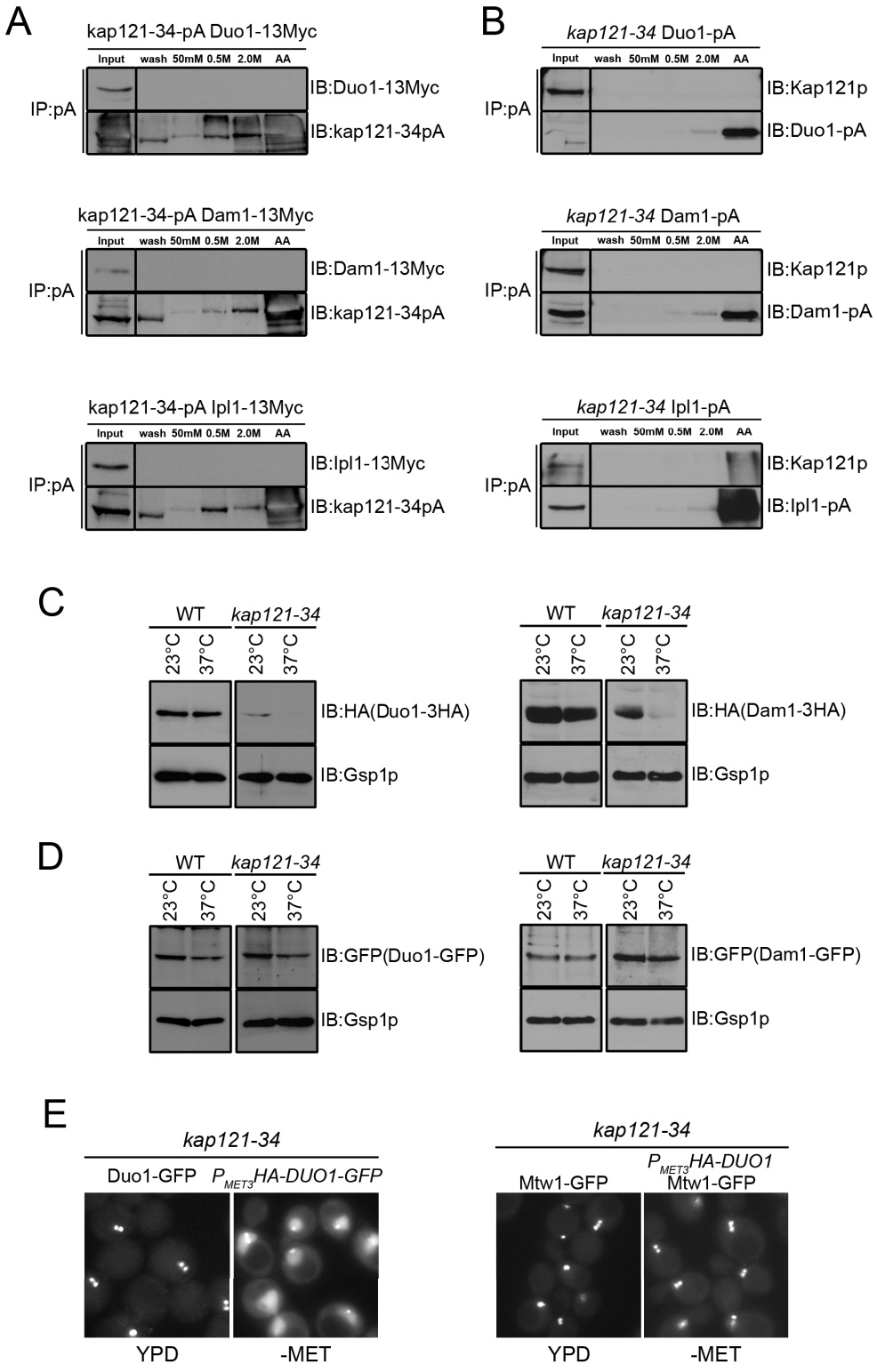


**Figure 4-8. kap121-34 fails to interact with the Dam1 complex or Ipl1.**

the *MET3* promoter (-Met) leads to increased nuclear levels of Duo1-GFP in *kap121-34* cells (Figure 4-8E, left panel). Importantly, overexpression of Duo1 ($P_{MET3}$-*HA-DUO1,* -Met) in *kap121-34* cells led to an increase in the number of mitotic cells with bi-oriented KTs as detected with Mtw1-GFP (Figure 4-8E, right panel). Thus, these data further support the conclusion that the KT bi-orientation defect detected in *kap121* mutant cells is linked to the loss of Dam1 complex stability. Consistent with this conclusion, we also detected a KT defect similar to that seen in *kap121-34* cells in a *duo1* mutant (*duo1-2*; Figure 4-9) defective for Dam1 complex assembly (Li et al., 2002; Westermann et al., 2005).

**4.3 Discussion**

We have uncovered a novel function for Kap121 in regulating mitotic KT bi-orientation in yeast. We have found that Kap121 contributes to the formation of stable bi-polar KT-MT interactions by physically associating with the Dam1 complex. The binding of Kap121 to the Dam1 complex is proposed to promote the stability of this assembly as the loss of Kap121 binding to Dam1/Duo1 leads to their destabilization and degradation. A proposed consequence of disrupting the Kap121/Dam1 complex is faulty KT-MT interactions, leading to erroneous mitotic KT alignment and chromosomal missegregation. Unlike importin/cargo interactions, we show that the Kap121/Duo1 complex is resistant to RanGTP-mediated dissociation, leading us to propose that this complex can form in the RanGTP-rich environment of the nucleoplasm, including at the KT-MT interface. We therefore propose a model in which Kap121 performs a "chaperone-like" function that contributes to the assembly and structural stability of the

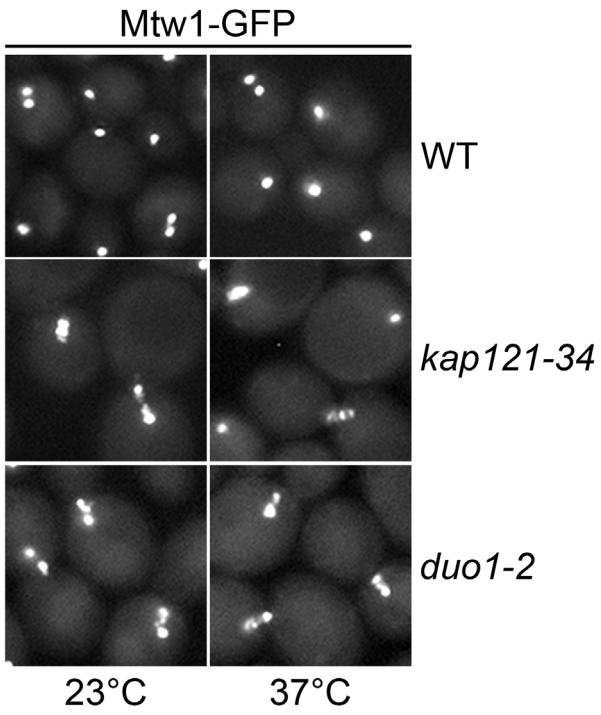


**Figure 4-9. *duo1-2* and *kap121-34* mutant cells produce similar KT bi-orientation defects.**

WT, *kap121-34* and *duo1-2* cells synthesizing Mtw1-GFP (KTs) were propagated overnight at 23°C and then shifted to 37°C for 3 h. The distribution of KTs was documented using epifluorescence microscopy.

Dam1 complex, either prior to, or following import into the nucleus and association of this complex with dynamic MT plus ends.

FACS analysis of *kap121-34* cells revealed that these mutant cells show defects in mitotic progression and also display errors in chromosome transmission (Makhnevych et al., 2003). Here we have demonstrated that this observed mitotic delay is alleviated by abrogation of the SAC (*mad1*Δ) at permissive temperatures for growth, and following growth at the non-permissive temperature, loss of the SAC in these cells leads to chromosome missegregation and cell death (Figure 4-3). As the SAC intimately monitors the state of KT-MT interactions during mitosis, we interpret the SAC-mediated delay in *kap121* Ts mutant cells to directly reflect interaction defects at the KT-MT interface.

Analysis of KT distribution in *kap121* Ts strains revealed striking defects in the ability of chromosomes to bi-orient on the mitotic spindle in these cells. This raised the question as to whether these defects arose as a consequence of alterations in Kap121-mediated transport. However, the state of Kap121-mediated cargo import did not correlate positively with the appearance of mitotic KT defects. For example, we showed that certain conditions that inhibit Kap121-mediated transport, such as the overproduction of Nup53 or expression of the Kap121-pA fusion protein, had no observable effects on sister KT bi-orientation (Figure 4-4). Furthermore, we found that while ectopic expression WT Kap121 suppresses the import defect of *kap121-34* cells, it failed to suppress the mitotic KT bi-orientation defect (Figure 4-4). Together, these data support the idea that the failure of chromosomes to bi-orient on the mitotic spindle in cells compromised for Kap121 function is unlikely to be due to the inhibition of Kap121 cargo import.

Since the inhibition of Kap121-mediated import does not perturb mitotic KT bi-orientation, this led us to speculate that Kap121 likely confers a more direct role in regulating mitotic chromosome alignment. In support of this hypothesis, we showed that Kap121 interacts physically with several proteins that reside at the KT-MT interface. Specifically, our data revealed that Kap121 binds Dam1, Duo1, and Ipl1 (Figure 4-5). Interestingly, the nuclear accumulation of these proteins was unaffected in cells in which Kap121-mediated import was inhibited (Figure 4-6). Moreover, the interaction of Kap121 with Duo1 was resistant to RanGTP-mediated dissociation, supporting the notion that these interactions can occur within the interior of the nucleus.

Importin/cargo complexes that confer RanGTP insensitivity are likely part of a general mechanism that enables Importins to function within the nuclear environment. For instance, Kap114 interacts with TATA-binding protein, Tbp1, in a manner that is resistant to dissociation by RanGTP (Pemberton et al., 1999). This RanGTP-resistant interaction enables Kap114 to target Tbp1 to chromatin, specifically to TATA-containing promoter regions (Pemberton et al., 1999). Intriguingly, the dissociation of this complex and deposition of Tbp1 onto chromatin require binding of both RanGTP and dsDNA containing TATA sequence to Kap114. In addition to this, the interaction of Kap121 with the SUMO isopeptidase, Ulp1, is resistant to RanGTP, and through this Ran-resistant interaction, Kap121 appears to contribute to the tethering of Ulp1 to the nucleoplasmic face of the NPC (Panse et al., 2003). Thus, in line with these observations, the observed RanGTP-resistant Kap121/Duo1 interaction led us to conclude that the binding of Kap121 to the Dam1 complex could occur at various locations in the cell including the nuclear interior at the KT-MT interface.

The Dam1 complex is an essential MT-bound assembly that loads onto MT plus end tips and is required for both establishment and maintenance of stable bi-polar KT-MT interactions (reviewed in Westermann et al., 2007). In effect, the Dam1 complex functions to link KTs to dynamic MT ends and maintain attachments between these structures during KT bi-orientation when significant forces are applied to sister KTs from opposing spindle MTs. Because this complex is required for maintaining stable, load-bearing KT-MT interactions, scenarios that lead to the loss of Dam1 complex functionality give rise to errors in mitotic KT bi-orientation (Hoffman et al., 1998; Cheeseman et al., 2001; Janke et al., 2002; Scharfenberger et al., 2003; Umbriet et al., 2014). Our data support a model where Kap121 is involved in regulating KT bi-orientation by influencing the functional integrity of the Dam1 complex. Consistent with this concept, the mitotic KT phenotypes observed in cells compromised for Kap121 function reflect the loss of Dam1 complex functional integrity. Particularly, we observed that the vast majority of mitotic *kap121-34* and *kap121-41* cells displays KTs that are either de-clustered along the spindle axis or collapsed into a single focus (Figures 4-1 and 4-2). Importantly, our analysis shows that the de-clustered KT phenotype parallels the distribution of mitotic KTs observed in cells lacking Duo1 function (*duo1-2,* 37 °C; Figure 4-9). In addition to this, KTs collapsed into a single focus are a frequent occurrence in *dam1-1* cells grown at the non-permissive temperature (Cheeseman et al., 2001; Gillett et al., 2004; Umbriet et al., 2014). The KT phenotypes associated with depletion of Kap121 ($P_{MET3}$-*KAP121*, +MET; Figure 1) appear more severe than those of the Ts mutants, with Mtw1-GFP foci randomly distributed throughout the nucleus and off the spindle axis, indicating that KTs are detached from spindle MTs. As Dam1 and Duo1

are required to maintain mitotic spindle integrity (Hoffman et al., 1998; Jones et al., 1999; Cheeseman et al., 2001), it is possible that following Kap121 depletion, additional spindle defects manifest, resulting in spindle collapse and detached KTs. However, this possibility remains to be assessed directly.

Our analysis of Kap121 has provided insight into the molecular basis for its contribution to mitotic KT bi-orientation. In addition to binding the Dam1 complex, the presence of Kap121 maintains the stability of key structural members of the Dam1 complex (Figure 4-8). Under conditions where Kap121 fails to physically associate with the Dam1 complex (kap121-34; Figure 4-8), the stability of both Dam1 and Duo1 is significantly compromised. From this, we propose that it is the loss of Dam1/Duo1 stability that leads to the observed mitotic KT bi-orientation defects in cells lacking Kap121 function (Figure 4-1). Importantly, conditions that stabilize Duo1, i.e. the addition of a large carboxy-terminal tag, or overproduction of Duo1 suppresses the KT bi-orientation defect in *kap121* mutant cells (Figures 4-6, 4-7 and 4-8). Similarly, Dam1-GFP also partially suppressed the KT bi-orientation defect. The less robust effect of the Dam1-GFP fusion might be explained by the fact the carboxy-terminus of Dam1 is required for its efficient interaction with Ndc80 and the addition of a large tag could affect this interaction (Lampert et al., 2010; Ramey et al., 2011a).

How Kap121 is involved in maintaining the stability of the Dam1 complex remains undetermined. Our data are consistent with several possible roles for Kap121. In one model, Kap121 could function as a constitutive and essential component of the Dam1 complex whose loss leads to destabilization of the complex. Arguing against this model is the observation that, unlike Duo1-GFP or Dam1-GFP, Kap121-GFP does not

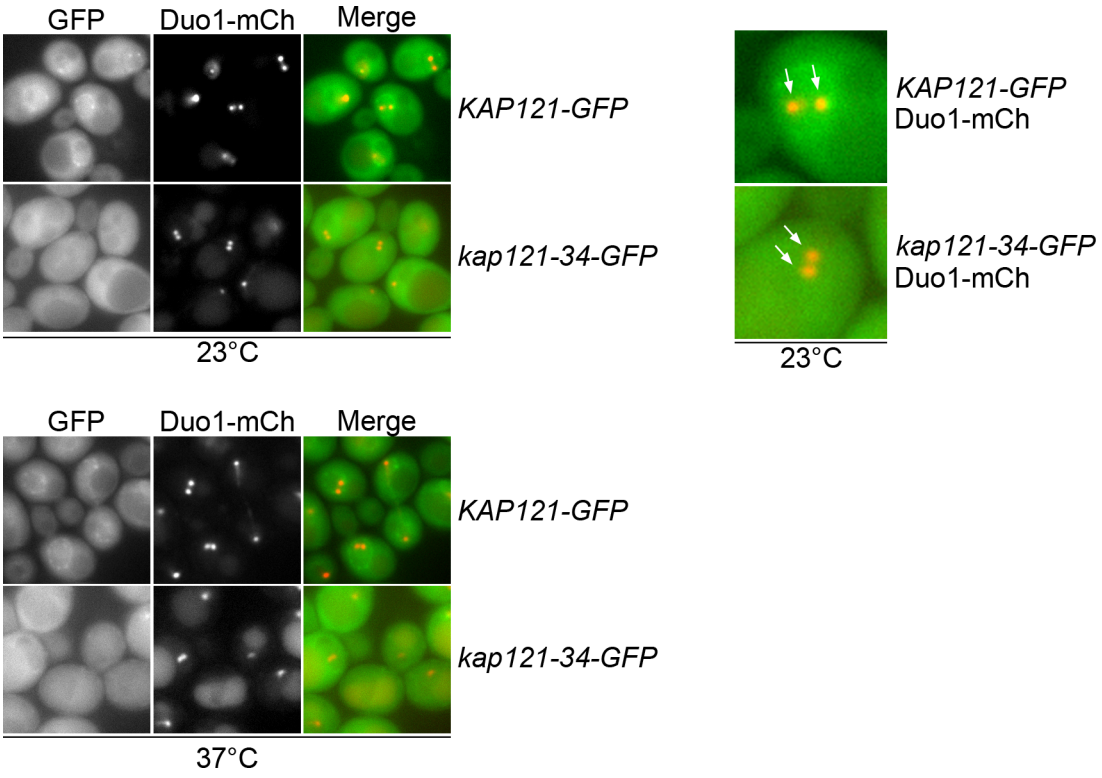


**Figure 4-10. Kap121-GFP is not observed at KTs.**

The localization of Kap121-GFP and kap121-34-GFP relative to Duo1-mCherry was followed in cells grown at 23°C and following shift to 37°C for 3 h using an epifluorescence microscope. Arrows point to Duo1-mCherry foci.

appear to visibly accumulate at KTs (Figure 4-10). Alternatively, Kap121 could contribute to the assembly of the Dam1 complex or its stable integration at the KT-MT interface. Such a "chaperone-like" role for Kap121 when compromised could give rise to partially assembled or mislocalized complexes susceptible to degradation. A conceptually similar function has been proposed for Importin-β in vertebrate cells. Importin-β functions in a manner analogous to a chaperone by binding positively charged proteins in the cytoplasm, including ribosomal proteins and histones, as part of a mechanism to suppress their aggregation and eventual degradation (Jakel et al., 2002). Of note, like histones and ribosomal proteins, both Dam1 and Duo1 are highly basic proteins with isoelectric points of 9.97 and 10.76, respectively (Westermann et al., 2005). Thus, the charged nature of these proteins likely renders them susceptible to non-specific, electrostatic interactions within the nuclear interior making them prone to aggregation. It is possible that Kap121 binds basic domains on Dam1 and Duo1 and functions to shield these positively charged residues from inappropriate interactions in the nuclear environment, thereby contributing to their stability. This also raises the possibility that the presence of a bulky epitope tag on the carboxy-terminus of Duo1 or Dam1 in the absence of Kap121 binding may, in effect, substitute for Kap121's physical association and function to shield positively charged domains within these proteins. Accordingly, within the carboxy-termini of both Dam1 and Duo1 is a stretch of basic amino acid residues that are thought to comprise the MT-binding domains of both proteins required for interacting with the highly acidic surface of MTs (Westermann et al., 2005; Wang et al., 2007; Ramey et al., 2011a; Ramey et al., 2011b).

Through our characterization of Kap121's role in KT bi-orientation, we have uncovered a novel essential role for Kap121 in KT function distinct from its role as a importin. On the basis of our analysis, this raises the possibility that similar functional relationships exist across eukaryotes. In vertebrates, the roles of both importins and exportins in regulating chromosome segregation have been established (see section 1.7.2). It is thus intriguing to consider the possibility that the vertebrate Ska1 complex, a MT-bound assemblage that is functionally homologous to the Dam1 complex, may be regulated, in part, through Kap function. In support of this, Ska1 contains a predicted NLS and, like Dam1 and Duo1, Ska1 is highly basic and susceptible degradation when other members of the Ska1 complex are compromised or absent (Gaitanos et al., 2009; Abad et al., 2014). Thus, it is plausible that Kaps play a related role in higher organisms, including regulating the assembly and structural stability of the Ska1 complex at the KT-MT interface.

# **Chapter V:** *Perspectives*[*]

[*] Portions of this chapter have been reproduced from: Cairo et al., *Nucleus,* 2013, 4, pp 367-373

## 5.1 Synopsis

The functional roles of Nups and Kaps in influencing chromosome transmission are necessary for the execution of an accurate mitosis. The work presented in this thesis establishes further functional links between the nuclear transport machinery and the mitotic apparatus. Specifically, we have uncovered a novel role for the SAC signaling protein Mad1 in the inhibition of Kap121-mediated import, and through this regulated transport inhibition, the environment of the nucleus changes to enhance the functional output of regulators of KT-MT interactions, namely Ipl1. In the second half of this thesis, we have uncovered a role for Kap121 in the regulation of KT-MT interactions through its association with the Dam1 complex. Kap121 binding to key structural members is thought to contribute to the overall stability of this MT-bound assembly thus promoting the integrity of KT-MT interactions *in vivo*. Within the upcoming sections, I will discuss these data in a broad and hypothetical context and speculate on future directions of where these findings could potentially lead.

## 5.2 Physiological output of the KTIP

Across species, activation and maintenance of SAC signaling rely upon the activity of a number of kinases (reviewed in Musacchio and Salmon, 2007; Foley and Kapoor, 2013; London and Biggins, 2014). In budding yeast, there are four major kinases that contribute to SAC signaling, i.e. Mps1, Bub1, Ipl1 and Cdk1 (Musacchio and Hardwick, 2002). In chapter III, we revealed that the KTIP fosters the formation of a nuclear environment that promotes the activity of the checkpoint kinase, Ipl1, during periods of SAC arrest by preventing the nuclear accumulation of the Ipl1 antagonist, Glc7 (Cairo et al., 2013a). Considering Glc7 functionally antagonizes the activity of multiple

kinases, this raises the possibility that the KTIP could also promote the activity of additional checkpoint kinases during SAC arrest. In particular, recent work has revealed an antagonistic functional relationship between Glc7 and Mps1 (London et al., 2012). Glc7 antagonizes Mps1 function by reversing Mps1-mediated phosphorylation events that occur at the KT, which contributes to the silencing of the SAC (London et al., 2012). Thus, linking these observations together, it is plausible that KTIP-mediated nuclear exclusion of Glc7 also works synergistically with Mps1 by promoting the maintenance of outer KT phosphorylation to promote SAC signaling. From this prediction, it would be of considerable interest to evaluate whether the phosphorylation of Spc105, or other Mps1 substrates, i.e. Mad1, is altered in the absence of the KTIP and whether this impacts the robustness of the SAC response.

In addition to the inhibition of Glc7's nuclear import, it is likely that the KTIP functions also to exclude a number of other cargos during SAC arrest. While a comprehensive list of Kap121 cargos has not been determined, two other cargos, Spo12 and Cdh1, are known regulators of mitotic progression (Chaves et al., 2001; Jacquenoud et al., 2002). Both proteins promote mitotic exit by regulating the localization and activity of Cdc14 and are considered antagonistic to metaphase arrest (Steigmeir et al., 2002; Visintin et al., 2008). Thus, the KTIP appears to contribute to the fidelity of chromosome segregation by limiting access to the nuclear environment of proteins that promote termination of the SAC and progression through mitosis under conditions of incomplete or improper KT-MT attachments. In doing so, the KTIP would assist in preventing mitotic slippage of arrested cells and the detrimental effects inherent therein, including defects leading to chromosome missegregation (Rossio et al., 2010). These roles for the

KTIP are presumed to be at least partially redundant, as mutations that repress the KTIP are viable and the SAC is functional.

In addition to Kap121 cargos, the flux of Kap121 into the nuclear compartment is also attenuated in nocodazole-arrested cells following KTIP activation (refer to Figure 7-1). Considering that Kap121 most likely interacts with the Dam1 complex in the nuclear interior, at the KT-MT interface (see chapter IV), it is plausible that the KTIP could function to restrict the access of this Kap to the Dam1 complex. Thus, under conditions of SAC arrest and KTIP activation, inhibited access of Kap121 to the Dam1 complex would potentially drive the partial or complete destabilization of this assemblage, thereby fostering the formation of mal- or unattached KTs. Thus, the prediction is that by compromising the functional/structural integrity of the Dam1 complex during SAC and KTIP activation through a lack of Kap121 binding, this would work synergistically with Ipl1-mediated phosphorylation to generate KTs detached from spindle MTs. Intriguingly, Ipl1-mediated phosphorylation of Dam1's carboxy-terminus has been shown to prevent the oligomerization of the Dam1 complex on MTs (Wang et al., 2007), thereby affecting the ability of this complex to bind and assemble on MTs. This supports the idea that preventing the proper assembly of the Dam1 complex by precluding Kap121 binding could potentially work in a synergistic manner with Ipl1-mediated phosphorylation of the Dam1 complex. However, as we have demonstrated that the inhibition of Kap121-transport in the absence of SAC-arrest does not impact KT-MT interactions (i.e. Nup53 overexpression, section 4.2.3), Kap121 would have to be released from the Dam1 complex in a regulated manner in SAC-arrested cells. Although this possibility remains hypothetical, it would be interesting to directly ascertain whether under conditions of

KTIP activation, the association of Kap121 with the Dam1 complex is lost and whether such a predicted change in interactions leads to alterations in the assembly state of the Dam1 complex.

**5.3 Mad1 and NPC molecular rearrangements**

During KTIP activation, Mad1 cycles dynamically between NPCs and KTs to drive NPC-structural rearrangements that alter the transport properties of NPCs. One outstanding question in uncovering a role for Mad1 in the KTIP is how Mad1's dynamic association with NPCs drives Nup-Nup rearrangements required to inhibit Kap121-mediated import. As discussed in chapter III, our results imply that post-translational modifications to individual NPC constituents may be important in altering Nup-Mad1 association in order to stabilize or induce the requisite Nup rearrangements. For example, Mps1-overexpression in a *nup60Δ* strain drives the dissolution of the intranuclear Mlp-bodies, suggesting that Mps1 modifies Mlps under these conditions (Figure 3-13). Thus, it is possible that Mps1-mediated phosphorylation of the Mlp proteins may inhibit Mad1 interactions with the nuclear basket while fostering Mad1 interactions with other NPC binding sites, such as Nup53. These orchestrated changes in the NPC binding partners of Mad1 may drive changes in Nup-Nup interactions, including rearrangements that expose the karyopherin-binding domain within Nup53. Furthermore, as Mad1 moves on and off NPCs, these Nup rearrangements are also envisaged to be cyclical. Thus, the capture of Kap121 by the Nup53 KBD and concomitant loss of cargo to the cytoplasm are predicted to be reversible and followed by the release of Kap121 from Nup53 and back to the cytoplasm as Mad1 dissociates and the Nups configure to their original state. As Kap121

occurs in excess of Nup53, such a cycling mechanism could prevent Kap121 from saturating these binding sites. A Kap121 "catch and release" mechanism, dependent upon Mad1 cycling, could ensure the continued availability of Nup53 binding sites required to inhibit Kap121-mediated transport.

### 5.4 KTIP in higher organisms

A comparison of eukaryotes from yeast to metazoans shows that the interactions between Mad1 and Nups are highly conserved. Mad1 has been found to associate with Nup53 and Mlp (Tpr) homologs in higher eukaryotes, as well as another nuclear basket component, Nup153, in mammalian cells (Hawryluk-Gara et al., 2008; Lee et al., 2008; Lussi et al., 2008; Lince-Faria et al., 2009). It remains to be determined whether these conserved interactions extend to the ability of Mad1 to regulate Nup function, as observed for the KTIP in yeast. A similar transport regulatory pathway might function during prophase when Mad1 associates with both KTs and NPCs in metazoan cells (Campbell et al., 2001). These cells also show NPC localization for Mps1 and Crm1 (Xpo1 homolog) during interphase, as well as KT localization of Crm1 in prophase, raising the possibility that Mps1 and Crm1 function to direct Mad1 translocation from NPCs to KTs as we proposed for yeast cells (Liu et al., 2003; Arnaoutov et al., 2005; Cairo et. al., 2013b). In addition, studies have shown that KT-localized metazoan Mad1 does cycle, but that only a fraction of the population is dynamic (~20%) with rapid recovery kinetics ($t_{1/2}$ ~6 s) (Howell et al., 2004; Shah et al., 2004). Whether this cycling population represents Mad1 exchange between NPCs and KTs to regulate nuclear transport remains to be determined.

The window for KTIP-like transport regulation in metazoans is short, as NE breakdown (NEBD) and NPC disassembly during late prophase eliminate the physical boundary between cytoplasm and nucleus. Even so, Nups and Kaps, free of intact NPCs, are repurposed during mitosis to play key roles in the regulation of the SAC, spindle assembly, and chromosome segregation (Wozniak et al., 2010). Furthermore, Nup-NTF interactions are also critical in NE and NPC reassembly near the end of mitosis (Guttinger et al., 2009). We speculate that Mad1 may play a role in modulating specific Nup-Nup or Nup-NTF interactions as a way of regulating their mitotic functions (Cairo et al., 2013a; Dasso, 2013).

A potential example is suggested by the interplay Mad1 has with Nup153 and Tpr (the vertebrate counterpart of Mlp1/Mlp2) during mitosis. During interphase, Nup153 and Tpr interact at the NPC nuclear basket where they both provide Mad1 binding sites (Lee et al., 2008; Lussi et al., 2010). However, after NEBD, Nup153-Tpr interactions are lost, but both Nups remain in complex with Mad1. These Nup-Mad1 complexes are thought to regulate Mad1 function during mitosis. Specifically, Tpr interacts with both Mad1 and Mad2 to facilitate the localization of these SAC regulators to detached KTs (Wozniak et al., 2010). The Nup153-Mad1 complex, however, does not appear to be critical for SAC function, but may promote SAC silencing by inhibiting Mad1 KT localization during prometaphase and removing Mad1 from spindles and/or the spindle matrix during metaphase (Lussi et al., 2010).

In addition to the potential role of Nups in impinging on the SAC functions of Mad1, we envisage a key role for Mad1 as a regulator of Nup-Nup interactions both during interphase and mitosis. As discussed above, the ability of yeast Mad1 to influence

Nup-Nup interactions during mitosis for the purpose of controlling mitotic nuclear transport events may also influence metazoan NPC function during mitotic prophase when the NE and NPCs are intact. However, it is also possible that, in cells undergoing an open mitosis, changes in Nup-Nup interactions driven by mitotic forms of Mad1 could instead impinge directly on the assembly state of NPCs, maintaining at least a subset of Nups in a disassembled state until the SAC is satisfied and anaphase is initiated. This model infers a regulatory role for KTs, through the actions of Mad1, in the disassembly and reassembly of NPCs during open mitosis. In this model, the inhibitory function of mitotic Mad1 is mechanistically analogous to that previously described for the nuclear transport factor Importin-β, which in mitotic extracts appears to bind various Nups and inhibit their assembly into subcomplexes (Walther et al., 2003a). In this example, it is proposed that Importin-β binds a subset of Nups until anaphase when the binding of RanGTP to Importin-β releases the Nups on the surface of decondensing chromatin prior to NPC assembly (Walther et al., 2003b). Similarly, Mad1-Nup complexes, established during SAC activation, could function to prevent the premature formation of Nup subcomplexes prior to anaphase onset, including nuclear basket structures containing the Mad1 binding partners Nup153 and Tpr.

### 5.5 Importins as intranuclear targeting factors

The RanGTP-rich environment of the nuclear interior imposes obvious functional limitations for Importins within the nucleus, particularly in yeast that undergo a closed mitosis. Nonetheless, there is accumulated evidence that several Importins carry out

functions inside the nucleus in yeast (Lee and Aitchison, 1999; Pemberton et al., 1999; Panse et al., 2003). As discussed in section 1.7.2, the ability of an import Kap to execute various activities in this compartment is contingent upon the ability of a given Kap to establish physical interactions that are resistant to RanGTP-mediated disassembly. What remains an enigma are the underlying molecular mechanisms that allow Importin/cargo complexes to bypass Ran-driven dissociation. The simplest molecular explanation for this phenomenon is that cargo binding could function to sterically block the Ran binding domain (positioned at the amino termini of β-Kaps), which could simply function to prevent RanGTP binding. Although cargo and Ran binding domains are positioned at the opposite ends of all β-Kaps, the inherent flexibility of these molecules through stacked heat repeats (see section 1.5.1) could allow for a scenario in which the cargo-binding domain is positioned in close proximity to the Ran-binding domain.

Ran-insensitivity could also be achieved by increasing the binding affinities between Kap and cargo. There are two scenarios through which this could arise and these including co-factor binding to a given Kap and post-translational modifications to either Kap or cargo. The first scenario has been demonstrated in yeast with Kap114. Specifically, the physical association of Kap114 with histones H2A and H2B is modulated by the co-factor Nap1, which binds directly to Kap114, increasing the affinity of this Kap for either protein (Mosammaparast et al., 2002). The augmented binding affinity enables Kap114 to bypass Ran-triggered dissociation, enabling this Kap to interact with either histone protein within the nucleoplasm. This is part of a mechanism that permits Kap114 to deposit both H2A and H2B at chromatin. In an analogous fashion, it is plausible that post-translational modifications to either Kap or cargo could feasibly

allow for RanGTP resistance. Consistent with this notion, as discussed in section 1.8.1, Kap-cargo binding affinities can be enhanced through post-translational modifications. Although there is a lack of documented examples where post-translational modifications enable Ran-resistance, Kap121 appears to possess a predicted sumoylation site within its sequence and there is preliminary evidence to suggest this protein is sumoylated *in vivo* (Diego Lapetina and Richard Wozniak, University of Alberta, personal communication). A nuclear specific modification such as sumoylation could be part of a mechanism where Kap/cargo complexes entering the nucleus are sumoylated resulting in resistance to Ran-GTP mediated dissociation. Although this possibility remains to be tested, it would be interesting to evaluate directly whether disrupting Kap121 sumoylation affects its Ran-GTP-insensitive interaction with either Duo1 or Ulp1 *in vivo*.

**5.6 Nups and chromosome segregation in yeast**

By directly interfacing with the mitotic apparatus, Nup subcomplexes and individual Nups confer paramount functional roles in regulating chromosome segregation (Guttinger et al., 2007; Wozniak et al., 2010). As discussed in section 1.9, the functions for Nups in regulating chromosome transmission have been best described in higher eukaryotes that undergo NEBD, at which point Nup-subcomplexes bind mitotic structures including KTs, centrosomes and the spindle (Guttinger et al., 2007; Hetzer, 2010). In yeast, outside of the role Nup53 and the KTIP exert in influencing chromosome segregation by regulating nuclear import, there is a lack of evidence to suggest that Nups can physically associate with the mitotic apparatus to influence chromosome segregation in these organisms. The presumption is that because yeast undergoes closed mitosis, and NPCs stay intact during M-phase, it is unlikely that individual Nups would associate with

mitotic structures located within the nuclear interior. However, despite this, there is accumulating evidence to suggest that the yeast core scaffold Nup, Nup170, may directly contribute to regulating chromosome transmission. An initial clue to suggest that Nup170 may be functionally linked to chromosome segregation came from an analysis showing that cells lacking Nup170 display chromosomal segregation defects (Kerscher et al., 2001). While the underlying molecular cause of these defects has not been clearly established, defects in nucleocytoplasmic transport have been ruled out, as the loss of Nup170 does not appear to impact active transport (Aitchison et al., 1995; Makio et al., 2009). However, *nup170Δ* cells appear to specifically possess centromeric transcriptional read-through defects, implying that the maintenance of heterochromatin structure at centromeres is defective (Kerscher et al., 2001). A key regulator of heterochromatin structure and nucleosome positioning at centromeres is Sth1, an essential catalytic member of the remodel the structure of chromatin (RSC) chromatin-remodeling complex (Cairns et al., 1996). Improper maintenance of heterochromatin at centromeres has been directly linked to KT structural defects and a reduction in the fidelity of chromosome transmission (Hsu et al., 2003; Verdaasdonk et al., 2012). Intriguingly, Nup170 interacts physically with Sth1 and the RSC chromatin-remodeling complex, and through this interaction, influences the topology of specific chromatin domains including telomeric and subtelomeric regions (Van de Vosse et al., 2013). Thus, from these observations, it is tempting to consider that Nup170 may influence the topology of centromeric chromatin through a functional relationship with Sth1. Consistent with this notion, Nup170 has been shown to physically associate with centromeric DNA through ChIP analysis in a manner that is Sth1-dependent (David Van de Vosse, University of Alberta, personal

communication). How Nup170 would function to promote proper chromatin structure at centromeres on a molecular level is uncertain, although, it is possible that this Nup could function to influence the activity, binding or assembly of Sth1 and the RSC complex at centromeric chromatin.

### 5.7 Kaps and KT assembly

KT assembly is an orchestrated process whereby individual KT subcomplexes come together in a temporally regulated manner to construct functional, higher order assemblies. For instance, the vertebrate KT undergoes dynamic structural changes over the course of the cell cycle as part of a mechanism required for KT assembly and disassembly. Specifically, while inner KT complexes remain constitutively associated with centromeric DNA sequence, the rest of the KT (>100 proteins) is built upon these centromeric KT complexes at the onset of mitosis (Cheeseman, 2014). How assembly of the outer KT is temporally restricted to mitosis remains poorly defined. However, it is tempting to consider that certain Kaps may potentially play a role in regulating this process in a manner that parallels their roles in spindle and NPC assembly. Consistent with this concept, it was recently demonstrated that the outer KT component, Ndc80, is specifically excluded from the nucleus during interphase and, upon the onset of mitosis, this protein is delivered to KTs for proper incorporation into these assemblies (Gascoigne and Cheeseman, 2014). What remains undefined is how both the nuclear exclusion and KT targeting of this outer KT protein are regulated.

The regulation of the dynamic subcellular localization of Ndc80 could be explained potentially by a functional relationship with a nuclear export factor such as

Crm1. In support of this idea, an inspection of the Ndc80 sequence reveals that it contains a predicted leucine rich NES, possibly recognized by Crm1 to drive both its nuclear exclusion and to regulate its KT targeting (La Cour et al., 2004). In addition to Ndc80, the outer KT components ZW10 and ROD also appear to contain predicted NESs (Robert Scott, University of Alberta, personal communication). Further investigation is needed to determine whether these NESs are functional, however, considering that Crm1 is involved in the targeting of other regulatory factors to KTs, including RanBP2 and RanGAP1, it is possible that this could be part of a general mechanism required for the spatiotemporal control of outer KT assembly upon the onset of mitosis.

*References*

Abad, M.A., B. Medina, A. Santamaria, J. Zou, C. Plasberg-Hill, A. Madhumalar, U. Jayachandran, P.M. Redli, J. Rappsilber, E.A. Nigg, and A.A. Jeyaprakash. 2014. Structural basis for microtubule recognition by the human kinetochore Ska complex. *Nature communications*. 5:2964.

Abruzzi, K.C., M. Magendantz, and F. Solomon. 2002. An alpha-tubulin mutant demonstrates distinguishable functions among the spindle assembly checkpoint genes in *Saccharomyces cerevisiae*. *Genetics*. 161:983-994.

Adam, S.A., K. Sengupta, and R.D. Goldman. 2008. Regulation of nuclear lamin polymerization by importin alpha. *The Journal of biological chemistry*. 283:8462-8468.

Aitchison, J.D., G. Blobel, and M.P. Rout. 1995. Nup120: a yeast nucleoporin required for NPC distribution and mRNA transport. *The Journal of cell biology*. 131:1659-1675.

Akey, C.W. 1989. Interactions and structure of the nuclear pore complex revealed by cryo-electron microscopy. *The Journal of cell biology*. 109:955-970.

Akey, C.W., and M. Radermacher. 1993. Architecture of the Xenopus nuclear pore complex revealed by three-dimensional cryo-electron microscopy. *The Journal of cell biology*. 122:1-19.

Akhtar, A., and S.M. Gasser. 2007. The nuclear envelope and transcriptional control. *Nature reviews. Genetics*. 8:507-517.

Akiyoshi, B., C.R. Nelson, J.A. Ranish, and S. Biggins. 2009a. Analysis of Ipl1-mediated phosphorylation of the Ndc80 kinetochore protein in Saccharomyces cerevisiae. *Genetics*. 183:1591-1595.

Akiyoshi, B., C.R. Nelson, J.A. Ranish, and S. Biggins. 2009b. Quantitative proteomic analysis of purified yeast kinetochores identifies a PP1 regulatory subunit. *Genes & development*. 23:2887-2899.

Akiyoshi, B., K.K. Sarangapani, A.F. Powers, C.R. Nelson, S.L. Reichow, H. Arellano-Santoyo, T. Gonen, J.A. Ranish, C.L. Asbury, and S. Biggins. 2010. Tension directly stabilizes reconstituted kinetochore-microtubule attachments. *Nature*. 468:576-579.

Alber, F., S. Dokudovskaya, L.M. Veenhoff, W. Zhang, J. Kipper, D. Devos, A. Suprapto, O. Karni-Schmidt, R. Williams, B.T. Chait, A. Sali, and M.P. Rout. 2007. The molecular architecture of the nuclear pore complex. *Nature*. 450:695-701.

Allen, N.P., L. Huang, A. Burlingame, and M. Rexach. 2001. Proteomic analysis of nucleoporin interacting proteins. *The Journal of biological chemistry*. 276:29268-29274.

Andrade, M.A., and P. Bork. 1995. HEAT repeats in the Huntington's disease protein. *Nature genetics*. 11:115-116.

Antonin, W., C. Franz, U. Haselmann, C. Antony, and I.W. Mattaj. 2005. The integral membrane nucleoporin pom121 functionally links nuclear pore complex assembly and nuclear envelope formation. *Molecular cell*. 17:83-92.

Araki, Y., C.K. Lau, H. Maekawa, S.L. Jaspersen, T.H. Giddings, Jr., E. Schiebel, and M. Winey. 2006. The Saccharomyces cerevisiae spindle pole body (SPB) component Nbp1 is required for SPB membrane insertion and interacts with the integral membrane proteins Ndc1 and Mps2. *Molecular biology of the cell*. 17:1959-1970.

Arnaoutov, A., Y. Azuma, K. Ribbeck, J. Joseph, Y. Boyarchuk, T. Karpova, J. McNally, and M. Dasso. 2005. Crm1 is a mitotic effector of Ran-GTP in somatic cells. *Nature cell biology*. 7:626-632.

Bansal, P.K., R. Abdulle, and K. Kitagawa. 2004. Sgt1 associates with Hsp90: an initial step of assembly of the core kinetochore complex. *Molecular and cellular biology*. 24:8069-8079.

Basu, J., H. Bousbaa, E. Logarinho, Z. Li, B.C. Williams, C. Lopes, C.E. Sunkel, and M.L. Goldberg. 1999. Mutations in the essential spindle checkpoint gene bub1 cause chromosome missegregation and fail to block apoptosis in Drosophila. *The Journal of cell biology*. 146:13-28.

Bayliss, R., T. Littlewood, and M. Stewart. 2000. Structural basis for the interaction between FxFG nucleoporin repeats and importin-beta in nuclear trafficking. *Cell*. 102:99-108.

Bayliss, R., T. Littlewood, L.A. Strawn, S.R. Wente, and M. Stewart. 2002. GLFG and FxFG nucleoporins bind to overlapping sites on importin-beta. *The Journal of biological chemistry*. 277:50597-50606.

Bayliss, R., K. Ribbeck, D. Akin, H.M. Kent, C.M. Feldherr, D. Gorlich, and M. Stewart. 1999. Interaction between NTF2 and xFxFG-containing nucleoporins is required to mediate nuclear import of RanGDP. *Journal of molecular biology*. 293:579-593.

Belgareh, N., G. Rabut, S.W. Bai, M. van Overbeek, J. Beaudouin, N. Daigle, O.V. Zatsepina, F. Pasteau, V. Labas, M. Fromont-Racine, J. Ellenberg, and V. Doye. 2001. An evolutionarily conserved NPC subcomplex, which redistributes in part to kinetochores in mammalian cells. *The Journal of cell biology*. 154:1147-1160.

Ben-Efraim, I., and L. Gerace. 2001. Gradient of increasing affinity of importin beta for nucleoporins along the pathway of nuclear import. *The Journal of cell biology*. 152:411-417.

Bernad, R., H. van der Velde, M. Fornerod, and H. Pickersgill. 2004. Nup358/RanBP2 attaches to the nuclear pore complex via association with Nup88 and Nup214/CAN and plays a supporting role in CRM1-mediated nuclear protein export. *Molecular and cellular biology*. 24:2373-2384.

Bharucha, J.P., J.R. Larson, L. Gao, L.K. Daves, and K. Tatchell. 2008. Ypi1, a positive regulator of nuclear protein phosphatase type 1 activity in Saccharomyces cerevisiae. *Molecular biology of the cell*. 19:1032-1045.

Bickel, T., and R. Bruinsma. 2002. The nuclear pore complex mystery and anomalous diffusion in reversible gels. *Biophysical journal*. 83:3079-3087.

Biggins, S. 2013. The composition, functions, and regulation of the budding yeast kinetochore. *Genetics*. 194:817-846.

Biggins, S., and A.W. Murray. 2001. The budding yeast protein kinase Ipl1/Aurora allows the absence of tension to activate the spindle checkpoint. *Genes & development*. 15:3118-3129.

Biggins, S., F.F. Severin, N. Bhalla, I. Sassoon, A.A. Hyman, and A.W. Murray. 1999. The conserved protein kinase Ipl1 regulates microtubule binding to kinetochores in budding yeast. *Genes & development*. 13:532-544.

Bischoff, F.R., and H. Ponstingl. 1991. Catalysis of guanine nucleotide exchange on Ran by the mitotic regulator RCC1. *Nature*. 354:80-82.

Bischoff, F.R., and H. Ponstingl. 1995. Catalysis of guanine nucleotide exchange of Ran by RCC1 and stimulation of hydrolysis of Ran-bound GTP by Ran-GAP1. *Methods in enzymology*. 257:135-144.

Boehmer, T., J. Enninga, S. Dales, G. Blobel, and H. Zhong. 2003. Depletion of a single nucleoporin, Nup107, prevents the assembly of a subset of nucleoporins into the nuclear pore complex. *Proceedings of the National Academy of Sciences of the United States of America*. 100:981-985.

Booth, J.W., K.D. Belanger, M.I. Sannella, and L.I. Davis. 1999. The yeast nucleoporin Nup2 is involved in nuclear export of importin alpha/Srp1. *The Journal of biological chemistry*. 274:32360-32367.

Brady, D.M., and K.G. Hardwick. 2000. Complex formation between Mad1, Bub1 and Bub3 is crucial for spindle checkpoint function. *Current biology : CB*. 10:675-678.

Breitkreutz, A., H. Choi, J.R. Sharom, L. Boucher, V. Neduva, B. Larsen, Z.Y. Lin, B.J. Breitkreutz, C. Stark, G. Liu, J. Ahn, D. Dewar-Darch, T. Reguly, X. Tang, R. Almeida, Z.S. Qin, T. Pawson, A.C. Gingras, A.I. Nesvizhskii, and M. Tyers. 2010. A global protein kinase and phosphatase interaction network in yeast. *Science*. 328:1043-1046.

Brinkley, B.R., and E. Stubblefield. 1966. The fine structure of the kinetochore of a mammalian cell in vitro. *Chromosoma*. 19:28-43.

Burke, B., and J. Ellenberg. 2002. Remodelling the walls of the nucleus. *Nature reviews. Molecular cell biology*. 3:487-497.

Cairns, B.R., Y. Lorch, Y. Li, M. Zhang, L. Lacomis, H. Erdjument-Bromage, P. Tempst, J. Du, B. Laurent, and R.D. Kornberg. 1996. RSC, an essential, abundant chromatin-remodeling complex. *Cell*. 87:1249-1260.

Cairo, L.V., C. Ptak, and R.W. Wozniak. 2013a. Dual personality of Mad1: regulation of nuclear import by a spindle assembly checkpoint protein. *Nucleus*. 4:367-373.

Cairo, L.V., C. Ptak, and R.W. Wozniak. 2013b. Mitosis-specific regulation of nuclear transport by the spindle assembly checkpoint protein Mad1. *Molecular cell*. 49:109-120.

Campbell, M.S., G.K. Chan, and T.J. Yen. 2001. Mitotic checkpoint proteins HsMAD1 and HsMAD2 are associated with nuclear pore complexes in interphase. *Journal of cell science*. 114:953-963.

Carazo-Salas, R.E., O.J. Gruss, I.W. Mattaj, and E. Karsenti. 2001. Ran-GTP coordinates regulation of microtubule nucleation and dynamics during mitotic-spindle assembly. *Nature cell biology*. 3:228-234.

Cassimeris, L., C.L. Rieder, G. Rupp, and E.D. Salmon. 1990. Stability of microtubule attachment to metaphase kinetochores in PtK1 cells. *Journal of cell science*. 96 ( Pt 1):9-15.

Caudron, M., G. Bunt, P. Bastiaens, and E. Karsenti. 2005. Spatial coordination of spindle assembly by chromosome-mediated signaling gradients. *Science*. 309:1373-1376.

Chang, W.L., and W.Y. Tarn. 2009. A role for transportin in deposition of TTP to cytoplasmic RNA granules and mRNA decay. *Nucleic acids research*. 37:6600-6612.

Chao, W.C., K. Kulkarni, Z. Zhang, E.H. Kong, and D. Barford. 2012. Structure of the mitotic checkpoint complex. *Nature*. 484:208-213.

Chaves, S.R., and G. Blobel. 2001. Nuclear import of Spo12, a protein essential for meiosis. *The Journal of biological chemistry*. 276:17712-17717.

Cheeseman, I.M. 2014. The kinetochore. *Cold Spring Harbor perspectives in biology*. 6:a015826.

Cheeseman, I.M., S. Anderson, M. Jwa, E.M. Green, J. Kang, J.R. Yates, 3rd, C.S. Chan, D.G. Drubin, and G. Barnes. 2002. Phospho-regulation of kinetochore-microtubule attachments by the Aurora kinase Ipl1. *Cell*. 111:163-172.

Cheeseman, I.M., J.S. Chappie, E.M. Wilson-Kubalek, and A. Desai. 2006. The conserved KMN network constitutes the core microtubule-binding site of the kinetochore. *Cell*. 127:983-997.

Cheeseman, I.M., and A. Desai. 2008. Molecular architecture of the kinetochore-microtubule interface. *Nature reviews. Molecular cell biology*. 9:33-46.

Cheeseman, I.M., M. Enquist-Newman, T. Muller-Reichert, D.G. Drubin, and G. Barnes. 2001. Mitotic spindle integrity and kinetochore function linked by the Duo1/Dam1 complex. *The Journal of cell biology*. 152:197-212.

Cheeseman, I.M., S. Niessen, S. Anderson, F. Hyndman, J.R. Yates, 3rd, K. Oegema, and A. Desai. 2004. A conserved protein network controls assembly of the outer kinetochore and its ability to sustain tension. *Genes & development*. 18:2255-2268.

Chen, R.H., J.C. Waters, E.D. Salmon, and A.W. Murray. 1996. Association of spindle assembly checkpoint component XMAD2 with unattached kinetochores. *Science*. 274:242-246.

Chi, Y.H., K. Haller, M.D. Ward, O.J. Semmes, Y. Li, and K.T. Jeang. 2008. Requirements for protein phosphorylation and the kinase activity of polo-like kinase 1 (Plk1) for the kinetochore function of mitotic arrest deficiency protein 1 (Mad1). *The Journal of biological chemistry*. 283:35834-35844.

Chial, H.J., M.P. Rout, T.H. Giddings, and M. Winey. 1998. Saccharomyces cerevisiae Ndc1 is a shared component of nuclear pore complexes and spindle pole bodies. *The Journal of cell biology*. 143:1789-1800.

Cho, U.S., and S.C. Harrison. 2012. Ndc10 is a platform for inner kinetochore assembly in budding yeast. *Nature structural & molecular biology*. 19:48-55.

Chook, Y.M., and G. Blobel. 1999. Structure of the nuclear transport complex karyopherin-beta2-Ran x GppNHp. *Nature*. 399:230-237.

Ciciarello, M., R. Mangiacasale, C. Thibier, G. Guarguaglini, E. Marchetti, B. Di Fiore, and P. Lavia. 2004. Importin beta is transported to spindle poles during mitosis and regulates Ran-dependent spindle assembly factors in mammalian cells. *Journal of cell science*. 117:6511-6522.

Ciferri, C., J. De Luca, S. Monzani, K.J. Ferrari, D. Ristic, C. Wyman, H. Stark, J. Kilmartin, E.D. Salmon, and A. Musacchio. 2005. Architecture of the human ndc80-hec1 complex, a critical constituent of the outer kinetochore. *The Journal of biological chemistry*. 280:29088-29095.

Ciferri, C., A. Musacchio, and A. Petrovic. 2007. The Ndc80 complex: hub of kinetochore activity. *FEBS letters*. 581:2862-2869.

Ciferri, C., S. Pasqualato, E. Screpanti, G. Varetti, S. Santaguida, G. Dos Reis, A. Maiolica, J. Polka, J.G. De Luca, P. De Wulf, M. Salek, J. Rappsilber, C.A. Moores, E.D. Salmon, and A. Musacchio. 2008. Implications for kinetochore-microtubule attachment from the structure of an engineered Ndc80 complex. *Cell*. 133:427-439.

Cimini, D., X. Wan, C.B. Hirel, and E.D. Salmon. 2006. Aurora kinase promotes turnover of kinetochore microtubules to reduce chromosome segregation errors. *Current biology : CB*. 16:1711-1718.

Cingolani, G., C. Petosa, K. Weis, and C.W. Muller. 1999. Structure of importin-beta bound to the IBB domain of importin-alpha. *Nature*. 399:221-229.

Ciosk, R., W. Zachariae, C. Michaelis, A. Shevchenko, M. Mann, and K. Nasmyth. 1998. An ESP1/PDS1 complex regulates loss of sister chromatid cohesion at the metaphase to anaphase transition in yeast. *Cell*. 93:1067-1076.

Clarke, P.R., and C. Zhang. 2008. Spatial and temporal coordination of mitosis by Ran GTPase. *Nature reviews. Molecular cell biology*. 9:464-477.

Connelly, C., and P. Hieter. 1996. Budding yeast SKP1 encodes an evolutionarily conserved kinetochore protein required for cell cycle progression. *Cell*. 86:275-285.

Cronshaw, J.M., A.N. Krutchinsky, W. Zhang, B.T. Chait, and M.J. Matunis. 2002. Proteomic analysis of the mammalian nuclear pore complex. *The Journal of cell biology*. 158:915-927.

D'Angelo, M.A., and M.W. Hetzer. 2008. Structure, dynamics and function of nuclear pore complexes. *Trends in cell biology*. 18:456-466.

D'Angelo, M.A., D.J. Anderson, E. Richard, and M.W. Hetzer. 2006. Nuclear pores form de novo from both sides of the nuclear envelope. *Science*. 312:440-443.

Dasso, M., H. Nishitani, S. Kornbluth, T. Nishimoto, and J.W. Newport. 1992. RCC1, a regulator of mitosis, is essential for DNA replication. *Molecular and cellular biology*. 12:3337-3345.

De Antoni, A., C.G. Pearson, D. Cimini, J.C. Canman, V. Sala, L. Nezi, M. Mapelli, L. Sironi, M. Faretta, E.D. Salmon, and A. Musacchio. 2005. The Mad1/Mad2 complex as a template for Mad2 activation in the spindle assembly checkpoint. *Current biology : CB*. 15:214-225.

De Souza, C.P., S.B. Hashmi, T. Nayak, B. Oakley, and S.A. Osmani. 2009. Mlp1 acts as a mitotic scaffold to spatially regulate spindle assembly checkpoint proteins in Aspergillus nidulans. *Molecular biology of the cell*. 20:2146-2159.

De Wulf, P., A.D. McAinsh, and P.K. Sorger. 2003. Hierarchical assembly of the budding yeast kinetochore from multiple subcomplexes. *Genes & development*. 17:2902-2921.

Debler, E.W., Y. Ma, H.S. Seo, K.C. Hsia, T.R. Noriega, G. Blobel, and A. Hoelz. 2008. A fence-like coat for the nuclear pore membrane. *Molecular cell*. 32:815-826.

DeLuca, J.G., Y. Dong, P. Hergert, J. Strauss, J.M. Hickey, E.D. Salmon, and B.F. McEwen. 2005. Hec1 and nuf2 are core components of the kinetochore outer plate essential for organizing microtubule attachment sites. *Molecular biology of the cell*. 16:519-531.

DeLuca, J.G., W.E. Gall, C. Ciferri, D. Cimini, A. Musacchio, and E.D. Salmon. 2006. Kinetochore microtubule dynamics and attachment stability are regulated by Hec1. *Cell*. 127:969-982.

DeLuca, J.G., and A. Musacchio. 2012. Structural organization of the kinetochore-microtubule interface. *Current opinion in cell biology*. 24:48-56.

Demirel, P.B., B.E. Keyes, M. Chaterjee, C.E. Remington, and D.J. Burke. 2012. A redundant function for the N-terminal tail of Ndc80 in kinetochore-microtubule interaction in Saccharomyces cerevisiae. *Genetics*. 192:753-756.

Denning, D.P., S.S. Patel, V. Uversky, A.L. Fink, and M. Rexach. 2003. Disorder in the nuclear pore complex: the FG repeat regions of nucleoporins are natively unfolded. *Proceedings of the National Academy of Sciences of the United States of America*. 100:2450-2455.

Denning, D.P., and M.F. Rexach. 2007. Rapid evolution exposes the boundaries of domain structure and function in natively unfolded FG nucleoporins. *Molecular & cellular proteomics : MCP*. 6:272-282.

Desai, A., S. Rybina, T. Muller-Reichert, A. Shevchenko, A. Shevchenko, A. Hyman, and K. Oegema. 2003. KNL-1 directs assembly of the microtubule-binding interface of the kinetochore in C. elegans. *Genes & development*. 17:2421-2435.

Devos, D., S. Dokudovskaya, F. Alber, R. Williams, B.T. Chait, A. Sali, and M.P. Rout. 2004. Components of coated vesicles and nuclear pore complexes share a common molecular architecture. *PLoS biology*. 2:e380.

Devos, D., S. Dokudovskaya, R. Williams, F. Alber, N. Eswar, B.T. Chait, M.P. Rout, and A. Sali. 2006. Simple fold composition and modular architecture of the nuclear pore complex. *Proceedings of the National Academy of Sciences of the United States of America*. 103:2172-2177.

Dewar, H., K. Tanaka, K. Nasmyth, and T.U. Tanaka. 2004. Tension between two kinetochores suffices for their bi-orientation on the mitotic spindle. *Nature*. 428:93-97.

Dhawale, S.S., and A.C. Lane. 1993. Compilation of sequence-specific DNA-binding proteins implicated in transcriptional control in fungi. *Nucleic acids research*. 21:5537-5546.

Dilworth, D.J., A. Suprapto, J.C. Padovan, B.T. Chait, R.W. Wozniak, M.P. Rout, and J.D. Aitchison. 2001. Nup2 dynamically associates with the distal regions of the yeast nuclear pore complex. *The Journal of cell biology*. 153:1465-1478.

Dingwall, C., J. Robbins, S.M. Dilworth, B. Roberts, and W.D. Richardson. 1988. The nucleoplasmin nuclear location sequence is larger and more complex than that of SV-40 large T antigen. *The Journal of cell biology*. 107:841-849.

Dishinger, J.F., H.L. Kee, P.M. Jenkins, S. Fan, T.W. Hurd, J.W. Hammond, Y.N. Truong, B. Margolis, J.R. Martens, and K.J. Verhey. 2010. Ciliary entry of the kinesin-2 motor KIF17 is regulated by importin-beta2 and RanGTP. *Nature cell biology*. 12:703-710.

Dobles, M., V. Liberal, M.L. Scott, R. Benezra, and P.K. Sorger. 2000. Chromosome missegregation and apoptosis in mice lacking the mitotic checkpoint protein Mad2. *Cell*. 101:635-645.

Doheny, K.F., P.K. Sorger, A.A. Hyman, S. Tugendreich, F. Spencer, and P. Hieter. 1993. Identification of essential components of the S. cerevisiae kinetochore. *Cell*. 73:761-774.

Dong, Y., K.J. Vanden Beldt, X. Meng, A. Khodjakov, and B.F. McEwen. 2007. The outer plate in vertebrate kinetochores is a flexible network with multiple microtubule interactions. *Nature cell biology*. 9:516-522.

Dorner, D., J. Gotzmann, and R. Foisner. 2007. Nucleoplasmic lamins and their interaction partners, LAP2alpha, Rb, and BAF, in transcriptional regulation. *The FEBS journal*. 274:1362-1373.

Doye, V., R. Wepf, and E.C. Hurt. 1994. A novel nuclear pore protein Nup133 with distinct roles in poly(A)+ RNA transport and nuclear pore distribution. *The EMBO journal*. 13:6062-6075.

Dultz, E., E. Zanin, C. Wurzenberger, M. Braun, G. Rabut, L. Sironi, and J. Ellenberg. 2008. Systematic kinetic analysis of mitotic dis- and reassembly of the nuclear pore in living cells. *The Journal of cell biology*. 180:857-865.

Emanuele, M.J., M.L. McCleland, D.L. Satinover, and P.T. Stukenberg. 2005. Measuring the stoichiometry and physical interactions between components elucidates the

architecture of the vertebrate kinetochore. *Molecular biology of the cell*. 16:4882-4892.

Enenkel, C., G. Blobel, and M. Rexach. 1995. Identification of a yeast karyopherin heterodimer that targets import substrate to mammalian nuclear pore complexes. *The Journal of biological chemistry*. 270:16499-16502.

Englmeier, L., J.C. Olivo, and I.W. Mattaj. 1999. Receptor-mediated substrate translocation through the nuclear pore complex without nucleotide triphosphate hydrolysis. *Current biology : CB*. 9:30-41.

Enquist-Newman, M., I.M. Cheeseman, D. Van Goor, D.G. Drubin, P.B. Meluh, and G. Barnes. 2001. Dad1, third component of the Duo1/Dam1 complex involved in kinetochore function and mitotic spindle integrity. *Molecular biology of the cell*. 12:2601-2613.

Faberge, A.C. 1973. Direct demonstration of eight-fold symmetry in nuclear pores. *Zeitschrift fur Zellforschung und mikroskopische Anatomie*. 136:183-190.

Fabre, E., and E. Hurt. 1997. Yeast genetics to dissect the nuclear pore complex and nucleocytoplasmic trafficking. *Annual review of genetics*. 31:277-313.

Fang, G. 2002. Checkpoint protein BubR1 acts synergistically with Mad2 to inhibit anaphase-promoting complex. *Molecular biology of the cell*. 13:755-766.

Fang, G., H. Yu, and M.W. Kirschner. 1998. The checkpoint protein MAD2 and the mitotic regulator CDC20 form a ternary complex with the anaphase-promoting complex to control anaphase initiation. *Genes & development*. 12:1871-1883.

Fatica, A., and D. Tollervey. 2002. Making ribosomes. *Current opinion in cell biology*. 14:313-318.

Feldherr, C.M., and D. Akin. 1993. Regulation of nuclear transport in proliferating and quiescent cells. *Experimental cell research*. 205:179-186.

Fernius, J., and K.G. Hardwick. 2007. Bub1 kinase targets Sgo1 to ensure efficient chromosome biorientation in budding yeast mitosis. *PLoS genetics*. 3:e213.

Feuerbach, F., V. Galy, E. Trelles-Sticken, M. Fromont-Racine, A. Jacquier, E. Gilson, J.C. Olivo-Marin, H. Scherthan, and U. Nehrbass. 2002. Nuclear architecture and spatial positioning help establish transcriptional states of telomeres in yeast. *Nature cell biology*. 4:214-221.

Field, M.C., and J.B. Dacks. 2009. First and last ancestors: reconstructing evolution of the endomembrane system with ESCRTs, vesicle coat proteins, and nuclear pore complexes. *Current opinion in cell biology*. 21:4-13.

Fletcher, L., T.J. Yen, and R.J. Muschel. 2003. DNA damage in HeLa cells induced arrest at a discrete point in G2 phase as defined by CENP-F localization. *Radiation research*. 159:604-611.

Foley, E.A., and T.M. Kapoor. 2013. Microtubule attachment and spindle assembly checkpoint signalling at the kinetochore. *Nature reviews. Molecular cell biology*. 14:25-37.

Fornerod, M., M. Ohno, M. Yoshida, and I.W. Mattaj. 1997. CRM1 is an export receptor for leucine-rich nuclear export signals. *Cell*. 90:1051-1060.

Franke, W.W., J.A. Kleinschmidt, H. Spring, G. Krohne, C. Grund, M.F. Trendelenburg, M. Stoehr, and U. Scheer. 1981. A nucleolar skeleton of protein filaments demonstrated in amplified nucleoli of Xenopus laevis. *The Journal of cell biology*. 90:289-299.

Fraschini, R., A. Beretta, L. Sironi, A. Musacchio, G. Lucchini, and S. Piatti. 2001. Bub3 interaction with Mad2, Mad3 and Cdc20 is mediated by WD40 repeats and does not require intact kinetochores. *The EMBO journal*. 20:6648-6659.

Fridkin, A., A. Penkner, V. Jantsch, and Y. Gruenbaum. 2009. SUN-domain and KASH-domain proteins during development, meiosis and disease. *Cellular and molecular life sciences : CMLS*. 66:1518-1533.

Fried, H., and U. Kutay. 2003. Nucleocytoplasmic transport: taking an inventory. *Cellular and molecular life sciences : CMLS*. 60:1659-1688.

Fujimura, K., T. Suzuki, Y. Yasuda, M. Murata, J. Katahira, and Y. Yoneda. 2010. Identification of importin alpha1 as a novel constituent of RNA stress granules. *Biochimica et biophysica acta*. 1803:865-871.

Fukuda, M., S. Asano, T. Nakamura, M. Adachi, M. Yoshida, M. Yanagida, and E. Nishida. 1997. CRM1 is responsible for intracellular transport mediated by the nuclear export signal. *Nature*. 390:308-311.

Fukuhara, N., E. Fernandez, J. Ebert, E. Conti, and D. Svergun. 2004. Conformational variability of nucleo-cytoplasmic transport factors. *The Journal of biological chemistry*. 279:2176-2181.

Gaitanos, T.N., A. Santamaria, A.A. Jeyaprakash, B. Wang, E. Conti, and E.A. Nigg. 2009. Stable kinetochore-microtubule interactions depend on the Ska complex and its new component Ska3/C13Orf3. *The EMBO journal*. 28:1442-1452.

Gall, J.G. 1967. Octagonal nuclear pores. *The Journal of cell biology*. 32:391-399.

Galy, V., J.C. Olivo-Marin, H. Scherthan, V. Doye, N. Rascalou, and U. Nehrbass. 2000. Nuclear pore complexes in the organization of silent telomeric chromatin. *Nature*. 403:108-112.

Gascoigne, K.E., and I.M. Cheeseman. 2013. CDK-dependent phosphorylation and nuclear exclusion coordinately control kinetochore assembly state. *The Journal of cell biology*. 201:23-32

Gassmann, R., A.J. Holland, D. Varma, X. Wan, F. Civril, D.W. Cleveland, K. Oegema, E.D. Salmon, and A. Desai. 2010. Removal of Spindly from microtubule-attached kinetochores controls spindle checkpoint silencing in human cells. *Genes & development*. 24:957-971.

Gestaut, D.R., B. Graczyk, J. Cooper, P.O. Widlund, A. Zelter, L. Wordeman, C.L. Asbury, and T.N. Davis. 2008. Phosphoregulation and depolymerization-driven movement of the Dam1 complex do not require ring formation. *Nature cell biology*. 10:407-414.

Gilchrist, D., and M. Rexach. 2003. Molecular basis for the rapid dissociation of nuclear localization signals from karyopherin alpha in the nucleoplasm. *The Journal of biological chemistry*. 278:51937-51949.

Gillett, E.S., C.W. Espelin, and P.K. Sorger. 2004. Spindle checkpoint proteins and chromosome-microtubule attachment in budding yeast. *The Journal of cell biology*. 164:535-546.

Godek, K.M., L. Kabeche, and D.A. Compton. 2015. Regulation of kinetochore-microtubule attachments through homeostatic control during mitosis. *Nature reviews. Molecular cell biology*. 16:57-64.

Goh, P.Y., and J.V. Kilmartin. 1993. NDC10: a gene involved in chromosome segregation in Saccharomyces cerevisiae. *The Journal of cell biology*. 121:503-512.

Goldfarb, D.S., A.H. Corbett, D.A. Mason, M.T. Harreman, and S.A. Adam. 2004. Importin alpha: a multipurpose nuclear-transport receptor. *Trends in cell biology*. 14:505-514.

Goldfarb, D.S., J. Gariepy, G. Schoolnik, and R.D. Kornberg. 1986. Synthetic peptides as nuclear localization signals. *Nature*. 322:641-644.

Gonen, S., B. Akiyoshi, M.G. Iadanza, D. Shi, N. Duggan, S. Biggins, and T. Gonen. 2012. The structure of purified kinetochores reveals multiple microtubule-attachment sites. *Nature structural & molecular biology*. 19:925-929.

Gorlich, D., M. Dabrowski, F.R. Bischoff, U. Kutay, P. Bork, E. Hartmann, S. Prehn, and E. Izaurralde. 1997. A novel class of RanGTP binding proteins. *The Journal of cell biology*. 138:65-80.

Gorlich, D., S. Kostka, R. Kraft, C. Dingwall, R.A. Laskey, E. Hartmann, and S. Prehn. 1995. Two different subunits of importin cooperate to recognize nuclear

localization signals and bind them to the nuclear envelope. *Current biology : CB*. 5:383-392.

Gorlich, D., and U. Kutay. 1999. Transport between the cell nucleus and the cytoplasm. *Annual review of cell and developmental biology*. 15:607-660.

Gorlich, D., M.J. Seewald, and K. Ribbeck. 2003. Characterization of Ran-driven cargo transport and the RanGTPase system by kinetic measurements and computer simulation. *The EMBO journal*. 22:1088-1100.

Goshima, G., and M. Yanagida. 2000. Establishing biorientation occurs with precocious separation of the sister kinetochores, but not the arms, in the early spindle of budding yeast. *Cell*. 100:619-633.

Grant, R.P., D. Neuhaus, and M. Stewart. 2003. Structural basis for the interaction between the Tap/NXF1 UBA domain and FG nucleoporins at 1A resolution. *Journal of molecular biology*. 326:849-858.

Gruss, O.J. 2010. Nuclear transport receptor goes moonlighting. *Nature cell biology*. 12:640-641.

Gruss, O.J., R.E. Carazo-Salas, C.A. Schatz, G. Guarguaglini, J. Kast, M. Wilm, N. Le Bot, I. Vernos, E. Karsenti, and I.W. Mattaj. 2001. Ran induces spindle assembly by reversing the inhibitory effect of importin alpha on TPX2 activity. *Cell*. 104:83-93.

Guan, T., R.H. Kehlenbach, E.C. Schirmer, A. Kehlenbach, F. Fan, B.E. Clurman, N. Arnheim, and L. Gerace. 2000. Nup50, a nucleoplasmically oriented nucleoporin with a role in nuclear protein export. *Molecular and cellular biology*. 20:5619-5630.

Guimaraes, G.J., Y. Dong, B.F. McEwen, and J.G. Deluca. 2008. Kinetochore-microtubule attachment relies on the disordered N-terminal tail domain of Hec1. *Current biology : CB*. 18:1778-1784.

Guttinger, S., E. Laurell, and U. Kutay. 2009. Orchestrating nuclear envelope disassembly and reassembly during mitosis. *Nature reviews. Molecular cell biology*. 10:178-191.

Haase, J., A. Stephens, J. Verdaasdonk, E. Yeh, and K. Bloom. 2012. Bub1 kinase and Sgo1 modulate pericentric chromatin in response to altered microtubule dynamics. *Current biology : CB*. 22:471-481.

Hanz, S., E. Perlson, D. Willis, J.Q. Zheng, R. Massarwa, J.J. Huerta, M. Koltzenburg, M. Kohler, J. van-Minnen, J.L. Twiss, and M. Fainzilber. 2003. Axoplasmic importins enable retrograde injury signaling in lesioned nerve. *Neuron*. 40:1095-1104.

Hardwick, K.G., E. Weiss, F.C. Luca, M. Winey, and A.W. Murray. 1996. Activation of the budding yeast spindle assembly checkpoint without mitotic spindle disruption. *Science*. 273:953-956.

Hawryluk-Gara, L.A., M. Platani, R. Santarella, R.W. Wozniak, and I.W. Mattaj. 2008. Nup53 is required for nuclear envelope and nuclear pore complex assembly. *Molecular biology of the cell*. 19:1753-1762.

Hayashi, I., and M. Ikura. 2003. Crystal structure of the amino-terminal microtubule-binding domain of end-binding protein 1 (EB1). *The Journal of biological chemistry*. 278:36430-36434.

He, X., D.R. Rines, C.W. Espelin, and P.K. Sorger. 2001. Molecular analysis of kinetochore-microtubule attachment in budding yeast. *Cell*. 106:195-206.

Hediger, F., K. Dubrana, and S.M. Gasser. 2002a. Myosin-like proteins 1 and 2 are not required for silencing or telomere anchoring, but act in the Tel1 pathway of telomere length control. *Journal of structural biology*. 140:79-91.

Hediger, F., F.R. Neumann, G. Van Houwe, K. Dubrana, and S.M. Gasser. 2002b. Live imaging of telomeres: yKu and Sir proteins define redundant telomere-anchoring pathways in yeast. *Current biology : CB*. 12:2076-2089.

Heessen, S., and M. Fornerod. 2007. The inner nuclear envelope as a transcription factor resting place. *EMBO reports*. 8:914-919.

Hetzer, M., D. Bilbao-Cortes, T.C. Walther, O.J. Gruss, and I.W. Mattaj. 2000. GTP hydrolysis by Ran is required for nuclear envelope assembly. *Molecular cell*. 5:1013-1024.

Hetzer, M.W. 2010. The nuclear envelope. *Cold Spring Harbor perspectives in biology*. 2:a000539.

Hetzer, M.W., T.C. Walther, and I.W. Mattaj. 2005. Pushing the envelope: structure, function, and dynamics of the nuclear periphery. *Annual review of cell and developmental biology*. 21:347-380.

Hinshaw, J.E., B.O. Carragher, and R.A. Milligan. 1992. Architecture and design of the nuclear pore complex. *Cell*. 69:1133-1141.

Hoelz, A., E.W. Debler, and G. Blobel. 2011. The structure of the nuclear pore complex. *Annual review of biochemistry*. 80:613-643.

Hofmann, C., I.M. Cheeseman, B.L. Goode, K.L. McDonald, G. Barnes, and D.G. Drubin. 1998. Saccharomyces cerevisiae Duo1 and Dam1, novel proteins involved in mitotic spindle function. *The Journal of cell biology*. 143:1029-1040.

Hornung, P., P. Troc, F. Malvezzi, M. Maier, Z. Demianova, T. Zimniak, G. Litos, F. Lampert, A. Schleiffer, M. Brunner, K. Mechtler, F. Herzog, T.C. Marlovits, and S. Westermann. 2014. A cooperative mechanism drives budding yeast kinetochore assembly downstream of CENP-A. *The Journal of cell biology*. 206:509-524.

Howell, B.J., B.F. McEwen, J.C. Canman, D.B. Hoffman, E.M. Farrar, C.L. Rieder, and E.D. Salmon. 2001. Cytoplasmic dynein/dynactin drives kinetochore protein transport to the spindle poles and has a role in mitotic spindle checkpoint inactivation. *The Journal of cell biology*. 155:1159-1172.

Howell, B.J., B. Moree, E.M. Farrar, S. Stewart, G. Fang, and E.D. Salmon. 2004. Spindle checkpoint protein dynamics at kinetochores in living cells. *Current biology : CB*. 14:953-964.

Hoyt, M.A., L. Totis, and B.T. Roberts. 1991. S. cerevisiae genes required for cell cycle arrest in response to loss of microtubule function. *Cell*. 66:507-517.

Hsia, K.C., P. Stavropoulos, G. Blobel, and A. Hoelz. 2007. Architecture of a coat for the nuclear pore membrane. *Cell*. 131:1313-1326.

Hsu, J.M., J. Huang, P.B. Meluh, and B.C. Laurent. 2003. The yeast RSC chromatin-remodeling complex is required for kinetochore function in chromosome segregation. *Molecular and cellular biology*. 23:3202-3215.

Hurd, T.W., S. Fan, and B.L. Margolis. 2011. Localization of retinitis pigmentosa 2 to cilia is regulated by Importin beta2. *Journal of cell science*. 124:718-726.

Hurwitz, M.E., C. Strambio-de-Castillia, and G. Blobel. 1998. Two yeast nuclear pore complex proteins involved in mRNA export form a cytoplasmically oriented subcomplex. *Proceedings of the National Academy of Sciences of the United States of America*. 95:11241-11245.

Hwang, L.H., L.F. Lau, D.L. Smith, C.A. Mistrot, K.G. Hardwick, E.S. Hwang, A. Amon, and A.W. Murray. 1998. Budding yeast Cdc20: a target of the spindle checkpoint. *Science*. 279:1041-1044.

Ikui, A.E., K. Furuya, M. Yanagida, and T. Matsumoto. 2002. Control of localization of a spindle checkpoint protein, Mad2, in fission yeast. *Journal of cell science*. 115:1603-1610.

Imamoto, N., and T. Funakoshi. 2012. Nuclear pore dynamics during the cell cycle. *Current opinion in cell biology*. 24:453-459.

Indjeian, V.B., B.M. Stern, and A.W. Murray. 2005. The centromeric protein Sgo1 is required to sense lack of tension on mitotic chromosomes. *Science*. 307:130-133.

Iouk, T., O. Kerscher, R.J. Scott, M.A. Basrai, and R.W. Wozniak. 2002. The yeast nuclear pore complex functionally interacts with components of the spindle assembly checkpoint. *The Journal of cell biology*. 159:807-819.

Iovine, M.K., J.L. Watkins, and S.R. Wente. 1995. The GLFG repetitive region of the nucleoporin Nup116 interacts with Kap95, an essential yeast nuclear import factor. *The Journal of cell biology*. 131:1699-1713.

Isgro, T.A., and K. Schulten. 2005. Binding dynamics of isolated nucleoporin repeat regions to importin-beta. *Structure*. 13:1869-1879.

Janke, C., J. Ortiz, T.U. Tanaka, J. Lechner, and E. Schiebel. 2002. Four new subunits of the Dam1-Duo1 complex reveal novel functions in sister kinetochore biorientation. *The EMBO journal*. 21:181-193.

Jans, D.A., C.Y. Xiao, and M.H. Lam. 2000. Nuclear targeting signal recognition: a key control point in nuclear transport? *BioEssays : news and reviews in molecular, cellular and developmental biology*. 22:532-544.

Jaquenoud, M., F. van Drogen, and M. Peter. 2002. Cell cycle-dependent nuclear export of Cdh1 may contribute to the inactivation of APC/C(Cdh1). *The EMBO journal*. 21:6515-6526.

Jiang, W., J. Lechner, and J. Carbon. 1993. Isolation and characterization of a gene (CBF2) specifying a protein component of the budding yeast kinetochore. *The Journal of cell biology*. 121:513-519.

Jokelainen, P.T. 1967. The ultrastructure and spatial organization of the metaphase kinetochore in mitotic rat cells. *Journal of ultrastructure research*. 19:19-44.

Jones, M.H., J.B. Bachant, A.R. Castillo, T.H. Giddings, Jr., and M. Winey. 1999. Yeast Dam1 is required to maintain spindle integrity during mitosis and interacts with the Mps1 kinase. *Molecular biology of the cell*. 10:2377-2391.

Joseph, J., S.T. Liu, S.A. Jablonski, T.J. Yen, and M. Dasso. 2004. The RanGAP1-RanBP2 complex is essential for microtubule-kinetochore interactions in vivo. *Current biology : CB*. 14:611-617.

Kaffman, A., and E.K. O'Shea. 1999. Regulation of nuclear localization: a key to a door. *Annual review of cell and developmental biology*. 15:291-339.

Kalab, P., K. Weis, and R. Heald. 2002. Visualization of a Ran-GTP gradient in interphase and mitotic Xenopus egg extracts. *Science*. 295:2452-2456.

Kalitsis, P., E. Earle, K.J. Fowler, and K.H. Choo. 2000. Bub3 gene disruption in mice reveals essential mitotic spindle checkpoint function during early embryogenesis. *Genes & development*. 14:2277-2282.

Kampmann, M., and G. Blobel. 2009. Three-dimensional structure and flexibility of a membrane-coating module of the nuclear pore complex. *Nature structural & molecular biology*. 16:782-788.

Kang, J., I.M. Cheeseman, G. Kallstrom, S. Velmurugan, G. Barnes, and C.S. Chan. 2001. Functional cooperation of Dam1, Ipl1, and the inner centromere protein (INCENP)-related protein Sli15 during chromosome segregation. *The Journal of cell biology*. 155:763-774.

Katsani, K.R., R.E. Karess, N. Dostatni, and V. Doye. 2008. In vivo dynamics of Drosophila nuclear envelope components. *Molecular biology of the cell*. 19:3652-3666.

Kawashima, S.A., Y. Yamagishi, T. Honda, K. Ishiguro, and Y. Watanabe. 2010. Phosphorylation of H2A by Bub1 prevents chromosomal instability through localizing shugoshin. *Science*. 327:172-177.

Kehlenbach, R.H., and L. Gerace. 2000. Phosphorylation of the nuclear transport machinery down-regulates nuclear protein import in vitro. *The Journal of biological chemistry*. 275:17848-17856.

Kemmler, S., M. Stach, M. Knapp, J. Ortiz, J. Pfannstiel, T. Ruppert, and J. Lechner. 2009. Mimicking Ndc80 phosphorylation triggers spindle assembly checkpoint signalling. *The EMBO journal*. 28:1099-1110.

Kerres, A., C. Vietmeier-Decker, J. Ortiz, I. Karig, C. Beuter, J. Hegemann, J. Lechner, and U. Fleig. 2004. The fission yeast kinetochore component Spc7 associates with the EB1 family member Mal3 and is required for kinetochore-spindle association. *Molecular biology of the cell*. 15:5255-5267.

Kerscher, O., P. Hieter, M. Winey, and M.A. Basrai. 2001. Novel role for a Saccharomyces cerevisiae nucleoporin, Nup170, in chromosome segregation. *Genetics*. 157:1543-1553.

Kim, S.H., D.P. Lin, S. Matsumoto, A. Kitazono, and T. Matsumoto. 1998. Fission yeast Slp1: an effector of the Mad2-dependent spindle checkpoint. *Science*. 279:1045-1047.

King, M.C., T.G. Drivas, and G. Blobel. 2008. A network of nuclear envelope membrane proteins linking centromeres to microtubules. *Cell*. 134:427-438.

King, M.C., C.P. Lusk, and G. Blobel. 2006. Karyopherin-mediated import of integral inner nuclear membrane proteins. *Nature*. 442:1003-1007.

King, R.W., J.M. Peters, S. Tugendreich, M. Rolfe, P. Hieter, and M.W. Kirschner. 1995. A 20S complex containing CDC27 and CDC16 catalyzes the mitosis-specific conjugation of ubiquitin to cyclin B. *Cell*. 81:279-288.

Kiseleva, E., T.D. Allen, S. Rutherford, M. Bucci, S.R. Wente, and M.W. Goldberg. 2004. Yeast nuclear pore complexes have a cytoplasmic ring and internal filaments. *Journal of structural biology*. 145:272-288.

Kitagawa, K., D. Skowyra, S.J. Elledge, J.W. Harper, and P. Hieter. 1999. SGT1 encodes an essential component of the yeast kinetochore assembly pathway and a novel subunit of the SCF ubiquitin ligase complex. *Molecular cell*. 4:21-33.

Kitagawa, R., and A.M. Rose. 1999. Components of the spindle-assembly checkpoint are essential in Caenorhabditis elegans. *Nature cell biology*. 1:514-521.

Kiyomitsu, T., H. Murakami, and M. Yanagida. 2011. Protein interaction domain mapping of human kinetochore protein Blinkin reveals a consensus motif for binding of spindle assembly checkpoint proteins Bub1 and BubR1. *Molecular and cellular biology*. 31:998-1011.

Kiyomitsu, T., C. Obuse, and M. Yanagida. 2007. Human Blinkin/AF15q14 is required for chromosome alignment and the mitotic checkpoint through direct interaction with Bub1 and BubR1. *Developmental cell*. 13:663-676.

Kline, S.L., I.M. Cheeseman, T. Hori, T. Fukagawa, and A. Desai. 2006. The human Mis12 complex is required for kinetochore assembly and proper chromosome segregation. *The Journal of cell biology*. 173:9-17.

Knauer, S.K., C. Bier, N. Habtemichael, and R.H. Stauber. 2006. The Survivin-Crm1 interaction is essential for chromosomal passenger complex localization and function. *EMBO reports*. 7:1259-1265.

Knockleby, J., and J. Vogel. 2009. The COMA complex is required for Sli15/INCENP-mediated correction of defective kinetochore attachments. *Cell cycle*. 8:2570-2577.

Kobayashi, J., and Y. Matsuura. 2013. Structural basis for cell-cycle-dependent nuclear import mediated by the karyopherin Kap121. *Journal of molecular biology*. 425:1852-1868.

Koffa, M.D., C.M. Casanova, R. Santarella, T. Kocher, M. Wilm, and I.W. Mattaj. 2006. HURP is part of a Ran-dependent complex involved in spindle formation. *Current biology : CB*. 16:743-754.

Kolling, R., T. Nguyen, E.Y. Chen, and D. Botstein. 1993. A new yeast gene with a myosin-like heptad repeat structure. *Molecular & general genetics : MGG*. 237:359-369.

Kops, G.J., and J.V. Shah. 2012. Connecting up and clearing out: how kinetochore attachment silences the spindle assembly checkpoint. *Chromosoma*. 121:509-525.

Kraemer, D.M., C. Strambio-de-Castillia, G. Blobel, and M.P. Rout. 1995. The essential yeast nucleoporin NUP159 is located on the cytoplasmic side of the nuclear pore complex and serves in karyopherin-mediated binding of transport substrate. *The Journal of biological chemistry*. 270:19017-19021.

Kubitscheck, U., D. Grunwald, A. Hoekstra, D. Rohleder, T. Kues, J.P. Siebrasse, and R. Peters. 2005. Nuclear transport of single molecules: dwell times at the nuclear pore complex. *The Journal of cell biology*. 168:233-243.

Kuijt, T.E., M. Omerzu, A.T. Saurin, and G.J. Kops. 2014. Conditional targeting of MAD1 to kinetochores is sufficient to reactivate the spindle assembly checkpoint in metaphase. *Chromosoma*. 123:471-480.

Kupke, T., L. Di Cecco, H.M. Muller, A. Neuner, F. Adolf, F. Wieland, W. Nickel, and E. Schiebel. 2011. Targeting of Nbp1 to the inner nuclear membrane is essential for spindle pole body duplication. *The EMBO journal*. 30:3337-3352.

la Cour, T., L. Kiemer, A. Molgaard, R. Gupta, K. Skriver, and S. Brunak. 2004. Analysis and prediction of leucine-rich nuclear export signals. *Protein engineering, design & selection : PEDS*. 17:527-536.

Lam, M.H., R.J. Thomas, K.L. Loveland, S. Schilders, M. Gu, T.J. Martin, M.T. Gillespie, and D.A. Jans. 2002. Nuclear transport of parathyroid hormone (PTH)-related protein is dependent on microtubules. *Molecular endocrinology*. 16:390-401.

Lampert, F., P. Hornung, and S. Westermann. 2010. The Dam1 complex confers microtubule plus end-tracking activity to the Ndc80 kinetochore complex. *The Journal of cell biology*. 189:641-649.

Lampert, F., C. Mieck, G.M. Alushin, E. Nogales, and S. Westermann. 2013. Molecular requirements for the formation of a kinetochore-microtubule interface by Dam1 and Ndc80 complexes. *The Journal of cell biology*. 200:21-30.

Lampert, F., and S. Westermann. 2011. A blueprint for kinetochores - new insights into the molecular mechanics of cell division. *Nature reviews. Molecular cell biology*. 12:407-412.

Lampson, M.A., and I.M. Cheeseman. 2011. Sensing centromere tension: Aurora B and the regulation of kinetochore function. *Trends in cell biology*. 21:133-140.

Lechner, J. 1994. A zinc finger protein, essential for chromosome segregation, constitutes a putative DNA binding subunit of the Saccharomyces cerevisiae kinetochore complex, Cbf3. *The EMBO journal*. 13:5203-5211.

Lee, D.C., and J.D. Aitchison. 1999. Kap104-mediated nuclear import. Nuclear localization signals in mRNA-binding proteins and the role of Ran and Rna. *The Journal of biological chemistry*. 274:29031-29037.

Lee, G.W., F. Melchior, M.J. Matunis, R. Mahajan, Q. Tian, and P. Anderson. 1998. Modification of Ran GTPase-activating protein by the small ubiquitin-related modifier SUMO-1 requires Ubc9, an E2-type ubiquitin-conjugating enzyme homologue. *The Journal of biological chemistry*. 273:6503-6507.

Lee, S.H., H. Sterling, A. Burlingame, and F. McCormick. 2008. Tpr directly binds to Mad1 and Mad2 and is important for the Mad1-Mad2-mediated mitotic spindle checkpoint. *Genes & development*. 22:2926-2931.

Lee, S.J., Y. Matsuura, S.M. Liu, and M. Stewart. 2005. Structural basis for nuclear import complex dissociation by RanGTP. *Nature*. 435:693-696.

Lee, S.J., T. Sekimoto, E. Yamashita, E. Nagoshi, A. Nakagawa, N. Imamoto, M. Yoshimura, H. Sakai, K.T. Chong, T. Tsukihara, and Y. Yoneda. 2003. The structure of importin-beta bound to SREBP-2: nuclear import of a transcription factor. *Science*. 302:1571-1575.

Lee, Y.T., J. Jacob, W. Michowski, M. Nowotny, J. Kuznicki, and W.J. Chazin. 2004. Human Sgt1 binds HSP90 through the CHORD-Sgt1 domain and not the tetratricopeptide repeat domain. *The Journal of biological chemistry*. 279:16511-16517.

Leslie, D.M., B. Grill, M.P. Rout, R.W. Wozniak, and J.D. Aitchison. 2002. Kap121-mediated nuclear import is required for mating and cellular differentiation in yeast. *Molecular and cellular biology*. 22:2544-2555.

Leslie, D.M., W. Zhang, B.L. Timney, B.T. Chait, M.P. Rout, R.W. Wozniak, and J.D. Aitchison. 2004. Characterization of karyopherin cargoes reveals unique mechanisms of Kap121-mediated nuclear import. *Molecular and cellular biology*. 24:8487-8503.

Li, J.M., Y. Li, and S.J. Elledge. 2005. Genetic analysis of the kinetochore DASH complex reveals an antagonistic relationship with the ras/protein kinase A pathway and a novel subunit required for Ask1 association. *Molecular and cellular biology*. 25:767-778.

Li, R., and A.W. Murray. 1991. Feedback control of mitosis in budding yeast. *Cell*. 66:519-531.

Li, Y., J. Bachant, A.A. Alcasabas, Y. Wang, J. Qin, and S.J. Elledge. 2002. The mitotic spindle is required for loading of the DASH complex onto the kinetochore. *Genes & development*. 16:183-197.

Li, Y., C. Gorbea, D. Mahaffey, M. Rechsteiner, and R. Benezra. 1997. MAD2 associates with the cyclosome/anaphase-promoting complex and inhibits its activity. *Proceedings of the National Academy of Sciences of the United States of America*. 94:12431-12436.

Lim, R.Y., B. Fahrenkrog, J. Koser, K. Schwarz-Herion, J. Deng, and U. Aebi. 2007. Nanomechanical basis of selective gating by the nuclear pore complex. *Science*. 318:640-643.

Lim, R.Y., N.P. Huang, J. Koser, J. Deng, K.H. Lau, K. Schwarz-Herion, B. Fahrenkrog, and U. Aebi. 2006. Flexible phenylalanine-glycine nucleoporins as entropic barriers to nucleocytoplasmic transport. *Proceedings of the National Academy of Sciences of the United States of America*. 103:9512-9517.

Lim, R.Y., K.S. Ullman, and B. Fahrenkrog. 2008. Biology and biophysics of the nuclear pore complex and its components. *International review of cell and molecular biology*. 267:299-342.

Lince-Faria, M., S. Maffini, B. Orr, Y. Ding, F. Claudia, C.E. Sunkel, A. Tavares, J. Johansen, K.M. Johansen, and H. Maiato. 2009. Spatiotemporal control of mitosis by the conserved spindle matrix protein Megator. *The Journal of cell biology*. 184:647-657.

Liu, Q., Q. Jiang, and C. Zhang. 2009. A fraction of Crm1 locates at centrosomes by its CRIME domain and regulates the centrosomal localization of pericentrin. *Biochemical and biophysical research communications*. 384:383-388.

Liu, S.M., and M. Stewart. 2005. Structural basis for the high-affinity binding of nucleoporin Nup1 to the Saccharomyces cerevisiae importin-beta homologue, Kap95. *Journal of molecular biology*. 349:515-525.

Liu, S.T., G.K. Chan, J.C. Hittle, G. Fujii, E. Lees, and T.J. Yen. 2003. Human MPS1 kinase is required for mitotic arrest induced by the loss of CENP-E from kinetochores. *Molecular biology of the cell*. 14:1638-1651.

Logan, M.R., T. Nguyen, N. Szapiel, J. Knockleby, H. Por, M. Zadworny, M. Neszt, P. Harrison, H. Bussey, C.A. Mandato, J. Vogel, and G. Lesage. 2008. Genetic interaction network of the Saccharomyces cerevisiae type 1 phosphatase Glc7. *BMC genomics*. 9:336.

Loiodice, I., A. Alves, G. Rabut, M. Van Overbeek, J. Ellenberg, J.B. Sibarita, and V. Doye. 2004. The entire Nup107-160 complex, including three new members, is targeted as one entity to kinetochores in mitosis. *Molecular biology of the cell*. 15:3333-3344.

London, N., and S. Biggins. 2014. Mad1 kinetochore recruitment by Mps1-mediated phosphorylation of Bub1 signals the spindle checkpoint. *Genes & development*. 28:140-152.

London, N., S. Ceto, J.A. Ranish, and S. Biggins. 2012. Phosphoregulation of Spc105 by Mps1 and PP1 regulates Bub1 localization to kinetochores. *Current biology : CB*. 22:900-906.

Longtine, M.S., A. McKenzie, 3rd, D.J. Demarini, N.G. Shah, A. Wach, A. Brachat, P. Philippsen, and J.R. Pringle. 1998. Additional modules for versatile and economical PCR-based gene deletion and modification in Saccharomyces cerevisiae. *Yeast*. 14:953-961.

Luo, X., G. Fang, M. Coldiron, Y. Lin, H. Yu, M.W. Kirschner, and G. Wagner. 2000. Structure of the Mad2 spindle assembly checkpoint protein and its interaction with Cdc20. *Nature structural biology*. 7:224-229.

Luo, X., Z. Tang, J. Rizo, and H. Yu. 2002. The Mad2 spindle checkpoint protein undergoes similar major conformational changes upon binding to either Mad1 or Cdc20. *Molecular cell*. 9:59-71.

Luo, X., Z. Tang, G. Xia, K. Wassmann, T. Matsumoto, J. Rizo, and H. Yu. 2004. The Mad2 spindle checkpoint protein has two distinct natively folded states. *Nature structural & molecular biology*. 11:338-345.

Lusk, C.P., G. Blobel, and M.C. King. 2007. Highway to the inner nuclear membrane: rules for the road. *Nature reviews. Molecular cell biology*. 8:414-420.

Lusk, C.P., T. Makhnevych, M. Marelli, J.D. Aitchison, and R.W. Wozniak. 2002. Karyopherins in nuclear pore biogenesis: a role for Kap121 in the assembly of Nup53 into nuclear pore complexes. *The Journal of cell biology*. 159:267-278.

Lussi, Y.C., D.K. Shumaker, T. Shimi, and B. Fahrenkrog. 2010. The nucleoporin Nup153 affects spindle checkpoint activity due to an association with Mad1. *Nucleus*. 1:71-84.

Lutzmann, M., R. Kunze, A. Buerer, U. Aebi, and E. Hurt. 2002. Modular self-assembly of a Y-shaped multiprotein complex from seven nucleoporins. *The EMBO journal*. 21:387-397.

Macara, I.G. 2001. Transport into and out of the nucleus. *Microbiology and molecular biology reviews : MMBR*. 65:570-594, table of contents.

Madison, D.L., P. Yaciuk, R.P. Kwok, and J.R. Lundblad. 2002. Acetylation of the adenovirus-transforming protein E1A determines nuclear localization by disrupting association with importin-alpha. *The Journal of biological chemistry*. 277:38755-38763.

Madrid, A.S., J. Mancuso, W.Z. Cande, and K. Weis. 2006. The role of the integral membrane nucleoporins Ndc1 and Pom152 in nuclear pore complex assembly and function. *The Journal of cell biology*. 173:361-371.

Mahajan, R., C. Delphin, T. Guan, L. Gerace, and F. Melchior. 1997. A small ubiquitin-related polypeptide involved in targeting RanGAP1 to nuclear pore complex protein RanBP2. *Cell*. 88:97-107.

Mahboubi, H., E. Seganathy, D. Kong, and U. Stochaj. 2013. Identification of Novel Stress Granule Components That Are Involved in Nuclear Transport. *PloS one*. 8:e68356.

Makhnevych, T., C.P. Lusk, A.M. Anderson, J.D. Aitchison, and R.W. Wozniak. 2003. Cell cycle regulated transport controlled by alterations in the nuclear pore complex. *Cell*. 115:813-823.

Makio, T., L.H. Stanton, C.C. Lin, D.S. Goldfarb, K. Weis, and R.W. Wozniak. 2009. The nucleoporins Nup170 and Nup157 are essential for nuclear pore complex assembly. *The Journal of cell biology*. 185:459-473.

Maldonado, M., and T.M. Kapoor. 2011. Constitutive Mad1 targeting to kinetochores uncouples checkpoint signalling from chromosome biorientation. *Nature cell biology*. 13:475-482.

Mansfeld, J., S. Guttinger, L.A. Hawryluk-Gara, N. Pante, M. Mall, V. Galy, U. Haselmann, P. Muhlhausser, R.W. Wozniak, I.W. Mattaj, U. Kutay, and W. Antonin. 2006. The conserved transmembrane nucleoporin NDC1 is required for nuclear pore complex assembly in vertebrate cells. *Molecular cell*. 22:93-103.

Mapelli, M., L. Massimiliano, S. Santaguida, and A. Musacchio. 2007. The Mad2 conformational dimer: structure and implications for the spindle assembly checkpoint. *Cell*. 131:730-743.

Marelli, M., J.D. Aitchison, and R.W. Wozniak. 1998. Specific binding of the karyopherin Kap121 to a subunit of the nuclear pore complex containing Nup53, Nup59, and Nup170. *The Journal of cell biology*. 143:1813-1830.

Marelli, M., C.P. Lusk, H. Chan, J.D. Aitchison, and R.W. Wozniak. 2001. A link between the synthesis of nucleoporins and the biogenesis of the nuclear envelope. *The Journal of cell biology*. 153:709-724.

Maresca, T.J., and E.D. Salmon. 2010. Welcome to a new kind of tension: translating kinetochore mechanics into a wait-anaphase signal. *Journal of cell science*. 123:825-835.

Martin-Lluesma, S., V.M. Stucke, and E.A. Nigg. 2002. Role of Hec1 in spindle checkpoint signaling and kinetochore recruitment of Mad1/Mad2. *Science*. 297:2267-2270.

Maskell, D.P., X.W. Hu, and M.R. Singleton. 2010. Molecular architecture and assembly of the yeast kinetochore MIND complex. *The Journal of cell biology*. 190:823-834.

Matsuura, Y., and M. Stewart. 2004. Structural basis for the assembly of a nuclear export complex. *Nature*. 432:872-877.

Mattaj, I.W. 2004. Sorting out the nuclear envelope from the endoplasmic reticulum. *Nature reviews. Molecular cell biology*. 5:65-69.

Mattaj, I.W., and L. Englmeier. 1998. Nucleocytoplasmic transport: the soluble phase. *Annual review of biochemistry*. 67:265-306.

Mattout, A., M. Goldberg, Y. Tzur, A. Margalit, and Y. Gruenbaum. 2007. Specific and conserved sequences in D. melanogaster and C. elegans lamins and histone H2A mediate the attachment of lamins to chromosomes. *Journal of cell science*. 120:77-85.

Matunis, M.J., E. Coutavas, and G. Blobel. 1996. A novel ubiquitin-like modification modulates the partitioning of the Ran-GTPase-activating protein RanGAP1 between the cytosol and the nuclear pore complex. *The Journal of cell biology*. 135:1457-1470.

McAinsh, A.D., J.D. Tytell, and P.K. Sorger. 2003. Structure, function, and regulation of budding yeast kinetochores. *Annual review of cell and developmental biology*. 19:519-539.

McCleland, M.L., R.D. Gardner, M.J. Kallio, J.R. Daum, G.J. Gorbsky, D.J. Burke, and P.T. Stukenberg. 2003. The highly conserved Ndc80 complex is required for kinetochore assembly, chromosome congression, and spindle checkpoint activity. *Genes & development*. 17:101-114.

McEwen, B.F., Y. Dong, and K.J. VandenBeldt. 2007. Using electron microscopy to understand functional mechanisms of chromosome alignment on the mitotic spindle. *Methods in cell biology*. 79:259-293.

Meluh, P.B., and D. Koshland. 1997. Budding yeast centromere composition and assembly as revealed by in vivo cross-linking. *Genes & development*. 11:3401-3412.

Miao, M., K.J. Ryan, and S.R. Wente. 2006. The integral membrane protein Pom34 functionally links nucleoporin subcomplexes. *Genetics*. 172:1441-1457.

Miranda, J.J., P. De Wulf, P.K. Sorger, and S.C. Harrison. 2005. The yeast DASH complex forms closed rings on microtubules. *Nature structural & molecular biology*. 12:138-143.

Mishra, K., and V.K. Parnaik. 1995. Essential role of protein phosphorylation in nuclear transport. *Experimental cell research*. 216:124-134.

Mishra, R.K., P. Chakraborty, A. Arnaoutov, B.M. Fontoura, and M. Dasso. 2010. The Nup107-160 complex and gamma-TuRC regulate microtubule polymerization at kinetochores. *Nature cell biology*. 12:164-169.

Mitchell, J.M., J. Mansfeld, J. Capitanio, U. Kutay, and R.W. Wozniak. 2010. Pom121 links two essential subcomplexes of the nuclear pore complex core to the membrane. *The Journal of cell biology*. 191:505-521.

Montpetit, B., N.D. Thomsen, K.J. Helmke, M.A. Seeliger, J.M. Berger, and K. Weis. 2011. A conserved mechanism of DEAD-box ATPase activation by nucleoporins and InsP6 in mRNA export. *Nature*. 472:238-242.

Mosammaparast, N., B.C. Del Rosario, and L.F. Pemberton. 2005. Modulation of histone deposition by the karyopherin kap114. *Molecular and cellular biology*. 25:1764-1778.

Mosammaparast, N., Y. Guo, J. Shabanowitz, D.F. Hunt, and L.F. Pemberton. 2002. Pathways mediating the nuclear import of histones H3 and H4 in yeast. *The Journal of biological chemistry*. 277:862-868.

Mosammaparast, N., K.R. Jackson, Y. Guo, C.J. Brame, J. Shabanowitz, D.F. Hunt, and L.F. Pemberton. 2001. Nuclear import of histone H2A and H2B is mediated by a network of karyopherins. *The Journal of cell biology*. 153:251-262.

Musacchio, A., and K.G. Hardwick. 2002. The spindle checkpoint: structural insights into dynamic signalling. *Nature reviews. Molecular cell biology*. 3:731-741.

Musacchio, A., and E.D. Salmon. 2007. The spindle-assembly checkpoint in space and time. *Nature reviews. Molecular cell biology*. 8:379-393.

Nachury, M.V., T.J. Maresca, W.C. Salmon, C.M. Waterman-Storer, R. Heald, and K. Weis. 2001. Importin beta is a mitotic target of the small GTPase Ran in spindle assembly. *Cell*. 104:95-106.

Nachury, M.V., and K. Weis. 1999. The direction of transport through the nuclear pore can be inverted. *Proceedings of the National Academy of Sciences of the United States of America*. 96:9622-9627.

Nakielny, S., and G. Dreyfuss. 1998. Import and export of the nuclear protein import receptor transportin by a mechanism independent of GTP hydrolysis. *Current biology : CB*. 8:89-95.

Nekrasov, V.S., M.A. Smith, S. Peak-Chew, and J.V. Kilmartin. 2003. Interactions between centromere complexes in Saccharomyces cerevisiae. *Molecular biology of the cell*. 14:4931-4946.

Nemergut, M.E., C.A. Mizzen, T. Stukenberg, C.D. Allis, and I.G. Macara. 2001. Chromatin docking and exchange activity enhancement of RCC1 by histones H2A and H2B. *Science*. 292:1540-1543.

Neuber, A., J. Franke, A. Wittstruck, G. Schlenstedt, T. Sommer, and K. Stade. 2008. Nuclear export receptor Xpo1/Crm1 is physically and functionally linked to the

spindle pole body in budding yeast. *Molecular and cellular biology*. 28:5348-5358.

Neville, M., and M. Rosbash. 1999. The NES-Crm1 export pathway is not a major mRNA export route in Saccharomyces cerevisiae. *The EMBO journal*. 18:3746-3756.

Nicklas, R.B., S.C. Ward, and G.J. Gorbsky. 1995. Kinetochore chemistry is sensitive to tension and may link mitotic forces to a cell cycle checkpoint. *The Journal of cell biology*. 130:929-939.

Niepel, M., C. Strambio-de-Castillia, J. Fasolo, B.T. Chait, and M.P. Rout. 2005. The nuclear pore complex-associated protein, Mlp2, binds to the yeast spindle pole body and promotes its efficient assembly. *The Journal of cell biology*. 170:225-235.

Obuse, C., O. Iwasaki, T. Kiyomitsu, G. Goshima, Y. Toyoda, and M. Yanagida. 2004. A conserved Mis12 centromere complex is linked to heterochromatic HP1 and outer kinetochore protein Zwint-1. *Nature cell biology*. 6:1135-1141.

Ohtsubo, M., H. Okazaki, and T. Nishimoto. 1989. The RCC1 protein, a regulator for the onset of chromosome condensation locates in the nucleus and binds to DNA. *The Journal of cell biology*. 109:1389-1397.

Onischenko, E., L.H. Stanton, A.S. Madrid, T. Kieselbach, and K. Weis. 2009. Role of the Ndc1 interaction network in yeast nuclear pore complex assembly and maintenance. *The Journal of cell biology*. 185:475-491.

Orjalo, A.V., A. Arnaoutov, Z. Shen, Y. Boyarchuk, S.G. Zeitlin, B. Fontoura, S. Briggs, M. Dasso, and D.J. Forbes. 2006. The Nup107-160 nucleoporin complex is required for correct bipolar spindle assembly. *Molecular biology of the cell*. 17:3806-3818.

Ossareh-Nazari, B., F. Bachelerie, and C. Dargemont. 1997. Evidence for a role of CRM1 in signal-mediated nuclear protein export. *Science*. 278:141-144.

Pagliuca, C., V.M. Draviam, E. Marco, P.K. Sorger, and P. De Wulf. 2009. Roles for the conserved spc105/kre28 complex in kinetochore-microtubule binding and the spindle assembly checkpoint. *PloS one*. 4:e7640.

Pangilinan, F., and F. Spencer. 1996. Abnormal kinetochore structure activates the spindle assembly checkpoint in budding yeast. *Molecular biology of the cell*. 7:1195-1208.

Panse, V.G., B. Kuster, T. Gerstberger, and E. Hurt. 2003. Unconventional tethering of Ulp1 to the transport channel of the nuclear pore complex by karyopherins. *Nature cell biology*. 5:21-27.

Patel, S.S., and M.F. Rexach. 2008. Discovering novel interactions at the nuclear pore complex using bead halo: a rapid method for detecting molecular interactions of high and low affinity at equilibrium. *Molecular & cellular proteomics : MCP*. 7:121-131.

Pemberton, L.F., G. Blobel, and J.S. Rosenblum. 1998. Transport routes through the nuclear pore complex. *Current opinion in cell biology*. 10:392-399.

Pemberton, L.F., and B.M. Paschal. 2005. Mechanisms of receptor-mediated nuclear import and nuclear export. *Traffic*. 6:187-198.

Pemberton, L.F., J.S. Rosenblum, and G. Blobel. 1999. Nuclear import of the TATA-binding protein: mediation by the karyopherin Kap114 and a possible mechanism for intranuclear targeting. *The Journal of cell biology*. 145:1407-1417.

Perriches, T., and M.R. Singleton. 2012. Structure of yeast kinetochore Ndc10 DNA-binding domain reveals unexpected evolutionary relationship to tyrosine recombinases. *The Journal of biological chemistry*. 287:5173-5179.

Petrovic, A., S. Pasqualato, P. Dube, V. Krenn, S. Santaguida, D. Cittaro, S. Monzani, L. Massimiliano, J. Keller, A. Tarricone, A. Maiolica, H. Stark, and A. Musacchio. 2010. The MIS12 complex is a protein interaction hub for outer kinetochore assembly. *The Journal of cell biology*. 190:835-852.

Pichler, A., and F. Melchior. 2002. Ubiquitin-related modifier SUMO1 and nucleocytoplasmic transport. *Traffic*. 3:381-387.

Pinsky, B.A., C.V. Kotwaliwale, S.Y. Tatsutani, C.A. Breed, and S. Biggins. 2006a. Glc7/protein phosphatase 1 regulatory subunits can oppose the Ipl1/aurora protein kinase by redistributing Glc7. *Molecular and cellular biology*. 26:2648-2660.

Pinsky, B.A., C. Kung, K.M. Shokat, and S. Biggins. 2006b. The Ipl1-Aurora protein kinase activates the spindle checkpoint by creating unattached kinetochores. *Nature cell biology*. 8:78-83.

Pinsky, B.A., C.R. Nelson, and S. Biggins. 2009. Protein phosphatase 1 regulates exit from the spindle checkpoint in budding yeast. *Current biology : CB*. 19:1182-1187.

Przewloka, M.R., W. Zhang, P. Costa, V. Archambault, P.P. D'Avino, K.S. Lilley, E.D. Laue, A.D. McAinsh, and D.M. Glover. 2007. Molecular analysis of core kinetochore composition and assembly in Drosophila melanogaster. *PloS one*. 2:e478.

Ptak, C., A.M. Anderson, R.J. Scott, D. Van de Vosse, R.S. Rogers, Y. Sydorskyy, J.D. Aitchison, and R.W. Wozniak. 2009. A role for the karyopherin Kap123 in microtubule stability. *Traffic*. 10:1619-1634.

Pyhtila, B., and M. Rexach. 2003. A gradient of affinity for the karyopherin Kap95 along the yeast nuclear pore complex. *The Journal of biological chemistry*. 278:42699-42709.

Radu, A., M.S. Moore, and G. Blobel. 1995. The peptide repeat domain of nucleoporin Nup98 functions as a docking site in transport across the nuclear pore complex. *Cell*. 81:215-222.

Ramey, V.H., H.W. Wang, Y. Nakajima, A. Wong, J. Liu, D. Drubin, G. Barnes, and E. Nogales. 2011a. The Dam1 ring binds to the E-hook of tubulin and diffuses along the microtubule. *Molecular biology of the cell*. 22:457-466.

Ramey, V.H., A. Wong, J. Fang, S. Howes, G. Barnes, and E. Nogales. 2011b. Subunit organization in the Dam1 kinetochore complex and its ring around microtubules. *Molecular biology of the cell*. 22:4335-4342.

Reddy, K.L., J.M. Zullo, E. Bertolino, and H. Singh. 2008. Transcriptional repression mediated by repositioning of genes to the nuclear lamina. *Nature*. 452:243-247.

Ribbeck, K., and D. Gorlich. 2001. Kinetic analysis of translocation through nuclear pore complexes. *The EMBO journal*. 20:1320-1330.

Ribbeck, K., and D. Gorlich. 2002. The permeability barrier of nuclear pore complexes appears to operate via hydrophobic exclusion. *The EMBO journal*. 21:2664-2671.

Ribbeck, K., G. Lipowsky, H.M. Kent, M. Stewart, and D. Gorlich. 1998. NTF2 mediates nuclear import of Ran. *The EMBO journal*. 17:6587-6598.

Ribbeck, K., T. Raemaekers, G. Carmeliet, and I.W. Mattaj. 2007. A role for NuSAP in linking microtubules to mitotic chromosomes. *Current biology : CB*. 17:230-236.

Rieder, C.L. 1981. The structure of the cold-stable kinetochore fiber in metaphase PtK1 cells. *Chromosoma*. 84:145-158.

Rieder, C.L., R.W. Cole, A. Khodjakov, and G. Sluder. 1995. The checkpoint delaying anaphase in response to chromosome monoorientation is mediated by an inhibitory signal produced by unattached kinetochores. *The Journal of cell biology*. 130:941-948.

Rieder, C.L., A. Schultz, R. Cole, and G. Sluder. 1994. Anaphase onset in vertebrate somatic cells is controlled by a checkpoint that monitors sister kinetochore attachment to the spindle. *The Journal of cell biology*. 127:1301-1310.

Rodriguez-Bravo, V., J. Maciejowski, J. Corona, H.K. Buch, P. Collin, M.T. Kanemaki, J.V. Shah, and P.V. Jallepalli. 2014. Nuclear pores protect genome integrity by assembling a premitotic and Mad1-dependent anaphase inhibitor. *Cell*. 156:1017-1031.

Roos, U.P. 1973. Light and electron microscopy of rat kangaroo cells in mitosis. II. Kinetochore structure and function. *Chromosoma*. 41:195-220.

Roscioli, E., L. Di Francesco, A. Bolognesi, M. Giubettini, S. Orlando, A. Harel, M.E. Schinina, and P. Lavia. 2012. Importin-beta negatively regulates multiple aspects of mitosis including RANGAP1 recruitment to kinetochores. *The Journal of cell biology*. 196:435-450.

Rosenberg, J.S., F.R. Cross, and H. Funabiki. 2011. KNL1/Spc105 recruits PP1 to silence the spindle assembly checkpoint. *Current biology : CB*. 21:942-947.

Rossio, V., E. Galati, M. Ferrari, A. Pellicioli, T. Sutani, K. Shirahige, G. Lucchini, and S. Piatti. 2010. The RSC chromatin-remodeling complex influences mitotic exit and adaptation to the spindle assembly checkpoint by controlling the Cdc14 phosphatase. *The Journal of cell biology*. 191:981-997.

Rousselet, A. 2009. Inhibiting Crm1 causes the formation of excess acentriolar spindle poles containing NuMA and B23, but does not affect centrosome numbers. *Biology of the cell / under the auspices of the European Cell Biology Organization*. 101:679-693.

Rout, M.P., and J.D. Aitchison. 2000. Pore relations: nuclear pore complexes and nucleocytoplasmic exchange. *Essays in biochemistry*. 36:75-88.

Rout, M.P., J.D. Aitchison, M.O. Magnasco, and B.T. Chait. 2003. Virtual gating and nuclear transport: the hole picture. *Trends in cell biology*. 13:622-628.

Rout, M.P., J.D. Aitchison, A. Suprapto, K. Hjertaas, Y. Zhao, and B.T. Chait. 2000. The yeast nuclear pore complex: composition, architecture, and transport mechanism. *The Journal of cell biology*. 148:635-651.

Rout, M.P., G. Blobel, and J.D. Aitchison. 1997. A distinct nuclear import pathway used by ribosomal proteins. *Cell*. 89:715-725.

Saitoh, H., R. Pu, M. Cavenagh, and M. Dasso. 1997. RanBP2 associates with Ubc9 and a modified form of RanGAP1. *Proceedings of the National Academy of Sciences of the United States of America*. 94:3736-3741.

Sandall, S., F. Severin, I.X. McLeod, J.R. Yates, 3rd, K. Oegema, A. Hyman, and A. Desai. 2006. A Bir1-Sli15 complex connects centromeres to microtubules and is required to sense kinetochore tension. *Cell*. 127:1179-1191.

Sarangapani, K.K., B. Akiyoshi, N.M. Duggan, S. Biggins, and C.L. Asbury. 2013. Phosphoregulation promotes release of kinetochores from dynamic microtubules via multiple mechanisms. *Proceedings of the National Academy of Sciences of the United States of America*. 110:7282-7287.

Sassoon, I., F.F. Severin, P.D. Andrews, M.R. Taba, K.B. Kaplan, A.J. Ashford, M.J. Stark, P.K. Sorger, and A.A. Hyman. 1999. Regulation of Saccharomyces cerevisiae kinetochores by the type 1 phosphatase Glc7. *Genes & development*. 13:545-555.

Schatz, P.J., F. Solomon, and D. Botstein. 1988. Isolation and characterization of conditional-lethal mutations in the TUB1 alpha-tubulin gene of the yeast Saccharomyces cerevisiae. *Genetics*. 120:681-695.

Schiestl, R.H., and R.D. Gietz. 1989. High efficiency transformation of intact yeast cells using single stranded nucleic acids as a carrier. *Current genetics*. 16:339-346.

Schirmer, E.C., and R. Foisner. 2007. Proteins that associate with lamins: many faces, many functions. *Experimental cell research*. 313:2167-2179.

Schjerling, P., and S. Holmberg. 1996. Comparative amino acid sequence analysis of the C6 zinc cluster family of transcriptional regulators. *Nucleic acids research*. 24:4599-4607.

Scharfenberger, M., J. Ortiz, N. Grau, C. Janke, E. Schiebel, and J. Lechner. 2003. Nsl1 is essential for the establishment of bipolarity and the localization of the Dam-Duo complex. *The EMBO journal*. 22:6584-6597.

Schramm, C., S. Elliott, A. Shevchenko, and E. Schiebel. 2000. The Bbp1-Mps2 complex connects the SPB to the nuclear envelope and is essential for SPB duplication. *The EMBO journal*. 19:421-433.

Schwoebel, E.D., B. Talcott, I. Cushman, and M.S. Moore. 1998. Ran-dependent signal-mediated nuclear import does not require GTP hydrolysis by Ran. *The Journal of biological chemistry*. 273:35170-35175.

Scott, R.J., L.V. Cairo, D.W. Van de Vosse, and R.W. Wozniak. 2009. The nuclear export factor Xpo1 targets Mad1 to kinetochores in yeast. *The Journal of cell biology*. 184:21-29.

Scott, R.J., C.P. Lusk, D.J. Dilworth, J.D. Aitchison, and R.W. Wozniak. 2005. Interactions between Mad1 and the nuclear transport machinery in the yeast Saccharomyces cerevisiae. *Molecular biology of the cell*. 16:4362-4374.

Seedorf, M., M. Damelin, J. Kahana, T. Taura, and P.A. Silver. 1999. Interactions between a nuclear transporter and a subset of nuclear pore complex proteins depend on Ran GTPase. *Molecular and cellular biology*. 19:1547-1557.

Severin, F., B. Habermann, T. Huffaker, and T. Hyman. 2001. Stu2 promotes mitotic spindle elongation in anaphase. *The Journal of cell biology*. 153:435-442.

Shah, J.V., E. Botvinick, Z. Bonday, F. Furnari, M. Berns, and D.W. Cleveland. 2004. Dynamics of centromere and kinetochore proteins; implications for checkpoint signaling and silencing. *Current biology : CB*. 14:942-952.

Shah, S., and D.J. Forbes. 1998. Separate nuclear import pathways converge on the nucleoporin Nup153 and can be dissected with dominant-negative inhibitors. *Current biology : CB*. 8:1376-1386.

Shepperd, L.A., J.C. Meadows, A.M. Sochaj, T.C. Lancaster, J. Zou, G.J. Buttrick, J. Rappsilber, K.G. Hardwick, and J.B. Millar. 2012. Phosphodependent recruitment of Bub1 and Bub3 to Spc7/KNL1 by Mph1 kinase maintains the spindle checkpoint. *Current biology : CB*. 22:891-899.

Sherman, F., G.R. Fink, J.B. Hicks. 1983. *Methods in yeast genetics: laboratory manual.* Cold Spring Harbor Laboratory, Cold Spring Harbor. 120p.

Sikorski, R.S., and P. Hieter. 1989. A system of shuttle vectors and yeast host strains designed for efficient manipulation of DNA in Saccharomyces cerevisiae. *Genetics*. 122:19-27.

Sillje, H.H., S. Nagel, R. Korner, and E.A. Nigg. 2006. HURP is a Ran-importin beta-regulated protein that stabilizes kinetochore microtubules in the vicinity of chromosomes. *Current biology : CB*. 16:731-742.

Siniossoglou, S., M. Lutzmann, H. Santos-Rosa, K. Leonard, S. Mueller, U. Aebi, and E. Hurt. 2000. Structure and assembly of the Nup84 complex. *The Journal of cell biology*. 149:41-54.

Sironi, L., M. Mapelli, S. Knapp, A. De Antoni, K.T. Jeang, and A. Musacchio. 2002. Crystal structure of the tetrameric Mad1-Mad2 core complex: implications of a 'safety belt' binding mechanism for the spindle checkpoint. *The EMBO journal*. 21:2496-2506.

Smith, A., A. Brownawell, and I.G. Macara. 1998. Nuclear import of Ran is mediated by the transport factor NTF2. *Current biology : CB*. 8:1403-1406.

Solsbacher, J., P. Maurer, F. Vogel, and G. Schlenstedt. 2000. Nup2, a yeast nucleoporin, functions in bidirectional transport of importin alpha. *Molecular and cellular biology*. 20:8468-8479.

Song, L., A. Craney, and M. Rape. 2014. Microtubule-dependent regulation of mitotic protein degradation. *Molecular cell*. 53:179-192.

Stade, K., C.S. Ford, C. Guthrie, and K. Weis. 1997. Exportin 1 (Crm1) is an essential nuclear export factor. *Cell*. 90:1041-1050.

Starr, D.A., and M. Han. 2003. ANChors away: an actin based mechanism of nuclear positioning. *Journal of cell science*. 116:211-216.

Steensgaard, P., M. Garre, I. Muradore, P. Transidico, E.A. Nigg, K. Kitagawa, W.C. Earnshaw, M. Faretta, and A. Musacchio. 2004. Sgt1 is required for human kinetochore assembly. *EMBO reports*. 5:626-631.

Stegmeier, F., R. Visintin, and A. Amon. 2002. Separase, polo kinase, the kinetochore protein Slk19, and Spo12 function in a network that controls Cdc14 localization during early anaphase. *Cell*. 108:207-220.

Stelter, P., R. Kunze, D. Flemming, D. Hopfner, M. Diepholz, P. Philippsen, B. Bottcher, and E. Hurt. 2007. Molecular basis for the functional interaction of dynein light chain with the nuclear-pore complex. *Nature cell biology*. 9:788-796.

Stewart, M. 2007. Molecular mechanism of the nuclear protein import cycle. *Nature reviews. Molecular cell biology*. 8:195-208.

Stoffler, D., B. Feja, B. Fahrenkrog, J. Walz, D. Typke, and U. Aebi. 2003. Cryo-electron tomography provides novel insights into nuclear pore architecture: implications for nucleocytoplasmic transport. *Journal of molecular biology*. 328:119-130.

Stommel, J.M., N.D. Marchenko, G.S. Jimenez, U.M. Moll, T.J. Hope, and G.M. Wahl. 1999. A leucine-rich nuclear export signal in the p53 tetramerization domain: regulation of subcellular localization and p53 activity by NES masking. *The EMBO journal*. 18:1660-1672.

Storchova, Z., J.S. Becker, N. Talarek, S. Kogelsberger, and D. Pellman. 2011. Bub1, Sgo1, and Mps1 mediate a distinct pathway for chromosome biorientation in budding yeast. *Molecular biology of the cell*. 22:1473-1485.

Strahm, Y., B. Fahrenkrog, D. Zenklusen, E. Rychner, J. Kantor, M. Rosbach, and F. Stutz. 1999. The RNA export factor Gle1 is located on the cytoplasmic fibrils of the NPC and physically interacts with the FG-nucleoporin Rip1, the DEAD-box protein Rat8/Dbp5 and a new protein Ymr 255. *The EMBO journal*. 18:5761-5777.

Strambio-de-Castillia, C., G. Blobel, and M.P. Rout. 1999. Proteins connecting the nuclear pore complex with the nuclear interior. *The Journal of cell biology*. 144:839-855.

Strambio-De-Castillia, C., M. Niepel, and M.P. Rout. 2010. The nuclear pore complex: bridging nuclear transport and gene regulation. *Nature reviews. Molecular cell biology*. 11:490-501.

Strawn, L.A., T. Shen, N. Shulga, D.S. Goldfarb, and S.R. Wente. 2004. Minimal nuclear pore complexes define FG repeat domains essential for transport. *Nature cell biology*. 6:197-206.

Strom, A.C., and K. Weis. 2001. Importin-beta-like nuclear transport receptors. *Genome biology*. 2:REVIEWS3008.

Strunnikov, A.V., J. Kingsbury, and D. Koshland. 1995. CEP3 encodes a centromere protein of Saccharomyces cerevisiae. *The Journal of cell biology*. 128:749-760.

Sudakin, V., G.K. Chan, and T.J. Yen. 2001. Checkpoint inhibition of the APC/C in HeLa cells is mediated by a complex of BUBR1, BUB3, CDC20, and MAD2. *The Journal of cell biology*. 154:925-936.

Sukegawa, J., and G. Blobel. 1993. A nuclear pore complex protein that contains zinc finger motifs, binds DNA, and faces the nucleoplasm. *Cell*. 72:29-38.

Sundin, L.J., G.J. Guimaraes, and J.G. Deluca. 2011. The NDC80 complex proteins Nuf2 and Hec1 make distinct contributions to kinetochore-microtubule attachment in mitosis. *Molecular biology of the cell*. 22:759-768.

Tan-Wong, S.M., H.D. Wijayatilake, and N.J. Proudfoot. 2009. Gene loops function to maintain transcriptional memory through interaction with the nuclear pore complex. *Genes & development*. 23:2610-2624.

Tanaka, K. 2012. Dynamic regulation of kinetochore-microtubule interaction during mitosis. *Journal of biochemistry*. 152:415-424.

Tanaka, K., E. Kitamura, Y. Kitamura, and T.U. Tanaka. 2007. Molecular mechanisms of microtubule-dependent kinetochore transport toward spindle poles. *The Journal of cell biology*. 178:269-281.

Tanaka, T., J. Fuchs, J. Loidl, and K. Nasmyth. 2000. Cohesin ensures bipolar attachment of microtubules to sister centromeres and resists their precocious separation. *Nature cell biology*. 2:492-499.

Tanaka, T.U. 2010. Kinetochore-microtubule interactions: steps towards bi-orientation. *The EMBO journal*. 29:4070-4082.

Tanaka, T.U., and A. Desai. 2008. Kinetochore-microtubule interactions: the means to the end. *Current opinion in cell biology*. 20:53-63.

Tanaka, T.U., N. Rachidi, C. Janke, G. Pereira, M. Galova, E. Schiebel, M.J. Stark, and K. Nasmyth. 2002. Evidence that the Ipl1-Sli15 (Aurora kinase-INCENP) complex promotes chromosome bi-orientation by altering kinetochore-spindle pole connections. *Cell*. 108:317-329.

Tanaka, T.U., M.J. Stark, and K. Tanaka. 2005. Kinetochore capture and bi-orientation on the mitotic spindle. *Nature reviews. Molecular cell biology*. 6:929-942.

Tatchell, K., V. Makrantoni, M.J. Stark, and L.C. Robinson. 2011. Temperature-sensitive ipl1-2/Aurora B mutation is suppressed by mutations in TOR complex 1 via the Glc7/PP1 phosphatase. *Proceedings of the National Academy of Sciences of the United States of America*. 108:3994-3999.

Tcheperegine, S.E., M. Marelli, and R.W. Wozniak. 1999. Topology and functional domains of the yeast pore membrane protein Pom152. *The Journal of biological chemistry*. 274:5252-5258.

Terasaki, M., P. Campagnola, M.M. Rolls, P.A. Stein, J. Ellenberg, B. Hinkle, and B. Slepchenko. 2001. A new model for nuclear envelope breakdown. *Molecular biology of the cell*. 12:503-510.

Terry, L.J., E.B. Shows, and S.R. Wente. 2007. Crossing the nuclear envelope: hierarchical regulation of nucleocytoplasmic transport. *Science*. 318:1412-1416.

Texari, L., G. Dieppois, P. Vinciguerra, M.P. Contreras, A. Groner, A. Letourneau, and F. Stutz. 2013. The nuclear pore regulates GAL1 gene transcription by controlling the localization of the SUMO protease Ulp1. *Molecular cell*. 51:807-818.

Tien, J.F., K.K. Fong, N.T. Umbreit, C. Payen, A. Zelter, C.L. Asbury, M.J. Dunham, and T.N. Davis. 2013. Coupling unbiased mutagenesis to high-throughput DNA sequencing uncovers functional domains in the Ndc80 kinetochore protein of Saccharomyces cerevisiae. *Genetics*. 195:159-170.

Tien, J.F., N.T. Umbreit, D.R. Gestaut, A.D. Franck, J. Cooper, L. Wordeman, T. Gonen, C.L. Asbury, and T.N. Davis. 2010. Cooperation of the Dam1 and Ndc80 kinetochore complexes enhances microtubule coupling and is regulated by aurora B. *The Journal of cell biology*. 189:713-723.

Tien, J.F., N.T. Umbreit, A. Zelter, M. Riffle, M.R. Hoopmann, R.S. Johnson, B.R. Fonslow, J.R. Yates, 3rd, M.J. MacCoss, R.L. Moritz, C.L. Asbury, and T.N. Davis. 2014. Kinetochore Biorientation in Saccharomyces cerevisiae Requires a Tightly Folded Conformation of the Ndc80 Complex. *Genetics*.

Tooley, J., and P.T. Stukenberg. 2011. The Ndc80 complex: integrating the kinetochore's many movements. *Chromosome research : an international journal on the molecular, supramolecular and evolutionary aspects of chromosome biology*. 19:377-391.

Tooley, J.G., S.A. Miller, and P.T. Stukenberg. 2011. The Ndc80 complex uses a tripartite attachment point to couple microtubule depolymerization to chromosome movement. *Molecular biology of the cell*. 22:1217-1226.

Torosantucci, L., M. De Luca, G. Guarguaglini, P. Lavia, and F. Degrassi. 2008. Localized RanGTP accumulation promotes microtubule nucleation at kinetochores in somatic mammalian cells. *Molecular biology of the cell*. 19:1873-1882.

Tu, L.C., and S.M. Musser. 2011. Single molecule studies of nucleocytoplasmic transport. *Biochimica et biophysica acta*. 1813:1607-1618.

Twyffels, L., C. Gueydan, and V. Kruys. 2014. Transportin-1 and Transportin-2: protein nuclear import and beyond. *FEBS letters*. 588:1857-1868.

Uhlmann, F., D. Wernic, M.A. Poupart, E.V. Koonin, and K. Nasmyth. 2000. Cleavage of cohesin by the CD clan protease separin triggers anaphase in yeast. *Cell*. 103:375-386.

Umbreit, N.T., D.R. Gestaut, J.F. Tien, B.S. Vollmar, T. Gonen, C.L. Asbury, and T.N. Davis. 2012. The Ndc80 kinetochore complex directly modulates microtubule dynamics. *Proceedings of the National Academy of Sciences of the United States of America*. 109:16113-16118.

Umbreit, N.T., M.P. Miller, J.F. Tien, J.C. Ortola, L. Gui, K.K. Lee, S. Biggins, C.L. Asbury, and T.N. Davis. 2014. Kinetochores require oligomerization of Dam1 complex to maintain microtubule attachments against tension and promote biorientation. *Nature communications*. 5:4951.

Van de Vosse, D.W., Y. Wan, D.L. Lapetina, W.M. Chen, J.H. Chiang, J.D. Aitchison, and R.W. Wozniak. 2013. A role for the nucleoporin Nup170 in chromatin structure and gene silencing. *Cell*. 152:969-983.

Vanoosthuyse, V., and K.G. Hardwick. 2009. A novel protein phosphatase 1-dependent spindle checkpoint silencing mechanism. *Current biology : CB*. 19:1176-1181.

Vassileva, M.T., and M.J. Matunis. 2004. SUMO modification of heterogeneous nuclear ribonucleoproteins. *Molecular and cellular biology*. 24:3623-3632.

Vasu, S., S. Shah, A. Orjalo, M. Park, W.H. Fischer, and D.J. Forbes. 2001. Novel vertebrate nucleoporins Nup133 and Nup160 play a role in mRNA export. *The Journal of cell biology*. 155:339-354.

Vasu, S.K., and D.J. Forbes. 2001. Nuclear pores and nuclear assembly. *Current opinion in cell biology*. 13:363-375.

Verdaasdonk, J.S., R. Gardner, A.D. Stephens, E. Yeh, and K. Bloom. 2012. Tension-dependent nucleosome remodeling at the pericentromere in yeast. *Molecular biology of the cell*. 23:2560-2570.

Vetter, I.R., A. Arndt, U. Kutay, D. Gorlich, and A. Wittinghofer. 1999. Structural view of the Ran-Importin beta interaction at 2.3 A resolution. *Cell*. 97:635-646.

Visintin, C., B.N. Tomson, R. Rahal, J. Paulson, M. Cohen, J. Taunton, A. Amon, and R. Visintin. 2008. APC/C-Cdh1-mediated degradation of the Polo kinase Cdc5 promotes the return of Cdc14 into the nucleolus. *Genes & development*. 22:79-90.

Voeltz, G.K., and W.A. Prinz. 2007. Sheets, ribbons and tubules - how organelles get their shape. *Nature reviews. Molecular cell biology*. 8:258-264.

Vorozhko, V.V., M.J. Emanuele, M.J. Kallio, P.T. Stukenberg, and G.J. Gorbsky. 2008. Multiple mechanisms of chromosome movement in vertebrate cells mediated through the Ndc80 complex and dynein/dynactin. *Chromosoma*. 117:169-179.

Walther, T.C., A. Alves, H. Pickersgill, I. Loiodice, M. Hetzer, V. Galy, B.B. Hulsmann, T. Kocher, M. Wilm, T. Allen, I.W. Mattaj, and V. Doye. 2003a. The conserved Nup107-160 complex is critical for nuclear pore complex assembly. *Cell*. 113:195-206.

Walther, T.C., P. Askjaer, M. Gentzel, A. Habermann, G. Griffiths, M. Wilm, I.W. Mattaj, and M. Hetzer. 2003b. RanGTP mediates nuclear pore complex assembly. *Nature*. 424:689-694.

Wang, H.W., V.H. Ramey, S. Westermann, A.E. Leschziner, J.P. Welburn, Y. Nakajima, D.G. Drubin, G. Barnes, and E. Nogales. 2007. Architecture of the Dam1 kinetochore ring complex and implications for microtubule-driven assembly and force-coupling mechanisms. *Nature structural & molecular biology*. 14:721-726.

Wang, Y., and D.J. Burke. 1995. Checkpoint genes required to delay cell division in response to nocodazole respond to impaired kinetochore function in the yeast Saccharomyces cerevisiae. *Molecular and cellular biology*. 15:6838-6844.

Watson, M.L. 1955. The nuclear envelope; its structure and relation to cytoplasmic membranes. *The Journal of biophysical and biochemical cytology*. 1:257-270.

Wei, R.R., J. Al-Bassam, and S.C. Harrison. 2007. The Ndc80/HEC1 complex is a contact point for kinetochore-microtubule attachment. *Nature structural & molecular biology*. 14:54-59.

Weirich, C.S., J.P. Erzberger, J.M. Berger, and K. Weis. 2004. The N-terminal domain of Nup159 forms a beta-propeller that functions in mRNA export by tethering the helicase Dbp5 to the nuclear pore. *Molecular cell*. 16:749-760.

Weis, K. 2003. Regulating access to the genome: nucleocytoplasmic transport throughout the cell cycle. *Cell*. 112:441-451.

Weiss, E., and M. Winey. 1996. The Saccharomyces cerevisiae spindle pole body duplication gene MPS1 is part of a mitotic checkpoint. *The Journal of cell biology*. 132:111-123.

Wiese, C., A. Wilde, M.S. Moore, S.A. Adam, A. Merdes, and Y. Zheng. 2001. Role of importin-beta in coupling Ran to downstream targets in microtubule assembly. *Science*. 291:653-656.

Wente, S.R., and M.P. Rout. 2010. The nuclear pore complex and nuclear transport. *Cold Spring Harbor perspectives in biology*. 2:a000562.

Westermann, S., A. Avila-Sakar, H.W. Wang, H. Niederstrasser, J. Wong, D.G. Drubin, E. Nogales, and G. Barnes. 2005. Formation of a dynamic kinetochore-microtubule interface through assembly of the Dam1 ring complex. *Molecular cell*. 17:277-290.

Westermann, S., I.M. Cheeseman, S. Anderson, J.R. Yates, 3rd, D.G. Drubin, and G. Barnes. 2003. Architecture of the budding yeast kinetochore reveals a conserved molecular core. *The Journal of cell biology*. 163:215-222.

Westermann, S., D.G. Drubin, and G. Barnes. 2007. Structures and functions of yeast kinetochore complexes. *Annual review of biochemistry*. 76:563-591.

Westermann, S., H.W. Wang, A. Avila-Sakar, D.G. Drubin, E. Nogales, and G. Barnes. 2006. The Dam1 kinetochore ring complex moves processively on depolymerizing microtubule ends. *Nature*. 440:565-569.

Wiese, C., A. Wilde, M.S. Moore, S.A. Adam, A. Merdes, and Y. Zheng. 2001. Role of importin-beta in coupling Ran to downstream targets in microtubule assembly. *Science*. 291:653-656.

Wigge, P.A., O.N. Jensen, S. Holmes, S. Soues, M. Mann, and J.V. Kilmartin. 1998. Analysis of the Saccharomyces spindle pole by matrix-assisted laser desorption/ionization (MALDI) mass spectrometry. *The Journal of cell biology*. 141:967-977.

Wigge, P.A., and J.V. Kilmartin. 2001. The Ndc80 complex from Saccharomyces cerevisiae contains conserved centromere components and has a function in chromosome segregation. *The Journal of cell biology*. 152:349-360.

Wilde, A., S.B. Lizarraga, L. Zhang, C. Wiese, N.R. Gliksman, C.E. Walczak, and Y. Zheng. 2001. Ran stimulates spindle assembly by altering microtubule dynamics and the balance of motor activities. *Nature cell biology*. 3:221-227.

Wilhelmsen, K., M. Ketema, H. Truong, and A. Sonnenberg. 2006. KASH-domain proteins in nuclear migration, anchorage and other processes. *Journal of cell science*. 119:5021-5029.

Wilhelmsen, K., S.H. Litjens, I. Kuikman, N. Tshimbalanga, H. Janssen, I. van den Bout, K. Raymond, and A. Sonnenberg. 2005. Nesprin-3, a novel outer nuclear membrane protein, associates with the cytoskeletal linker protein plectin. *The Journal of cell biology*. 171:799-810.

Windecker, H., M. Langegger, S. Heinrich, and S. Hauf. 2009. Bub1 and Bub3 promote the conversion from monopolar to bipolar chromosome attachment independently of shugoshin. *EMBO reports*. 10:1022-1028.

Winey, M., L. Goetsch, P. Baum, and B. Byers. 1991. MPS1 and MPS2: novel yeast genes defining distinct steps of spindle pole body duplication. *The Journal of cell biology*. 114:745-754.

Wool, I.G., Y.L. Chan, and A. Gluck. 1995. Structure and evolution of mammalian ribosomal proteins. *Biochemistry and cell biology = Biochimie et biologie cellulaire*. 73:933-947.

Worman, H.J., and G. Bonne. 2007. "Laminopathies": a wide spectrum of human diseases. *Experimental cell research*. 313:2121-2133.

Wozniak, R.W., G. Blobel, and M.P. Rout. 1994. POM152 is an integral protein of the pore membrane domain of the yeast nuclear envelope. *The Journal of cell biology*. 125:31-42.

Wozniak, R.W., M.P. Rout, and J.D. Aitchison. 1998. Karyopherins and kissing cousins. *Trends in cell biology*. 8:184-188.

Yamada, J., J.L. Phillips, S. Patel, G. Goldfien, A. Calestagne-Morelli, H. Huang, R. Reza, J. Acheson, V.V. Krishnan, S. Newsam, A. Gopinathan, E.Y. Lau, M.E. Colvin, V.N. Uversky, and M.F. Rexach. 2010. A bimodal distribution of two distinct categories of intrinsically disordered structures with separate functions in FG nucleoporins. *Molecular & cellular proteomics : MCP*. 9:2205-2224.

Yamagishi, Y., C.H. Yang, Y. Tanno, and Y. Watanabe. 2012. MPS1/Mph1 phosphorylates the kinetochore protein KNL1/Spc7 to recruit SAC components. *Nature cell biology*. 14:746-752.

Yang, Q., M.P. Rout, and C.W. Akey. 1998. Three-dimensional architecture of the isolated yeast nuclear pore complex: functional and evolutionary implications. *Molecular cell*. 1:223-234.

Yang, W., J. Gelles, and S.M. Musser. 2004. Imaging of single-molecule translocation through nuclear pore complexes. *Proceedings of the National Academy of Sciences of the United States of America*. 101:12887-12892.

Yang, W., and S.M. Musser. 2006. Visualizing single molecules interacting with nuclear pore complexes by narrow-field epifluorescence microscopy. *Methods*. 39:316-328.

Yaseen, N.R., and G. Blobel. 1997. Cloning and characterization of human karyopherin beta3. *Proceedings of the National Academy of Sciences of the United States of America*. 94:4451-4456.

Yoon, H.J., and J. Carbon. 1999. Participation of Bir1, a member of the inhibitor of apoptosis family, in yeast chromosome segregation events. *Proceedings of the National Academy of Sciences of the United States of America*. 96:13208-13213.

Young, J.C., V.R. Agashe, K. Siegers, and F.U. Hartl. 2004. Pathways of chaperone-mediated protein folding in the cytosol. *Nature reviews. Molecular cell biology*. 5:781-791.

Yuan, S., and Z. Sun. 2013. Expanding horizons: ciliary proteins reach beyond cilia. *Annual review of genetics*. 47:353-376.

Zhang, C., M.W. Goldberg, W.J. Moore, T.D. Allen, and P.R. Clarke. 2002. Concentration of Ran on chromatin induces decondensation, nuclear envelope formation and nuclear pore complex assembly. *European journal of cell biology*. 81:623-633.

Zhang, C., M. Hughes, and P.R. Clarke. 1999. Ran-GTP stabilises microtubule asters and inhibits nuclear assembly in Xenopus egg extracts. *Journal of cell science*. 112 ( Pt 14):2453-2461.

Zuccolo, M., A. Alves, V. Galy, S. Bolhy, E. Formstecher, V. Racine, J.B. Sibarita, T. Fukagawa, R. Shiekhattar, T. Yen, and V. Doye. 2007. The human Nup107-160 nuclear pore subcomplex contributes to proper kinetochore functions. *The EMBO journal*. 26:1853-1864.

# **Chapter VI:** *Appendix*

Presented within this Appendix are the results of experiments that have not been published and are also not apart of any of the preceding results chapters contained within this thesis. The data contained within this section consist of the localization of Kap121-GFP in cells depleted of Cdc20 grown in the presence or absence of the MT-destabilizing drug, nocodazole (Figure 7-1).

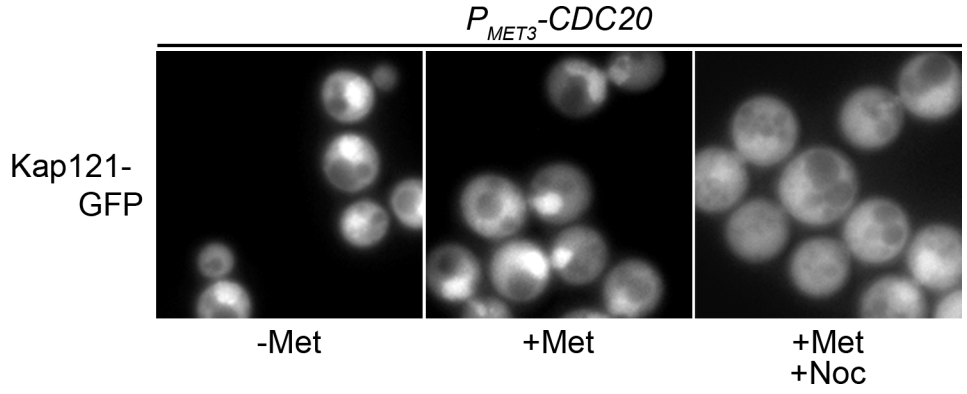


**Figure 7-1. Nuclear accumulation of Kap121-GFP is inhibited in metaphase-arrested cells treated with nocodazole.**

*$P_{MET3}$-CDC20* cells producing Kap121-GFP were grown overnight at 23°C in medium lacking methionine (-Met). Methionine was added to the medium alone (+Met) or with nocodazole (+Met +Noc), and the cultures were incubated for 2.5 h to deplete Cdc20 and induce a metaphase arrest. The subcellular distribution of Kap121-GFP was followed using an epifluorescence microscope.